



HAL
open science

Genome wide analysis for novel regulators of growth and lipid metabolism in drosophila melanogaster

Muhammad Kashif Zahoor

► **To cite this version:**

Muhammad Kashif Zahoor. Genome wide analysis for novel regulators of growth and lipid metabolism in drosophila melanogaster. Agricultural sciences. Université Paris Sud - Paris XI, 2011. English. NNT : 2011PA112039 . tel-00664844

HAL Id: tel-00664844

<https://theses.hal.science/tel-00664844>

Submitted on 27 Nov 2014

HAL is a multi-disciplinary open access archive for the deposit and dissemination of scientific research documents, whether they are published or not. The documents may come from teaching and research institutions in France or abroad, or from public or private research centers.

L'archive ouverte pluridisciplinaire **HAL**, est destinée au dépôt et à la diffusion de documents scientifiques de niveau recherche, publiés ou non, émanant des établissements d'enseignement et de recherche français ou étrangers, des laboratoires publics ou privés.

**GENOME WIDE ANALYSIS FOR NOVEL REGULATORS OF GROWTH
AND LIPID METABOLISM IN *DROSOPHILA MELANOGASTER***

Thesis submitted to obtain the degree of
DOCTOR OF THE UNIVERSITE PARIS-SUD XI

Discipline : Génétique

l'École Gènes, Génomes, Cellules

Presented by

Muhammad Kashif ZAHOOR

Jury:

Prof. Laurent THEODORE

Président

Dr. François LEULIER

Rapporteur

Dr. Frédérique PERONNET

Rapporteur

Dr. Mario PENDE

Examineur

Dr. François ROUYER

Examineur

Dr. Jacques MONTAGNE

Directeur de Thèse

This thesis is dedicated to

my parents

Acknowledgement

I feel much honor to express my ineffable gratitude and profound indebtedness to my venerable supervisor Dr. Jacques Montagne for his exceptional guidance, sagacious suggestions and precept advice in every aspect, hour-lasting thought-provoking discussion and exploratory criticisms, from bench work to manuscript writing and sympathetic attitude throughout the course of study. I am thankful for having an opportunity to work with such a dedicated scientist, who has influenced and enhanced my passion for science.

I am heartily grateful to the members of my thesis jury committee; Dr. Laurent Théodore, Dr. François Leulier, Dr. Frédérique Perronet, Dr. Mario Pende and Dr. François Rouyer; for their precious time, valuable comments and suggestions for this research work. With deep emotion of gratitude, I offer my appreciation to Dr. Pierre Capy, Director de l'école doctoral; for his encouragement to complete my research work.

I have no words to express my feelings to Dr. Jean Philippe Parvy; many thanks for his interest, guidance, research expertise, valuable suggestions and productive discussions during the study. It is a pleasure to thank Brigitte Maroni, and Mickaël Poidevin who made profound efforts to make this thesis possible. I am also very much indebted to Laura Napal, Caroline Lecerf and Thomas Rubin for sharing with me the cheerful as well as gloomy moments and particularly their exclusive cooperation and necessary help during the study. A deep appreciation goes to Souhir, Peng, Fabien, Ekram, Diana, Laïtita, Yousra, Haela, Rabih, Demian and all the past and present lab members for their help and support. I offer also my deep regards to all the people of CGM who supported me in any respect during the completion of the project.

I feel pleasure in transcribing my cordial thanks to my long-time friends Muhammad Shoaib, Kashif Saeed, Zaeem Noman, Saeed Chatha, Adnan Ahmed Dogar, Amer Yousaf, Taj Muhammad, Syed Asim Ali, Aamer Baqai, Khurram Khurshid, Husain Pervez, Kashif Mehmood, Naeem Iqbal, Tenzila Khan and Batool Bukhari; for their moral support throughout my course of study.

Last, but not least, I would like to pay my deepest gratitude to my parents and family members for their affection, amicable attitude and prayers for my success, consistent encouragement and cordial cooperation throughout my life. No words can really express the feelings that I have for my beloved parents. May Allah give them a long, happy life. Ameen!

Muhammad Kashif Zahoor

Table of contents

Acknowledgement	iii
Table of contents	v
List of Figures	viii
List of Tables	x
Nomenclature	xi
Abstract	xiii
Chapter 1 - Introduction	1
1.1 - Cellular signaling regulating growth and metabolism	1
1.1.1 - Cellular signaling.....	3
1.1.2 - Signal transduction pathways	3
1.2 - Target of rapamycin (TOR).....	5
1.2.1 - A central controller of cell growth.....	6
1.2.2 - TORC1 is sensitive to rapamycin and regulates cell growth	10
1.2.3 - TORC2 is insensitive to rapamycin.....	11
1.2.4 - PI3K-TORC1 signaling pathway	13
1.2.5 - Nutrients: a stimulus for TORC1	15
1.2.6 - Regulation of the translation initiation and elongation by TORC1	16
1.2.7 - Regulation of ribosome biogenesis by TORC1	17
1.2.8 - TOR and regulation of autophagy.....	20
1.2.9 - Metabolic functions of TOR signaling	23
1.2.9.1 - Drosophila as a system for studies of lipid metabolism	24
1.2.9.2 - Structure of a lipid droplet.....	26
1.3 - S6 Kinase.....	28
1.3.1 - Ribosomal protein S6 phosphorylation	28
1.3.2 - Identification of the S6K1	29
1.3.3 - Activation of S6K.....	33
1.3.4 - An overview of S6K function	35
1.3.4.1 - S6K1 deletion in the mouse	35
1.3.4.2 - dS6K and the regulation of growth.....	36
1.4 - Archipelago: A key regulator of protein degradation	40
1.4.1 - The F-box hypothesis	41

1.4.2 - Phosphorylation is required for FBP target recognition	41
1.4.3 - Ubiquitination and proteasomal degradation	42
1.4.4 - Molecular and biological function of <i>Archipelago (ago)</i>	45
1.4.4.1 - Archipelago in cell cycle and genomic instability	45
1.4.4.2 - Archipelago as a regulator of Cyclin E and dMyc	46
1.4.4.3 - Archipelago and tracheogenesis	47
1.4.4.4 - Archipelago controls Rb/E2F regulated apoptosis	48
1.4.4.5 - Archipelago as a tumour suppressor	49
1.5 - RNAi Screening for regulators of growth and metabolism	51
1.5.1 - RNA interference (RNAi) and its mechanism	52
1.5.2 - Utility of RNAi technique	53
1.5.3 - <i>Drosophila</i> : A model for genetic screens	54
1.5.4 - RNAi screen for regulators of Steroidogenesis at the ring gland	57
1.5.5 - RNAi screen for regulators of lipid metabolism at the fat body.....	61
1.5.6 - RNAi screen for negative regulators of dS6K-dependent-growth	62
1.5.7 - A protein-protein interaction network through RNAi	64
Chapter 2 - Materials & Methods.....	66
2.1 - RNAi screen for regulators of steroidogenesis at the ring gland	66
2.2 - RNAi screen for regulators of lipid metabolism at the fat body	67
2.3 - Lipid droplet staining	67
2.4 - RNAi screening for negative regulators of dS6K-dependent-growth	68
2.5 - Fly strains used during the study	68
2.6 - Immunostaining.....	69
2.7 - Eye/thorax measurement:.....	70
2.8 - Microscopy	70
2.9 - Protein-protein interaction network data analysis.....	71
2.10 - Quantitative PCR (q-PCR)	71
2.11 - Western blotting	72
2.12 - <i>Drosophila</i> cell culture.....	74
Chapter 3 - Results	75
3.1 - Project goals	75
3.2 - RNAi screening procedure.....	77
3.3 - RNAi screening for novel regulators of steroidogenesis	80
3.4 - RNAi screening for new regulators of lipid metabolism	83
3.5 - RNAi screening for negative regulators of dS6K-dependent-growth	91
3.6 - Interaction map for dS6K-based growth regulators	99
3.7 - Identification of upstream regulators of dS6K.....	103

3.8 - Mammalian homologs of the most relevant dS6K modulators.....	106
3.9 - Archipelago is a negative regulator of dS6K levels	112
3.9.1 - Identification of Archipelago as a negative interactor of dS6K.....	112
3.9.2 - A putative Ago interaction motif in dS6K	114
3.9.3 - Genetic interaction between <i>dS6K</i> and <i>ago</i> mutants	118
3.9.4 - Ago regulates dS6K levels.....	122
Chapter 4 - Discussion and Perspectives.....	129
4.1 - Comparison of genome-wide RNAi screen in <i>Drosophila</i>	129
4.2 - RNAi screening for new regulators of lipid metabolism.....	132
4.3 - RNAi screening for negative regulators of dS6K-dependent-growth	135
4.4 - Regulation of dS6K activity	137
4.5 - Does Archipelago control dS6K degradation?.....	140
References	143

List of Figures

Figure 1 - mTOR signaling	9
Figure 2 - The domain structure of TOR protein	9
Figure 3 - TOR complex 1 (TORC1) and TOR complex 2 (TORC2)	12
Figure 4 - Regulation of cell growth and cell cycle progression by TOR	19
Figure 5 - Interrelations between TOR signaling, autophagy and cell growth	22
Figure 6 - Structure of a lipid droplet	31
Figure 7 - Comparison of carboxy-terminal domain of ribosomal protein S6.....	31
Figure 8 - The domain structure of S6K1, S6K2 and the dS6K	32
Figure 9 - Model of S6K1 activation	34
Figure 10 - <i>dS6K</i> and the regulation of growth.....	39
Figure 11 - The SCF complex and the Ubiquitination pathway.....	44
Figure 12 - The domain structure of Archipelago (Ago) in <i>Drosophila</i> , human and <i>C. elegans</i>	50
Figure 13 - Dicer and RISC (RNA-induced silencing complex)	55
Figure 14 - RNAi interference in <i>Drosophila</i>	55
Figure 15 - The structure and location of the ring gland in drosophila larva	60
Figure 16 - The dynamics of ecdysteroids levels and the development of drosophila	60
Figure 17 - Schematic diagram of the genome-wide RNAi screen for novel regulators of dS6K-dependent growth	78
Figure 18 - Schematic diagram of the genome-wide RNAi screen for novel regulators of lipid metabolism and steroidogenesis	79
Figure 19 - The phenotypic classification of the Phm screen.....	82
Figure 20 - Lipid droplets labelled with LSD2-GFP fusion protein	87
Figure 21 - Changes in the size of lipid droplet (LD) by <i>Rheb</i> ^{RNAi}	87
Figure 22 - The phenotypic classification of the Lipid droplet screen	88
Figure 23 - Changes in the size of lipid droplet (LD) by <i>Fas</i> ^{RNAi}	90

Figure 24 - Modulation of the bend-down wing phenotype due to dS6K over-expression	95
Figure 25 - A brief summary of RNAi lines identified in a screen for modulators of the dS6K-dependent wing phenotype.....	96
Figure 26 - A representation of dS6K interactors	101
Figure 27 - A protein-protein interaction network centered on dS6K-dependent growth.....	102
Figure 28 - Western blot analysis to the extracts of S2 cells for dS6K and P-dS6K.....	105
Figure 29 - Sequence analysis of CG8318 (Neurofibomin 1, NF1)	109
Figure 30 - Sequence analysis of CG1283 (Cdep)	110
Figure 31 - Sequence analysis of CG15010 (Archipelago).....	111
Figure 32 - Genetic interaction at the wing between <i>dS6K</i> and <i>ago</i> ^{RNAi}	113
Figure 33 - Efficiency of <i>ago</i> ^{RNAi} through quantitative PCR.....	113
Figure 34 - The Ago substrates share a putative interactive motif.....	116
Figure 35 - Genetic interaction between <i>ago</i> ^{RNAi} and different variants of <i>dS6K</i>	117
Figure 36 - Genetic interaction between <i>dS6K</i> and <i>ago</i> in homozygous mutant eyes	120
Figure 37 - A representation of the eye/thorax ration between <i>dS6K</i> and <i>ago</i> mutants.....	121
Figure 38 - Immunostaining to dS6K in wing imaginal disc of the 3 rd instar larvae	123
Figure 39 - dS6K expression level and flip-out clones	124
Figure 40 - dS6K expression level in <i>ago</i> mutant clones	127
Figure 41 - Western blot analysis to dS6K in <i>ago</i> ^{RNAi} and <i>ago</i> mutant larval extracts	128

List of Tables

Table 1 - Drosophila homologs of F-box components and related genes	50
Table 2 - List of RNAi lines identified in screen for LD size.....	89
Table 3 - List of RNAi lines identified as strong enhancers of dS6K-dependent growth.....	97

Nomenclature

Abbreviations

4E-BP	4E binding protein
<i>ago</i>	Archipelago
<i>ap</i>	Apterous
CDKs	Cyclin dependent kinases
Cyc E	Cyclin E
DABCO	1,4-diazabicyclo[2.2.2]octane
DAPI	Diamidino-2-phenylindol dihydrochloride
DHR3	Drosophila hormone receptor 3
<i>dS6K</i>	Drosophila S6 kinase
dsRNA	Double-stranded RNA
EGFR	Epidermal growth factor receptor
eIF4E	Eukaryotic translation initiation factor 4 E
ERTs	Endoreplicating tissues
FBPs	F-box binding proteins
Fbw7	F-box WD 7
FRB	FKBP12-rapamycin binding domain
FRT	Flp recognition target
GAP	GTPase-activating protein
GFP	Green fluorescent protein
IGF	Insulin like growth factors
LD	Lipid droplet
LSD2	lipid storage droplet-2
PAGE	Polyacrylamide gel electrophoresis

PAT-domain	<u>P</u> erilipin, <u>A</u> DRP and <u>T</u> IP47-related protein domain
PBS	Phosphate buffer saline
PDK1	Phosphoinositide-dependent protein kinase 1
PI3K	Phosphatidylinositol 3-kinase
PKB	Protein kinase B
<i>ppl</i>	pumpless
Raptor	<u>R</u> egulatory <u>A</u> ssociated <u>P</u> rotein of m <u>T</u> OR
Rheb	Ras homolog enriched in brain
RING	Really interesting new gene
RISC	RNA induced silencing complex
RNAi	RNA interference
RPS6	Ribosomal protein S6
S6K1	S6 kinase 1
SCF	Skp-Cullin-F-box
SDS	Sodium dodecyl sulfate
siRNA	Small interfering RNA
TAG	Triglycerides
TEMED	N, N, N', N'-Tetramethylethylenediamine
TOR	Target of rapamycin
TORC1	Target of rapamycin complex1
TORC2	Target of rapamycin complex2
Tris	Trishydroxymethylaminomethane
TSC1	Tuberous sclerosis complex1
TSC2	Tuberous sclerosis complex2
UAS	Upstream activating sequence
VDRC	Vienna Drosophila Research Center
WD	Tryptophan-Aspartic Acid

Abstract

The evolutionary conserved insulin and nutrient signaling network regulates growth and metabolism. Nutrients are directly utilized for growth or stored, mostly as triglycerides. In *Drosophila*, activation of insulin/nutrient signaling in the fat body (the fly equivalent of liver and adipose tissue), causes an increase in fat stores composed of several small-size lipid droplets (LDs). Conversely, fasting produces an increase in LD size and a decrease in fat contents. The TOR kinase and its substrate S6 kinase (S6K) play a central role in this response, and particularly in *Drosophila*, they have been shown to orchestrate cell-autonomous and hormone-controlled growth. However, despite extensive research studies on different model organisms (mouse, fly, worm) to decipher the molecular and physiological functions of S6K, nothing is known about how its degradation is regulated.

Taking advantage of the inducible RNA interfering (RNAi) library from NIG (Japan), we have performed three genetic screens to identify novel regulators of steroidogenesis, lipid metabolism and dS6K-dependent growth. First, RNAi lines were screened in the ring gland; an organ that controls the progression of the developmental steps by producing the steroid hormone ecdysone. Out of 7,000 genes screened, 620 positive candidates were identified to produce developmental arrest and/or overgrowth phenotypes. Then, we challenged 4,000 genes by RNAi screening able to recapitulate the larger sized LD phenotype as obtained upon starvation, leading to the identification of 24 potential candidates. Finally, the RNAi lines were screened for their ability to enhance a growth phenotype dependent of the *Drosophila* S6K (dS6K). Out of 7,000 genes screened, 45 genes were identified as potential negative regulators of dS6K. These genes were further used to design a novel protein-protein interaction network centered on dS6K through the available data from yeast-2-hybrid (Y2H) assay. The most potent interactors were then analyzed by treatment of cultured S2 cells with the corresponding double strand RNA (dRNA). Western blotting thus, allowed us to discriminate between the gene products that regulate dS6K levels versus those that regulate its phosphorylation, as a hallmark for

its kinase activity. Interestingly, *archipelago (ago)*, which encodes a component of an SCF-ubiquitin ligase known to regulate the degradation of dMyc, Cyclin E and Notch, was identified as a negative regulator of dS6K-dependent growth. Based on the Y2H available data showing that Ago and dS6K interact each other and the presence of a putative Ago-interaction motif in dS6K, we hypothesized that Ago causes an ubiquitin-mediated degradation of dS6K. Our molecular data showed that loss of *ago* caused an elevated level of dS6K, which confirms a role of Ago in controlling dS6K degradation. Altogether our findings emphasize the importance of the saturating screening strategies in *Drosophila* to identify novel regulators of metabolic and signaling pathways.

Chapter 1

Introduction

1.1 - Cellular signaling regulating growth and metabolism

The fundamental cellular activities in eukaryotes are organized in a coordinated fashion through complex interrelating networks of cellular signaling which regulate growth and development process. One of the major, still incompletely understood problems in biology is how the final size and organ proportions of an organism are achieved (Mirth and Riddiford, 2007). The highly sophisticated and synchronized tissue growth requires crosstalk between energy producing and energy consuming tissues of the animal. The final body size of an individual is determined by genetic and environmental factors. All animal species have their genetically determined optimal size, which can vary tremendously even between closely related species. Among the most important environmental factors that contribute to determining the growth rate and final size of animals is nutrition (Hietakangas and Cohen, 2009). In multicellular animals, however, each cell also needs to receive information about the nutritional status of the whole animal. This kind of systemic regulation through signaling pathways allows the animal to coordinate growth between tissues and adjust growth rates and consumption of energy stores during periods of nutrient limitation. The insulin/IGF pathway regulates growth

mainly through the phosphatidylinositol 3-kinase (PI3K)/PKB protein kinase signaling pathway, which converges with the cellular nutrient-sensing pathways mainly at TOR (target of rapamycin) (Hietakangas and Cohen, 2009). As the main nodal point in nutrient sensing in all eukaryotes is the protein kinase TOR, it regulates and adjusts cell growth, largely by determining the rate of protein biosynthesis (Schmelzle and Hall, 2000). The TOR kinase is present in two complexes; TORC1 and TORC2 which have important roles in growth control, but they act in different ways. Two key substrates of TORC1 are S6 kinase (S6K) and eukaryotic initiation factor 4E binding protein (4E-BP) regulating mainly growth and metabolism of an organism (Martin and Hall, 2005; Kim et al., 2003; Loewith et al., 2002).

At the cellular level, the biological processes of cell proliferation, cell growth, cell differentiation, autophagy and apoptosis are all tightly coupled to appropriate alterations in metabolic status. In the case of cell growth and cell proliferation, this requires redirecting metabolic pathways to provide the fuel and basic components for new cells. Ultimately, the successful co-ordination of cellular biology with cellular metabolism underscores a wide range of multicellular processes during the course of development of an organism (Sethi and Vidal-Puig, 2010). Therefore, the processes that govern growth regulation are probably closely coupled to ones regulating metabolism. The evolutionary conserved insulin/TOR signaling pathway plays its role the regulation of growth as well as glucose and lipid metabolism (Colombani et al., 2003; Arquier and Leopold, 2007; Wullschleger et al., 2006; Ducharme and Bickel, 2008). Different components of the insulin/TOR signaling pathway are being individually delineated in a range of experimental systems, i.e. *Drosophila*, mouse and yeast. Therefore, our understanding of how different components of cell growth and metabolism machinery are regulated and how they integrate with each other still needs a lot of efforts of elucidation.

S6 kinase is an evolutionary conserved determinant of growth through increased protein biosynthesis. Although several studies have shown how S6 kinase is regulated; however with particular context to the ultimate fate of S6 kinase, nothing is known about its degradation. Moreover, the regulation of metabolism particularly lipid metabolism which provides energy and macromolecules to the growing cells still needs detailed insights. In this thesis, we have used the model organism *Drosophila melanogaster* in order to

investigate the regulation of growth and lipid metabolism. Below here, a concise introductory note on cellular signaling pathways is discussed briefly.

1.1.1 - Cellular signaling

For the survival of an organism, it needs to react to an alternating environment and adjusts its behavior to meet the prevailing conditions. The reaction of a metazoan animal is the result of a perception event which is followed by a coordinated response of various specialized cell types. This response ultimately leads to a change in the animal behavior. This coordinated action of metazoan operations relies on communication between cells. Hence, individual cells are faced with the same requirements as the organism as a whole, they need to receive information and respond in an appropriate manner. For the purpose of cellular communication, cells have evolved signaling mechanisms to elicit and receive information through different interactions. These mechanisms, i.e. cellular signaling pathways; collect and integrate information about extracellular conditions, are important for survival, growth and the differentiation (Sethi and Vidal-Puig, 2010).

Through information collection from its external milieu, a cell is able to respond to changes in nutrient and growth factor composition and abundance by modulating its protein post-translational modifications profile. These alterations can lead to responses such as regulation of growth and metabolism, cell division, cell death, and modulation of cellular cytoskeleton. The response of a given cell to a given signal is dictated by its repertoire of molecular signal transduction mechanisms. These mechanisms consist of different receptors and intracellular signaling pathway components such as kinases which are all coordinated into a signaling cascade to govern a given biological process (Marshall, 2006; Hietakangas and Cohen, 2009; Sethi and Vidal-Puig, 2010).

1.1.2 - Signal transduction pathways

A signaling pathway comprises of several intracellular transducers. These are typically kinases and phosphatases which by incorporating or removing a phosphate group alter

the physiochemical properties of a substrate protein or a second messenger such as inositol-lipids (Graves and Krebs, 1999; Vanhaesebroeck, 2001). A signaling pathway may consist of several kinases which sequentially phosphorylate each other in a specified order. For instance, PI3K/TOR signaling pathway comprises different events of sequential phosphorylation and then downstream triggers S6 kinase signaling (Volarevic and Thomas, 2001; Oldham et al., 2000).

A characteristic consequence of a protein phosphorylation event is a conformational change in its three dimensional structure, which exposes its catalytic cleft to interact with its substrates. A good example of such a regulation is the activation of Protein kinase B (PKB/Akt) and S6 kinase (S6K) (Dutil and Newton, 2000; Calleja et al., 2007; Volarevic and Thomas, 2001; Oldham et al., 2000; Montagne and Thomas, 2004). In addition to kinases and phosphatases, a signaling pathway may contain several other adapter proteins which may facilitate protein-protein interactions and enzymatic activity (Pratt et al., 2008). For example, PKB/Akt is known to associate with more than ten different proteins having a role in its stabilization, kinase activity and intracellular transport (Du and Tschlis, 2005; Radimerski et al., 2002b; Potter et al., 2002; Rintelen et al., 2001). PKB is thought to have an activation of mTORC1 and ultimately makes a link between nutrients and insulin signaling pathways impinging on TOR kinase (White, 2003; Oldham et al., 2000).

Although there are multiple developmental outputs, there are a limited number of signaling pathways controlling cell fate decisions, including Wnt, TGF- β , Hedgehog, receptor tyrosine kinase, nuclear receptor, Jak/STAT and Notch pathways (Lodish et al., 2008). Each of these signaling pathways is used over and over throughout the development of an organism to activate the target gene expression corresponding to various developmental contexts. Mechanisms of signal transduction utilized by each of these pathways are very different from one another, but the output is the same, the activation of target genes (Barolo and Posakony, 2002).

A primary role of signaling pathways is to regulate a particular cellular process. In spite of different signaling pathways, we know less concerning the signaling pathways that control cell growth, specifically those associated with the regulation of protein synthesis

(Volarevic and Thomas, 2001). The main key player which regulates growth and metabolic processes is TOR kinase (Bryk et al., 2010). The downstream effector of TOR, 4E-BP regulates organismal lipid homeostasis rather than growth (Teleman et al., 2005a). Lipid metabolism is essential for growth and generates much of the energy needed for normal developmental process as well as during periods of food deprivation. The regulation process of lipid metabolism is partly monitored by TOR signaling pathway which also responds to cellular levels of amino acids (Laplante and Sabatini, 2009; Bryk et al., 2010). Especially from growth point of view, the whole activities centres on the downstream target of TOR; the S6 kinase signaling and then ultimately upon translational machinery. In parallel, a great deal of information has been accumulated concerning the signaling pathways and the regulatory phosphorylation sites involved in controlling S6K activation (Meyuhas, 2008). One main substrate of S6 kinase is ribosomal protein S6 (RPS6), which has been implicated in the protein synthetic apparatus. (Hietakangas and Cohen, 2009; Volarevic and Thomas, 2001). Below are briefly introduced central signaling systems involved in the regulation of growth and metabolism important for this work.

1.2 - Target of rapamycin (TOR)

In the 1970s, a bacterial strain; Streptomycete (*Streptomyces hygroscopicus*) isolated from a soil sample of the Easter Island (Rapa Nui in the local language) was found to inhibit growth of a variety of fungi (Sehgal et al., 1975). The antifungal principle was subsequently extracted and termed as rapamycin. It was discovered that rapamycin selectively blocked S6K1 activation in mammalian cells (Chung et al., 1992). Thereafter, a tremendous amount of efforts has provided an exciting insight into a central growth regulatory signaling component named TOR, which is an evolutionary conserved element from yeast to man (Hanrahan and Blenis, 2006; Dann and Thomas, 2006; Hietakangas and Cohen, 2009).

The conserved serine/threonine protein kinase TOR was originally identified in budding yeast, where gain-of-function mutations in the *TOR1* and *TOR2* genes were shown to confer resistance to rapamycin that inhibits yeast growth (Heitman et al., 1991). Over the

last few years, TOR has been emerged as a critical regulator of the protein synthesis and cell growth in *Caenorhabditis elegans*, *Drosophila melanogaster*, yeast, plants, and mammals. Unlike yeast, which in some cases possesses two *TOR* genes, higher eukaryotes possess only a single *TOR* gene (Lee et al., 2005; Crespo et al., 2005). In addition to regulating protein synthesis, mTOR (also known as FRAP, RAFT, RAPT, or SEP) signaling may also regulate transcription, cell proliferation, cytoskeletal rearrangements, ribosome biogenesis and autophagy (Fig. 1) (Hay and Sonenberg, 2004; Schmelzle and Hall, 2000; Martin and Hall, 2005; Hietakangas and Cohen, 2009; Soulard and Hall, 2007).

Eukaryote TORs are large proteins (about 280 kDa) that share 40%–60% identity in their primary sequence and belong to a group of kinases known as the phosphatidylinositol kinase-related kinase (PIKK) family. PIKK family members contain a carboxy-terminal serine/threonine protein kinase domain that resembles the catalytic domain of phosphatidylinositol 3-kinases (PI3Ks) and PI4Ks. At the amino-terminal region, the FKBP12-rapamycin binding domain (FRB) is located and the FAT (FRAP, ATM, and TTRAP) and FATC domains are located towards the carboxy-terminal part (Fig. 2). Single amino acid substitutions in FRB yield TOR proteins (such as TOR1-1 and TOR2-1) that are no longer bound and inhibited by the FKBP12-rapamycin complex. These domains are always found together in all PIKKs, suggesting that they may interact with each other. The amino-terminal portion of TOR contains tandem HEAT repeats that may form an extended super helical array with large interfaces for protein-protein interactions (Wullschleger et al., 2006).

1.2.1- A central controller of cell growth

Genetic studies from multiple model organisms have demonstrated that TOR is an essential regulator of cell and tissue growth. Net tissue growth depends on the rate at which cells grow and divide. Both cell size and cell proliferation are regulated by TOR signaling (Zhang et al., 2000; Stanfel et al., 2009; Hietakangas and Cohen, 2009). Deletion of *CeTOR* in the nematode worm *Caenorhabditis elegans* causes developmental arrests (Long et al., 2002). *TOR* mutant *Drosophila* shows a small cell size phenotype

and reduced body size, which is consistent with a role of *dTOR* in regulating cell growth (Oldham et al., 2000; Zhang et al., 2000). It has been also shown that *dTOR* affects the timing of neuronal cell differentiation. Hyperactivation of dTOR signaling leads to accelerated differentiation, whereas inhibition of dTOR signaling retards differentiation (Bateman and McNeill, 2004). Interestingly, ablation of *dTOR* in the fat body results in a systemic defect in larval growth (Colombani et al., 2003). Thus, in addition to controlling growth of the cell in which it resides, dTOR can also influence growth of distant cells and organs during development via a humoral mechanism. Studies in yeast demonstrated that TOR regulates growth both at cellular and systemic levels. (Loewith et al., 2002; Friberg, 2006). When growth conditions are favourable, TOR is active and yeast cells maintain a robust rate of ribosome biogenesis, translation initiation, and nutrient import. However, rapidly growing yeast cells treated with rapamycin, starved for nitrogen, or depleted of both *TOR1* and *TOR2* downregulate general protein synthesis, upregulate macroautophagy and activate several stress-responsive transcription factors (Stanfel et al., 2009; Wullschleger et al., 2006). Thus, conditional rapamycin-sensitive TOR signaling promotes anabolic processes and antagonizes catabolic processes. Many of these rapamycin-sensitive readouts of TOR are conserved in mammals. For example, TOR is also required for development in mice. Homozygous *mTOR*^{-/-} embryos resemble embryos starved of amino acids and die shortly after implantation due to impaired cell proliferation in both embryonic and extra-embryonic compartments (Gangloff et al., 2004; Martin and Sutherland, 2001; Murakami, 2004). Exposure of early mouse embryos to rapamycin also arrests cell proliferation indicating that rapamycin-sensitive *mTOR* function is essential during this stage of development (Martin and Sutherland, 2001).

mTOR exists in two distinct complexes within cells; one that contains raptor, GβL, mTOR (mammalian target of rapamycin complex 1, mTORC1), and another containing rictor, GβL, and mTOR (mammalian target of rapamycin complex 2, mTORC2). The identification of the two distinct multiprotein complexes has provided a molecular basis for understanding the complexity of mTOR signaling. mTORC1 is sensitive to rapamycin and mediates the temporal control of cell growth by regulating protein synthesis and mass accumulation through its substrates, S6K1 and 4E-BPs (Martin and Hall, 2005; Hara et al., 2002; Kim et al., 2003; Hay and Sonenberg, 2004; Loewith et al.,

2002). As the cell growth in higher organisms is tightly coupled to nutrient availability, growth factors and energy status of the cell. It seems that mTORC1 integrates all three inputs to control cell growth (Martin and Hall, 2005) (see below). mTORC2 is rapamycin insensitive and mediates the spatial control of cell growth by regulating a Rho/GTPase signaling pathway, which impinges on the actin organization (Sarbasov et al., 2004) (see below). mTORC2 is also implicated in phosphorylation of PKB on Ser₄₇₃ (Bayascas and Alessi, 2005; Sarbasov et al., 2005b). This observation suggests the existence of feedback mechanism in which TORC2 activation leads to positive regulation of PKB signaling pathway. In summary, all the findings suggest that metazoan TOR coordinates growth and development in response to the nutritional cues.

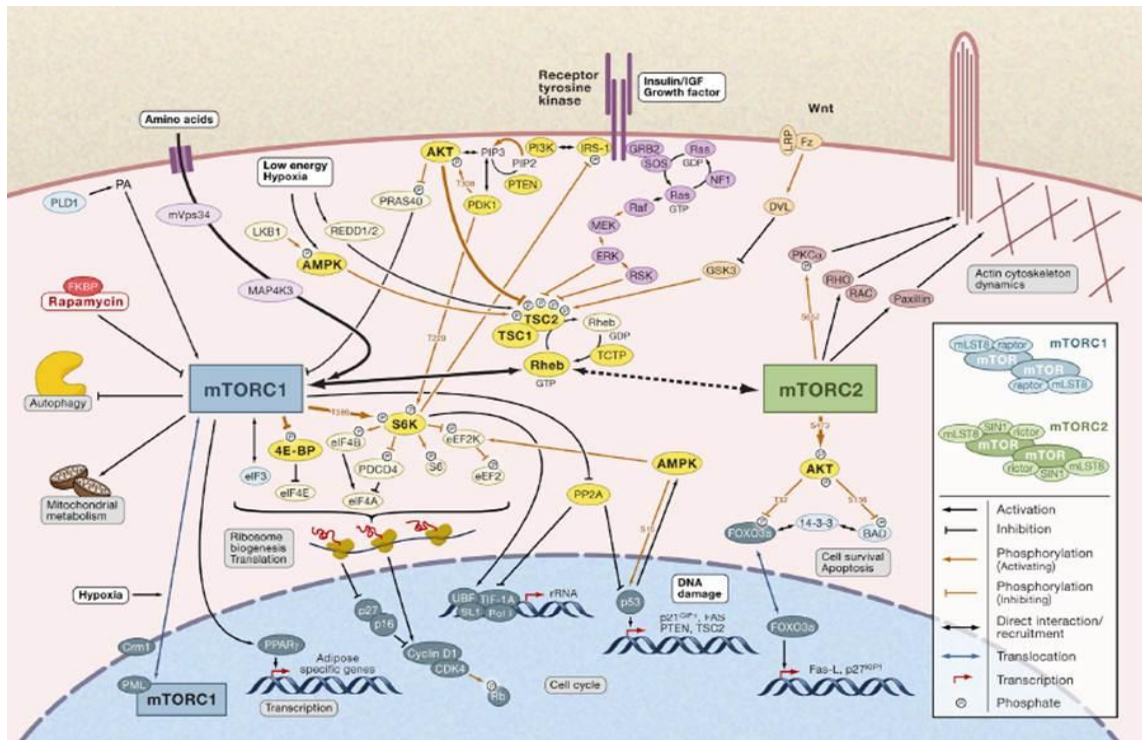


Figure 1 - mTOR signaling

TOR intercepts different signaling pathways and thereby controls processes such as transcription, translation, ribosome biogenesis, autophagy, mitochondrial metabolism, apoptosis, and the reorganization of the actin cytoskeleton (From Soulard and Hall, 2007).



Figure 2 - The domain structure of TOR protein

All TOR proteins contain in their carboxy-terminus about a 250 amino acid region that shows homology to the catalytic subunit of PI-3/4 kinases (violet). Despite the homology to lipid kinases, the TOR kinase domain phosphorylates serine and threonine residues of target proteins. The central about 550 residue long FAT domain occurs always in tandem with the 35 residue encompassing FATC motif at the very carboxy-terminal end. The FRB (FKBP-rapamycin binding) domain is located between the FAT and the kinase domains. Two amino-terminal domains composed of HEAT repeats are supposed to mediate protein-protein interactions (drawn from Wullschleger et al., 2006).

1.2.2 - TORC1 is sensitive to rapamycin and regulates cell growth

As discussed above, the genetic studies in yeast demonstrated that TOR signaling regulates cell growth and overall growth of an organism. The biochemical purification of TOR1 and TOR2 from yeast led to the identification of two distinct TOR protein complexes, TORC1 and TORC2, which account for the differential sensitivity of TOR signaling to rapamycin (Fig. 3). The TORC1 contains KOG1, TCO89, LST8, and either TOR1 or TOR2 (Loewith et al., 2002; Reinke et al., 2004; Wullschleger et al., 2006). KOG1 and LST8 have obvious mammalian sequence homologs, raptor and mLST8 also known as GβL, respectively. When mTORC1 is bound by FKBP12-rapamycin, the mTORC1 kinase activity is abrogated both *in vivo* and *in vitro* (Hara et al., 2002; Jacinto et al., 2004; Kim et al., 2002; Sarbassov et al., 2004). The disruption of TORC1 mimics rapamycin treatment, suggesting that TORC1 mediates the rapamycin-sensitive temporal control of cell growth (Loewith et al., 2002).

Raptor (Regulatory Associated Protein of mTOR) is a large protein (150 kDa) containing a highly conserved amino-terminal domain followed by several HEAT repeats and seven carboxy-terminal WD40 repeats (Hara et al., 2002; Kim et al., 2002). The interactive domains in raptor and mTOR have been difficult to map which suggests that multiple contact sites exist between these two proteins. The knockdown of KOG1/raptor in mammals, *S. cerevisiae*, and *Drosophila* phenocopies rapamycin treatment and depletion of TOR indicates that raptor functions positively in mTOR signaling (Hara et al., 2002; Jacinto et al., 2004; Kim et al., 2002; Sarbassov et al., 2004). It has been suggested that raptor acts as an adaptor to recruit substrates to mTOR (Choi et al., 2003; Hara et al., 2002; Nojima et al., 2003; Schalm et al., 2003), whereas Kim et al. described that upstream signals regulate the raptor-mTOR interaction and thereby monitor the activity of mTORC1 (Kim et al., 2002). The mechanism by which FKBP12-rapamycin binding inhibits mTORC1 is not known and may indeed involve more than one mechanism (Wullschleger et al., 2006). Under some experimental conditions, FKBP12-rapamycin dissociates raptor-mTOR which suggests that FKBP12-rapamycin blocks access to the substrates (Kim et al., 2002). Jacinto et al. observed that FKBP12-rapamycin inhibits mTORC1 autophosphorylation, meaning thereby that FKBP12-rapamycin inhibits intrinsic mTORC1 kinase activity and the access to an extrinsic substrate (Jacinto et al.,

2004). Raptor also serves as a scaffold for the interaction between mTOR which is required for mTOR mediated 4E-BP1 phosphorylation and elevates mTOR kinase activity towards S6K1 (Hara et al., 2002; Schalm and Blenis, 2002). Thus, in nutshell, TORC1 is sensitive to rapamycin and TORC1-raptor interaction leads towards the cell growth.

1.2.3 - TORC2 is insensitive to rapamycin

In yeast, TORC2 contains AVO1, AVO2, AVO3, BIT61, LST8, and TOR2, but not TOR1 (Fig. 3) (Wullschleger, 2006; Loewith et al., 2002; Reinke et al., 2004). FKBP12-rapamycin does not bind to TORC2. The disruption of TORC2 mimics TOR2 depletion which suggests that TORC2 mediates the rapamycin-insensitive spatial control of cell growth (Loewith et al., 2002). TORC2 is a multimeric super complex, i.e., TOR2-TOR2 interaction gives rise to a TORC2-TORC2 dimer assembly (Wullschleger et al., 2005). Yeast and mammalian TORC1 are also multimeric, as is *Drosophila* TOR. The elegant genetic study of Zhang et al. demonstrated that dTOR is multimeric, but they did not determine whether the multimerization corresponded to dTORC1 or dTORC2. Multimerization may play a role in the regulation of TORC kinase activity because multimeric TORC2 appears to be more active kinase than monomeric TORC2 (Zhang et al., 2006).

Mammalian TORC2 (mTORC2) contains mTOR, rictor, and mLST8, but not raptor. Rictor (also known as mAVO3) is a large protein (about 200 kDa) but contains no obvious catalytic motifs. The knockdown of *mTOR* or *rictor* results in loss of both actin polymerization and cell spreading which is consistent with the results obtained from studies in yeast and *Dictyostelium discoideum*. Moreover, mTORC2 is neither bound by FKBP12-rapamycin nor FKBP12-rapamycin affects mTORC2 kinase activity *in vitro*, suggesting that TORC2 is insensitive to rapamycin (Jacinto et al., 2004; Sarbassov et al., 2004).

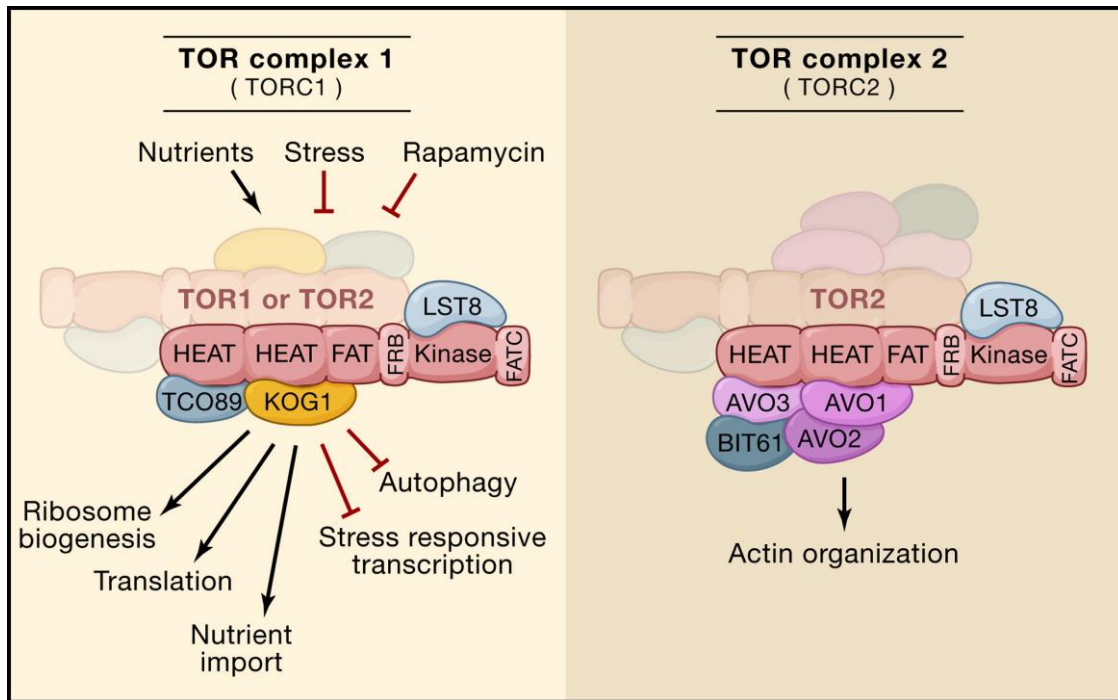


Figure 3 - TOR complex 1 (TORC1) and TOR complex 2 (TORC2)

TOR-associated proteins (KOG1, TCO89, LST8, AVO1–3, and BIT61) and their potential interactor domains in TOR (HEAT, FAT, FRB, Kinase, and FATC). Both TORC1 and TORC2 are likely dimers of multi-proteins containing complexes. TORC1 mediates the rapamycin-sensitive signaling branch that couples growth to amino acid sensing. Stimuli that positively regulate TORC1 and TORC1 outputs that promote growth are depicted with black arrows. Inputs that negatively regulate TORC1 and the stress- and starvation-induced processes that TORC1 regulates negatively are depicted with red bars. TORC2 signaling is rapamycin insensitive and is required for the organization of the actin cytoskeleton (From Wullschleger et al., 2006).

1.2.4 - PI3K-TORC1 signaling pathway

The mTOR pathway responds to growth factors via the PI3K pathway. The activation of PI3K signaling pathway is initiated by the binding of growth factors, such as insulin and insulin growth factor-1 (IGF-1) to their tyrosine kinase receptors, G-protein coupled receptors, but also by direct interaction with oncogenic Ras (Katso et al., 2001; Cantley et al., 2002). The activation of PI3K leads to production of the lipid second messenger phosphatidylinositol 3,4,5-trisphosphates (PIP3) from phosphatidylinositol 4,5-diphosphates (PIP2) (Cantley, 2002). The tumor suppressor phosphatase and tensin homologue (PTEN) reverses the action of PI3K by dephosphorylating (PIP3) and, therefore, is an essential suppressor of PI3K signaling pathway (Fig. 1). Phosphatidylinositol 3, 4,5- trisphosphate recruits proteins containing pleckstrin homology (PH) domain to the plasma membrane, thereby coupling PI3K signals to downstream effector molecules (Katso et al., 2001). Activation of protein kinase B (PKB), following membrane translocation is essential in mediating the effects of PI3K, not only on cell growth, but also in regulating other metabolic and anti-apoptotic effects (Alessi et al., 1996). PKB is activated by phosphorylation on two key residues: Thr₃₀₈ by the phosphoinositide-dependent protein kinase (PDK1) and Ser₄₇₃ by mTORC2 (Sarbasov et al., 2005a; Alessi et al., 1997). PKB activation is thought to regulate the activation of mTORC1 (White, 2003). The activation of mTOR by PKB is indirect and involves inactivation of an inhibitor of cell growth, tumor suppressor tuberous sclerosis complex (TSC) composed of hamartin (TSC1) and tuberlin (TSC2) heterodimer proteins (Martin and Hall, 2005). *TSC* mutations are associated with an autosomal dominant genetic disorder, *tuberous sclerosis* (TS), a disease that is associated with cancer susceptibility, including hamartomas in various organs (Hodges et al., 2001). One feature of these tumors is that they contain large cells. In *Drosophila*, Radimerski et al. showed that the absence of *Tsc1/2* leads to the constitutive dS6K activation and the inhibition of dPKB. And also the inhibition of the dPKB could be rescued by the loss of *dS6K*. In contrast, the dPTEN has little effect on dS6K but negatively regulates dPKB. They also demonstrated that reduced dS6K signaling rescued the early larval lethality associated with the loss of *dTSC1/2* function which suggested that the S6K pathway is a promising target for the treatment of Tuberous sclerosis complex (Radimerski et al.,

2002a). Furthermore, the mutations in either *dTSC1* or *dTSC2* have also been identified in screens for genes that suppress cell growth (Tapon et al., 2001). It has been suggested that phosphorylation of TSC2 at PKB phosphorylation sites is important for inhibition of TSC complex and cell growth (Manning et al., 2002; Inoki et al., 2002; Potter et al., 2002). However, Dong and Pan presented a report in *Drosophila* that is in contrast with this hypothesis (Dong and Pan, 2004). *TSC2* null flies are successfully rescued using wild-type *TSC2* or PKB phosphorylation-site mutants of *TSC2*. These rescued mutant flies have similar sized cells compared with wild-type-rescued flies, suggesting that phosphorylation of TSC2 by PKB has no effect on function of TSC2 under conditions of normal PKB activation during *Drosophila* development. It is still possible that under non-physiological conditions, PKB-mediated phosphorylation of TSC2 could be relevant for regulation of cell growth (Fig. 1).

TSC2 has a GTPase-activating protein domain (GAP) and acts as a GTPase-activating protein for the small G protein Rheb (Li et al., 2004). Rheb (Ras homolog enriched in brain) was first identified as an enhancer of cell growth that was epistatic to the TSC complex in *Drosophila*, and places TOR and S6K downstream of Rheb (Stocker et al., 2003). Rheb binds directly to the kinase domain in mTOR and activates mTOR in a GTP dependent manner (Long et al., 2005a). It has been suggested that GTP loading of Rheb, rather than mediating mTORC1 recruitment, enables Rheb to induce a conformational change in mTORC1 leading to mTORC1 activation and phosphorylation of downstream targets S6 kinase 1 (S6K1) and 4E binding protein 1 (4E-BP1) (Long et al., 2005a; Inoki et al., 2002; Jaeschke et al., 2002). In *Drosophila*, these two key substrates of TORC1 are S6 kinase and eukaryotic initiation factor 4E binding protein (4E-BP), which are the downstream effectors of PI3K-TORC1 signaling pathway, ultimately regulating the mechanisms of growth and the metabolism (Martin and Hall, 2005; Kim et al., 2003; Loewith et al., 2002; Teleman et al., 2005a; Meyuhas, 2008).

To summarize, PI3K signaling pathway results in active PKB and PDK1. The latter can directly activate S6K (detail in section 1.3.3) whereas PKB inhibits the TSC complex thus releasing Rheb from the TSC inhibition. This, together with nutrient stimulation leads to fully active TOR that can phosphorylate S6K, 4E-BP to stimulate growth. In addition, more complexity was added to this portrait that S6K negatively modulates the

effect of Insulin/insulin-like growth factors by phosphorylating IRS proteins. Thus, insulin or IGF activates a negative feedback mechanism in order to regulate its own activity (Fig. 1).

1.2.5 - Nutrients: a stimulus for TORC1

The nutrients fuel the growth and the development of living organisms. As already discussed in detail; the eukaryotic machinery that allows unicellular and multicellular organisms to utilize nutrients efficiently involves the highly conserved protein TOR. The regulation of TOR by nutrients is conserved from yeast to man (Martin and Hall, 2005; Jacinto and Lorberg, 2008). One possibility is that nutrients are the primary stimulus, whereas growth factor signaling may modulate the intensity of growth in certain tissues or during specific developmental stages. Alternatively, the primary stimulus in higher organisms might be growth factor signaling, whereas the nutrient signals subsequently modify the potency of the response. The activated mTORC1 regulates the translation through the hierarchical phosphorylation event either by an activation of S6K1/2 or by an inactivation of eukaryotic translation initiation factor 4 (eIF4E) inhibitor, 4E-BP1 (Hay and Sonenberg, 2004). It is poorly understood how cellular responses mechanistically regulate mTORC1 signaling. It seems that the stability of the mTOR-raptor interaction strengthens during nutrient deprivation, which correlates with a decrease in *in vitro* kinase activity of mTORC1. Amino acids have been proposed to activate mTORC1 via inhibition of TSC1-TSC2 or through stimulation of Rheb. The stimulation of leucine-starved cells with leucine reduces the amount of raptor associated with mTORC1 and correlates with increased mTORC1 *in vitro* kinase activity (Kim et al., 2002). This regulation requires GβL, otherwise the absence of which causes the interaction between mTOR and raptor insensitive to nutrients (Kim et al., 2003).

Gao et al. demonstrated that inactivation of TSC2 renders cells resistant to amino acid withdrawal which suggests that the amino acids mediate signals through the TSC1-TSC2 (Gao et al., 2002). Other studies have proposed a model in which amino acids signal to mTORC1 independently of TSC2. Amino acid withdrawal still downregulates mTORC1 signaling in *TSC2*-deficient cells and overexpression of *Rheb* in *Drosophila* and

mammalian cells allows TORC1 signaling in the absence of amino acids (Smith et al., 2005; Saucedo et al., 2003; Garami et al., 2003). Furthermore, the binding of Rheb to mTOR is regulated by amino acid sufficiency, whereas GTP charging of Rheb is independent of amino acids (Long et al., 2005b) which suggests that the amino acid signal impinges on Rheb. However, Smith et al. failed to detect amino acid regulated binding of Rheb to mTOR (Smith et al., 2005). TORC1 responds to nutrients despite the absence of functional Rheb and TSC orthologs in *S. cerevisiae*, whereas withdrawal of amino acids in mammalian cells alters the binding of raptor to mTOR (Kim et al., 2002). These latter observations may suggest that amino acids are sensed by mTORC1 directly. In addition to nutrients and growth factors, mTORC1 seems to be a major integrator of the signals that convey the overall status of the cellular environment to the protein synthetic machinery and cell growth. Clearly, the mechanism by which nutrient status is communicated to mTORC1 requires further study.

1.2.6 - Regulation of the translation initiation and elongation by TORC1

The importance of translation and ribosome biogenesis for cell growth has been well pointed out. The main mechanism by which TORC1 regulates tissue growth is by adjusting protein biosynthesis, which is a rate limiting process in cell growth (Hietakangas and Cohen, 2009). Two key substrates of TORC1 are involved in the initiation of cap-dependent translation of mRNAs, ribosomal protein S6 kinase (S6K) and eukaryotic initiation factor 4E binding protein (4E-BP) (Fig. 4) (Tee and Blenis, 2005). In an un-phosphorylated state, 4E-BP binds to the eukaryotic initiation factor 4E (eIF4E). TORC1-mediated phosphorylation of 4E-BP leads to its dissociation from eIF4E, which enables the association of eIF4G and assembly of the translation pre-initiation complex (Jackson et al., 2010; Hietakangas and Cohen, 2009; Hayashi and Proud, 2007). TORC1 activates S6K by phosphorylating the hydrophobic motif site, which allows S6K to be further phosphorylated by PDK1. The activated S6K, in turn, phosphorylates 40S ribosomal protein S6 and eIF4B, which contributes to the association of eIF4B with the translation preinitiation complex (Holz et al., 2005). In addition to its role in translation initiation, S6K has been shown to phosphorylate the eukaryotic

elongation factor 2 (eEF2) kinase which is associated with stimulation of peptide chain elongation (Wang and Klionsky, 2003). TORC1 is also thought to regulate translation of a specific group of mRNAs containing 5'-terminal oligopyrimidine (5'-TOP) tracts in an S6K-independent manner (Patursky-Polischuk et al., 2009; Pende et al., 2004). These transcripts encode ribosomal proteins and translation elongation factors, thereby providing a translational control-based mechanism to regulate ribosome biogenesis. Combining these various activities, TORC1 controls the rate of protein production in three ways: by controlling the rate of initiation of mRNA translation and the rate of elongation of the nascent polypeptides and indirectly by controlling translation of ribosomal proteins (Hietakangas and Cohen, 2009).

1.2.7 - Regulation of ribosome biogenesis by TORC1

Ribosomes are the molecular machines that translate mRNA into protein, and consist of two subunits. Each subunit is a complex of ribosomal RNA (rRNA) and core ribosomal proteins. The mammalian ribosome is composed of a 40S small ribosomal subunit, which is made up of 33 proteins as well as the 18S rRNA, and a 60S large ribosomal subunit, a complex of 47 proteins and the 28S, 5.8S and 5S rRNA (Wool, 1996). In addition to its role in regulation of translational initiation and elongation, TORC1 also regulates transcription. In yeast, several transcriptional downstream effectors of TOR have been identified (Rohde et al., 2008). The transcriptional program downstream of TORC1 has a role in controlling the production of ribosomes and consequently the cellular biosynthetic capacity. This ensures maintenance of balance between the rate of translation and the amount of ribosomes available. There is emerging evidence from multiple experimental systems that the regulation of ribosome biogenesis is a major contributor to TOR-mediated regulation of tissue growth (Wullschleger et al., 2006).

In *Drosophila* cells, the majority of TORC1-regulated genes are involved in various aspects of ribosome biogenesis, and many of these genes have a role in promoting cell growth (Guertin et al., 2006). For instance, a majority of TORC1-regulated genes appear to be targets of *dMyc*, the *Drosophila* ortholog of the oncogene *c-Myc* (Teleman et al., 2008). Inhibition of TORC1 activity leads to a rapid downregulation of *dMyc* expression,

leading to a perturbation of ribosome biogenesis machinery which provides an explanation for the TORC1-regulated transcriptional program in *Drosophila*. Therefore, Myc activity is essential for TORC1-mediated tissue growth (Hietakangas and Cohen, 2009).

Myc overexpression in mice can induce the transcription of multiple genes involved in ribosome synthesis (Kim et al., 2000). The *Drosophila melanogaster* genes *minifly* and *pitchoune* have been found to be required for ribosomal RNA (rRNA) processing and are also important for growth (Giordano et al., 1999; Zaffran et al., 1998). Notably, *pitchoune* appears to be a target of *Myc* in flies (Zaffran et al., 1998). Therefore, concisely proposed that ribosome biogenesis is mediated through TORC1 and TORC1-regulated target genes.

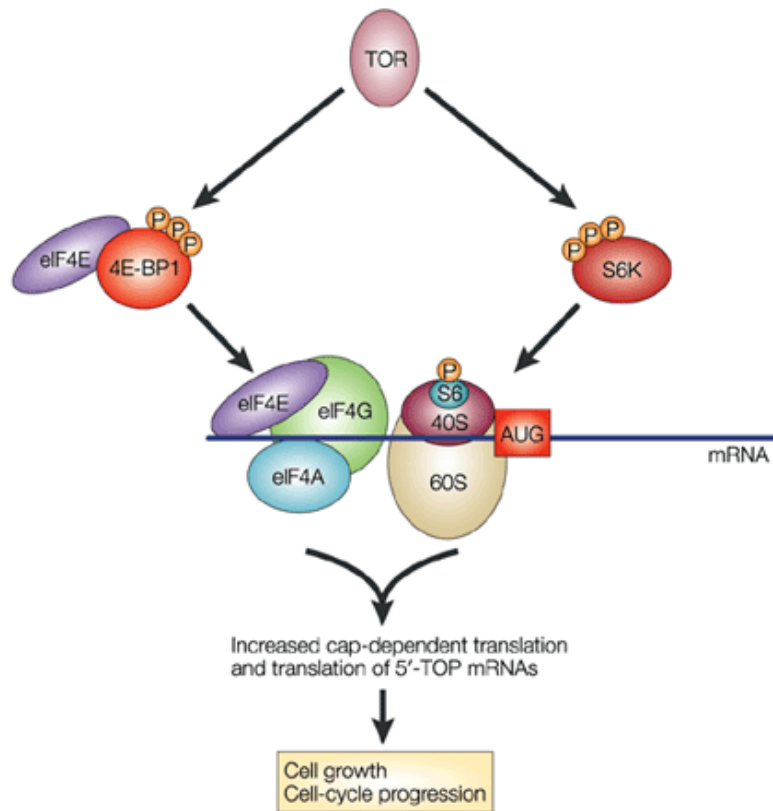


Figure 4 - Regulation of cell growth and cell cycle progression by TOR

TORC1 promotes cap dependent translation by activating S6K and inhibiting 4E-BP. This regulation promotes bulk protein biosynthesis and subsequent cell growth. (From Tee and Blenis, 2005).

1.2.8 - TOR and regulation of autophagy

For the continuity of normal development of an organism, a constant supply of nutrients is required to provide energy necessary for growth and metabolism. To achieve this, eukaryotic cells have evolved a variety of mechanisms to adjust their metabolic activities in response to changes in nutrient levels. Under starvation conditions, energy demanding functions such as protein synthesis and cell cycle progression are rapidly suppressed; and patterns of gene expression, protein stability, and nutrient uptake are adjusted so that cell physiology and metabolism match the supply and quality of nutrients (Scott et al., 2004).

Central among the responses to nutrient deprivation is autophagy which is a cellular process of bulk degradation of organelles and cytoplasmic contents upon starvation and/or the process of recycling of these structures (Mizushima et al., 2002; Wang and Klionsky, 2003). The process of autophagy involves the encapsulation of the material to be degraded in double membrane vesicles named ‘autophagosomes’ which fuse with the lytic vacuole (yeast) or with lysosomes (Stromhaug and Klionsky, 2001). The resulting breakdown products can be an essential source of nutrients under starvation conditions, as the mutations in many of the approximately 20 *ATG* genes required for autophagy in *S. cerevisiae* cause lethality under starvation conditions (Klionsky et al., 2003). Furthermore, in yeast, TOR is thought to control the autophagic machinery in part by regulating the activity of a complex containing the serine-threonine kinase Atg1 and by regulating expression of *ATG8* (Kamada et al., 2000; Kirisako et al., 1999). Autophagy also plays an important housekeeping role in turnover of damaged organelles, in cellular remodelling during development, and in some types of programmed cell death (Levine and Klionsky, 2004). Many of the cellular processes to changes in nutrient levels, including autophagy are regulated by TOR (Fig. 5). Inactivation of *TOR* by mutation or by treatment with the drug rapamycin induces autophagy despite the presence of ample nutrients indicates that TOR acts to suppress autophagy under non-starvation conditions (Jacinto and Hall, 2003; Noda and Ohsumi, 1998; Scott et al., 2004). It has been also shown in mammalian system that the mTOR is likely to be involved in the regulation of autophagy (Dennis et al., 1999). In higher eukaryotes, starvation-induced autophagy is also suppressed by components of the Insulin/PI3K pathway upstream of the TOR (Melendez et al., 2003).

Apart from their role in suppressing autophagy, the insulin/PI3K and TOR pathways are well established as potent oncogenic activators of cell growth (Kozma and Thomas, 2002). As the growth rate of a cell reflects the balance between anabolic processes (protein synthesis) and catabolic processes (protein degradation), therefore, this raised the possibility that TOR may regulate growth in part through suppression of autophagy (Fig. 5). In *Drosophila*, in late larval stages and during metamorphosis, cytoplasmic contents within the fat body are degraded by autophagy (Rusten et al., 2004). Scott et al. provided a genetic evidence that under conditioning of low TOR signaling, autophagy functions primarily to promote normal cell functioning and survival, rather than to suppress cell growth (Scott et al., 2004). Thus in a variety of signaling and developmental contexts, TOR acts as a negative regulator of autophagy and promotes protein synthesis and growth as long as there is a provision of nutrients (Schmelzle and Hall, 2000). These findings also suggest that autophagy is a default mechanism that requires permanent active repression by a TOR dependent mechanism if the cell is to grow in the absence of nutrients.

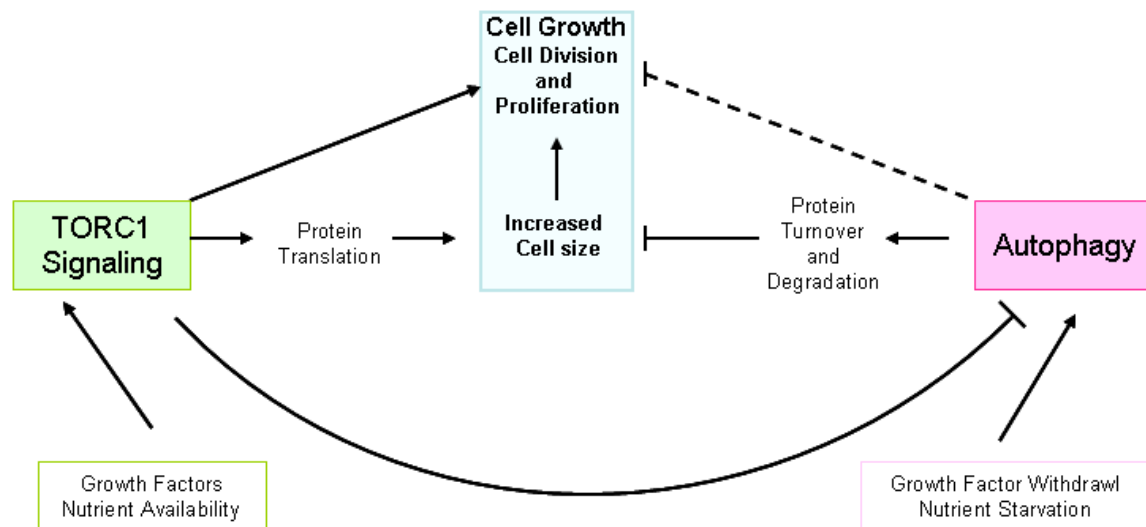


Figure 5 - Interrelations between TOR signaling, autophagy and cell growth

TORC1 signaling promotes cell growth through its effects both on increasing cell proliferation and increasing cell size, and also through its inhibitory effects on autophagy. TORC1 increases protein synthesis and cell size through intermediates such as 4E-BP and S6K. In contrast, autophagy is believed to inhibit cell growth at least in part by promoting protein organelle turnover. Note that the presence of growth factors and nutrients are all required for the full activation of TORC1 signaling, whereas the absence of any of these factors is sufficient to induce autophagy. (drawn from Wang and Levine, 2010).

1.2.9 - Metabolic functions of TOR signaling

The target of rapamycin (TOR) signaling pathway responds to cellular levels of amino acids and ATP through its upstream effectors, the tuberous sclerosis complex (TSC1 & TSC2) and Rheb GTPase. Insulin/TOR signaling pathway directs critical changes in cellular physiology that link growth, translation, and autophagy to the nutrient status of the animal (Edgar, 2006; Hay and Sonenberg, 2004). For example, TOR kinase is active in the presence of sufficient nutrients, phosphorylating S6 kinase (S6K), regulating protein synthesis and hence facilitates growth (Hietakangas and Cohen, 2009). In addition, Akt mediated phosphorylation of a key transcriptional effector of insulin signaling, dFOXO, renders it inactive by restricting it to the cytoplasm (Baker and Thummel, 2007). In contrast, TOR activity is reduced under starvation conditions, leading to a decreased translational capacity. The non-phosphorylated dFOXO translocates into the nucleus, triggering a transcriptional program that includes the upregulation of 4E-BP, which controls lipid mobilization (Teleman et al., 2005a). Furthermore, a hypomorphic *dTOR* allele has been described with reduced fat body lipid levels and increased β -hydroxybutyrate levels, indicating an increased conversion of lipids into ketone bodies and reduced glucose levels. These findings provide a new genetic system to better characterize the effects of TOR signaling on the energy metabolism (Luong et al., 2006).

Although amino acid levels are known to modulate TOR activity, the mechanisms that underlie this response remain poorly understood. Genetic characterization of the *Slimfast* amino acid transporter has provided some initial clues into this pathway, indicating that it functions as a nutrient sensor in the larval fat body and controlling a systemic response which links amino acid levels with organismal growth. The observation that fat body specific inactivation of either *slimfast* or *dTOR* leads to similar phenotypes supports the notion that Slimfast can signal through dTOR in the fat body to globally regulate growth and metabolism in response to amino acid levels. This fat body amino acid sensor pathway can override insulin signaling in peripheral tissues through inhibition of PI3K activity, apparently through one or more unidentified factors that emanate from the fat body (Colombani et al., 2003).

1.2.9.1 - *Drosophila* as a system for studies of lipid metabolism

The mammalian genome is thought to have been duplicated two times which in some cases makes phenotypic characterization of a specific gene deficiency difficult (Miklos and Rubin, 1996). Therefore, in some instances it is more attractive to study gene function in less complex organisms, such as *Drosophila melanogaster*, in which individual genes are usually represented in a single copy. Additionally, the mammalian signaling pathways are largely conserved in *Drosophila* which offers a powerful genetic system and thereby, provides a unique opportunity to uncover critical new insights into the central regulatory pathways that are conserved through evolution. Therefore, the past few years have seen a shift in direction, in which *Drosophila* is being increasingly exploited to understand the regulatory mechanisms of metabolism (Beller et al., 2008). Furthermore, the *Drosophila* genetic system has been implicated also in the better understanding and the treatment of human disease risk factors, such as diabetes and obesity (Baker and Thummel, 2007). Indeed, even the relatively few *Drosophila* data in literature described, have changed our understanding of vertebrate metabolic control. For example, contrary to studies in mammalian cell culture, 4E-BP regulates organismal lipid homeostasis rather than growth (Teleman et al., 2005a). Similarly, the discovery of evolutionarily conserved essential regulators of lipid metabolism in *Drosophila*, such as *melted* and *adipose*, provide new directions for understanding the control of these pathways in humans and also raise the possibility that mutations in these genes may be risk factors for human metabolic disorders (Teleman et al., 2005b). Therefore, growing studies and research work have been emerged in which *Drosophila* has been constantly embarked as a model system for the study of lipid metabolism (Baker and Thummel, 2007; Beller et al., 2008; Farese and Walther, 2009; DiAngelo and Birnbaum, 2009; Beller et al., 2010).

Lipid metabolism is essential for growth and generates much of the energy needed for normal developmental process as well as during periods of food deprivation. The larvae of *Drosophila* have been used extensively to study for regulation of growth and lipid metabolism (Colombani et al., 2003). The bulk of the *Drosophila* larva is made up of endoreplicating tissues (ERTs) that are histolyzed during the pupal phase to support metamorphosis. During metamorphosis, mitotic tissues known as imaginal discs are

recognized into the adult fly. In insects and particularly in *Drosophila*, lipids are stored in a specialized tissue that resembles the adipose tissue of mammals, the fat body. The fat body is an ERT, which is particularly sensitive to nutrients and alters its morphology dramatically in response to amino acid starvation (Britton and Edgar, 1998). Several earlier observations have suggested that the fat body can modulate the growth of other tissues according to nutrient levels. The experiments described by Colombani et al. reinforced the idea that the fat body of *Drosophila* can act as a nutrient sensor that influences the growth of other tissues. In contrast, the growth of the mitotic imaginal discs is less impaired. The diet-derived lipids, exported from the midgut as lipoproteins, are taken up from the hemolymph by the fat body via a mechanism involving low-density lipoprotein (LDL) receptor-like molecules called lipophorin receptors. These lipids accumulate in fat body cells in the form of intracellular droplets but, when larvae are food deprived, there is a net efflux of lipid into the hemolymph. The mobilization process is regulated by TSC/TOR signaling and a nutrient sensor in the fat body that monitors amino-acid levels via the Slimfast (Slif) amino-acid channel (Colombani et al., 2003). Starvation induced fat release is accompanied by increased lipolysis, at least in part associated with upregulation of Brummer, an ATGL (Adipose Triglyceride Lipase) related lipase localized to lipid droplets. Fat mobilization is also influenced by LSD2 (lipid storage droplet-2), a lipid droplet protein related to a mammalian negative regulator of TAG (Triglycerides) hydrolysis called PERILIPIN. In addition to its involvement in lipid storage and release, the fat body produces a humoral signal regulating larval tissue growth in response to food availability. In addition, *Drosophila* maintains appropriate circulating sugar levels, compensating for changing environmental conditions and storing excess energy in the forms of glycogen and lipid. These reserves are mobilized during periods of energy need, such as nutrient depletion (Rusten et al., 2004; Scott et al., 2004). Many of the analogous organ systems that control nutrient uptake, storage, and metabolism in humans are present in the fruit fly. Digestion and nutrient absorption occur in the *Drosophila* midgut, the functional equivalent of the stomach and intestine. The fat body acts like the mammalian liver and white adipose tissue, metabolizing nutrients and storing large reserves as stores. Hence, the central pathways of intermediary metabolism and regulators of homeostasis are present in the fly which demonstrates that most of the essential metabolic functions have been conserved

through evolution (Baker and Thummel, 2007). In nutshell, based on functional analogy and the powerful genetic system, *Drosophila* could serve as a good model for metabolic studies.

1.2.9.2 - Structure of a lipid droplet

The earliest descriptions of lipid droplets date to the 19th century. The identification through light microscopy and the speculation of their origin gave an importance to lipid droplets and in the meantime a respectable name was given to these organelles: liposome (Farese and Walther, 2009). However, in the late 1960s, the organelles were called by many names, including lipid droplets, lipid bodies, fat bodies fat droplets, and adiposomes. In plants, they are often called oil bodies. As the field continuously rapidly evolved, it seemed to be settling on the name “lipid droplets” (LDs) (Martin and Parton, 2006; Farese and Walther, 2009).

These universal organelles are found in most eukaryotic cells and range greatly in size (< 1–100 μm); the diameter varies tremendously depending on the cell type (Murphy, 2001; Farese and Walther, 2009). However their structure appears to be fairly consistent and each consists of a phospholipid monolayer that surrounds a core of neutral lipids, such as sterol esters or triacylglycerols (Fig. 6). Numerous proteins, many of which play functional roles in LD biology, decorate their surfaces (Farese and Walther, 2009; Goodman, 2008; Beller et al., 2006; Cermelli et al., 2006). The mechanism of LD formation is uncertain; the prevailing model posits that LDs form at the ER, where the enzymes that catalyze neutral lipid synthesis are located. Eventually, the growing oil droplet buds from the ER membrane, forming a detached cytosolic LD, or stays in contact with the ER membrane and forms a specialized LD and ER domain (Farese and Walther, 2009; Martin and Parton, 2006). The ability to isolate LDs to high purity, together with the modern techniques of proteomics, has allowed an elucidation of the LD proteome under different experimental conditions. This has yielded maps of the ‘housekeeping’ proteins of LDs, as well as unexpected insights into their possible interactions with other organelles. Among the several proteins that have been identified on LDs, are intimately linked to vesicular transport, membrane fusion and cytoskeletal

motility (Beller et al., 2006; Cermelli et al., 2006; Martin and Parton, 2006). Some of the best-understood LD components are members of the PAT-domain (Perilipin, ADRP and TIP47-related protein domain) family of proteins (Farese and Walther, 2009; Tansey et al., 2004). The term PAT domain refers to a region of sequence similarity that is present in the founding members of this family: perilipin, adipose differentiation-related protein (ADRP; also called adipophilin) and tail-interacting protein of 47 kDa (TIP47). PAT domain proteins including LSD2 (lipid storage droplet-2) are evolutionarily conserved with homologs in both *Dictyostelium discoideum* and *D. melanogaster* (Miura et al., 2002). Adipophilin is a ubiquitously expressed protein in all mammalian cell types and found only in lipid droplets (Brasaemle et al., 1997; Heid et al., 1998). Perilipin, a structurally related protein, associates with lipid droplets in adipocytes and steroidogenic cells (Greenberg et al., 1991). In these cells, it restricts the access of hormone-sensitive lipase and other cytosolic lipases to the lipid droplet under basal conditions and facilitates lipase access to the droplet under lipolytically stimulating conditions (Brasaemle et al., 2000). The first genetic study of an essential enzyme in lipolysis, the ATGL (Adipose Triglyceride Lipase) homolog Brummer, foreshadowed genetic studies of its vertebrate counterpart in mice (Gronke et al., 2005; Haemmerle et al., 2006). Furthermore, Rusten et al. investigated the starvation induced autophagy at deferent developmental stages in the fat body of *Drosophila*. The larvae fed on amino acid-deficient food display a quick starvation-induced response in the fat body, leading to the aggregation of the storage vesicles, the lipid droplets (LDs) (Rusten et al., 2004). Therefore, LDs are being used for the study of metabolism studies as a quick tool. The phenotype of these vesicles can be traced out easily and, hence, has been retained to study a gene function in *Drosophila* (Britton et al., 2002; Colombani et al., 2003; Zhang et al., 2000; Beller et al., 2008; Farese and Walther, 2009; DiAngelo and Birnbaum, 2009; Beller et al., 2010).

1.3 - S6 Kinase

1.3.1 - Ribosomal protein S6 phosphorylation

As described earlier, higher eukaryotic ribosomes consist of two subunits designated as 40S (small) and 60S (large) subunits. The 40S subunit comprises a single molecule of RNA, termed 18S rRNA, and 33 proteins; by contrast, the 60S subunit has three RNA molecules, termed 5S, 5.8S and 28S rRNA, and 47 proteins (Wool, 1996). It was discovered in 1970s that the 30 kDa ribosomal protein S6 became phosphorylated in the liver of partially hepatectomized rats (Gressner and Wool, 1974). Following partial hepatectomy, the remaining hepatocytes re-enter the cell cycle and proliferate to regenerate the liver. In the same organ, *in vivo* S6 phosphorylation was induced after refeeding starved rats. Starvation induces hepatic autophagy and atrophy, which was reversed upon refeeding (Kozma et al., 1989). In addition, a variety of hormones and growth factors have been reported to induce S6 phosphorylation. Thus S6 phosphorylation appears to correlate with increased rates of protein synthesis and hence cell growth. It has been also described that protein phosphorylation can modify enzymatic activity or create a binding site for other proteins, so it has been speculated that S6 phosphorylation may serve to increase translation rates when cells are to grow (Stewart and Thomas, 1994). In support of this notion, S6 is positioned in the small head region of the 40S ribosomal subunit at the interface with the 60S subunit. There, S6 is thought to contact mRNA and the 28S rRNA directly (Nygard and Nilsson, 1990).

Subsequent analysis revealed that S6 became phosphorylated at multiple sites in an ordered fashion. The mammalian S6 phosphorylation sites were identified as Ser₂₃₅, Ser₂₃₆, Ser₂₄₀, Ser₂₄₄ and Ser₂₄₇ all located in the carboxyl-terminal region (Bandi et al., 1993; Volarevic and Thomas, 2001). The ribosomal protein S6, including its phosphorylation sites, is highly conserved among vertebrates (Meyuhas, 2008). In fact, five phosphorylation sites in the carboxyl-terminus of *Drosophila* S6 (dS6) have been identified (Volarevic and Thomas, 2001; Radimerski et al., 2000). Furthermore, the *S. cerevisiae* and *S. pombe* orthologue, ribosomal, protein S10, also contains two phosphorylation sites (Johnson and Warner, 1987). Thus ribosomal protein phosphorylation appears to be conserved from yeast to man (Fig. 7), suggesting that it

has been implicated for its function in translational control. Of all ribosomal proteins, it is the ribosomal protein S6 (RPS6) that has attracted much attention, since it is the first, and was for many years the only one that has been shown to undergo inducible phosphorylation. It is only recently that the role of RPS6 and its post-translational modification has been started being disclosed by genetic targeting of the *RPS6* gene and of the respective kinases (Meyuhas, 2008). However it must be emphasized that direct evidence for regulation of protein synthesis by S6 phosphorylation needs further investigations.

1.3.2 - Identification of the S6K1

Keeping in view that ribosomal protein S6 phosphorylation correlates with increased translation and growth, efforts started focusing on the identification of *in vivo* S6 kinase in order to understand the molecular signaling pathway that communicate extra-cellular stimuli to the ribosome (Meyuhas, 2008). Although a number of kinases were initially implicated in S6 phosphorylation based on *in vitro* activities; it has been generally accepted that the S6K family of kinases mediates this response (Volarevic and Thomas, 2001). S6K (S6 kinase) is a protein kinase belonging to the AGC (protein kinase A/ protein kinase G/ protein kinase C) kinase family and a key regulator of protein synthesis (Jacinto and Lorberg, 2008). Characterization of an S6 kinase at a molecular level was first described in *Xenopus* oocytes wherein a dominant form of S6 kinase detected after mitogen stimulation, had been purified as a 90-kDa polypeptide (Erikson and Maller, 1985), later termed as p90 ribosomal protein S6 kinase (p^{90RSK}). Purification of the avian and mammalian RPS6 recovered 65-70 kDa polypeptides that are currently referred to as S6K (Meyuhas, 2008).

Mammalian cells contain two forms of S6K, S6K1 & S6K2 (Fig. 8), which is encoded by two different genes and shares a very high level of overall sequence homology. S6K1 has cytosolic and nuclear isoforms (p^{70S6K1} and p^{85S6K1}, respectively), whereas both S6K2 isoforms (p^{54S6K2} & p^{56S6K2}) are primarily nuclear, and partly associated with the centrosome (Rossi et al., 2007; Meyuhas, 2008)). Analysis of RPS6 phosphorylation in mouse cells deficient in either *S6K1* or *S6K2* suggested that both are required for full S6

phosphorylation, with the predominance of *S6K2* (Pende et al., 2004). Notably, the phosphorylation of the evolutionary conserved sites of *Drosophila* RPS6 has been carried out by dS6K that is encoded by a single gene (Fig. 8) (Watson et al., 1996).

The S6 kinase signaling pathway, which in many cell types, is triggered by the recruitment of phosphatidylinositide-3OH kinase (PI3K) to the activated receptor and the production of phosphatidylinositol-3,4,5-trisphosphate (PIP3). The mechanism by which kinase activation is presumed to take place has been elucidated by the dissection of the primary structure of S6Kl into domains and to the identification of specific regulatory phosphorylation sites (Volarevic et al., 2000). There are five distinct domains that cooperate to bring about S6 kinase activation. The first is an acidic domain that extends from the short amino-terminus to the beginning of the catalytic domain and confers rapamycin sensitivity on the kinase (Dennis et al., 1996). The second is the catalytic domain, which contains the mitogen-induced phosphorylation site T₂₂₉, residing within the activation loop. The catalytic domain, and sequence immediately after the amino terminal to the T₂₂₉ phosphorylation site are highly conserved in the protein A, protein G, and protein C (AGC) family of protein kinases. The third domain is the linker domain, which connects the catalytic domain to the autoinhibitory domain (Pullen and Thomas, 1997). The linker domain is also highly conserved in the AGC family of serine threonine kinases and contains two phosphorylation sites, S₃₇₁ and T₃₈₉, which are essential for S6Kl activation (Pearson et al., 1995). Immediately, downstream of the auto-inhibitory domain is the amino terminus, which has been implicated in the interaction of the kinase with other proteins (Burnett et al., 1998).

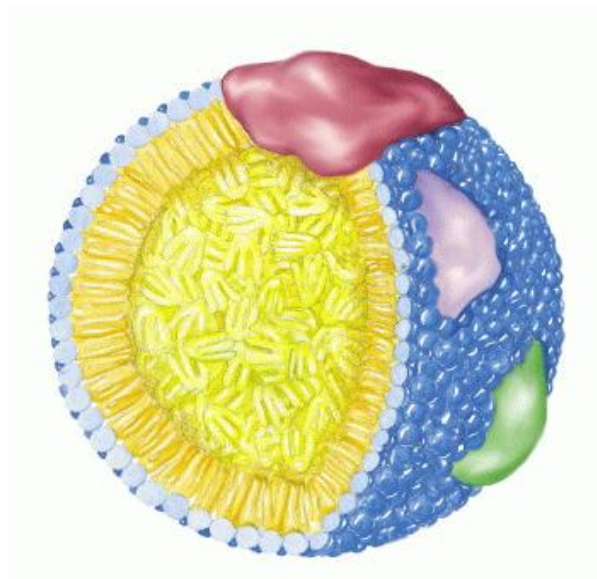


Figure 6 - Structure of a lipid droplet

Lipid droplets are the lipid storage organelles of all organisms, and share a simple, stereotyped structure of a hydrophobic core built of the storage lipids (triacylglycerols), surrounded by a phospholipid monolayer to which numerous proteins are attached (From Beller et al., 2006).

<u>Organism (Species)</u>	<u>Sequence (phosphorylated Serine residues)</u>
<i>Saccharomyces cerevisiae</i>	AEKAEIRKRRASSLKA ²³⁶
<i>Saccharomyces pombe</i>	KREVVKARRASSLKK ²³⁹
<i>Drosophila melanogaster</i>	RRRSASIRESKSSVSSDKK ²⁴⁸
<i>Oncorhynchus mykiss</i>	RRLSSLRASTSKSESSQK ²⁴⁹
<i>Oncorhynchus mykiss</i>	RRLSSLRASTSKSESSQK ²⁴⁹
<i>Rattus norvegicus</i>	RRLSSLRASTSKSESSQK ²⁴⁹
<i>Mus musculus</i>	RRLSSLRASTSKSESSQK ²⁴⁹
<i>Xenopus laevis</i>	RRLSSLRASTSKSESSQK ²⁴⁹
<i>Homo sapiens</i>	RRLSSLRASTSKSESSQK ²⁴⁹

Figure 7 - Comparison of carboxy-terminal domain of ribosomal protein S6

Carboxy-terminal domain of ribosomal protein S6 along with the phosphorylation sites in different species are shown (From Meyuhas, 2008; Volarevic and Thomas, 2001).

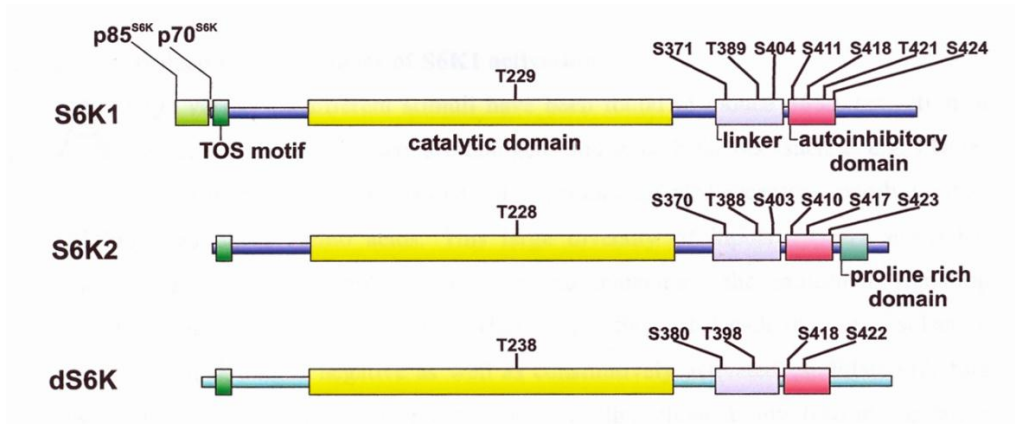


Figure 8 - The domain structure of S6K1, S6K2 and the dS6K

S6K1 exists in two isoforms, p70^{S6K} and p85^{S6K} which are generated from alternative translation start sites within the same transcript. Different domains of S6K: TOS-motif (green box), linker domain (purple box) and the auto-inhibitory domain (red box) are shown. Note that S6K2 contains a unique proline-rich sequence in its carboxyl-terminus. The conserved regulatory phosphorylation sites are also indicated (From Radimerski, 2002).

1.3.3 - Activation of S6K

The basic mechanism of the kinase activation was preceded by the identification of the signaling components that mediate S6K1 activation. Activation of S6K1 requires phosphorylation of four S/T-P sites, which reside in the auto-inhibitory domain (Dennis et al., 1998). This event, in combination with phosphorylation of S₃₇₁ in the linker domain, facilitates T₃₈₉ phosphorylation, which also resides in the linker domain, and provides a docking site for the phosphoinositide-dependent protein kinase, (PDK1) (Biondi et al., 2001). PDK1 docks on T₃₈₉ and phosphorylates T₂₂₉ in the activation loop of the kinase, leading to kinase activation (Fig. 9). The critical event then in activating S6K is phosphorylation of T₃₈₉ (Dennis et al., 1998). A number of kinases have been suggested as potential T₃₈₉ kinases, including protein kinase B and PDK1 (Burgering and Coffey, 1995; Balendran et al., 1999). However, it has been found that the mammalian target of rapamycin, mTOR, is a potent T₃₈₉ kinase (Dennis et al., 1998). As already discussed in detail, mTOR is a member of the PI3K related family of protein kinases, acts as an amino acid and energy effector. If either amino acids, especially branch-chain amino acids, or ATP levels drop, mTOR activity decreases leading to inhibition of S6K1 (Dennis et al., 2001) The phosphorylation sites and the domain structure are well conserved in drosophila S6 kinase (Stewart et al., 1996; Watson et al., 1996).

The protein phosphatase 2A (PP2A), a conserved component of the insulin pathway in flies and in mammals, dephosphorylates S6K. *PP2A* knockout flies showed elevated S6K phosphorylation, thereby making an activation of S6K. In addition, the B' subunit of protein phosphatase 2A (PP2A-B') interacts with S6K (Hahn et al., 2010). Downstream of S6K, there are alleles of the kinase which are either rapamycin resistant or dominant interfering has provided evidence that the kinase regulates the expression of a family of mRNAs at the translational level (Fumagalli, 2000). This family is small, may be representing one to two hundred gene products. However, they can account for up to 20-30% of the mRNA in the cell and they largely encode for the components of translational apparatus, particularly of ribosomal proteins (Meyuhas, 2008).

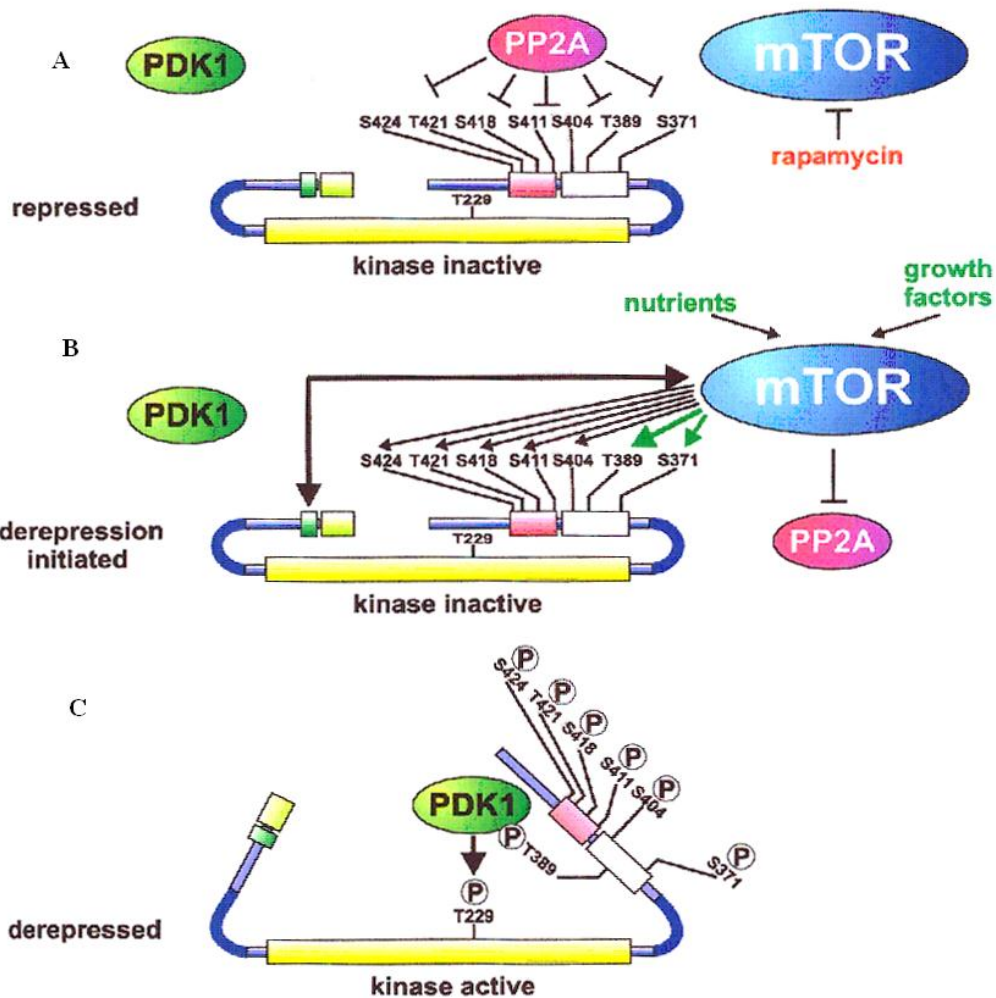


Figure 9 - Model of S6K1 activation

S6K1 remains repressed in an inactive conformation in the absence of stimuli. The protein phosphatase PP2A has been implicated in binding to and inactivating S6K1 (A). Growth factors and nutrients are thought to induce m-TOR-mediated phosphorylation of S6K1 (B). In a first step, it is thought that the Ser/Thr-Pro sites in the autoinhibitory domain become phosphorylated. Phosphorylation of the sites in the autoinhibitory domain is thought to facilitate mTOR-mediated phosphorylation of key regulatory sites within the linker domain (Ser₃₇₁ and Thr₃₈₉), leading to a depressed kinase conformation. Finally, PDK1 docks onto S6K1 phosphorylated at Thr₃₈₉ and activates the kinase by inducing phosphorylation at the activation loop site (Thr₂₂₉) in the catalytic domain (C) (From Radimerski, 2002).

1.3.4 - An overview of S6K function

1.3.4.1 - *S6K1* deletion in the mouse

The physiological importance of S6K1 in mammalian cells has been largely addressed in tissue culture model systems. However, in order to obtain a corroborative *in vivo* data in animal to support and elicit a role of S6K1 in cell growth, initial studies employed micro-injection of neutralizing antibodies against S6K1 in rat embryonic fibroblast cells. These studies suggested that the kinase was essential for G1 phase progression and entry into the S-phase (Lane, 1993). Contrary to this, the disruption of *S6K1* in the embryo stem (ES) cells showed a reduction in the proliferation rate as compared to the parental cells. This study suggested that *S6K1* had a positive effect on proliferation but not essential. The translation rates of 5'TOP mRNAs in *S6K1* null ES cells, which lack S6K phosphorylation, did not change significantly in the presence or absence of serum, and the percentage of mRNAs recruited in the polysome fraction was intermediate compared to the control cells. Furthermore, the overall protein synthesis was repressed to similar extents by rapamycin treatment in both *S6K1* null and wild type ES cells, while 5'TOP mRNA translation was only mildly affected in the former cells. Thus, in the absence of S6K1, the translational control of 5'TOP mRNAs was deregulated possibly by a compensatory mechanism that could involve the down-regulation of a putative repressor protein that normally binds 5'TOP mRNA (Kawasome et al., 1998).

In 1998, Shima et al. reported *S6K1* knockout mice with small size phenotype which was particularly pronounced during embryogenesis (Shima et al., 1998). The proliferation of *S6K1* null mouse embryonic fibroblast (MEFs) in culture was intact as well as the regulation of 5'TOP mRNA translation which is in contradiction to the findings of Kawasome et al. It would be noteworthy that following starvation and refeeding, the induction of S6 phosphorylation in the liver was normal. This suggested that a distinct rapamycin sensitive kinase is the physiological S6 kinase, or possibly that it functions in a redundant manner in the absence of S6K1. The *S6K1* homolog termed as *S6K2* was upregulated in all the tissues examined of the *S6K1* null mice and it was revealed that S6K2 was capable to phosphorylate the ribosomal protein S6. The catalytic and regulatory domains as well as the regulatory phosphorylation sites are conserved between S6K1 and S6K2 (Shima et al., 1998). However, S6K2 contains a proline rich

region (Fig. 8) in the carboxyl-terminal tail and is less sensitive to inhibition by rapamycin compared to S6K1 (Gout et al., 1998; Saitoh et al., 1998). The presence and upregulation of *S6K2* may obscure and compensate some functions of *S6K1* and also the characterization of the *S6K1* and *S6K2* double knockout mouse is anticipated. In spite of the apparent normal S6 phosphorylation and the regulation of 5'TOP mRNA translation in mice lacking *S6K1*, the small mouse phenotype indicates that *S6K2* cannot compensate for all the functions of *S6K1*.

Hence, S6K is an evolutionary conserved determinant of growth through increased protein biosynthesis. The downstream target of S6K, the 40S ribosomal protein S6 has been thought to regulate the translation of 5'TOP mRNAs which encode proteins important for translational machinery. However, many reports questioned this model since S6 phosphorylation and translation of 5'TOP mRNAs are not correlated (Pende et al., 2004). Furthermore, S6 phosphorylation is not affected in *S6K1*^{-/-} mice, even though these mice have a reduction in size compared to wild type. In addition, the protein S6 was also phosphorylated in an *S6K1*^{-/-} and *S6K2*^{-/-} double mutant mouse (Pende et al., 2004). This suggested that S6 might be phosphorylated by other kinases. Moreover, in *C. elegans*, *rsks-1* (S6K homolog) could possibly affect growth through regulation of ribosome biosynthesis (Friberg, 2006). Future studies will shed light on the regulation of ribosome biosynthesis and protein levels and also the biochemical function of S6K in more detail for the overall scenario of the regulation of cell growth.

1.3.4.2 - dS6K and the regulation of growth

The *Drosophila* genome contains a single *S6K* gene, termed as *dS6K*, which is highly homologous to mammalian *S6K1* and *S6K2*. The dS6K protein has an overall identity of 57% with either *S6K1* or *S6K2* and 78% identity in the catalytic domain. The organization of functional domains and key phosphorylation sites is also conserved between the two enzymes. In addition, it has been proposed that upstream elements and downstream effectors of S6K are conserved in mammals and flies (Stewart et al., 1996; Watson et al., 1996). The two *S6K* homolog which are actually expressed in mammals could overlap in their individual function (Shima et al., 1998). This functionality, hence,

represents an enormous challenge to unravel the role of S6K signaling pathway in a simpler genetically amenable model organism, such as *Drosophila*. In *Drosophila*, the dS6K activity is sensitive to rapamycin *in vivo* and the kinase readily phosphorylates 40S ribosomal subunit protein S6 *in vitro*. Also the growth factor treatment of *Drosophila* cells in culture induces S6 phosphorylation in an ordered fashion on five carboxyl-terminal residues (Stewart et al., 1996; Radimerski et al., 2000).

It has been known in enormous literature, the mammalian signaling pathways are largely conserved in *Drosophila* which offers its powerful genetic system to uncover novel components in signaling cascades. Therefore, to elucidate the cell growth functioning of *dS6K*, Montagne et al., did a pioneer work and identified a P-element insertion in the 5' non-coding region of the *dS6K* gene. They described that this mutation led to the strongly reduced female fertility and a developmental delay of about 3-days. Furthermore, only 25% of the expected number of homozygous flies emerged as adults. As the P-element insertion did not completely abolish *dS6K* transcription, null alleles were generated by imprecise excision of the transposable element. The homozygotes with a *dS6K* null mutation (*dS6K^{1/1}*) displayed a strong developmental delay of 5-days and were reduced in overall body size (Fig. 10). Montagne et al. noticed that the reduced size-phenotype also comprised of female sterility, inability to fly and reduced adult life-span. Most importantly, they suggested that the flies lacking *dS6K* were reduced in overall body size due to smaller but not less cells. Moreover, the cell cycle phasing (G1/G2 distribution) in flies lacking *dS6K* was normal. However, the cells appeared to proliferate at a reduced rate and divided at a smaller size. Furthermore, analysis of the developing wing disc revealed that the effect on cell size was displayed throughout development (Montagne et al., 1999).

As described above elsewhere, S6K is implicated in the regulation of translational components that make up the protein synthetic apparatus. The *dS6K* mutants were speculated to mimic ribosomal protein mutants, termed Minutes, a name derived from the strong reduction in bristle size (Lambertsson, 1998). *Minutes* are classified as recessive lethal mutations in ribosomal protein genes, which lead to dominant phenotypes in heterozygotes. The resulting phenotype includes a delay in development as well as short and slender bristles despite of normal overall body size. As bristle

formation requires strong protein synthesis, bristle size can be viewed as a marker for translational capacity of the cell that generates it. Interestingly, the *dS6K* mutant phenotype was quite distinct from that of *Minutes*. Both of the mutations displayed a delay in development and comprised of reduced ribosome content. However, the *dS6K* mutants did not exhibit a strong reduction in bristle size (Montagne et al., 1999). The phenotypical differences compared to *Minutes* were rather inconsistent with *dS6K* solely regulating ribosome production. This is to mention that the absence of *dS6K*, possibly due to lack of S6 phosphorylation affects both the ribosome biogenesis and the individual phase of translation. Given the relatively strong phenotype of *dS6K* null flies, it was surprising that targeted overexpression of *dS6K* in various tissues using the Gal4-UAS system did not induce any obvious phenotype except in the dorsal wing compartment when transgene expression was driven with *apterous*-Gal4 (*ap-Gal4*; the *apterous* promoter is restricted to the dorsal compartment of the wing). The *ap-Gal4* directed UAS-*dS6K* expression forces the wing to bend downwards as the dorsal and ventral epithelial sheaths form the adult wing, suggesting that the expression of an extra copy of the *dS6K* gene in the dorsal compartment of the wing caused only those cells to grow larger and not the cells in the ventral compartment. Although the resulted phenotype due to *dS6K* overexpression was very impressive; however, it should be pointed-out that very subtle changes in cell growth could account for the bending down of the wing. In fact, less than 1% increase in the size of the dorsal surface versus the ventral surface would be sufficient to induce such phenotype. Furthermore, Wu et al. described the role of hunger-driven behaviours which are actually regulated by neural ribosomal *dS6K* (Wu et al., 2001). Also, Vargas et al. defined the role of *dS6K* in maintaining the dietary switch followed by mating and then increased preference for nutrients such as yeast; a major protein source. They suggested that TOR signaling plays an important role in maintaining a nutrient balance in *Drosophila* (Vargas et al., 2010).

To summarize, in fact; the TOR signaling pathway regulates a balance of nutrients (Vargas et al., 2010). But, more specifically to the viewpoint of *dS6K* and growth; the most important and pioneer work has been demonstrated by Montagne et al., which shows that the *dS6K* regulates cell size, growth, and proliferation in a cell autonomous manner without impinging on cell number (Montagne et al., 1999).

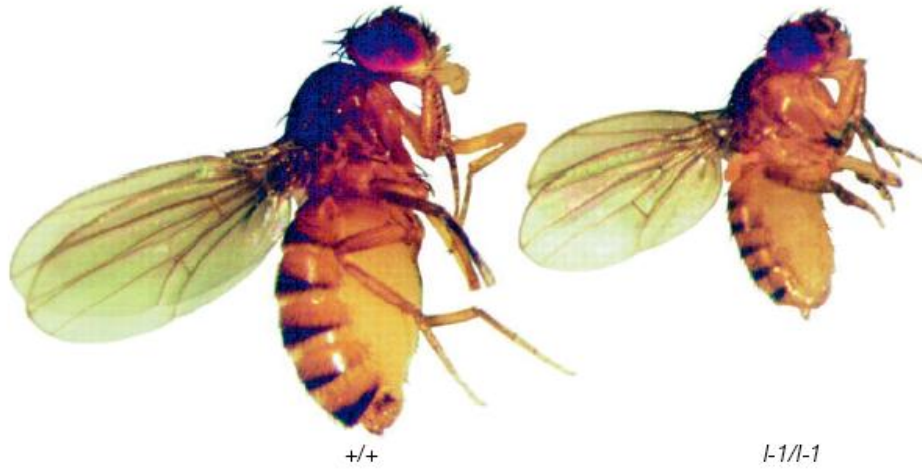


Figure 10 - *dS6K* and the regulation of growth

dS6K is implicated in the regulation of growth. Homozygous *dS6K* null mutation (*dS6K^{l-1}*) flies (right) are reduced in overall body size compared to control (left). It is worth noting that the flies lacking *dS6K* are reduced in size due to smaller but not less cells (From Montagne et al., 1999).

1.4 - Archipelago: A key regulator of protein degradation

The regulation of tissue growth requires a precise control of gene expression by which the developmental program generates an organism of a characteristic size and form (Hariharan and Bilder, 2006). A significant feature of all living organisms is their utilization of proteins to construct molecular machineries that undertake the complex network of cellular activities. The posttranscriptional control of protein abundance has recently emerged as an important aspect of developmental biology (Ho et al., 2008). Perturbations of the mechanisms that regulate normal growth are observed in disease states caused by an aberrant growth such as cancer. By characterizing these abnormal features that can alter the normal regulation of tissue growth, the signaling pathways could be reconstructed that function together to control the growth process. These pathways form the crucial link between the patterning mechanisms which specify the overall form of the organism and the cellular pathways that regulate growth (Hariharan and Bilder, 2006). In *Drosophila*, mutations that alter tissue growth have provided a valuable entry points into the study of growth regulatory pathways. The tissue overgrowth almost always results from a perturbation of specific pathways that function to restrict growth and maintain normal organ size. Therefore, studies of mutations in genes that can be termed growth-suppressors or tumors-suppressors have advanced our understanding of the genetic regulation of tissue growth in *Drosophila* and mammals (Vidal and Cagan 2006; Hariharan and Haber, 2003).

The cellular activities in eukaryotes are organized in a coordinated fashion through complex interrelating networks maintained largely by generation and destruction of proteins. An important index for accomplishing this cellular balance is the dynamic protein levels (Ho et al., 2008; Tetzlaff et al., 2004). By regulated processes like synthesis and degradation, protein turnover are under delicate temporal and spatial controls. In particular, the regulation of protein degradation is of great importance and although it has been studied less than protein synthesis. One major route of protein destruction is coordinated by a set of conserved molecules, the F-box proteins, which recruit specific substrates and regulate their abundance in the context of SCF-E3 ligases (see below).

1.4.1 - The F-box hypothesis

During 1990s, a region of homology was initially observed in proteins containing β -transducin repeats like Cdc4, Met30, and β -TrCP (Kumar and Paietta, 1995). This homologous sequence was not characterized until the discovery of a novel gene, *Skp1p* (Bai et al., 1996). Moreover, two-hybrid assay conducted for Cyclin F-binding proteins identified the human counterpart Skp1 (Durfee et al., 1993). *Skp1* genes are crucial for cell cycle regulation and influential in determining the stability of certain proteins. Alignments of Skp1p interacting protein sequences by Elledge and colleagues revealed a 40-amino acid sequence required for binding to Skp1p. It was not until then that a name, F-box was coined for this motif, and subsequently onward the F-box hypothesis arose. The term F-box was named after Cyclin F, the first defined F-box protein (FBP) (Bai et al., 1996). Soon after, proteins carrying the F-box motif were found to be evolutionarily conserved in various species. To date, numbers of identified FBPs range from about 11 in *Saccharomyces cerevisiae*, 33 in *Drosophila melanogaster* (Table 1) and approximately 600 in *Arabidopsis thaliana*. F-box proteins are evolutionally conserved among eukaryotes like *C. elegans* and *D. melanogaster*, *H. sapiens*, *S. cerevisiae* (Ho et al., 2006; Ho et al., 2008).

The importance of F-box proteins are being dictated in several ways. F-box proteins (FBPs) are responsible for the substrate specificity of SCF complexes (Skp1, Cull1, and FBP) (Fig. 11) that serve as the variable adaptors to recruit specific protein substrates to SCF complexes (Skowyra et al., 1997). FBPs proteins connect the ubiquitination machinery and diverse cellular processes by exerting control over the stability of substrate proteins. FBPs also function in many different biochemical contexts and are involved in DNA replication, transcription, cell differentiation and cell death (Ho et al., 2006; Kanemori and Sagata, 2006).

1.4.2 - Phosphorylation is required for FBP target recognition

FBPs in SCF complexes are known to provide specificity when deciding which substrate is going to be degraded. Mostly, the substrate phosphorylation is a common prerequisite for FBP target recognition. It is critical that one or more residues of the substrate are

phosphorylated prior to the FBP-substrate interaction. For example, the two serine residues in the motif need to be phosphorylated sequentially before binding to β -TrCP (Spencer et al., 1999). Another well-known mammalian FBP, Fbw7/hCdc4, recognizes LL**T**PP**Q**SG sequence deduced from Cyclin E (Ho et al., 2008; Orlicky et al., 2003; Moberg et al., 2001). Within the Cyclin E, Thr-380 is the crucial phospho-residue with an immediately adjacent proline residue. Some Fbw7 substrates also carry a phosphorylated serine at the +4 position after the threonine. Many substrates include more than one serine/threonine (S/T) residues, as in the case of Sic1p which is the substrate of the yeast Cdc4p. Therefore, the sequential phosphorylation events are important for substrate binding and hence their degradation (Ho et al., 2008).

1.4.3 - Ubiquitination and proteasomal degradation

The proteins targeted for degradation by the proteasomal pathway are first ubiquitinated. i.e., a small molecule ubiquitin (Ub) is covalently attached to the protein (Pickart, 2004). Ubiquitination plays a key regulatory role in the Ub-proteasomal degradation pathway which involves three major enzymes: E1 activating enzyme, E2 conjugating enzyme, and E3 ubiquitin ligases. E1 and E2 enzymes are responsible for activating and conjugating the Ub moieties, respectively, whereas E3 ligases are important for transferring Ub moieties from the E2 enzyme onto the recognized substrates destined for destruction by the 26S proteasome (Pickart, 2001; Cardozo and Pagano, 2004). Two types of E3 ligases, HECT-domain and RING-domain type (Really Interesting New Gene) are known which utilize different mechanisms to transfer the Ub adducts to substrates (Pickart et al., 2001; Petroski and Deshaies, 2005). The RING-domain E3s transfer Ub directly onto substrates from the E2 enzymes; whereas, HECT-domain E3s act slightly different, i.e. the Ub is transferred first to the HECT E3s, and then targeted to the substrates (Fig. 11).

The best characterized RING ligases, the SCF (Skp–Cullin–F-box) complex, is composed of four major components: Skp1, Cull1/Cdc53, Roc1/Rbx1/Hrt1, and an F-box protein (Fig. 11) (Ho et al., 2006; Cardozo and Pagano, 2004). Within the SCF complex, Cull1 is the scaffold protein that interacts with Roc1 at its carboxyl-terminus to recruit Ub-conjugated E2. The amino-terminus of Cull1 interacts with Skp1 which binds to the

F-box motif of an F-box protein (Fig. 11). The carboxyl-terminal part of the FBPs usually consists of substrate-binding domains of various types, such as Trp-Asp (WD) repeats and leucine-rich repeats (LRR), both of which have been demonstrated to bind to already phosphorylated substrates. Depending on the motifs at the carboxyl-terminus, FBPs are categorized into three major families (Table 1): the FBW family contains F-box proteins with WD repeats whereas those from the FBL family contain LRRs. The third family, FBX, consists of F-box proteins with other protein-protein interaction domains at the carboxyl-terminus such as carbohydrate-interacting (CASH), zinc-finger, and proline-rich domains (Cardozo and Pagano, 2004).

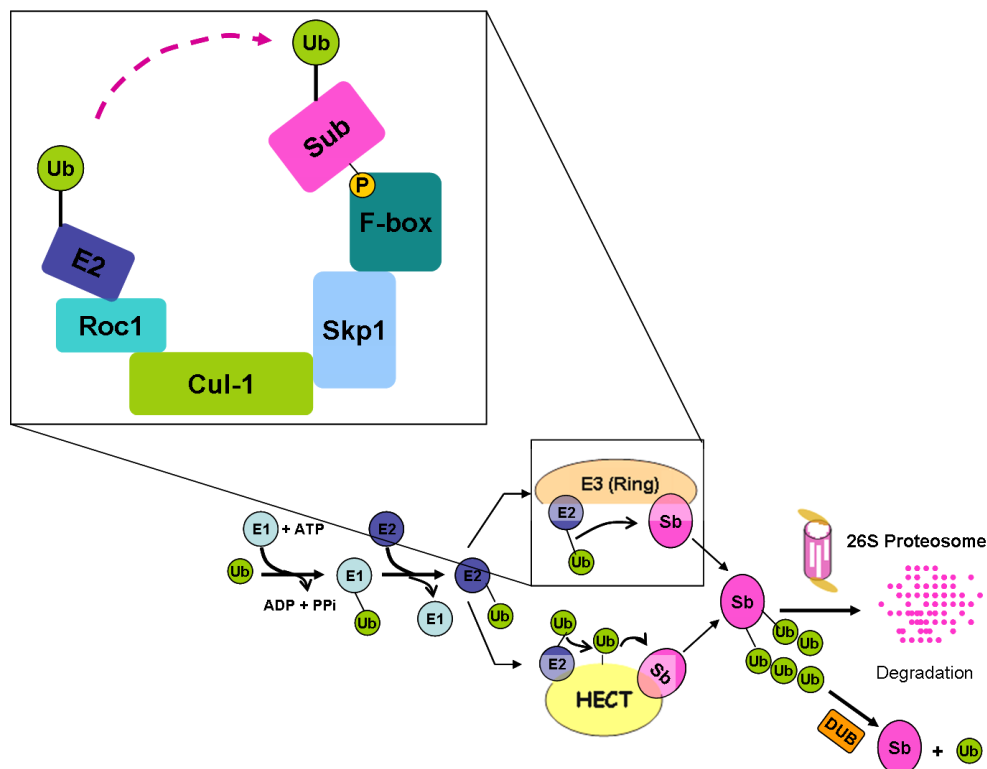


Figure 11 - The SCF complex and the Ubiquitination pathway

The SCF complex consists of four major components: Skp1, Cul1, ROC1 and an F-box protein. Skp1 is a scaffold protein, its C-terminus interacts with Roc1, which contains a characteristic RING-finger domain to recruit Ub-E2; the N-terminus interacts with Skp1, which binds the conserved F-box domain of an F-box protein. The protein degradation pathway is mediated by ubiquitin (Ub); a small peptide of 76 amino acids, covalently attached to substrates targeted for degradation by three consecutive enzymatic reactions. The E1 activating enzyme forms a high-energy thioester bond with Ub by consuming ATP, and transfers the bound Ub to the E2 conjugating enzyme. Using Ub from E2, E3 ligases recognize protein substrates and catalyze Ub conjugation and polymerization. The HECT ligases form a thioester linkage with Ub from E2 and then transfer Ub to the substrate (Sb), whereas RING ligases interact with both Ub-E2 and the substrate for ubiquitination. The poly-Ub chains on the substrate are recognized by the 26S proteasome for subsequent proteolysis. Ubiquitination is reversible, by deubiquitinating enzymes, which are thiol proteases that cleave poly-Ub chains or Ub conjugated proteins. The Ub degradation pathway can be regulated in the processes of substrate recognition, Ub conjugation, deubiquitination and recruitment to the 26S proteasome (drawn from Ou et al., 2003; Dubois-Dalcq et al., 1999; Ho et al., 2006).

1.4.4- Molecular and biological function of *Archipelago* (*ago*)

Archipelago (*ago*) has been localized to position 64B on the left arm of chromosome 3 through meiotic and deletion mapping. All of the three *ago* alleles (*ago*¹, *ago*³, *ago*⁴) have mutations in an open reading frame designated CG15010 which has been demonstrated through sequencing of the transcriptional units. *ago* encodes a 1,326-amino-acid protein that contains an F-box and seven WD repeats in its carboxy-terminal portion. As already described, F-boxes and WD motifs are found in those proteins which function as the substrate-recognition component of SCF-type ubiquitin ligase complexes. The Ago protein in its C-terminal portion is most similar to that encoded by an amino-terminally truncated human expressed sequence tag (EST) previously designated FLJ11071, which has been further renamed as human Ago. This protein is also referred to as hCdc4. Furthermore, an homolog gene in *Caenorhabditis elegans* also exists which is named as *sel-10* (Hubbard et al., 1997). Two of the mutations (*ago*⁴: Ala 1,117 to Val, *ago*³: Gly 1,131 to Glu) are missense mutations that map to the fourth WD repeat. Each alters a residue that is conserved among the three proteins. The third mutation (*ago*¹: Gln 1,195 to stop) results in premature termination of translation early in the sixth WD repeat (Fig. 12) (Moberg et al., 2001). Below here, some of the biological functions of *ago* are briefly discussed.

1.4.4.1 - Archipelago in cell cycle and genomic instability

Central to the cell developmental mechanism is the process of the cell cycle, a basic cyclic progression formed by repetitive events including the S phase for the replication of DNA and the M phase for initiation of genome segregation. Cells grow and divide through checkpoints at each stage of the cell cycle while correct timing is under the control of cyclin proteins and the serine/threonine protein kinases known as cyclin-dependent kinases (CDKs) (Ekholm and Reed, 2000). The endocycle is a developmentally specialized cell cycle that lacks M phase and consists of only S and G phases. Endoreplicating cells acquire high ploidies by multiple rounds of replication without cell divisions. Following the cell proliferative phase of *Drosophila* embryogenesis, many tissues initiate endocycles that lack all visible aspects of mitosis. These tissues include the gut, epidermis, fat body, malpighian tubules, trachea and

salivary glands, which continue to endocycle during larval development long after they are fully differentiated. Some adult tissues, including ovarian follicle and nurse cells, and sensory neurons in the wing, also employ endocycles (Asano, 2009). One central regulator of all *Drosophila* endocycles is the S phase kinase, Cyclin E/Cdk2. The *cyclin E* gene is transcribed prior to the onset of endocycle S and is required for these cycles (Knoblich et al., 1994). Szuplewski et al presented a novel cell cycle regulator, called *minus*, which influences Cyclin E turnover in *Drosophila* and proposed that Minus contributes to cell cycle regulation in part by selectively controlling turnover of Cyclin E. Minus protein has also been known to interact physically with Cyclin E and the SCF Archipelago/Fbw7/Cdc4 ubiquitin ligase complex (Szuplewski et al., 2009). It has been described that Cyclin E is regulated by Ago (see below) (Moberg et al., 2001) and hence, perturbation in Ago causes a continuous overexpression of Cyclin E which inhibits endocycle progression in *Drosophila* and eventually causes a genomic instability (Follette et al., 1998; Weiss et al., 1998; Edgar and Orr-Weaver, 2001).

1.4.4.2 - Archipelago as a regulator of Cyclin E and dMyc

Hariharan et al. performed a genetic screen in *Drosophila* to identify genes involved in controlling cell numbers and growth during development and found Archipelago (*ago*) as a candidate gene (Moberg et al., 2001). The screen was done by generating clones of homozygous mutant tissue in fly eyes and selecting the mutant cells that had a proliferative advantage over the wild type cells. Within the *ago* mutant clones, distance between adjacent photoreceptor clusters was increased compared to the wild-type, indicating an over-proliferation in the mutant tissue. This over-proliferation of *ago* mutant tissue is not due to irregular apoptosis event since there is no significant decrease in the extent of cell death. Due to a role in cell proliferation, loss of *ago* could lead to an increased level of a positive cell cycle regulator. Several cyclins and CDKs were examined, and the Cyclin E was found to accumulate in the *ago* mutant clones in third instar eye imaginal discs. Nevertheless, the mRNA level of *cyclin E* remains unchanged within *ago* mutant clones, suggesting a post-transcriptional modification of Cyclin E by Ago (Moberg et al., 2001).

Myc genes encode basic-helix-loop-helix-zipper (bHLHZ) domain transcription factors and dimerize with Max family proteins through the bHLHZ domain to promote cell growth and proliferation (Grandori et al., 2000; Donaldson and Duronio, 2004). In *Drosophila*, overexpression of *dMyc* causes cell over growth as evidenced through an increased size of developing tissues (Neufeld and Edgar, 1998; Johnston and Gallan, 2002). Moberg et al. performed interaction screens using the Ago F box/WD domain as a bait to search for additional substrates of Ago and recovered dMyc (Moberg et al., 2004). While both dMyc and Cyclin E promote S phase entry, only dMyc was found to have effect on growth (Neufeld and Edgar, 1998). As overexpression of *dMyc* causes cell over growth, the phenotype was recapitulated and found to be consistent with *ago* mutant tissue phenotypes. The *dMyc* mutant flies were smaller than the wild-type flies in body size, and losing a copy of wild-type *ago* gene under the *dMyc* mutant background restores the body size defect to the extent of 12 to 15%. Similar to Cyclin E, protein levels of dMyc were also elevated in *ago* mutant clones and its mRNA level remains the same. Direct interaction between dMyc and Ago were also observed by cell transfection and co-immunoprecipitation analyses (Moberg et al., 2004). To summarize in brief, Ago regulates the degradation of dMyc and the increased cell growth observed in tissues which ectopically expressed *dMyc* mainly accounts for the *ago* mutant phenotype.

1.4.4.3 - Archipelago and tracheogenesis

In *Drosophila melanogaster*, tubular morphogenesis underlies formation of the tracheal system, a network of interconnected tubes that duct air throughout the developing organism. The central components of the *Drosophila* fibroblast growth factor (FGF) pathway associated with tracheogenesis are encoded by the breathless (*btl*) and branchless (*bnl*) genes, which encode an FGF-like receptor and an FGF-like secreted ligand respectively (Klambt et al., 1992; Sutherland et al., 1996). The role of this receptor/ligand pair in controlling tracheal outgrowth is based upon a simple model in which the restricted expression of *bnl* in cells outside the tracheal placode represents a directional cue for the migration of *btl*-expressing cells within the tracheal placode, which is dependent upon the tracheless (*trh*) gene (Isaac and Andrew, 1996). Mutation of any one of these core components; *btl*, *bnl*, or *trh* produces a failure of tracheal

branching. Mortimer and Moberg showed that Ago acts upstream of tracheless (Trh) and breathless (btl) and is required for controlling the levels of tracheless (Trh) transcription factor. Ago binds directly to Trh and stimulates its proteasomal degradation (Mortimer and Moberg, 2007). This novel role for Ago in tracheal development is supported by an independent finding which demonstrated that the homozygosity for a genomic deletion containing *ago* locus is associated with cell migration defects in embryonic tracheal development (Myat, 2005). dVHL (Von Hippel-Lindau) protein is a central player in the hypoxic response pathway in embryonic and larval tracheal cells and has been revealed to strongly interact with Ago. dVHL is a substrate adaptor component of an ubiquitin ligase that subsequently polyubiquitinates HIF-1 α (Hypoxia induced factor) and targets it for degradation by the proteasome. Thus, both of these two proteins, dVHL and Ago synergize with each other to regulate the process of tracheogenesis in *Drosophila* (Mortimer and Moberg, 2009).

1.4.4.4 - Archipelago controls Rb/E2F regulated apoptosis

Recently, Nicholson et al. found that due to unrecognized mechanism the loss of *ago* has different effects on the size of different tissues in the adult head. There is no solid reason to elaborate that *ago* loss induces hyperplasia of some of organs but paradoxically reduces the size of the adult eye. This reflects a requirement for *ago* to restrict apoptotic activity of the *rb1/de2f1* pathway. Adjacent to the eye-specific morphogenetic furrow (MF), *ago* mutant cells displayed an elevated level of dE2f1 activity and expressed the prodeath dE2f1 targets *hid* and *rpr*. Furthermore, the *ago* mutant cells also showed high rates of apoptosis (Nicholson et al., 2009). Eye overgrowth resulting from loss of *ago* was retarded by apoptosis that could occur as *ago* mutant cells encounter the MF. Blocking this death led to eye hypertrophy, demonstrating that *ago* mutations could synergize with anti-apoptotic mutations to drive organ overgrowth. The pattern of apoptosis in *ago* mutant eye discs resembled that caused by loss of the retinoblastoma homolog *rbf1* (Moon et al., 2006). In summary, these data linked two tumor suppressor genes *ago* and *rbf1* in a common developmental pathway and also displayed a role of *ago* as a required regulator of the *rbf1/de2f1* pathway.

1.4.4.5 - Archipelago as a tumour suppressor

The regulation of tissue growth is, perhaps, the most important means by which the developmental program generates an organism of a characteristic size and form. The perturbations in the mechanisms that regulate normal growth lead to an aberrant growth such as cancer (Hariharan and Bilder, 2006). In *Drosophila*, analysis of the growth restrictive role of *archipelago* in proliferating larval imaginal disc cells has provided an excellent model to understand the tumor suppressive properties of *ago* mammalian orthologs (Moberg et al., 2004). Elevated levels of Cyclin E have been reported in a subset of human tumors, notably of the breast and ovary (Keyomarsi and Herliczek, 1997). Moberg et al. examined human ovarian cancer cell lines and demonstrated that, 3 out of 10 had mutations in the human *Fbw7* gene, the homolog of *ago*. The Cyclin E was upregulated in these ovarian cancer cell lines as well, implicating a role of *ago* in human cancer pathogenesis (Moberg et al., 2001). Spruck et al. observed that the F-box protein hCdc4 was mutated in at least 16% of human endometrial tumors. Furthermore, mutations were found either in the substrate-binding domain of the protein or at the amino terminus, suggesting a critical role for the region of hCdc4 upstream of the F-box (Spruck et al., 2002). In addition, there are many reports which show that this highly conserved mammalian *ago* ortholog (variously termed *Fbw7*, *Fbxw7*, *hAgo*, *hCDC4*, or *hSel-10*) is a mutational target in a rapidly expanding array of human cancers (Balakrishnan et al., 2007; Calhoun et al., 2003; Malyukova et al., 2007; Minella et al., 2007).

Table 1 - Drosophila homologs of F-box components and related genes

F-box component	Homologs and related genes	Reported components	Proposed substrates
F-box (33)	Fbw (3): <i>ago</i> , <i>slimb</i> , CG9144	Slimb	Arm, Ci, Cactus, Paired
		Ago	Cyc E*, Trh*, Myc*, CG13822, CG4998, RpS3, Hippo, Scf, Dys, CG2165, Plex A
	Fbl (11): <i>ppa</i> , CG14891, CG7148, CG12402, CG13213, CG14937, CG11033, CG8873, CG8272, CG9003, CG1839	Ppa	Paired
	Fbx (19): <i>morgue</i> , CG9461, CG11044, CG9772, CG9316, CG2247, CG4643, CG13766, CG6758, CG12765, CG13770, CG5003, CG7707, CG10855, CG4911, CG3428, CG2010, CG1866, CG5961	Morgue	DIAP1

Abbreviations: Ago, Archipelago; Arm, Armadillo; Ci, *Cubitus interruptus*; CycE, Cyclin E; Dys, Dysfusion; Scf, supercoiling factor; Trh, Trachealess; Fbw, F-box proteins with WD repeats; Fbl, F-box proteins with leucine-richrepeats; Fbx, F-box proteins with other motifs or without recognizable motifs (drawn from (Ho et al., 2006)) (*Reported substrates and other interactors of Ago; drawn from Moberg et al., 2001; Moberg et al., 2004; Mortimer and Moberg, 2007; <http://thebiogrid.org>; <http://bond.unleashedinformatics.com>).

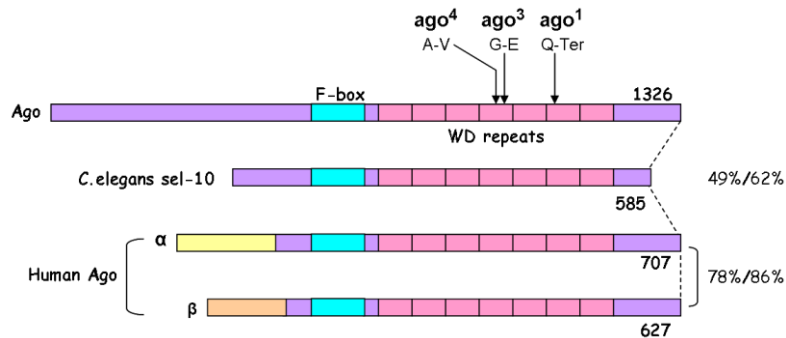


Figure 12 - The domain structure of Archipelago (Ago) in *Drosophila*, human and *C. elegans*

Archipelago (*ago*) encodes a protein with an F-box and WD repeats. The domain structure; the F-box (light blue), WD-repeat region (pink) and the *ago* alleles are shown. The N-terminal domains of the two human and the unique *C. elegans* and *Drosophila* Ago are indicated; note the absence of conserved domain. The degree of conservation in the F-box/WD region between *Drosophila*, human *ago* and *C. elegans* sel-10 is also indicated (identity/similarity).

1.5 - RNAi Screening for regulators of growth and metabolism

The fruit fly, *Drosophila melanogaster* has been a valuable model organism in which genetic screens have been used to study a variety of cellular and developmental processes for close to a century (Nagy et al., 2003; St Johnston, 2002). Traditionally, the power of *Drosophila* genetics relied on forward genetic screens to identify genes which affect a given biological process. Forward genetic screens uncover many genes required for specific processes, but other genes can be missed due to limitations of the screening process. For example, embryonic screens may not uncover some mutations because the genes are expressed during oogenesis contributed by the mother and mask a mutation in the zygotic gene (St Johnston, 2002). Patterning of the early embryo body axes is directed by mRNAs that are deposited in the oocyte by the mother and localized at the specific positions within the embryo. The genes providing the mRNA are known as the maternal effect genes as they are expressed in the mother rather than the embryo. Moreover, of the 14,600 predicted open reading frames in *Drosophila* genome, only approximately 3600 have been associated with mutant phenotypes. It is not entirely clear why so many genes have been missed in forward genetic screens (Adams et al., 2000; Kuttenukeuler and Boutros, 2004). Recently, the availability of *Drosophila* genome sequences enables a genetic approach to be utilized to determine the function of predicted classes of gene products (Mohr et al., 2010). Since many developmental processes as well as known human disease genes are conserved between flies and vertebrates (St Johnston, 2002), studies in the fly may provide useful insights into understanding the signaling pathways and also the causes of diseases in humans (Hietakangas and Cohen, 2009). Hence, taking advantage of the conserved genomic analogy between fly and humans and also the availability of RNAi library, a reverse genetic approach through an RNAi screen has been followed-out to look for regulators of growth, development and metabolism in *Drosophila melanogaster*. A short note on RNAi and its utility in drosophila is briefly discussed below.

1.5.1 - RNA interference (RNAi) and its mechanism

RNA interference (RNAi) is a mechanism for directly knocking down expression of genes with known sequence and has proven to be a powerful reverse genetic approach. (Fire, 1999; Fire, 2007). RNAi was originally discovered in *Caenorhabditis elegans* when injection of double-stranded RNA (dsRNA) into the worm was shown to result in degradation of the corresponding mRNA and silencing of the gene product (Fire et al., 1998). Injection with dsRNA proved to be much more potent in knocking down mRNA levels than injection with either sense or anti-sense RNA alone. In addition to injection of dsRNA, RNAi has been demonstrated in *C. elegans* by feeding on *E. coli* engineered to express dsRNA of a nematode gene (Timmons and Fire, 1998) and soaking the worms in a solution of dsRNA (Tabara et al., 1998).

RNA interference refers to the use of double-stranded RNA (dsRNA) to target mRNAs for degradation leading to silencing of gene expression. The dsRNA sequence is utilized by RNA machinery to produce a protein-RNA complex that degrades the corresponding mRNA, thereby producing an extremely specific means of silencing genes, as other non-specific mRNAs are not affected (Zamore et al., 2000). It has been proposed that the biological roles of RNAi may be to maintain the integrity of the genome by suppressing mobilization of transposons or to prevent an accumulation of repetitive sequences in the germline (Aravin et al., 2001). In addition, RNAi is speculated to be a defence against viral infections as well as a regulator of gene expression (Zamore, 2001).

RNA interference is a two-step process. The RNAi pathway is initiated through ATP-dependent cleavage of the dsRNA into small interfering RNAs (siRNAs) 21-25 nt in length by Dicer, a Ribonuclease (RNaseIII), (Bernstein et al., 2001; Elbashir et al., 2001; Zamore et al., 2000). Dicer is a member of the RNaseIII family of dsRNA specific endonucleases (Bernstein et al., 2001), and similar to other family members produces a small interfering RNAs (siRNA) product consisting of a 5' phosphate and 3' hydroxyl with two unpaired nucleotides at each end (Elbashir et al., 2001). The siRNAs then interact with a multi-protein complex that is not able to mediate RNAi until the ATP-dependent unwinding of the siRNA duplex is initiated (Nykanen et al., 2001). Upon duplex unwinding, the complex undergoes a conformational change producing an active RNA induced silencing complex (RISC) (Fig. 13). The siRNA antisense strand of the

activated RISC complex can recognize and hybridize with corresponding target mRNA leading to cleavage of the mRNA by the RISC complex (Hammond et al., 2000; Nykanen et al., 2001) and subsequently, regulating the expression of a protein-coding gene (Hannon and Conklin, 2004).

1.5.2 - Utility of RNAi technique

The availability of genomic sequences from *Caenorhabditis elegans*, *Drosophila melanogaster*, *Mus musculus* and human have provided a source of target sequences against which RNAi can be utilized as a reverse genetic tool to begin understanding the function of many genes with previously unknown function. RNAi has been effectively used as a tool to perform multiple screens in *C. elegans* (Gonczy et al., 2000), *Drosophila* embryos (Ivanov et al., 2004; Kim et al., 2004; Kutteneuler and Boutros, 2004), and *Drosophila* cell culture to identify genes involved in numerous biological processes including cell cycle regulators, cell morphology, growth and viability and signaling pathways (Bai et al., 2009; Doumanis et al., 2009; Bjorklund et al., 2006; Clemens et al., 2000). RNAi techniques both *in vivo* and in cultured cells have been increasingly used to explore functions of uncharacterized genes by loss-of-function analysis (Kutteneuler and Boutros, 2004). The first large-scale RNAi screens covering single chromosomes of *C. elegans* genome identified 90 percent of embryonic lethal alleles that were known from previous studies and provided evidence for the efficiency of RNAi approaches (Fraser et al., 2000; Gonczy et al., 2000). Subsequent genome-wide screens for developmental defects identified phenotypes for more than 1,700 genes in the *C. elegans* genome (Kamath et al., 2003). Therefore, genome-wide RNAi screens in *C. elegans* impressively demonstrated the versatility of this approach and demonstrated how biologically significant insights can be gained using a variety of phenotype based assays (Kutteneuler and Boutros, 2004).

1.5.3 - *Drosophila*: A model for genetic screens

Experimentally introduced dsRNA can trigger the RNAi effect in a wide range of experimental organisms, providing a powerful method for disrupting gene function (Fire et al., 1998). *Drosophila* is one of the major model organisms in which genetic screens have been used to study a variety of cellular and developmental processes (St Johnston, 2002; Nagy et al., 2003). In *Drosophila*, several methods have been used to deliver dsRNA. The simplest method works for cultured cells; dsRNA is added directly to the culture medium which silences gene function within 72 h. This can be a powerful method for working out signal transduction pathways, cell biological phenomena and the mechanism of RNAi itself (Adams et al., 2001; Giet and Glover, 2001; Adams and Sekelsky, 2002; Caplen et al., 2000; Clemens et al., 2000). Two methods that use RNAi have been developed in *Drosophila*. The first relies on the delivery of dsRNA to embryos by microinjection. The main advantage of this method is that both maternally supplied mRNA and zygotically expressed mRNA are degraded. Also, the results are obtained within a few days of injection but the injected dsRNA might not produce a phenotype in every embryo, and the severity of the phenotype might vary between embryos (Kennerdell and Carthew, 2000; Adams and Sekelsky, 2002). Furthermore, the injection procedure itself can cause aberrant phenotypes or death in some embryos. Unfortunately, microinjection of dsRNA into *Drosophila* embryos does not efficiently interfere with gene function later in development. An alternative that works at all stages and in all tissues is to generate the dsRNA *in vivo* (Kennerdell and Carthew, 2000). This can be accomplished by expressing an RNA with a long inverted repeat that can fold back on itself to become double stranded. A principal advantage of this promising RNAi approach is the possibility of interfering with gene function in specific tissues or at specific times during development by using the Gal4–UAS system (Fig. 14) (Brand and Perrimon, 1993).

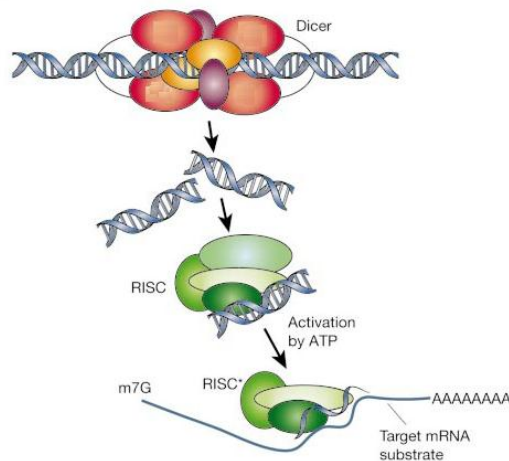


Figure 13 - Dicer and RISC (RNA-induced silencing complex)

RNAi is initiated by the Dicer enzyme which processes double-stranded RNA into ~22-nucleotide small interfering RNAs. The siRNAs are incorporated into a multi-component nuclease, RISC. RISC must be activated from a latent form, containing a double-stranded siRNA to an active form, RISC*, by unwinding of siRNAs. RISC* then uses the unwound siRNA as a guide to the substrate selection (drawn from Hannon, 2002).

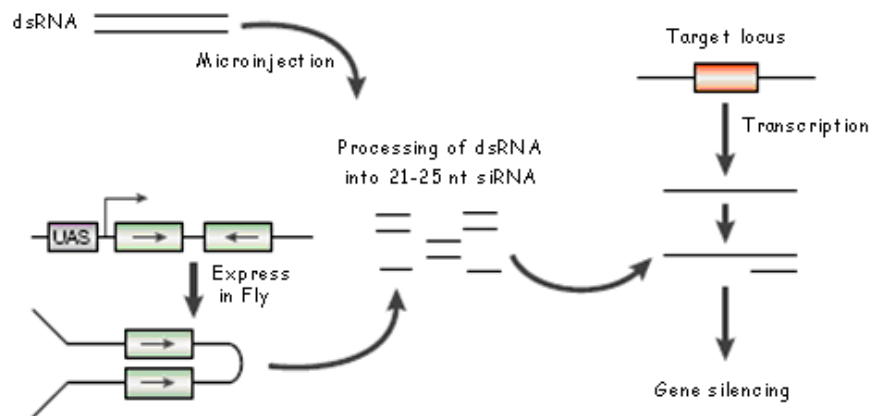


Figure 14 - RNAi interference in *Drosophila*

Double-stranded RNA (*dsRNA*) that is homologous to the target gene by either of two methods. Injection of *in vitro* transcribed RNA into individual embryo or expression of an inverted repeat *in vivo*. The dsRNA is processed into 21-25 nucleotide (nt) small interfering RNAs by the Dicer ribonuclease. The siRNA is used to guide the sequence specific degradation of mRNA, leading to post-transcriptional silencing of the target locus (drawn from Adams and Sekelsky, 2002).

In order to assess phenotypes on a genome-wide scale, an RNAi library was constructed comprising 21,000 dsRNAs that covered all predicted open reading frames in the *Drosophila* genome to comprehensively characterize cell growth and survival phenotypes (Hild et al., 2003). Using approximately 4,400 dsRNAs derived from the *Drosophila* expressed sequence tag project, Lum et al. searched for Hedgehog pathway components using a *luciferase* reporter gene assay. They screened for both negative regulators of the pathway, which could activate the reporter gene in absence of a stimulus, and for positive regulators that are required to transmit the signal from the membrane to the nucleus. By these means, they identified several known and novel components, including casein kinase 1 α , which has also been implicated in Wnt signaling (Lum et al., 2003). Wnt and Hedgehog pathways, which were first discovered as regulators of early embryonic development, but later have been shown to be indispensable for many other processes during development and disease in higher vertebrates (Pospisilik et al., 2010).

In genetic screens for early embryonic defects, independent alleles with similar phenotypes often uncovered multiple components in the same cellular pathway (Kennerdell and Carthew, 1998). Furthermore, many genes are used at multiple developmental stages enabling phenotypes of lethal mutations to be analyzed in embryos, but there are drawbacks to analyzing embryonic phenotypes (St Johnston, 2002). Therefore, classical genetics may be limited by its inability to identify zygotic and maternal effects mutations simultaneously, and many mutations were not uncovered. Nevertheless, RNAi has been shown to reduce levels of both maternal and zygotic mRNA enabling further analysis of these previously uncharacterized gene products (Adams and Sekelsky, 2002).

A genetic screen for growth regulators in *Drosophila* revealed a new member of the TOR signaling pathway, *melted* (Teleman et al., 2005b). This gene encodes a protein with a pleckstrin homology (PH) domain that is essential for its function. Melted can bind TSC1 and recruit the TSC1/2 complex to cell membranes, suggesting it can act upstream of TOR. The *melted* mutants have reduced lipids but display no apparent defects in circulating sugar levels. Although the mechanisms remain unclear, Melted may help to facilitate the phosphorylation of dFOXO and TSC2 by Akt in response to

insulin input. Consistent with the proposal that Melted limits the dFOXO response, the dFOXO target 4E-BP is highly upregulated in starved *melted* mutants, and reduced dFOXO levels can suppress the lipid metabolic defects of *melted* mutants (Teleman et al., 2005b). The identification of *melted* homologs in *C. elegans*, mice, and humans sets the stage for further studies to understand its role in TOR and FOXO signaling as well as lipid metabolism.

Recently, most of the RNAi screening is being carried-out in cultured cells. Both *in vivo* and *in vitro* approaches have different advantages and constraints. RNAi in cultured cells has the advantage of speed, reduced phenotype complexity and easily quantifiable phenotypes and also cell culture models can provide a convenient platform to study signal transduction pathways, they fail to recapitulate the complexity of signaling within intact organs and/or in the whole organism (Mohr et al., 2010; Doumanis et al., 2009; Kuttenukeuler and Boutros, 2004). In contrast, the main disadvantage of large-scale and genome-wide genetic screens is that they are costly, labor intensive, and time consuming (Aerts et al., 2009). However, RNAi experiments *in vivo* provide immediate insights into biological processes in a relevant setting and the results seem to be more reliable and applicable at an organism level (Aerts et al., 2009). Therefore, the physiological significance of results obtained in tissue culture should be corroborated in an animal model system. Such studies have been greatly facilitated by the development of certain tools to either disrupt or over-express nearly any gene of interest in a genetically suitable model organism such as *Drosophila* (Kuhnlein, 2010; Grewal, 2009).

1.5.4 - RNAi screen for regulators of Steroidogenesis at the ring gland

Growth and metabolism are coordinated according to genetic and environmental cues. Furthermore, multicellular organisms have to orchestrate the maintenance and adjustment of the correct proportions of organs and tissues throughout life. The accomplishment of this commitment mainly remains perplexing. However, systemic growth factors such as hormones which transmit signals to target cells are known to play an important part in this regulation. Nutrient availability is important for the production

and secretion of hormones (Ikeya et al. 2002) and hence thereby regulating the whole scenario of growth, development and the metabolism processes.

In insects, as in all animals, many aspects of development are under hormonal control. The most important insect hormones are the ecdysteroid molting hormone (EC), which is secreted from the prothoracic glands, and the sesquiterpenoid juvenile hormone (JH), which is secreted from the corpus allatum (CA). In the larvae of *Drosophila*, ecdysteroids and juvenile hormones are produced by the ring gland, which is composed of the prothoracic gland, the corpus allatum, and the corpora cardiaca (Fig. 15). Ecdysteroids are actually synthesized from the dietary cholesterol which is converted through a multistep enzymatic pathway to Ecdysone (E). The peripheral hydroxylation of Ecdysone leads to the biologically active compound 20-hydroxyecdysone (20-HE). The ecdysteroids are required for morphogenetic events and for cuticle deposition in embryos. During larval development, ecdysteroid levels rise briefly controlling the transition from one stage to the next. At the end of the third instar, a large pulse of molting hormone, the commitment peak apparently causes the epidermis to become committed to trigger the onset of metamorphosis. This process ends with another pulse of molting hormone; the prepupal or molting peak is responsible for adult head eversion and the differentiation of adult structures (Fig. 16). The precise timing of these events suggests that steroid hormone synthesis and/or degradation are tightly regulated. Any perturbation in the titer of ecdysteroids could lead to the changes in the phenotype. For instance, an RNAi to DHR3 directed in the prothoracic gland causes giant L3 larvae, a phenotype that could be rescued with ecdysone feeding (Parvy et al., unpublished results). DHR3 is a nuclear receptor and has been known for its positive regulation of growth (Montagne et al., 2010). Furthermore, it has been shown that β -Ftz-F1 another nuclear receptor is necessary for synthesis of the steroidogenic enzymes (Parvy et al., 2005). More recently, Parvy et al (unpublished results) have shown that RNAi to other nuclear receptors also interfere with the progression of larval developmental steps, which opened new doors of the regulation of the ecdysteroid biogenesis and, hence the control of development in *Drosophila*. As DHR3 regulates dS6K-dependent growth and also the dS6K has been shown to play a role in metabolism, it is conceivable that all these processes; growth, development and metabolism are connected with one another through

different effectors. Consistently, it is known that nutrition modifies the timing of development by acting on the production of the ecdysone at the prothoracic gland (PG) and that the TOR signaling plays a critical role in controlling this process. The levels of ecdysone are regulated by a neurohormone PTTH (prothoracicotropic hormone) (Gilbert et al., 2002), which may regulate TOR signaling (Layalle et al. 2008).

Keeping in view this prospect, a genome wide RNAi screening project was designed for the regulators of growth, development and metabolism in *Drosophila*. Meanwhile, National Institute of Genetics, Japan (NIG) started a mega project to launch an RNAi library containing inducible UAS-RNAi lines directed against every *Drosophila* gene. Thanks to a collaborative project between NIG and the platform of Centre de Génétique Moléculaire (CGM), we were able to utilise these UAS-RNAi lines to screen for regulators of the steroidogenesis. As the UAS-RNAi collection spans the whole genome of *Drosophila*, thereby, this RNAi library provided us a convenient mean for saturating genetic screen. We expressed these inducible RNAi lines in the ring gland by using *phm-Gal4* driver. As already described, that an RNAi to DHR3 when expressed in the ring gland caused an increase the larval size. This way, the larval phenotype served as a tool to screen for novel regulators of development which potentially regulate the process of steroidogenesis. The novel candidates which regulate the process of development at different stages through controlling the ecdysteroid biogenesis could be further selected for future studies.

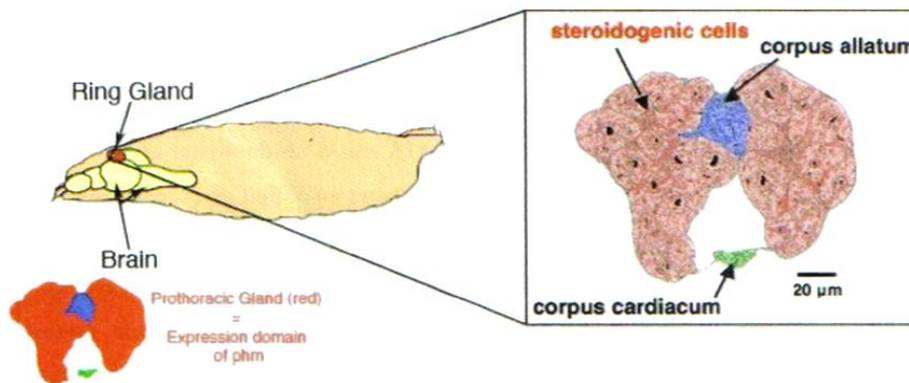


Figure 15 - The structure and location of the ring gland in drosophila larva

The ring gland is present only in the larval stage and degenerated during metamorphosis. It is composed of the prothoracic gland, the corpus allatum, and the corpora cardiaca. The prothoracic gland comprised of steroidogenic cells (red); the corpus allatum (blue) which produces the JH and the corpora cardiaca (green) which regulates certain neuropeptides and metabolic hormones are shown.

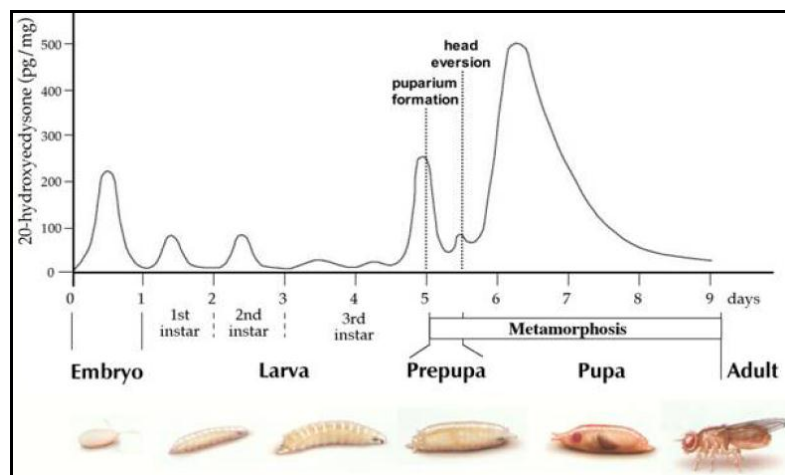


Figure 16 - The dynamics of ecdysteroids levels and the development of drosophila

The transient increase in ecdysteroids levels during the course of development in drosophila. The ecdysteroids are required for morphogenetic events and for cuticle deposition in embryos. During larval and pupal stages, ecdysteroid levels rise briefly controlling the transition from one stage to the next and regulate the onset of metamorphosis.

1.5.5 - RNAi screen for regulators of lipid metabolism at the fat body

The ability to manipulate the fly genome in virtually any way desired, combined with a range of newly available genomic resources, allow the researcher to define the molecular mechanisms of gene function at a level of resolution not possible in more complex organisms. The similar proteomic composition of lipid droplets and the regulation of many of the genes under starvation establish parallels between fly and mammalian system (Gronke et al., 2005; Zinke et al., 2002). This analogy of lipid physiology indicates that the studies in *Drosophila* could provide new insights into how lipid homeostasis is maintained (Cermelli et al., 2006). The *Drosophila* larval fat body combines the hepatic and adipose functioning and hence, serves as a most sophisticated and convenient tissue for the dissection of metabolic function (Colombani et al., 2003). Fat body cells accumulate large stores of carbohydrates, lipids and proteins that are normally used during metamorphosis. During the third instar of larvae, this accumulation of nutrients causes opacity of fat body cells. If the larva is starved, remobilization of these stored metabolites causes shrinkage of fat body cells which become clear. Close investigation of fat body cells reveals that starvation provokes large increase of cytoplasmic vesicles while after storage and; otherwise during normal feeding conditions many more vesicles are visible but their size is significantly reduced (Hietakangas and Cohen, 2009). Moreover, it has been also reported that under starvation, in late larval stages and during metamorphosis, cytoplasmic components within the fat body are degraded by autophagy to provide nutrients to developing imaginal tissues (Juhasz et al., 2003; Rusten et al., 2004). Starvation has also been shown to induce alterations in the morphology of fat body cells, including aggregation of lipid droplets and mobilization of nutrient stores (Britton et al., 2002; Colombani et al., 2003; Zhang et al., 2000), and to cause a marked reduction in fat body cell size (Scott et al., 2004). Interestingly modulation of a number of growth or metabolic regulators (Hietakangas and Cohen, 2009; Britton et al., 2002; Beller et al., 2008) phenocopies the starvation induced phenotype in the fat body (DiAngelo and Birnbaum, 2009). These regulators include intermediates in the insulin and nutrient network, as well as amino acid transporters, lipase and *microRNA* (Colombani et al., 2003; Britton et al., 2002; Teleman et al., 2006).

The modulating lipid droplet phenotype can serve as a phenotypic tool and a good read-out to find new components of a signaling cascade and to further explore the metabolic functioning of genes (Grewal, 2009). Since, no studies to date have exploited one of the main strengths of *Drosophila*; the ability to conduct large-scale genome-wide genetic screen in larvae for regulators of lipid metabolism. We benefited the RNAi library of the NIG fly stock to screen for new regulators of metabolism. For the screening of novel regulators which are potentially implicated in the lipid metabolism, the larval fat body was used as a tool. Moreover; the easiness of dissection, the tools available for fat body screening and the easy detection of lipid droplets, we have thus decided to use the lipid droplet phenotype as a convenient tool to screen for specific regulators.

This screening approach holds the promising commitment of extending our understanding of the regulation of lipid metabolism in a new and unexpected direction. It is likely that we have much to look forward to in the next few years, as further studies exploit the humble fruit fly to reveal new insights into the regulation of lipid homeostasis.

1.5.6 - RNAi screen for negative regulators of dS6K-dependent-growth

The mechanisms that regulate the growth and size of different organs and tissues during the course of development are among the least known biological processes (Leever and McNeill, 2005). The *Drosophila* wing serves as a good model system to analyze growth regulation (Martin and Morata, 2006). It is formed by the cells of the wing imaginal disc, which initially contains about 40 cells (Lawrence and Morata, 1977) that proliferate during the larval period to reach about 50,000 cells. There are about 10-11 divisions in the progeny of the initial cell, each of them takes about 10 hours (Garcia-Bellido and Merriam, 1971). Shortly after the beginning of pupariation, cell divisions cease and the differentiation of the adult structures begins. The disc is subdivided during embryogenesis into anterior (A) and posterior (P) compartments which appear to grow independently (Lawrence and Morata, 1977) and during second instar larval stage into dorsal (D) and ventral compartments (V) (Diaz-Benjumea and Cohen, 1993). The TOR (target of rapamycin) has been revealed as an effector of an insulin- and nutrient

signaling pathway which regulates growth as well as metabolism. As stated earlier that the key downstream effector of insulin- and nutrient-mediated dTOR (*Drosophila* target of rapamycin) is dS6K (*Drosophila* ribosomal protein S6 kinase) which acts as a regulator of growth (Montagne et al., 1999). Using the *ap*-Gal4 driver, ectopic expression of *dS6K* within the dorsal compartment of the developing wing imaginal disc induced a moderate overgrowth and caused a bending down of the adult wing (Montagne et al., 1999). It has been described that the *Drosophila* PDK1 (*dPDK1*) when co-induced with *dS6K* in the dorsal compartment of the wing disc caused an enhancement of the wing bending-down phenotype, whereas expression of *dPDK1* alone had no effect to this phenotype (Radimerski et al., 2002). It has been also described that the expression of a particular phosphorylation-site mutants of *dS6K* caused an enhancement or suppression of the wing phenotype depending upon the increase or decrease in the activation state of dS6K, respectively (Barcelo and Stewart, 2002). These findings demonstrated that the wing bending-down phenotype varies according to the dS6K activity. Thus, this sensitized phenotype was used in a gain-of-function genetic strategy to identify novel positive regulators of dS6K-dependent growth. During the screen, approximately 5,000 Enhancer-Promoter (EP) lines were co-induced with *dS6K* in the developing dorsal wing compartment. Since several enhancers, but too many suppressors were found, this study revealed that the bent-down wing phenotype could be efficiently used for enhancement, but not for suppression. In this screening for new positive regulators of dS6K-dependent growth, the *Drosophila* hormone receptor 3 (*DHR3*) was found to be one of the strongest enhancers (Montagne et al., 2010).

It is to be worth noting that expression of *dS6K* in other tissues did not produce any significant phenotype (Montagne et al., 1999). Therefore, larval wing imaginal disc which gives rise to future wing, proved to be a valuable and suitable tool for the search of growth regulators interacting with *dS6K*. Taking advantage from the UAS-RNAi lines from NIG, we started a project in order to find out novel regulators of dS6K signaling. We have exploited the sensitized phenotype, such that ectopic expression of *dS6K* within the developing dorsal compartment causes the wing to bend-down. Using this sensitized phenotype we performed a genome-wide RNAi screening to identify novel potential regulators, which negatively regulate dS6K-dependent growth.

1.5.7 - A protein-protein interaction network through RNAi

The genetic approaches mainly focus on generating data on a gene-by-gene basis and creating a protein-protein interaction network which then prove to be a valuable information data. Hence, genetic screens, either for specific phenotypes or for modifiers of gene function, are thus a valuable source of large-scale interaction data (Aerts et al., 2009). But the high quality functional annotations through computational predictions of gene function alone remain much higher than genetic screening data (Adie et al., 2006). However, protein interaction networks summarize large amounts of protein-protein interaction data, both from individual, small scale experiments and from automated high-throughput screens. Sometimes, it seems that genetic interactions in model organisms constitute a potentially invaluable source of *in vivo* interaction data for systems biology provided that throughput and speed can be increased. For example, the BioGRID database currently contains approximately 53,000 genetic interactions compared to almost 100,000 physical interactions (Stark et al., 2006). On the experimental side, the first direct large-scale protein interaction data were presented in 2000 (Ito et al., 2001); both studies used yeast two-hybrid technology. Two years later, the first large-scale protein complex purification data sets were published.

The recently developed RNA interference (RNAi) technology has created an unprecedented opportunity which allows the function of individual genes in whole organisms or cell lines to be interrogated at genome-wide scale. Therefore, a genome-wide or even large-scale screening approach and side by side the computational predictions and/or annotations of gene-gene or gene-pathway associations, simultaneously both are biologically meaningful (Aerts et al., 2009). However, multiple issues, such as off-target effects or low efficacies in knocking down certain genes, have produced RNAi screening results that are often noisy and that potentially yield both high rates of false positives and false negatives (Wang et al., 2009). By analyzing 24 genome-wide RNAi screens interrogating various biological processes in *Drosophila*, Wang et al found that RNAi positive hits were significantly more connected to each other when analyzed within a protein-protein interaction network. Based on this finding, Wang et al developed a network-based approach to identify false positives (FPs) and false negatives (FNs) in these screening results. Using two genome-wide RNAi screens and integrating

these screening results with protein-protein interaction (PPI) network extensively validated this approach from multiple aspects (Wang et al., 2009).

Keeping in view the practical application of the genome-wide RNAi screening data we have also generated a protein-protein interaction network using different web based sources. An interaction network of all the candidate genes have been presented in the manuscript which is, in fact centrally based on dS6K-dependant growth.

Chapter 2

Materials & Methods

2.1 - RNAi screen for regulators of steroidogenesis at the ring gland

The transgenic RNAi male flies were generated through P-element insertion carrying a *white* gene (P{w⁺, UAS-RNAi}) which gives red color eyes (NIG, Japan). During preparatory step, the UAS-RNAi males were first crossed with double balancer flies (Sp; MKRS/SM5-TM6B). This double balancer line consists of the genetic markers for larvae, pupae and the adults. The red eye colored (Pw⁺) UAS-RNAi males with Cyo wing phenotype and carrying tubby marker (UAS-RNAi/ SM5-TM6B) were crossed to virgin *Phm*-Gal4 flies at 25°C. By using *Phm*-Gal4 line, Gal4 is expressed under the control of the promoter of *phantom* gene in the steroidogenic cells of the ring gland which permits the expression of RNAi in these cells. Hence, the individuals of the following cross give rise to the expression of an RNAi restricted to the steroidogenic cells of the ring gland. The UAS-mCD6;GFP was also used simultaneously as a marker to the cells where the Gal4 has been expressed. The *Phm*-Gal4 line was also balanced by SM5-TM6B; therefore, the heterozygotes *Phm*-Gal4/ UAS-RNAi would lose the

larval/pupal phenotype and could easily be analysed for the phenotype of developmental arrest and hence, looking for candidates potentially involved in the process of steroidogenesis.

2.2 - RNAi screen for regulators of lipid metabolism at the fat body

Initially, for the screening at fat body; 4-5 UAS-RNAi males were crossed to seven virgin females of *ppl-Gal4/UAS-LSD2-GFP* at 25°C, and let these flies laying eggs for 2 days. Five to six days AED (after egg deposition), third instar feeding larvae were collected and transferred to small petri-dishes with fresh food and let them feeding for at least 4 hrs. under optimal conditions. Full fed third instar larvae were then dissected and the fat body was collected quickly on slides for microscopic analysis using both normal and fluorescent light.

For “flip-out” clones (Struhl and Basler, 1993) in the larvae by using heat shock promoter (*hsflp*), the UAS-RNAi males were crossed with flip-out flies and 24-48 hrs. later, the tubes were heat shocked for 12 minutes at 37°C. After 5-6 days of egg laying, the third instar larvae were transferred to new food media in petri-dishes for feeding of 4 hrs. The fat body was then dissected in saline buffer and analysed under microscope for lipid droplet phenotype using fluorescent light. The selected candidate genes were further analyzed through a starvation of overnight. For this purpose, the third instar larvae were put into 10% sucrose solution for overnight (at least 12 hrs.) and then dissected for phenotypic analysis of lipid droplets.

2.3 - Lipid droplet staining

Nile red was reported as a selective fluorescent stain for the detection of intracellular lipid droplets by fluorescent microscopy (Greenspan and Yudkovitz, 1985). Dissection of the fat body was carried-out in PBS (immediately collected in microtiter-plate on ice (PBS), the GFP discs were protected from light as much as possible). Fixation was performed in 20 % paraformaldehyde (PFA) (in PBS) at Room Temp. for 20 min. After

removing the fixation solution, Nile red was added to the secondary antibodies solution in dilution 1:1000 (Bulankina, 2003). To visualize the nuclei, DAPI (0.2%) was also added. After, the fat body was washed with PBT as well as PBS respectively. Then pipetting with the cut-end tip, the fat body was mounted on slides by using citiflour and used quickly for phenotypic analysis or stored at 4°C.

Oil Red O (ORO) staining was also performed as a visual marker to evaluate the lipid droplet contents of the fat body cells. Dissection of the fat body was carried-out in PBS (1X) and fixation was done in paraformaldehyde (4% in PBS) in PBS at Room Temp. for 10 min. After removing the fixation solution, the specimens were rinsed twice with distilled water, incubated for 20 to 30 min in Oil Red O stain (6 ml of 0.1% Oil Red O in isopropanol and 4 ml distilled water: prepared fresh and passed through a 0.45-mm syringe filter) (Gutierrez et al., 2007). Stained fat body was mounted in citiflour and scored for lipid droplet phenotype quickly or stored at 4°C.

2.4 - RNAi screening for negative regulators of dS6K-dependent-growth

To screen for negative regulators of dS6K-dependent growth, 6-7 virgins of *ap-Gal4>UAS-dS6K* line were crossed with 4-5 UAS-RNAi males. All the crosses were done at 25°C. The selected candidate UAS-RNAi lines were re-crossed with *ap-Gal4>UAS-dS6K* and *ap-Gal4* flies both at 25°C and 29°C. Notably, the UAS-RNAi males were crossed to *ap-Gal4* line to eliminate an RNAi line which itself gives an effect. The analysis of the wing phenotype of all the crosses of UAS-RNAi lines were made very carefully by using normal microscope (Leica MZ 6).

2.5 - Fly strains used during the study

The following alleles or transgenic lines were used: W^{1118} , *ap-Gal4>UAS-dS6K/CyoGal80*, *ap-Gal4/CyoGal80*, *UAS-dS6K/SM5-TM6B*, *ago¹FRT80B/TM6B*, *ago³FRT80B/TM6B*, *ago¹Df(3L)H99,FRT80B/TM6B*, *ago¹hid⁰⁵⁰¹⁴*, *FRT80B/TM6B*,

ey-Gal4, *Da-Gal*, *act-Gal4*, *ppl-Gal4*, *ppl-Gal4>LSD2-GFP*, *eyFLP;ey-Gal4*;"M"-
FRT80B/SM5-TM6B, *hs-flp;α-tub>FRT-stop-FRT>UAS-GAL4-UAS-GFP/SM5-*
TM6B, *α-tub>dS6K/Cyo*, *α-tub>dS6K/TM3*, *α-tub>dS6K;ago¹FRT80B/SM5-TM6B*, *α-*
tub>dS6K;ago³FRT80B/SM5-TM6B, *α-tub>dS6K;ago^{RNAi}*, *ago^{RNAi};α-tub>dS6K*, 16989
(w¹¹¹⁸;P{EP}ago^{EP1135}/TM6B, Tb), 20064 (*yw;P{EPgy2}ago^{EY01092}/TM3*, SbSer),
20064/SM5-TM6B, *FRT-20064*, *UAS-dS6K;ago^{RNAi}/SM5-TM6B*, *UAS-*
dS6K;ago³FRT80B/SM5-TM6B, *UAS-dS6K;ago¹FRT80B/SM5-TM6B*, *UAS-*
dS6K;ago¹Df(3L)H99FRT80B/SM5-TM6B, *dS6Kago¹FRT80B/SM5-TM6B*,
dS6Kago³FRT80B/SM5-TM6B, *dS6Kago¹Df(3L)H99FRT80B/SM5-TM6B*, *dS6K*
ago³Df(3L)H99FRT80B/SM5-TM6B, *ago^{RNAi};UAS-dS6K^{STDE}*, *UAS-dS6K^{TE};ago^{RNAi}*,
UAS-dS6K^{STDETE};ago^{RNAi}, *α-tub>dS6K;ago¹hidFRT80B/SM5-TM6B*, *α-tub>dS6K;*
ago¹H99FRT80B/SM5-TM6B, *α-tub>dS6K;H99FRT80B/SM5-TM6B*, *ap-Gal4> UAS-*
dS6K^{TE}/CyoGal80, *ap-Gal4> UAS-dS6K^{STDETE}/CyoGal80*, *ap-Gal4;UAS-*
dS6K^{STDE}/CyoGal80, *Sp;MKRS/SM5-TM6B*, *w¹¹¹⁸;P{Ubi-*
GFP(S65T)nls}3LP{neoFRT}80B/TM3, Sb (stock: 5630), *w¹¹¹⁸;P{neoFRT}82BP{Ubi-*
GFP(S65T)nls}3R/TM6B, Tb (stock: 5628), *Sco/CyotubGal80*, *yw;TM3/TM6GFP*,
Sp/Cyo;MKRS/TM6B.

For RNAi screening, UAS-RNAi lines were used from NIG Japan; and for further experiments, RNAi lines were ordered from VDRC. Flies were balanced using double balancer *yw; Sp; MKRS/SM5-TM6B* for subsequent crosses.

2.6 - Immunostaining

Dissection of the discs/tissues was carried-out in PBS (immediately collected in microtiter-plate on ice (PBS), the GFP discs were protected from light as much as possible). Fixation was performed in 4% Formaldehyde in PBS at room temp. (RT) for 30 min. After washing of discs with PBT at least 3 times for about 10 min each, permeabilisation and blocking for 40 min at RT with PTF were done. Following immediately, incubation with PTF diluted primary antibody was carried out for overnight at 4°C. Then the discs/tissues were washed 2-times with PBT for 5-10 min, following 1-wash for 5 min at RT with PTF and 1- wash for 5-10 min at RT with PBT were carried

out. Then incubation with secondary was performed for 2 hrs at RT (0.1% PTF + 2/100 DAPI + 1/500 Ab). TOPRO-3 (diluted in DABCO) was also used to stain the nucleic acid. The tissues/discs were washed 3-times with PBT and at the last kept in PBS at RT. The mounting was done in citiflour and kept at 4°C for microscopic analysis.

The following primary antibodies were used: anti-dS6K (rabbit, 1:50) (Montagne, 1999 #8), Anti-dS6K P (Cell Signaling Technology®), anti-βgal (rabbit, 1:200, DSHB), anti-GFP (mouse, 1:500, Roche Cat: 11814460001) and anti-Gal-4 (mouse, 1:200; Abcam). Secondary Antibodies included Alexa 488 (anti-rabbit, Invitrogen: A-11078), Alexa 488 (goat anti-mouse, Invitrogen: A-21121), Alexa 568 (goat anti-rabbit, Invitrogen Lot: 633962A) and Alexa 594 (anti-rabbit, Molecular Probes: A-21441).

2.7 - Eye/thorax measurement:

Eyes and thorax of flies were photographed with a microscopic attached camera (Leica MICRO MECANIQUE), and then were redrawn with Adobe Photoshop. The pixel sizes were counted for eye and thorax separately for each fly by CoralDraw Graphics Suit 12. Males and females were photographed and measured separately.

2.8 - Microscopy

The lipid droplet phenotype was always analyzed using “objective” of 40X magnification with a drop of Oil (Zeiss Immersol 518F) at camera-fitted Leica fluorescence microscope (Leitz DMRD). The images were imported into Adobe Photoshop, assembled and converted to merged ones. For confocal microscopy (Nikon; Eclipse TE2000U), preferably an objective of 60X magnification was used with a drop of oil (Zeiss Immersol 518F). But in some cases, to better visualize the slides, an objective of 100X magnification was also used with a drop of oil. An average of at least 3 images, along with 1 μm size of each stack was performed. The images were imported into ImageJ and Adobe Photoshop, then assembled and converted to merge images accordingly.

2.9 - Protein-protein interaction network data analysis

To generate a protein-protein interaction signaling network, two main websites “BioGRID^{3.0}” (Biological General Repository for Interaction Datasets) and “BOND^{OA}” (Biomolecular Object Network databank) were used (<http://thebiogrid.org/>; <http://bond.unleashedinformatics.com/>). Both of these websites contain a huge protein-protein interaction database based on yeast-two-hybrid assay. There are different enhancer/suppression interactions of the proteins which exist at these websites. For the reconstruction the dS6K-based growth networking pathway, only the physical interactions of the selected candidate genes were scored.

2.10 - Quantitative PCR (q-PCR)

For RNA extraction, twenty 20 adult flies were collected in a 1.5-ml eppendorf tube (with lid) with 100 μ l beads and placed at -20°C . After thawing on ice, 500 μ l of TRIZOL[®] Reagent was added to each tube and homogenized for 30 s by Precellys 24. The samples were incubated at room temperature for 5 min., then 100 μ l of chloroform was added and vortexed for 2×30 s. The samples were centrifuged at $12,000 \times g$ for 15 min at 4°C . The supernatant was collected (250 μ l, aqueous phase) in a clean tube. Then 250 μ l of isopropanol (stored at room temperature) was added to precipitate RNA and mixed gently by inverting the tube three times. The samples were then centrifuged immediately at $12,000 \times g$ for 15 min at 4°C . The supernatant was removed by inverting the tube and the RNA pellet was washed with 400 μ l 70% ethanol (room-temperature) and centrifuged at $12,000 \times g$ for 10 min at 4°C . The supernatant was poured without disturbing the pellet, and then the pellet was air-dried for about 10 min. and finally redissolved with 50 μ l of water. The RNA concentration was determined using UV spectrophotometry (Romeo and Lemaitre, 2008).

For cDNA synthesis, filter tips were used to prevent contamination of the samples by foreign amplicons. The reverse transcription was performed in a 20 μ l final volume. For each experiment, two control samples were included: one without RNA and the other without Superscript-II (SSII-RT; Invitrogen). The followed protocol was: In a clean 0.2-

ml PCR tube add: RNA (500 ng/ μ l) 2 μ l, Random hexamers (50 ng/ μ l) 2 μ l, dNTPs mix (10 mM) 1 μ l, H₂O 7.5 μ l, denature samples at 65°C for 10 min., Quick-chill on ice and centrifuge briefly. In each tube add: 5 \times SSII-RT buffer 4 μ l, Dithiothreitol (DTT) (0.1 M) 2 μ l, RNaseOUT™ RRI 0.5 μ l, SSII-RT 0.5 μ l, Place the tubes in a thermal cycler (heated lid at 70°C) and run the following: Incubate at 42°C for 50 min., Denature at 60°C for 15 min. Dilute RT products to 1/20 in water and store diluted RT products at –20°C (Romeo and Lemaitre, 2008).

For RT-PCR and gene expression quantification, the experiment was performed in 10- μ l plates using the LightCycler® 480 System. A control sample containing water was included instead of RT product. The following PCR master mix was prepared for each sample: Light cycler® 480 SYBR Green I master 5 μ l, forward primer 100 μ M 0.125 μ l, reverse primer 100 μ M 0.125 μ l, PCR-grade H₂O 2.5 μ l. In each plate -96 PCR master mix 8 μ l and diluted RT product 2 μ l was added. The following program was followed using the LightCycler® 480SW 1.5: denaturation: 95°C for 10 min., Cycling repeated 40 times: 95°C for 10 s, 60°C for 15 s, 72°C for 20 s, melting curve: 95°C for 5 s, 60°C for 5 s, 72°C for 15 s, 70°C→95°C with 0.1°C/s ramping ((Romeo and Lemaitre, 2008)). The absolute quantification was monitored using the LightCycler® software and the gene expression level (R) was calculated as described by Romeo and Lemaitre (Romeo and Lemaitre, 2008).

2.11 - Western blotting

Protein extraction was performed as follows: L2 larvae of *ago*^{RNAi} were collected and transferred to a fresh food and left feeding until they reached to L3. Full fed L3 larvae were collected in PBS and transferred to 1.5 ml eppendorf tubes. *ago* mutants are lethal at early larval stage, and we were able to find L2 transheterozygotes (*ago*^{1/ago}³), therefore L2 larvae were collected for protein extraction. Batches of 50 larvae were prepared and immediately put into liquid nitrogen. The larvae could be stored in liquid nitrogen for weeks (Radimerski, 2002). Extraction of protein was done by adding a 400 μ l of protein extraction buffer (Extraction buffer, EB: (NaCl 120mM, Tris 50mM, NaF 20mM, Benzamidine, EDTA 1mM, EGTA 6mM, PPI 15mM, NP-40 (nonidet-p40) (1%)

2 ml make up vol. upto 180 ml and adjust to pH6.8 with 4M HCl, sterile filter)(Protein Extraction buffer 10 ml: EB 800 μ l, Complete inhibitor 200 μ l (mini tablet: 1 tablet in 1.4 ml EB), Pepstatin 3-4 μ l (-20°C; 1.4 mg in 1ml EtOH), Aprotinin 10 μ l (0.2 mM stock), Leupeptin 2 μ l (2mM stock), PMSF 3 μ l (protease inhibitor; 100mM stock in 100 EtOH), Pnpp 30 μ l (1M in EB) stock (phosphatase inhibitor), β -glycol 30 μ l (1M in EB) stuff (phosphatase inhibitor) directly to the frozen larvae and squashed with a plastic pestle fitting the eppendorf tube. Cell debris was removed by centrifugation at 14000 rpm for 8 min at 4°C. The supernatant was transferred to a new eppendorf tube and 5 μ l kept aside for Bradford. Laemmli buffer (4X stock) (Tris 2.5ml (0.25M); pH:6.8, SDS 0.8g (8%), β -mercaptethanol 2ml (20%), Glycerol 5.5ml (60%), Bromophenol blue 0.02%) was added to the supernatants (1:3) and kept at 95°C for 5 min. and then stored at -20°C.

Electrophoresis was conducted at 30 mA in an electrophoresis tank in 1X running buffer (5X stock: Tris base 15.1g (25mM), Glycerine 94g (250mM), SDS 50ml (10%), water 950ml). Proteins separated by SDS-PAGE were then transferred onto nitrocellulose membrane for western blot analysis. Eight pieces of whatman paper (10"x10"cm) and one piece of nitrocellulose membrane were prepared. Four sheets of whatman paper immersed in the blot buffer (methanol 200ml, glycerine 2.93g, Tris base 5.81g, SDS 0.37g, water to make up vol. 1L) and placed in the chamber. The gel was also soaked in the blot buffer before placing on the paper. Then the membrane dipped in the blot buffer was placed on top of it and the air bubbles were removed. Another whatman layer of four sheets was dipped in the buffer and placed on top of the gel. A glass pipette was rolled on top of the stack to remove air bubbles. The proteins were transferred onto the membrane using 10mA current for 90 min. After the transfer, membrane was briefly washed with PBS, incubated in PBST (PBS 1X, 0.5% Tween) containing 5% milk powder for 1 hour at room temperature to block all non-specific interaction sites on the membrane. After blocking, the primary antibodies diluted in PBST, were added onto the membrane and incubated overnight in the cold room (constantly vortexing at low speed). The non-specifically bound antibody was washed off by incubating the blot with PBST, changing the buffer once every 10 min for three times. The membrane was then subsequently incubated with the respective secondary antibody coupled to horseradish

peroxidase for 1 h at room temperature and washed again 5 times for 5 min. The nitrocellulose membrane was incubated at room temperature for 1 min in enhancer and peroxide solutions mixed in a 1:1 ratio (enhanced chemoluminescent kit; PIERCE). The membrane was wrapped in a polythene sheet and signals were detected accordingly.

2.12 - *Drosophila* cell culture

RNAi assays in S2 cells were performed in the following way. Double stranded RNA (dsRNA) molecules were synthesized by *in vitro* transcription from PCR generated templates having a T7 promoter attached to both ends (T7 MEGAscript Kit (Ambion)). The length of the RNA molecules ranged to 500 base pairs. We followed the protocol of Ramadan et al. during the whole experiment (for detail see Ramadan et al., 2007). We used exponentially growing S2 cells in Schneider's *Drosophila* medium (Sigma) with serum and placed 500µl of them in 12-well plates at the final concentration of 4×10^5 cells/ml along with 4 µg of dsRNA per well. Then, after 3 days of incubation; 500 µl of new medium was added with serum and without serum concomitant with 4 µg of dsRNA per well. The cells were serum starved for one day. At the 4th day, cells were harvested and washed with PBS 1X. The cells were lysed for protein extraction (Radimerski et al., 2002a). Protein concentration was estimated using a spectrophotometer and the Bradford assay with a kit from BioRad. The proteins were resolved through SDS-PAGE and transferred to a nitrocellulose membrane. Western blot assay was performed using antibodies against dS6K, P-dS6K and secondary anti-rabbit IgG, separately (see above). After reaction using enhanced chemoluminescent kit (PIERCE), the signals were detected by LAS3000 (Fugifilm apparatus) and processed accordingly.

Chapter 3

Results

3.1- Project goals

The cellular growth in response to nutrition is centred on TOR kinase, which in turn modulates protein translation machinery, and ribosome biogenesis. With an increase in growth, there is increasing demand of energy which is produced through metabolism. Finally, the *Drosophila* TOR signaling pathway also controls the developmental timing through the regulation of the synthesis of steroid hormone ecdysone, which controls larval developmental steps. Therefore, the whole research activities of our group are linked to growth, development and entangle also to the metabolism. To better understand the mechanisms of regulation of these three processes in *Drosophila*, we took advantage of the availability of RNAi collections of the National institute of Genetics (NIG, Japan), and embarked on a saturating screening project. Three different strategies were designed:

1. *RNAi screening for novel regulators of steroidogenesis*
2. *RNAi screening for regulators implicated in lipid metabolism*
3. *RNAi screening for negative regulators of dS6K-dependent growth*

Although I was also involved in the preparative steps of the first screen, but my PhD work mainly concerned with the two latter screens. All these three screens are directly or partially linked to the TOR signaling pathway.

When the larvae have reached a minimum viable weight, they possess sufficient nutritional stores to undergo metamorphosis. The transition from feeding and growth to pupariation at the onset of metamorphosis is triggered by the production of a peak of ecdysone in the prothoracic gland (PG). The TOR kinase has been proposed to constitute the physiological node between nutritional status and ecdysone production, since its inhibition through over-expression of the tumor suppressor TSC1/TSC2 in the PG causes a delay in developmental timing and organismal overgrowth (Layalle et al. 2008). In order to explore the systemic control of developmental steps mediated by ecdysone, our RNAi screen (1) is aimed to find-out novel regulators of steroidogenesis in *Drosophila*.

Microarrays approaches recently showed that the TOR signaling pathway regulates the expression of genes encoding enzymes of lipid metabolism (Li et al., 2010). Consistently, metabolic studies in *Drosophila* revealed that the TOR kinase directly controls lipid metabolism, as its down-regulation induces an increase of the size of the lipid droplets (LDs) in the fat body, a phenotype that is also observed following starvation (Colombani et al., 2003). Therefore, in another screen (2), we focused our attention to recapitulate the starvation induced lipid droplet phenotype using the UAS-RNAi lines to find out novel regulators of lipid metabolism.

A well-known direct target of TOR is the S6 kinase, whose *Drosophila* homologue (*dS6K*) has been described to be a regulator of size gauging (Montagne et al., 1999). A genetic screen for positive regulators of dS6K has been successfully performed in our laboratory using a sensitized dS6K-dependent growth, leading to the identification of a novel positive regulator of growth (Montagne et al., 2010). Our genome-wide screen (3) to identify novel negative regulators of dS6K-dependent growth followed the same strategy using the RNAi collection.

In the following sections, first I would like to describe our general screening plans in order to compare these in discussion; and the percentage of positive hits which has

been retain through each strategy. With that respect, the screen at the PG will be described first, since I have been involved only in the preparative steps. I will then present the results of the screen at the fat body and eventually expose the screen for dS6K negative regulators. The last section will concern the detailed studies that we performed for the most relevant negative regulator of dS6K-dependent growth.

3.2 - RNAi screening procedure

To carry out a genome-wide RNAi screen, the drosophila fly stock had been received regularly from the RNAi library of NIG, Japan. The inducible RNAi lines are expressed under UAS/Gal4 system and carry a P-element containing a w^+ gene as a visible eye marker. Because this P-element (P{ w^+ , UAS-RNAi}) was randomly inserted on chromosomes, different types of eye colours could be observed, i.e., ranging from yellow, orange or red eyes. It is to mention that mostly the P-element was inserted on 2nd or 3rd chromosome. Very rarely, we received few RNAi lines with P-element inserted on X-chromosome or on 4th chromosome. Out of all, many of the UAS-RNAi lines were homozygous viable and also few were not stably balanced. Therefore most of the homozygous lethal lines and ill-balanced RNAi lines were established in front of a balancer chromosome.

As the phenotype screened for dS6K-dependent growth was analyzed in adult flies, the inducible RNAi male flies from the NIG stock were directly crossed to the corresponding virgin females, which contain a Gal4 transgene to induce both dS6K and the RNAi simultaneously in the dorsal compartment of the developing wing (Fig. 17). In contrast, the two other screened phenotypes were analyzed in larvae. Therefore, to ascertain for the expression of an RNAi, we made use of a visible larval marker; by crossing first the UAS-RNAi males with virgin females carrying the combined balancers on 2nd and 3rd chromosomes (SM5-TM6B). For both screens, the offspring males carrying the UAS-RNAi in front of the combined SM5-TM6B balancers were then crossed to the corresponding virgin females (Fig. 18). This way, the *Tubby* marker that labelled the combined SM5-TM6B balancers served as a tracker to select those larvae which express the RNAi.

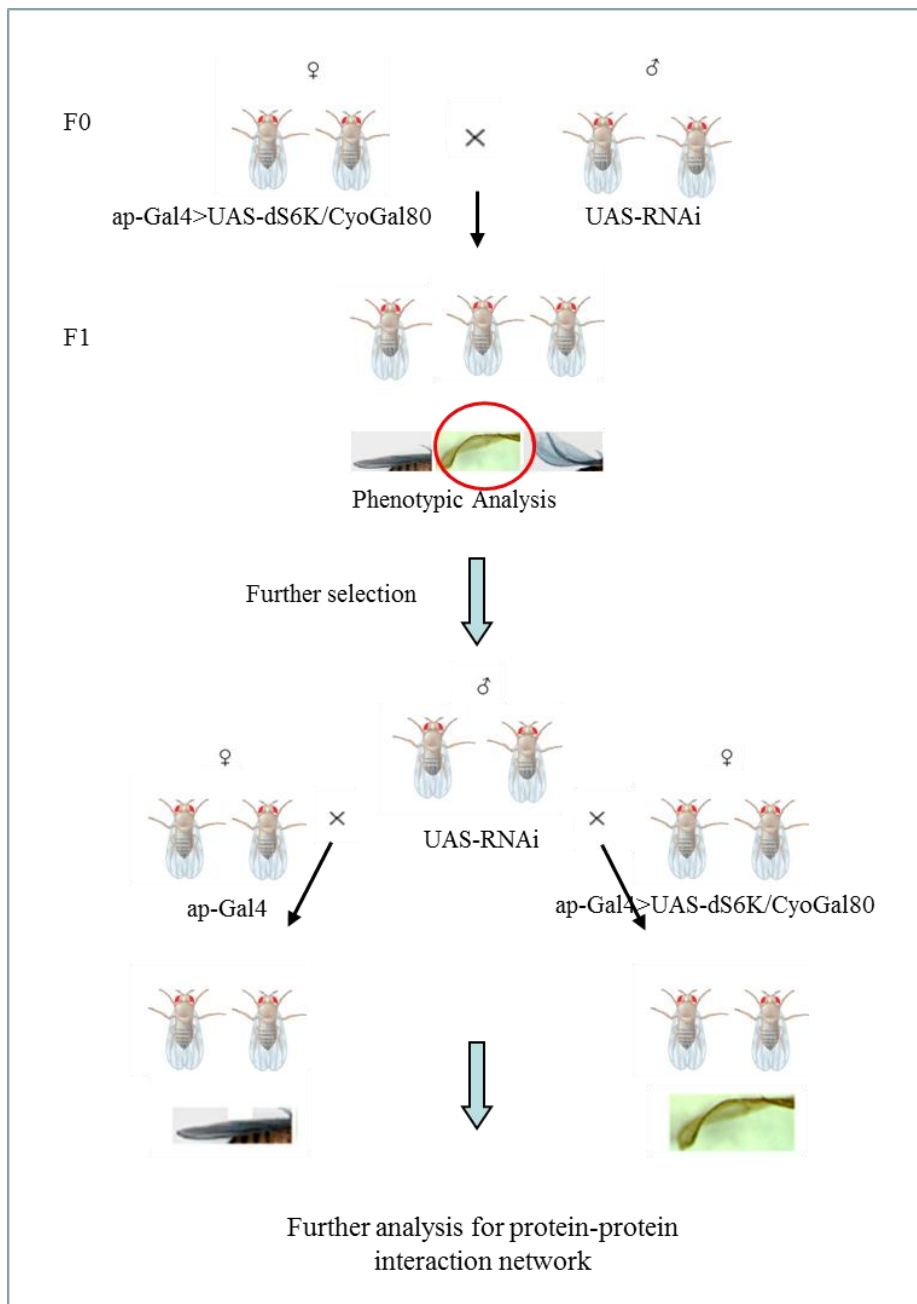


Figure 17 - Schematic diagram of the genome-wide RNAi screen for novel regulators of dS6K-dependent growth

(Top) Males carrying the inducible RNAi (*UAS-RNAi*) were crossed to virgin females of the genotype *ap-Gal4,UAS-dS6K* (F0 flies). The offspring (F1 generation) was scored for the enhancement of the adult bent-down wing phenotype. (Bottom) The corresponding lines were tested second time (right) and further analyzed to discard the RNAi lines that produced a bent-down of the wing when induced alone (left). The selected candidates were further used to generate an interaction network.

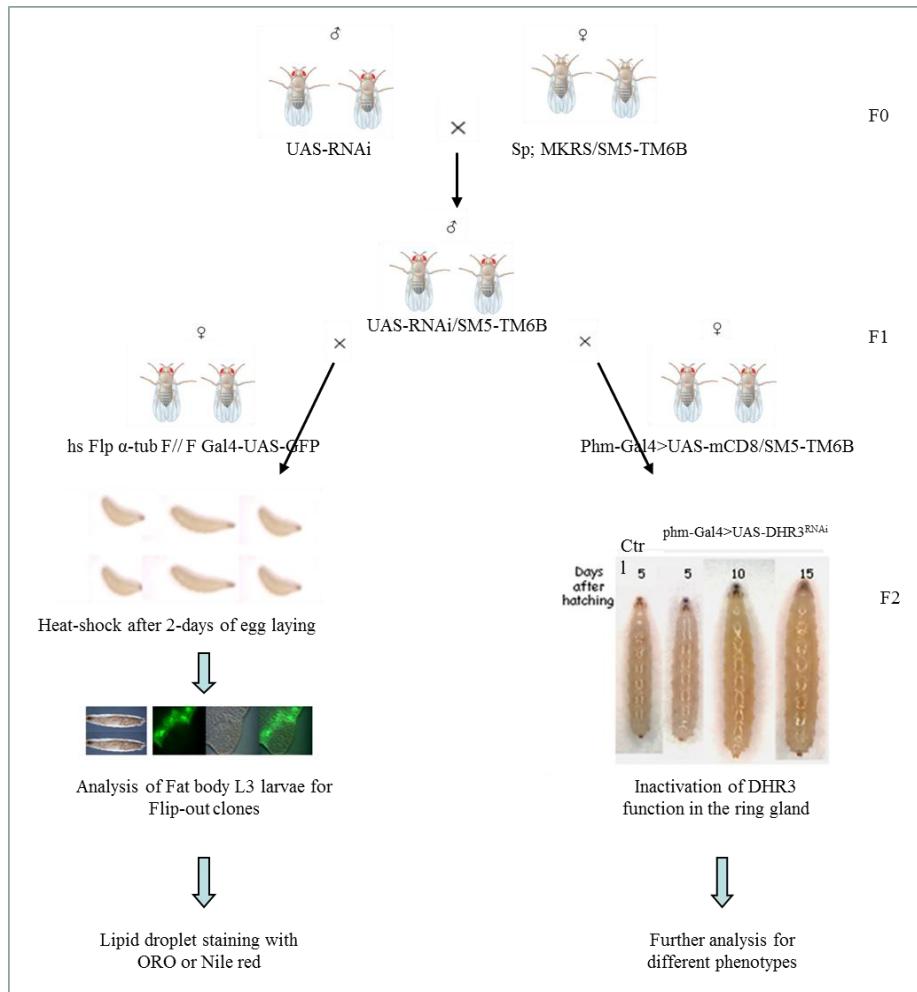


Figure 18 - Schematic diagram of the genome-wide RNAi screen for novel regulators of lipid metabolism and steroidogenesis

The inducible RNAi males (UAS-RNAi) were crossed to virgin females of Sp;MKRS/SM5-TM6B double balancer flies (F0). The balanced RNAi males (UAS-RNAi/SM5-TM6B) were crossed separately to the corresponding virgin females expressing Gal4 (F1) either in the steroidogenesis organ (*phm* screen) (right) or in randomly induced clones (lipid metabolism screen) (left). The phenotypes of the *Tubby*⁺ larvae, pupae and/or adults were analyzed carefully during screening for steroidogenesis (F2). For lipid metabolism screen, the tubes were heat-shocked after two days of egg-laying. At the 5th day, the *Tubby*⁺ L3 larvae were dissected for lipid droplet analysis in the fat body (F2). The fat body for the positive candidates was then stained with ORO (oil red O) or Nile red for further analysis of lipid droplet phenotype.

3.3 - RNAi screening for novel regulators of steroidogenesis

In *Drosophila*, nutrition modifies the timing of development by acting on the production of the ecdysone at the PG, a process that is in part controlled by the neurohormone PTTH (Prothoracicotropic hormone) (Gilbert et al., 2002), which may regulate TOR signaling (Layalle et al. 2008). Ecdysone signaling actually triggers a cascade of nuclear receptors and we recently observed that specific RNAis to these receptors also impede the progression of the developmental steps, a phenotype that could be suppressed by feeding ecdysone (Parvy et al, unpublished results). Therefore, we performed a genome-wide RNAi screen to find-out new regulators participating in the production or secretion of Ecdysone and ultimately regulating the steroidogenesis in drosophila. The transgenic RNAi lines were expressed in the steroidogenic cells of the ring gland using *phm*-Gal driver. However, as the phenotype had been followed during larval development, the RNAi transgenes inserted on second or third chromosomes were first balanced over the combined SM5-TM6B balancers. My contribution to this screen concerns this preparative steps, since SM5-TM6B balanced males were also used in the screen for LD size described below. Nonetheless, I briefly describe this; also I will present a comparative analysis for screening procedures in the discussion section. Following the crosses with the *phm*-Gal4 driver, *Tubby*⁺ larvae, which correspond to the bone fide animals to score, were carefully analyzed. A total of about 11,000 inducible RNAi lines were screened, predicted to approximately 7,000 genes corresponding to roughly half of the genome of *Drosophila melanogaster*. This way, more than 620 candidate genes were retained, as their RNAi induced a phenotype ranging from early developmental arrest to extension of growth period and eclosion of giant adults. All these candidates were then classified into 15-different groups regarding their annotated functions at flybase (Fig. 19A), or into 9-different phenotypic groups regarding the stage of developmental arrest (Fig. 19B). Identification of RNAi to genes previously described to regulate steroidogenesis were also found in the screen, i.e. *ras* (Caldwell et al. 2005), which makes a confirmation to the efficiency of the screen for potential candidates regulating steroidogenesis. Beside a high number of unknown genes, the selected candidates fall into several functional groups which govern basal cellular activity: metabolism, signaling, chromatin structure,

transcription, translation and protein maturation. A few of these candidates concerned with steroidogenesis or intracellular trafficking are rather directly linked to ecdysone production or secretion, as the process of synthesis takes place in various sub-cellular compartments. Neither the significance of the observed phenotypes, nor the function of the selected candidates will be further discussed, since it was not the focus of my PhD work. The comparative analysis for screening procedures will mostly concern the number of candidate genes identified, regarding the screening strategy.

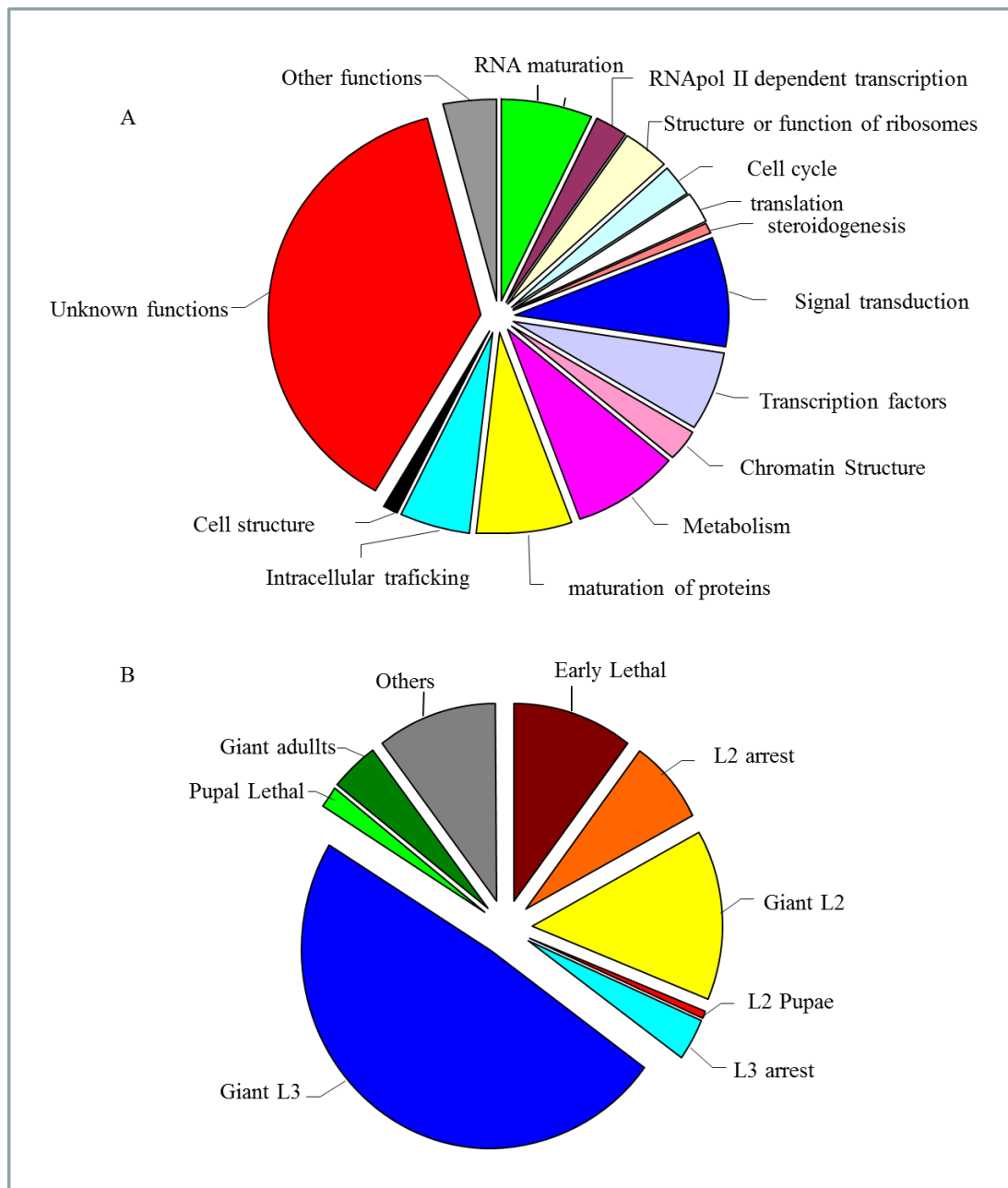


Figure 19 - The phenotypic classification of the Phm screen

(A) The 620 candidate genes retained in the screen for regulators of steroidogenesis were categorized into 15 sub-groups regarding their biological functions. The largest sub-group represents genes, which have not been annotated yet. (B) The observed phenotypes were categorized into 9 sub-groups. Formation of the giant third instar larvae (L3) was the most frequent phenotype found in the screen. The different other indicated phenotypes are described in the text.

3.4 - RNAi screening for new regulators of lipid metabolism

When drosophila larvae are fully fed, they accumulate lipids in fat body cells (Britton et al., 2002; Scott et al., 2004). Under starvation conditions, the stores of lipids in the fat body cells are remobilized, which results in an increase of the size of LDs (Juhász et al., 2003; Rusten et al., 2004; Gutierrez et al., 2007). Interestingly modulation of a number of growth or metabolic regulators phenocopies the starvation induced phenotype in the fat body (Colombani et al., 2003; Hietakangas and Cohen, 2009; Britton et al., 2002; Beller et al., 2008). Therefore, taking advantage of the UAS-RNAi library from NIG, we screened these lines to identify novel regulators of lipid storage and metabolism at the fat body of 3rd instar larvae.

As for the screen for ecdysone production at the PG described above, the screened phenotype was monitored in larvae and thus the UAS-RNAi inserted on the second or the third chromosomes were first balanced in front of the combined SM5-TM6B balancers (Fig. 18). Initially, the RNAi transgenic lines were expressed within the entire larval fat body using the *ppl*-Gal4 driver, combined to an UAS-LSD2-GFP transgene. Because the LSD2-GFP fusion protein surrounds the LDs, the green fluorescence served as a read-out to score the characteristic LD phenotype (Fig. 20). Fat body of third instar larvae were dissected and directly analyzed under light and fluorescent microscopes. We analyzed the phenotype of LDs both under full fed as well as under starvation conditions. This way, using the *ppl*-Gal4 driver line, we selected candidate genes, which displayed various types of phenotypes, i.e., small, large, medium sized LDs, scattered, oblong and spherical shaped LDs (data not shown). However, it was laborious and time consuming as we always needed an external control for each set of dissection, while the number of selected UAS-RNAi lines were also increasing. Approximately, seventy five UAS-RNAi lines were selected out of total of four hundred fifty lines, the phenotype of which finally appeared to be poorly relevant (data not shown).

Considering that too many genes were selected using the *ppl*-Gal4 driver, we switched to the flip-out strategy. In this setting, a silent Gal4 transgene is induced by an Flp/FRT-dependent recombination to generate random marked clones that expressed UAS-GFP and UAS-RNAi together. Clones within the fat body, were obtained by a

37°C heat-shock treatment to induce the *Flp* recombinase in 24-48 hrs old larvae (α -tub>FRT-w⁺ STOP-FRT>Gal4, UAS-GFP) and analyzed 3 days later. This process induces recombination between the FRT sites and removes the w⁺ STOP cassette in clones, thus allowing the expression of Gal-4 to activate the UAS-GFP and the UAS-RNAi transgenes simultaneously. The technique was advantageous, since the LDs of the UAS-RNAi expressing clones (GFP positive cells) could be directly compared to the LDs of the neighboring cells as internal control (GFP negative cells). Moreover, we performed a pilot experiment using a transgenic RNAi line to *Rheb* (*Ras* homolog enriched in brain) to check the feasibility, and to improve the specificity of our screening. Consistent with its function as an activator of the TOR/S6K signaling cassette (Saucedo et al., 2003; Stocker et al., 2003), the clonal expression of *Rheb*-RNAi provoked a dramatic increase in the size of LDs coupled to a decrease in LDs number (Fig. 21). In nutshell, the flip-out technique was found to be more efficient and faster to screen for regulator of lipid metabolism and of the TOR/S6K pathway as compared to the strategy using the *ppl-Gal4* driver. Our pilot experiment through the flip-out technique gave a break-through and a sound basis to our screening scheme; therefore, we also re-screened the already selected candidates using *ppl-Gal4* line.

Altogether, a total of 7,300 lines roughly corresponding to 4,000 distinct genes were screened-out and scored only for an increase in LD size. This way, twenty four (24) candidate lines were found to slightly modulate the LD phenotype (Fig. 22; Table 2). The selected lines were further analyzed through Nile Red or Oil Red O (ORO) staining to visualize the lipid droplets phenotypes in more detail, but did not further improve the selection (data not shown). For most of the RNAi lines retained, we observed a decrease of number of LDs concurrent to the increase in LD size of clonal cells, as compared to the surrounding control wild-type fat body cells. Few lines produced smaller sized LDs phenotypes and an increased number of LDs per cell (data not shown). Since the Vienna Drosophila Research Center (VDRC) also provides transgenic RNAi collection, the more significant candidates were further tested using this library. A major issue of the RNAi usage is the existence of “off-targets”, namely alternative genes, which may be affected by the RNAi. Considering that the template to produce the precursor dsRNA derived from a few hundred nucleotide genomic

sequence, this precursor can potentially produce many small interfering RNAs (siRNAs); some of these may affect an unexpected gene. The transgenic RNAi lines of VDRC were generated later and regarding the issue of off-targets, were designed to have much less potential unrelated hits. Therefore, we further analyzed our selected candidate lines using RNAi collection of VDRC.

This screen for modulator of LD size led to the identification of various candidate genes (Table 2): Eight of these encode enzymes of lipid metabolism (*sxe2*, *thiolase*, *start1*, CG3961, CG5122, CG4630, *cyp4g* and α/β hydrolase), three encode ribosomal proteins (*mRpS31*, *mRpS35* and *mRpL28*), four encode potential signaling molecules (*Pak3*, *twins*, CG2165 and *Rack1*) and four others encoded proteins involved in neurological activity (*Fasciclin2*, *period*, *dunce* and *RhoGAP93B*). Regarding the latter group, one candidate gene, *Fasciclin2* gene (*Fas2*) was found to produce a slightly larger sized lipid droplet phenotype (Fig. 23). Since three *Fasciclin* genes (*Fas1*, *Fas2* and *Fas3*) have been described in *Drosophila*, RNAi lines from VDRC that affect specifically each of these genes were tested. The fat body of third instar larvae expressing flip-out clones to each of these RNAi line was dissected and carefully analyzed for the phenotype of LDs both under full fed as well as starvation conditions. Strikingly, we did not find a larger sized lipid droplet phenotype compared to larger size of lipid droplets with RNAi to *Rheb*. However, an RNAi line to *Fas3* (CG5803) was found to produce a moderate increase of LD size, coupled to a decrease in LDs number (Fig. 23). These findings suggest that one of the *Fasciclin* genes might affect lipid metabolism to control the size of LDs. However, three other candidate genes affecting LDs size (*dunce*, *period* and *RhoGAP93B*) have been previously described to act on neuronal activity support the notion that some genes are involved in both processes of nervous system and lipid metabolism. Another gene, *Pak3* (CG14895) showed a slight increase in the phenotype of LDs compared to controls (data not shown). *Pak3* has been annotated to have a serine/threonine kinase activity acting as a signaling molecule. In addition, *Pak3* had also been found through an RNAi screen to cause an axon guidance defect and hence might be involved in the development of the nervous system (Winter, 2005). However, we tested an RNAi to *Pak3* from VDRC for

further analysis. A subtle modulation in LD phenotype was observed (data not shown), which need to be further analyzed.

It is worth noting that, none of the selected candidate lines did produce an LD phenotype as severe as the one induced by *Rheb*^{RNAi} (Fig. 21). Moreover, an RNAi screen in *Drosophila* S2 cells has been published by Guo et al. during the course of our screen. In this study, they searched for any kind of modulation in the LD phenotype and categorized these LD phenotypes into five distinct groups, and showed that about 1.5% of all the genes are involved in lipid-droplet formation and regulation (Guo et al., 2008). We, therefore, did not further continue screening at the fat body and concentrated on the other screen (see below in the corresponding section).

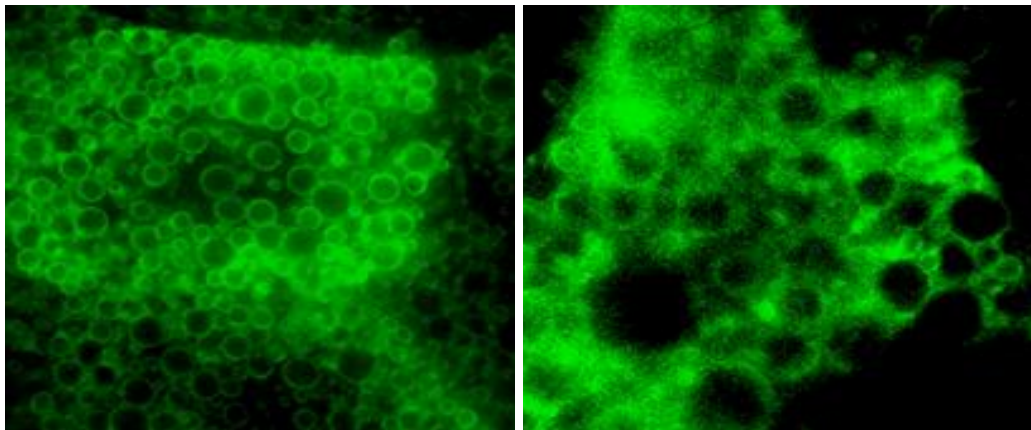


Figure 20 - Lipid droplets labelled with LSD2-GFP fusion protein

Variation of size of the lipid droplets labelled with an Lsd2-GFP fusion protein upon gene disruption by UAS-RNAi induced within the entire fat body. The ppl-Gal4>UAS-Lsd2-GFP were crossed to an RNAi that induced a decrease of LD size (left) as compared to a mock RNAi without consequence (right).

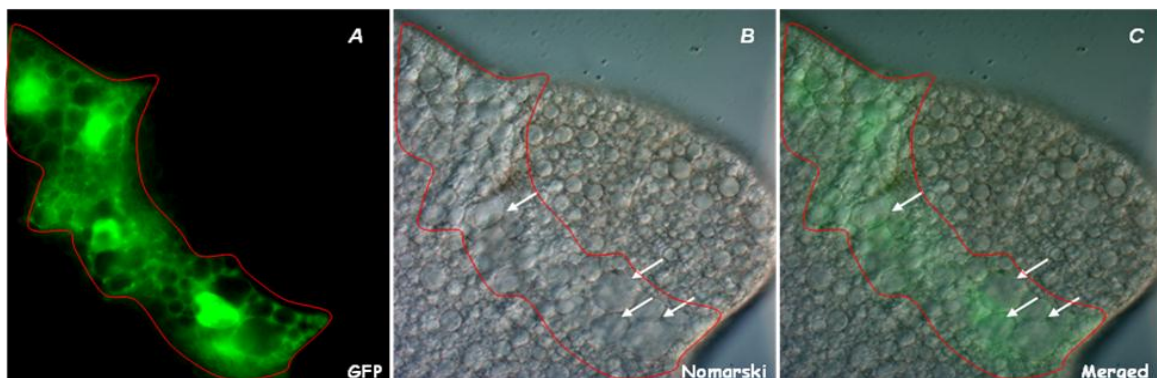


Figure 21 - Changes in the size of lipid droplet (LD) by *Rheb*^{RNAi}

A pilot experiment using *Rheb* shows efficacy of flip-out technique. Note that the size of LDs is significantly increased (GFP positive cells), and the number of LDs per cell in clones is decreased compared to the surrounding control cells (GFP negative cells). Gal4 expressing clones were randomly induced by heat-shock to activate a UAS-GFP and a UAS-*Rheb*-RNAi. The GFP positive clones are detected in fluorescence (A) whereas LDs are visualized in Nomarski (B). Both pictures are merged (C).

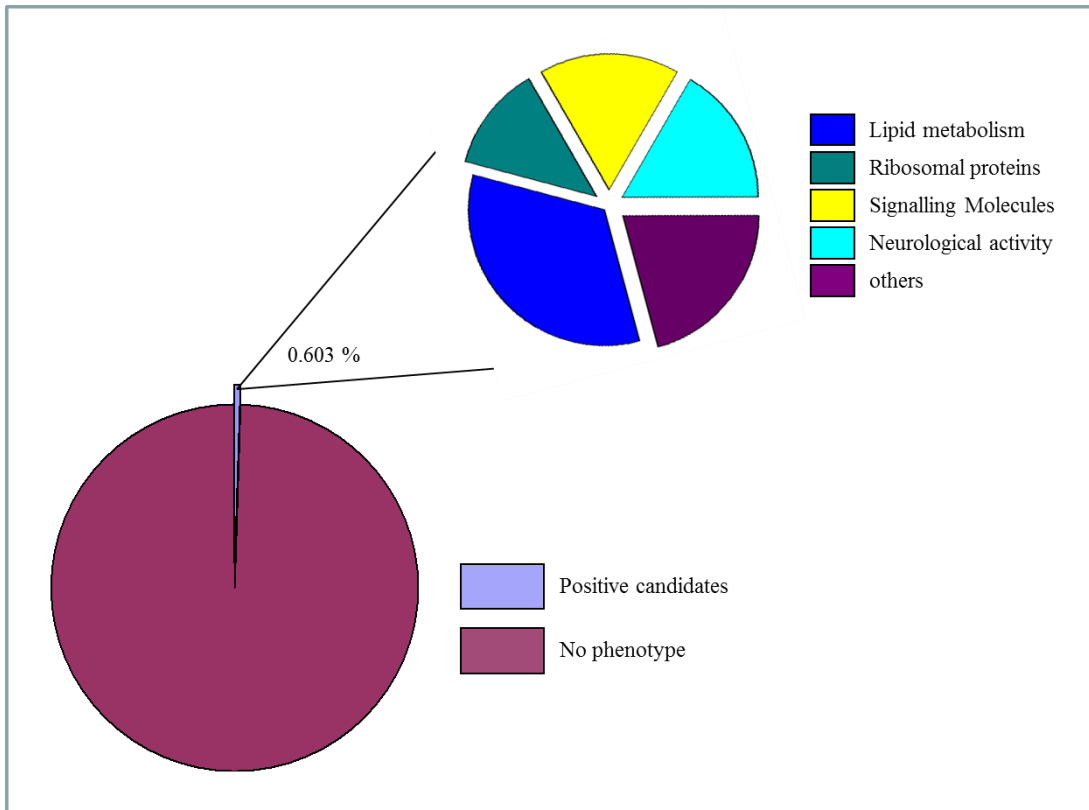


Figure 22 - The phenotypic classification of the Lipid droplet screen

Approximately 7,300 UAS-RNAi lines were used in the screen for regulators of lipid metabolism. A total of 24 candidates were retained and categorized into 5 sub-groups regarding their biological function (right).

Table 2 - List of RNAi lines identified in screen for LD size

No.	CG number	Line # *	Gene	Comments
1	3665	3	fasciclin 2	learning, memory, nervous system, organ development
2	14895	2	Pak 3	receptor signaling protein serine/threonine kinase activity
3	2647	1	period	circadian clock, mating, circadian behavior, memory
4	4979	3	sxe2	phosphatidylserine phospholipase activity, lipid metabolic process
5	4581	3	thiolase	long-chain-3-hydroxyacyl-CoA dehydrogenase activity
6	12819	3	slender lobes	Molecular function unknown, involved in nucleolus organization
7	10792	3	dunce	synaptic transmission, nervous system, short-term memory
8	2165	2	CG2165	calcium-transporting ATPase activity
9	3522	2	start1	cholesterol transporter activity, steroid biosynthetic process
10	10139	2	CG10139	Unknown function
11	3961	3	CG3961	long-chain-fatty-acid-CoA ligase activity, metabolic process
12	5122	3	CG5122	carnitine O-acetyltransferase activity, biological process unknown
13	5904	2	mRpS31	structural constituent of ribosome, translation
14	10697	2	Ddc	amino-acid decarboxylase activity, dopamine and serotonin biosynthesis
15	3421	2	RhoGAP93B	protein binding, axon guidance
16	4630	2	CG4630	carnitine transporter activity, transmembrane transport
17	3972	1	Cyp4g1	electron carrier activity, lipid metabolic process
18	2101	3	mRpS35	structural constituent of ribosome, translation
19	18033	1	CG18033	transcription repressor activity
20	3488	2	α/β hydrolase2	lipase activity, lipid metabolic process
21	6235	2	twins	protein phosphatase, regulation of mitosis;, Wnt signaling pathway
22	10959	3	CG10959	zinc ion binding; nucleic acid binding, biological process unknown
23	7111	1	Rack1	protein kinase C binding, wing disc development, oogenesis
24	3782	2	mRpL28	structural constituent of ribosome, translation

The selected candidate genes identified in the screen for LD size are shown in the table. The putative molecular and biological functions are taken from flybase (Anonymous, 2003). Genes are indicated by their name or CG (computational gene) number. The asterisk (line# *) indicates the specific number used by NIG to design each RNAi line for a given gene.

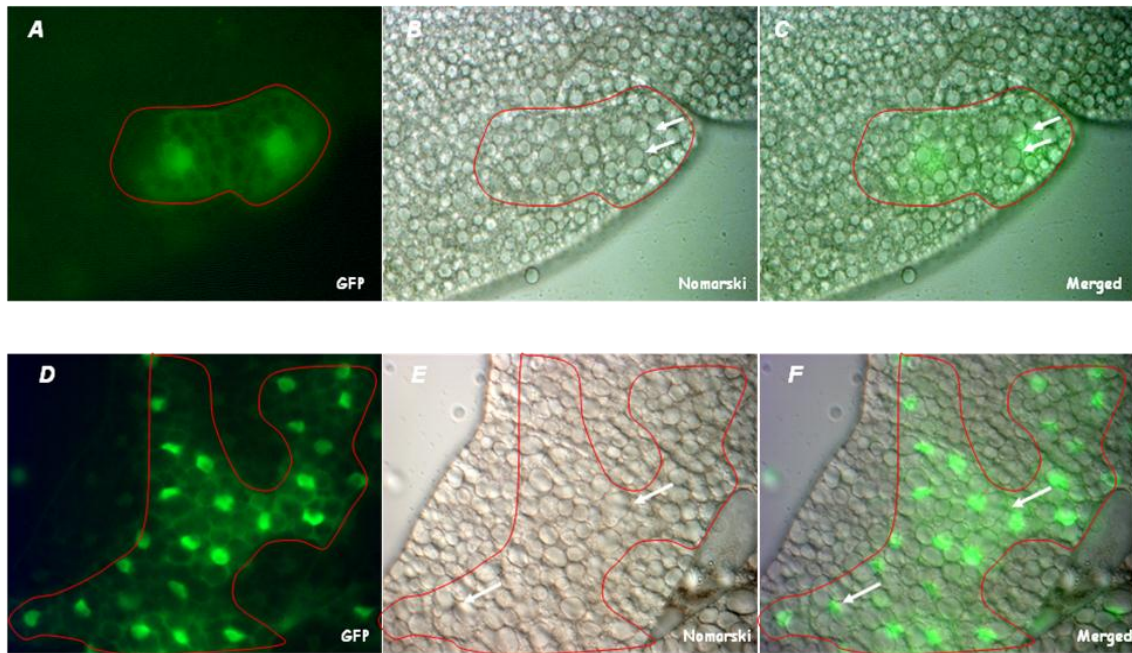


Figure 23 - Changes in the size of lipid droplet (LD) by *Fas*^{RNAi}

Upper panel (A-C): An RNAi to *Fasciclin2* (*Fas2*) gene (CG3665) randomly induced in a GFP-marked clone shows an increase of LD size (arrows).

Lower panel (D-E): An RNAi to *Fasciclin3* (from VDRC) in GFP-marked clones induces a weak increase of the size of the LD (arrows). The number of LDs per cell in clones is slightly decreased as compared to the adjacent control cell (GFP negative cells).

3.5 - RNAi screening for negative regulators of dS6K-dependent-growth

An ectopic expression of *dS6K* within the developing dorsal wing compartment using the *apterous*-Gal4 (*ap*-Gal4) driver induces a moderate overgrowth of this compartment and lead to a bending-down phenotype of the adult wing (Montagne et al., 1999). It has been discussed earlier that this bend-down phenotype of the adult wing varies according to the activation status of *dS6K* mutants (Barcelo and Stewart, 2002) and can be modulated by the *Drosophila* PDK1 (dPDK1) (Radimerski et al., 2002). This sensitized genetic phenotype has been retained by our research group to search for novel modulators of dS6K-dependent growth. Following a gain-of-function strategy, a collection of approximately 5000 Enhancer-Promoter (EP)-lines were coexpressed together with *dS6K* in the developing dorsal wing compartment. The offspring was then scored for enhancement or suppression of the bending-down of the adult wing. This study identified novel positive regulator of dS6K, including the nuclear receptor *DHR3* (*Drosophila* hormone receptor 3), which was further shown to be a positive regulator of growth (Montagne et al., 2010). Moreover, it was observed in this study that the enhancement of the bent-down wing phenotype is a rare event and for most of the cases resulted from a specific interaction, whereas, suppression of this phenotype is very frequent and most likely reflects a non-specific interaction (Montagne et al., 2010). Considering that the enhancement of the bending down results on cell growth increase and that the EP induction normally induces over-expression of the neighboring gene, this strategy may allow the identification of only positive regulators of dS6K-dependent growth.

Taking advantage of the UAS-RNAi library of NIG, we performed a loss-of-function genome-wide RNAi screen to further identify novel regulators of dS6K signaling. Using the *ap*-Gal4 driver, each RNAi line was co-expressed with *dS6K* in the developing dorsal wing compartment and the adult wing was scored for enhancement or suppression of the bent-down wing phenotype. As expected, suppression appeared to be a frequent event (data not shown) and thus, was considered to be irrelevant,

whereas, enhancement was observed with very low frequency (Fig. 24). Considering that an RNAi disrupts gene expression, and that enhancement of the wing phenotype reflects an increase of cellular growth, the candidate genes indentified in the screen are expected to act as negative regulators of dS6K-dependent growth. In the first step of the screening procedure, approximately 11,000 UAS-RNAi lines corresponding to roughly 7,000 genes were co-induced with *dS6K* in the developing dorsal compartment of the wing disc and scored for the enhancement of the dS6K-dependent wing phenotype. All the crosses were performed at 25°C and the RNAi lines which non-specifically disrupt the wing development (i.e. Cyo-like, strong Cyo, flat, crumbled) were discarded (data not shown). In this way, three hundred fifty seven of the UAS-RNAi lines were found to produce a strong bending-down of the adult wing. These lines were further analyzed for the effect on the wing when induced alone with *ap-Gal4* driver. The UAS-RNAi which alone produced a strong bent-down of the adult wing was then discarded, since it was supposed to affect growth independent of dS6K. For example, an RNAi to CG8931 when induced alone produced a bent-down wing phenotype that was almost the same as the phenotype produced in combination with dS6K (compare Fig. 24E and 24E'). Moreover, one of the candidates was discarded (CG5580), as it has been described to control dorsal/ventral patterning of the developing wing and thus, most likely affects our expression system (data not shown).

The selected candidates were further analyzed using the corresponding RNAi line from the library of VDRC for confirmation of dS6K specific interaction (data not shown). Moreover, to narrow the selection criteria, we also tested UAS-RNAi to the potential off-target genes of the selected RNAi lines. When co-expression of dS6K and an RNAi line to a potential off-target could reproduce the wing bend-down phenotype, the initially selected candidate was considered to be irrelevant and the corresponding RNAi line was discarded (data not shown). Following this additional selection step, several false positives were discarded. At higher temperature, the UAS-GAL4 system is known to be more efficient. Hence, to confirm the strong genetic interactions, the selected lines were then co-induced with *dS6K* both at 25°C and 29°C. This way, the selected UAS-RNAi lines were categorized into weak, mild and strong enhancers (Fig. 25). As depicted in the graph, 50 RNAi lines (0.45 %) produced a strong enhancement,

109 (0.99 %) produced a mild enhancement and 198 (1.8 %) produced a weak enhancement of the bent-down wing phenotype (Fig. 25). The selected 50 strong enhancer RNAi lines correspond to 45 different genes (Table 3), and out of these five genes showed an extreme bend-down phenotype when co-expressed with dS6K.

Finally, we focused only on the 45 candidate genes which produced a strong enhancement of the bent-down wing phenotype and were definitely confirmed through all the screening steps (Table 3). These selected candidates include eight genes encoding metabolic enzymes (CG4581, CG8798, CG3522, CG9165, CG3626, CG8349, CG6917, CG6947), three genes encoding enzymes with ubiquitin ligase activity (CG15010, CG5603, CG12799) and seven genes encoding signaling molecules (CG12015, CG8318, CG13850, CG1283, CG13229, CG5279, CG8985), the three latter encoding G-protein coupled receptors. Two selected candidate genes have not been annotated with any function at flybase, however, these genes encode for proteins with either F-box domain or WD-40 repeats (CG3909 and CG5961). These domains are particularly important for target protein interaction and then degradation. Therefore, as for the gene encoding enzyme with ubiquitin ligase activity, the gene products might be involved in targeting a substrate to the proteasome to control its subsequent degradation.

As mentioned above, two UAS-RNAi lines for each single gene are normally available. For some genes, both RNAi lines were found as enhancers of the bent-down wing phenotype further validating our screening strategy. Those RNAi lines were specific to the CG15010, CG12015, CG1283, CG9165 and CG6917 genes (Table 3); for each of them, none of the potential off-target genes tested were found to enhance the bent-down wing phenotype (data not shown), arguing that the corresponding gene products might be *bona fide* negative regulators of dS6K dependent growth.

Systematic studies aimed to establish a physical interactive inventory between the *Drosophila* gene products have been previously performed following the yeast-two-hybrid strategy (Giot et al., 2003). Databases revealed that seven proteins (CG15010/Archipelago, CG8843/Sec5, CG8128, CG10622/Such, CG10295/Pak, CG14216 and CG12019/Cdc37) can physically interact with dS6K in yeast two-hybrid (Y2H) assay (Formstecher et al., 2005). Three of those were found through our RNAi

screen, CG12019 (*cdc37*), CG15010 (*ago*) and CG8843 (*sec5*), although the former showed a mild-type enhancement of the bend-down phenotype. Since the NIG collection does not uncover the entire *Drosophila* genome, RNAi lines specific to the other dS6K physical interactors were ordered from VDRC and analyzed. In summary, out of the seven physical dS6K interactors, three were found to be potential negative regulators of dS6K-dependent growth (CG12019/Cdc37, CG15010/Ago and CG8843/Sec5). No strong enhancement of wing bend-down phenotype was observed with RNAi to the other four genes, neither at 25°C nor at 29°C, which exclude them as negative regulators of dS6K-dependent growth. Two genes CG8985 and CG13229 involved in G-protein coupled receptor signaling pathways, were found through our screen, but appeared to be off-targets of each other. This finding suggests that either several G-protein coupled receptors converge on dS6K signaling or that only one of them is specific for dS6K. It is to be worth noting that the RNAi to CG2165 and CG11081 (*plexA*) produced a strong enhancement of the bent-down wing phenotype (Table 3) and that the corresponding gene product for either of them has been described to physically interact with CG15010 (*ago*) in two-hybrid assay. Altogether, these data strongly argue for the specificity of our screening scheme.

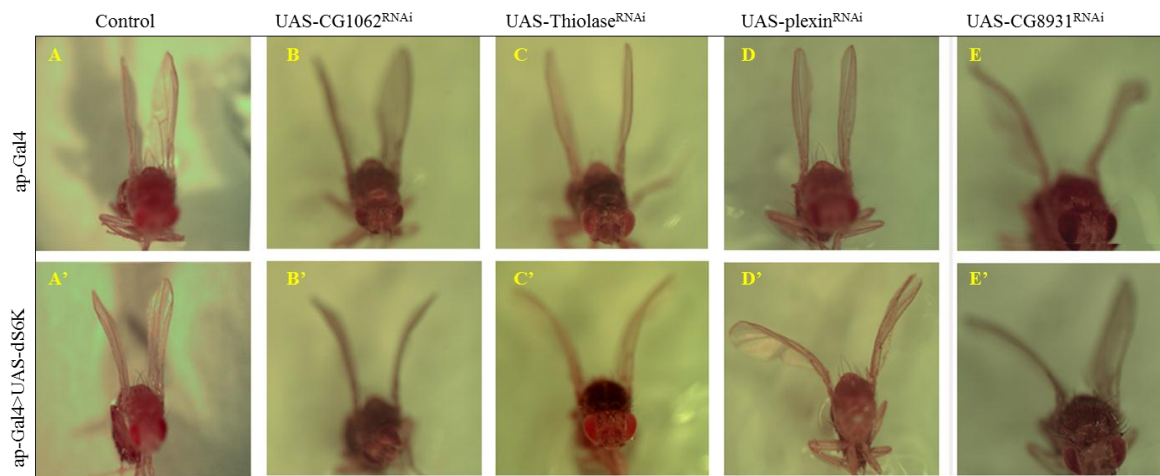


Figure 24 - Modulation of the bend-down wing phenotype due to dS6K over-expression

The bending down of the adult wing due to dS6K overexpression in the dorsal compartment of the developing wing disc (A') is enhanced by co-induction of RNAi to CG1062 (B'), Thiolase (C') and plexin (D'). Induction of these RNAi lines alone (B, C and D), does not modify the wild type wing phenotype (A). The bending down phenotype is enhanced by an RNAi to CG8931 when co-induced with dS6K (E'). However induction of the CG8931^{RNAi} alone is sufficient to induce a bend-down phenotype (E).

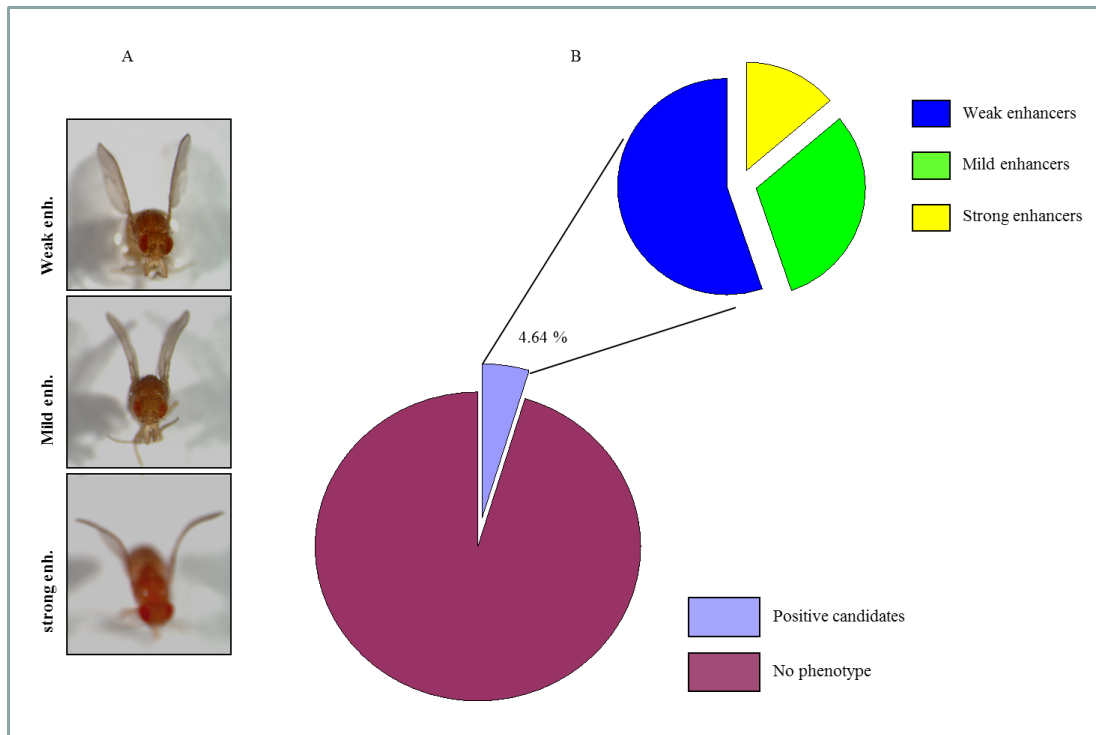


Figure 25 - A brief summary of RNAi lines identified in a screen for modulators of the dS6K-dependent wing phenotype

Approximately 11,000 UAS-RNAi lines were used in the screen of wing phenotype. (A) A total of 357 enhancers were found and categorized into weak (top), mild (middle) and strong (bottom) enhancers, respectively. (B) The weak enhancers correspond to 1.8%, the mild enhancers to 0.99% and the strong enhancers to 0.454% of the total lines used. About 96.75% of the UAS-RNAi lines did not enhance the dS6K-dependent bending down of the wing.

Table 3 - List of RNAi lines identified as strong enhancers of dS6K-dependent growth

No.	CG number	lines (n)	Gene	Comments
1	1062	1	CG1062	neurexin binding, phagocytosis, engulfment
2	1233	1	CG1233	zinc ion binding, biological process unknown
3	1283 *	2	CG1283	actin binding; Rho GEF domain Ezrin/radixin/moesin
4	2165	1	CG2165	calcium-transporting ATPase activity
5	2921	1	unknown	Domain of unknown function DUF89
6	3522	1	start1	cholesterol transporter activity, steroid biosynthetic process
7	3626	1	CG3626	phosphatase regulator activity, glycine catabolic process
8	3909	1	unknown	G-protein β , WD-40 repeat subgroup
9	4420	1	unknown	aspartic-type endopeptidase, proteolysis, ubiquitin domain
10	4581	1	Thiolase	long-chain-3-hydroxyacyl-CoA dehydrogenase activity
11	5084	1	CG5084	Unknown function
12	5279 *	1	Rhodopsin 5	G-protein coupled photoreceptor activity, absorption of visible light
13	5603	1	cylindromatosis	ubiquitin-specific protease activity, defense response
14	5961	1	unknown	F-box domain, Skp2-like
15	6917	2	Estrase-6	carboxylesterase activity, pheromone biosynthesis, courtship behavior
16	6947	1	peritrophin-like	peritrophic membrane component; chitin metabolism
17	7235	1	Hsp60C	ATPase activity, oogenesis, spermatogenesis
18	7447	1	slowdown	EGF-like calcium binding, muscle attachment
19	8034	1	unknown	transMb transport; Major facilitator superfamily MFS-1
20	8036	1	CG8036	transketolase activity, cytoplasmic microtubule organization
21	8318 *	1	Nf1	Ras GTPase activator activity, regulation of growth
22	8349	1	CG8349	cytidine deaminase activity
23	8411	1	gcl	protein binding, negative regulation of transcription
24	8798	1	CG8798	serine-type endopeptidase activity, proteolysis
25	8843	1	sec5	specific transcriptional repressor activity, immune response
26	8985	1	DmsR-1	G-protein coupled receptor protein signaling pathway
27	9104	1	channel	dentrite morphogenesis
28	9165	2	CG9165	hydroxymethylbilane synthase, peptidyl-pyrromethane cofactor linkage
29	9188	1	sip2	protein binding, biological process unknown
30	10139 *	1	CG10139	Unknown function
31	11081	1	plexin A	protein binding, nervous system
32	12015	2	RabX6	GTPase activity, small GTPase mediated signal transduction
33	12026	1	unknown	Lipoma HMGIC fusion partner-like protein
34	12455	1	unknown	CG42817/CG42818
35	12799	1	Ubc84D	ubiquitin-protein ligase activity, regulation of protein metabolic process
36	12819	1	slender lobes	Molecular function unknown, involved in nucleolus organization
37	12918	1	unknown	Protein of unknown function DUF3456

38	13229	1	CG13229	G-protein coupled receptor protein signaling pathway
39	13850	1	CG13850	protein kinase activity, ATP binding, apoptosis
40	15009	1	ImpL2	Molecular function unknown, involved in cell adhesion
41	15010 *	2	Archipelago	ubiquitin-protein ligase activity, negative regulation of growth
42	15254	1	unknown	Peptidase M12A
43	15258	1	unknown	Unknown function
44	18247	1	shark	scavenger; epithelial cell apical/basal polarity, JNK cascade;
45	31826	1	transport	(Ra) retinaldehyde-binding; Phosphatidylinositol transfer

The selected candidate genes identified in the *ap*-screen are listed. The putative molecular and biological functions are taken from flybase (Anonymous, 2003). Genes are indicated by their name or CG number. The asterisks indicate the RNAi lines, which produced an extreme enhancement of the wing bend-down phenotype.

3.6 - Interaction map for dS6K-based growth regulators

Taking advantage of the protein-protein interaction data based on yeast two hybrid (Y2H) assay (Formstecher et al., 2005), we analyzed all the gene products of the candidates RNAi lines which were selected as strong enhancers through the screen for dS6K growth modulators. The candidate genes were analyzed using “The bioGRID” (<http://thebiogrid.org>) and “BOND” (<http://bond.unleashedinformatics.com/>) web-based sources. Gene products that have been identified in Y2H assay to physically interact with dS6K with high confidence are limited to seven candidates: Sec5 (CG8843), Ago (CG15010), Suchb (CG10622), Pak (CG10295), Cdc37 (CG12019), CG8128 and CG14216. In addition, several genetic, molecular and pharmacological studies in various species including *Drosophila melanogaster*, have formally demonstrated that PDK1, TOR, Raptor and Rheb act as positive regulators of dS6K activity, whereas the *TSC1/2* tumor suppressor act as a repressor (Rintelen et al., 2001; Radimerski et al., 2002a; Radimerski et al., 2002b; Kim et al., 2002; Stocker et al., 2003; Saucedo et al., 2003; Zhang et al., 2003). Figure 26 recapitulates the gene products that have been shown to tightly regulate dS6K activity (green boxes), the seven gene products that physically interact with dS6K in Y2H (pink boxes) and all the candidates selected through our screen which produced a strong enhancement (blue-outlined boxes). Figure 27 represents a physically-interacting molecular network based on Y2H-assay that we were able to draw using available protein-protein interaction information database. For simplicity, the candidates (23 candidates) for which no interaction data is available, have been removed. All the proteins drawn are physically linked, few of these have not been selected through our screen (grey boxes), but they were necessary to establish the physical interacting-network between our selected candidates (Fig 27). In addition to the selected candidates (blue-outlined boxes), some of the genes have been tested in the dS6K modulator screen but their corresponding RNAi did not produce any phenotypic enhancement (black-outlined boxes), although two of these candidates, i.e. RNAi to CG4998 and *cact* (yellow boxes) produced a weak enhancement (data not shown). Further investigations for all these interactors using the “bioGRID” and “BOND” sources revealed that CG6947 genetically interacts through CG1921 with Ras85D, sina, svp, EGFR, Notch, Dpp and TGF- β (not indicated

in Fig. 27). Similarly CG18247 genetically interacts with CG2275, which itself interacts with EGFR, Ras85D, phyl and phl (not indicated in Fig. 27). These genetic interactions validate the relevance of this network. Interestingly, all the gene products of the network are linked together, so that any of the candidates can be physically associated with another one. These findings emphasize the role of various regulatory processes including signaling pathways, cell cycle control and protein degradation; and further suggest that these cellular processes interact together to coordinate the process of growth.

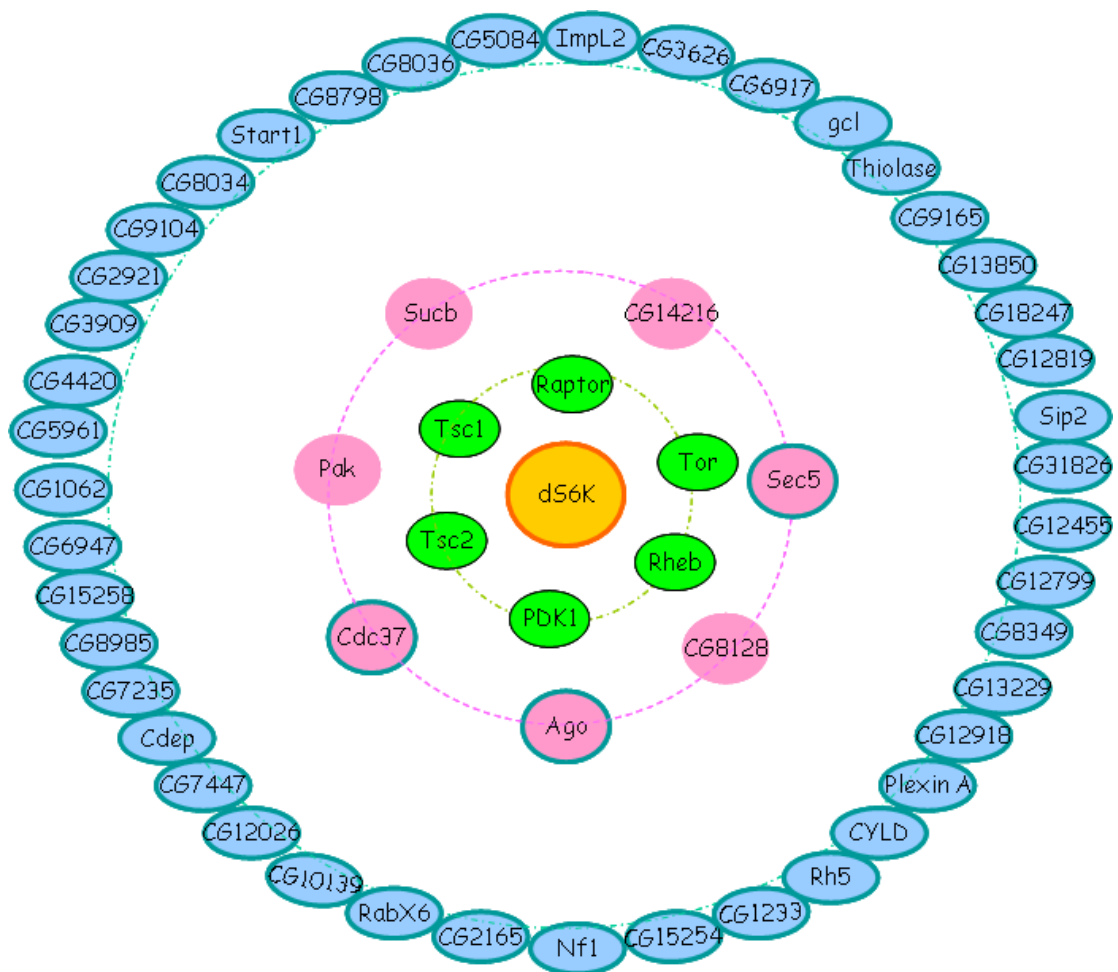


Figure 26 - A representation of dS6K interactors

All the candidates selected in the RNAi screen are shown (blue circled). Proteins reported to physically interact with dS6K (pink boxes), and the known direct regulators of dS6K activity (green boxes) are indicated. The candidates which are physically interacting with dS6K (pink color) have been tested; three of them were found to be enhancers (blue circle).

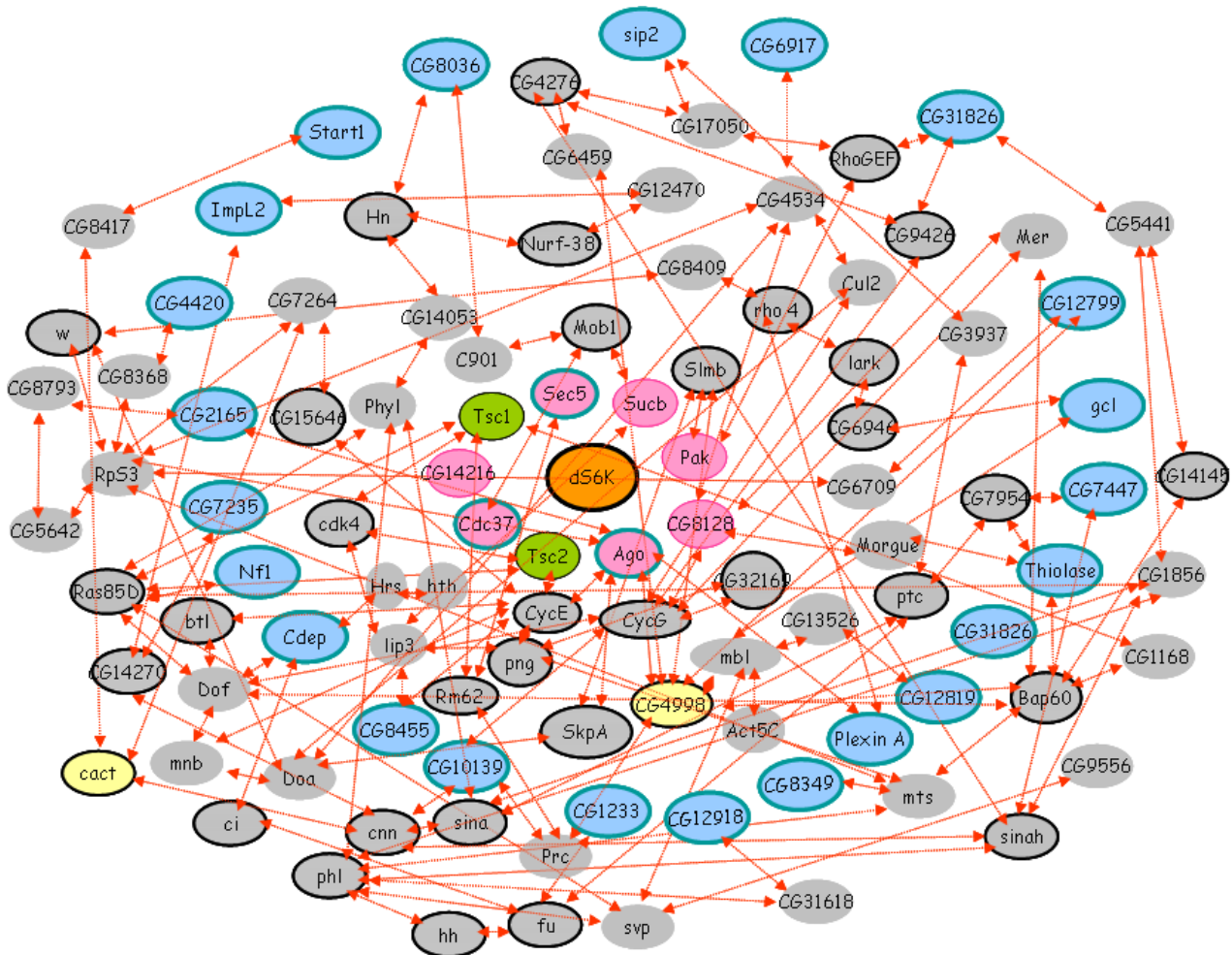


Figure 27 - A protein-protein interaction network centered on dS6K-dependent growth

The candidates selected in the screen are shown (blue circled) (for simplicity, the candidates for which no information is available, have been removed). The proteins that are reported to physically interact with dS6K (pink boxes), and the Tsc1/2 repressors of dS6K activity (green boxes) are indicated. Additional gene products necessary to establish the physical interactive network are represented (grey boxes). RNAi to some of these additional gene products have been tested in the screen and did not strongly enhance the bent-down wing phenotype (grey boxes with dark grey circles). Two genes, i.e. *cact* and CG4998 were found to be mild enhancers (grey circled, yellow boxes).

3.7 - Identification of upstream regulators of dS6K

In an attempt to discriminate whether a candidate gene is acting upstream or downstream of dS6K, we ubiquitously expressed the RNAi lines corresponding to the 45 strong enhancers retained in the screen. Larval extract were then prepared, scored and analyzed by Western-blotting with antibodies specific to either dS6K or to its active phosphorylated site (P-dS6K). All of these RNAi lines were viable in this genetic setting. However the effects on dS6K levels and/or phosphorylation varied a lot and were not reproducible in distinct experiments (data not shown). This variability may in part reflect the difficulty to precisely synchronise the larvae with respect to feeding and developmental stage. It may also be a consequence of the RNAi knock down that varies a lot depending on the experiment. In addition, we observed that ubiquitous expression of the RNAi did not produce lethality, whereas some mutant are described to be homozygous lethal, as previously reported for *ago* (Moberg et al., 2001). These different phenotypic effects suggest that induction of the RNAi lines in our genetic setting can never totally abolished the gene expression.

The *Drosophila* derived S2 cells have been described to provide an appropriate system to suppress an upstream regulator through direct application of specific double strand RNA (dsRNA) and then to monitor kinase activity or levels of a given intermediate of the insulin and nutrient signaling network (Clemens et al. 2000, Radimerski et al. 2002a, Kim et al. 2008). Therefore, we analyzed the expression and activity profiles of dS6K for few of the candidates. Five of the 45 candidate genes retained in the latter screen, i.e. CG15010, CG1283, CG8318, CG10139 and CG5279 (Table 3), were categorized as the most potent interactors, since co-induction of their specific RNAi with dS6K produced an extreme enhancement of the bent-down wing phenotype. Specific dsRNA fragments to these 5 candidate genes and to 3 other candidates (CG1233, CG12819 and CG11081) were produced and incubated with cultured S2 cells. Cell extracts were then analyzed by Western-blotting using specific antibodies to either the full-length dS6K or to its phosphorylated T398 residue to evaluate dS6K levels or activity state, respectively (Fig. 28). To precisely assess the eventual variation of dS6K levels or activity, western-blotting was performed to α -Tubulin as internal controls. Specific signals (Fig. 28 A,A') were quantified using the Scion imaging

software and the dS6K specific values were normalized to the α -Tubulin corresponding values (Fig. 28B,B',C,C'). In S2 cells complemented with serum, a moderate increase in dS6K levels was observed upon dsRNA treatment to CG15010, CG10139 and CG1283 but not to CG8318 and CG5279 (Fig. 28A,B). The phosphorylation of the T398 residue of dS6K (P-dS6K) was strongly increased under treatment of dsRNA to CG10139, CG1283 and CG8318, whereas it was decreased under treatment of dsRNA to CG15010 (Fig. 28A,C). Similar western-blotting assay was performed in serum-deprived S2 cells. In this setting, a clear increase in dS6K levels (Fig. 28A',B') concurrent to a decrease in T398 phosphorylation (Fig. 28A',C') were observed in S2 cells treated with dsRNA to CG15010. However, none of the other dsRNA produced a noticeable effect on either dS6K levels or T398 phosphorylation. The weak variations that can be observed were not reproduced in other experiments (data not shown) and therefore, are likely unspecific. When selected through the dS6K modifier screen, the RNAi to CG12819, CG11081 and CG1233 were classified as strong but not extreme enhancers. Unexpectedly, none of the corresponding dsRNA when added to S2 cells produced a clear reproducible effect (Fig 28 and data not shown). Altogether, these findings suggest that our screen clearly identifies one gene product (CG15010), which potentially regulates dS6K levels, and 3 gene products (CG1283, CG8318, CG10139), which play on T398 phosphorylation and subsequently on dS6K activity in serum stimulated S2 cells. This further reveals that relevant modifiers for dS6K-dependent growth could be identified following extreme enhancement of the sensitized bent-down wing phenotype.

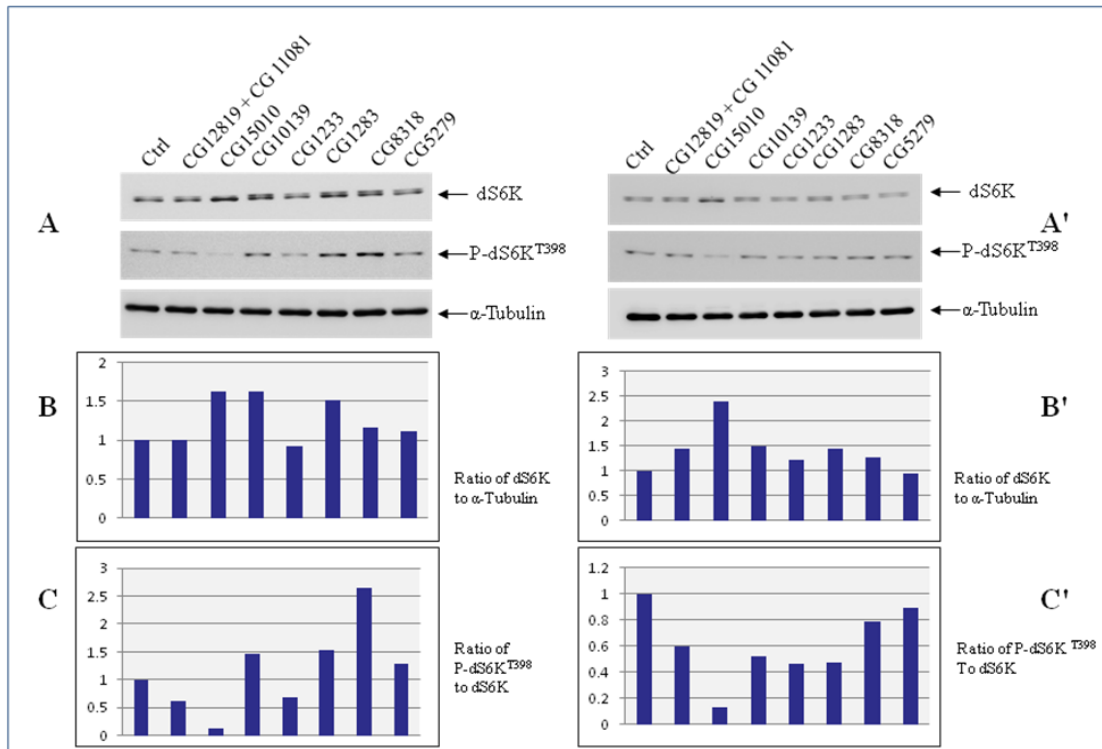


Figure 28 - Western blot analysis to the extracts of S2 cells for dS6K and P-dS6K

Left panel: (A) Western-blotting with S2 Cells extracts grown on serum, using antibody specific to dS6K (top), phospho-T398 residue of dS6K (middle) and α -Tubulin (bottom). S2 Cells were treated with dsRNAs to extreme enhancers (CG1283, CG5279, CG8318, CG10139, CG15010) and few strong enhancers (CG12819, CG11081, CG1233). (B) Quantification of the intensity of the bands indicates that dS6K levels are mildly increased with RNAi to CG15010, CG10139 and CG1283. (C) Quantification of the intensity of the bands indicates that phosphorylated dS6K is significantly increased with RNAi to CG10139, CG1283 and CG8318.

Right panel: (A'): Western-blotting with serum-deprived S2 Cells using the same specific antibodies and dsRNA used in (A). Quantification of the intensity of the bands shows that treatment of dsRNA to CG15010 provokes a significant increase of dS6K levels (B') coupled to a severe decrease in T398 phosphorylation (C'). The band intensity was quantified using ImageJ.

3.8 - Mammalian homologs of the most relevant dS6K modulators

The *Drosophila* gene CG10139 encodes a small protein of 224 amino acids that does not match to any mammalian counterpart. Protein blast search could identify homologues only in insects. No typical conserved domain is reported, except a potential pyrolysyl-tRNA synthetase domain with low homology with a bacterial enzyme. Neither phenotypic mutant analysis nor biological function is reported for this gene in *Drosophila melanogaster* (Giot et al., 2003).

The gene CG8318 encodes a unique gene, which has been extensively investigated in *Drosophila*, showing that it plays an important role in learning and memory (Buchanan and Davis 2010), although the initial characterisation revealed a role in the control of growth (The et al., 1997). Protein blast identifies a single mammalian homologue named as Neurofibromin 1 (NF1). It is described as a tumor suppressor, whose mutation also induces neurological disabilities in patient. The *Nf1* gene encodes a big protein of almost 3000 amino acids, which functions as a guanosine triphosphatase (GTPase) activating protein for Ras (Ras-GAP), stimulating the intrinsic activity of Ras-GTPase thereby inhibiting the biological activation of Ras. The protein structure of NF1 indicates that it contains two conserved domains: a Sec14p-like lipid binding domain spanning amino acids 1612-1758 in drosophila and 1583-1729 in mouse; and a RasGTPase activating domain spanning amino acids 1247-1573 in drosophila and 1205-1551 in mouse (Fig. 29). Three distinct studies in mammals recently showed that NF1 also acts as a repressor of the mTOR/S6K pathway (Johannessen et al. 2005; Dasgupta et al. 2005; Johannessen et al. 2008), which firmly validates the specificity of our *Drosophila*-modifier screen to identify negative regulators of dS6K-dependent growth.

The gene CG1283 also called *Cdep* (Chondrocyte-derived ezrin-like domain containing protein) encodes a protein member of the FARP (Fibrinogen/angiopoietin-related protein) family, for which 2 homologues have been found in mammalian species, Farp1 and Farp2; the latter exhibiting a higher degree of homology with Cdep (Fig. 30). Protein structure analysis reveals several conserved domains: the FERM (Farp ezrin moesin radixin) domain, found in cytoskeletal-associated proteins, a GEF

(Guanine nucleotide exchange factor) domain for Rho and 2 PH (pleckstrin homology) domains (Fig. 30A). Little is reported in literature for proteins of the Farp family. A recent study in breast cancer reveals that Farp1 is a TGF- β target induced in the switch from cohesive to single cell motility. Therefore, *Cdep* is certainly one of the most interesting candidates found in our dS6K-modifier screen that should be further investigated

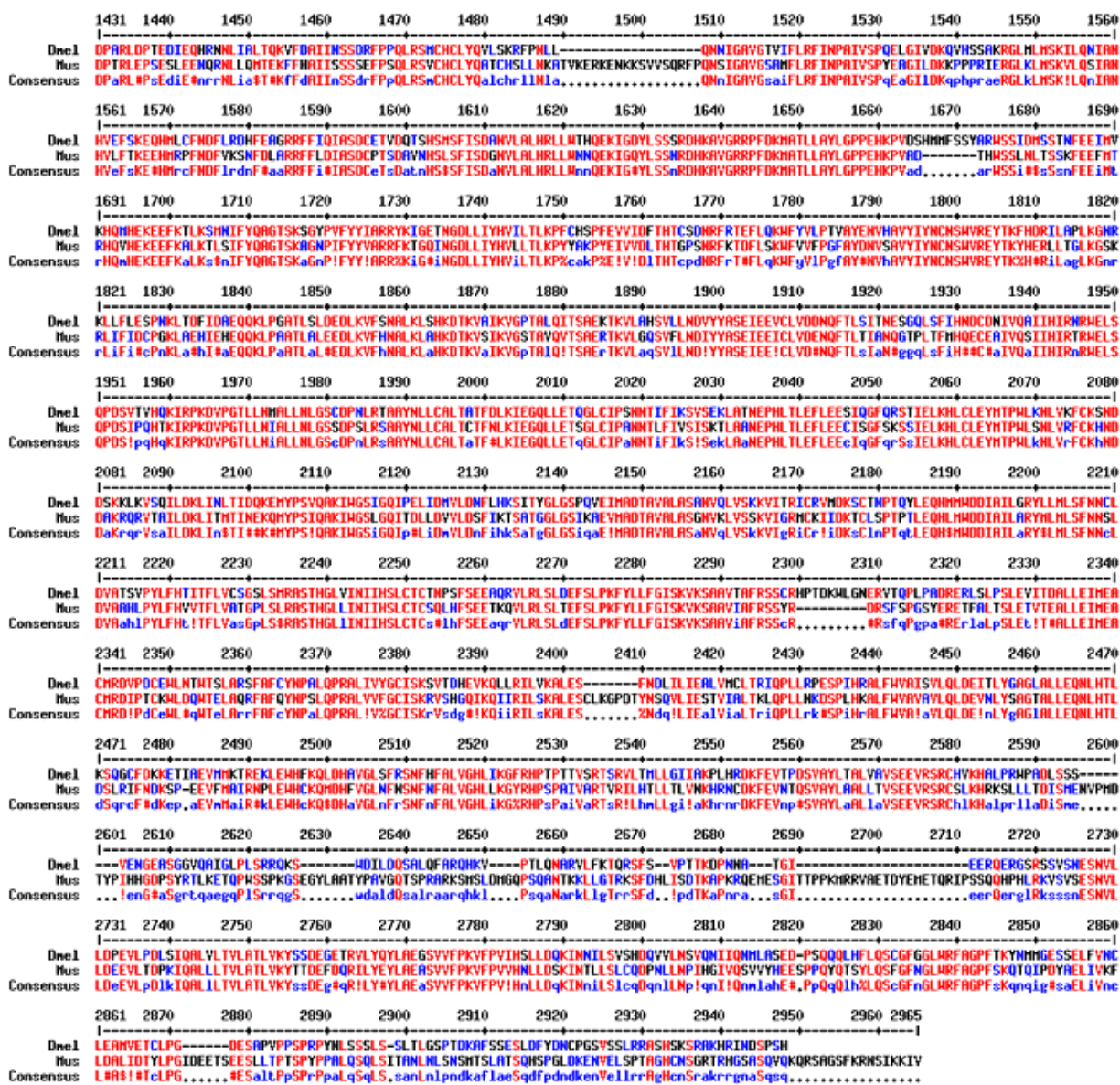
The gene CG15010 also known as *archipelago* (*ago*) has been extensively described in the introduction. Protein blast analysis identified a unique homolog in mammals, the *FBW7* gene which is mutated in several human tumors. Sequence homology only concerns the C-terminal half, where the F-box and the seven WD repeats are located (Fig. 12 & Fig. 31). These proteins are reported to be a part of the E3-ubiquitine ligase complex that targets the substrate to proteasomal degradation. Consistently, our results suggest that Ago may regulate dS6K degradation. Since nothing is known to date about the regulation of dS6K degradation, we then, decided to further investigate the potential interaction between Ago and dS6K.

A



B

	1	10	20	30	40	50	60	70	80	90	100	110	120	130
Dne1	MTQKPGEWASALLARFEDQLPNRIGAYGTQARRMSQDQLVACLTHISRYRFSLVISGLTKMLQRVNEARLQNRHEPERCYFESLVIITLTLERCLTNQTKDARFEERANVKLLREISQFVVDVQSDNP													
Hus	MARRPVEKQVAVYSRFDEQLPIKTQQNTHTKVSTENHKECLINISKYKFSLVISGLTILKNVNMRRIFGEAREKMLYLSQL--ITLDTLEKCLAGQPKDTRLOETPLVKQLPEICHLHTCREGNGQ													
Consensus	.aaqrPgEMaQaRlLaRF#QLPNriGaqTqarnSq#qnkaCLINISrYrFSLVISGLTkiLqrVn#aaiaqrnaaerercYleqL..ITLdTLERCLanQPKDARi#EamNvKqLrLEicqFIdcr#q#kq													
	131	140	150	160	170	180	190	200	210	220	230	240	250	260
Dne1	MRAQLKALASKVLFALSNHFSAVFNRSARIQELTSCSEENPDYNDIELTQHIDHMIKLTLLQETITKFRS--KRAPPILLVSLERAIHNIHIEYHPQEFQDLQRGTNRDSTCNEPLHDFVEYFKTE													
Hus	MARELNSASGVLFSLSCNFMVAVSRISTRLQELTYVCEEDVVDVHDIELQYINVDCAKLRLLKETAFKFKALKKVAVLAVINSLERAFNNHVEYDPDEFKLYQIPQDMARECAEKLFDLVDF--AE													
Consensus	MRA#LraLAgVLFaLScNfNvAVFNRISaRIQELTeCSE#pDgnDIELiQhI#DcaLkrLLqETafKfra,KraaqLalinSLEKAIHNI#Enp#EFqdlqrqgr#rDiaeCaELnDlV#gf,aE													
	261	270	280	290	300	310	320	330	340	350	360	370	380	390
Dne1	NKKSKTLVAPLQMLLLILNPSCLERVYVNELOQSEKEKEKQEKVASKSAQSTSRQKDFSAKQFIESIKRGLGQHSPOKVTESARIACVKLCKRSTYINNTDSNNVVFKLVOFFINDLKALLFNPAKPF													
Hus	STKRAAVVAPLQITLLILCPETIQDTSKDVVD-----ESWINKKLLDLSLAKLAGGSRQLTESARIACVKLCKRSTYINNEED--NSVIFLLVDSHVYDLKMLLNFNPKPF													
Consensus	nkKraaVAPLQIiLLiLnPeci#a!sn#lq#.....#k#inaKq#i#SirraLaqggSrqiTESARIACVKLCKRSTYINNEED..NnV#FILLVDF#nDLKaLlFNPAKPF													
	391	400	410	420	430	440	450	460	470	480	490	500	510	520
Dne1	RGQGYNFADLELHLDICLVSCFRINPHNIEALKYCLMLSSPQRYHFVIVCSLLRLRHLYVDFRLDHNKPFRIYVNPRLSNHPQDQVHYRSARELRLFDTLNKAQGGYLAHTPLRYITSLTLKSKDTQ--													
Hus	RGS--QPADVLDLHLDICLVSCFRISPHNHDHFKICLADNSPSTFHYVLVNSL-----HRIITNSALDHPKIDAVYCHSVELRNFGETLHKAYVGGCGAHPAIRNRPSTLFEKVKSLK													
Consensus	Rgq..#fAD!#LHLDICLVSCFRINPHn#a!k!CLaqsSPqaZHXVIVnSL.....hriIn#paLdHPqIDaVhcrSaELR#f#tLnKRCQGGaHPaIRnRpsLTLKSkDtq..													
	521	530	540	550	560	570	580	590	600	610	620	630	640	650
Dne1	-KGLTRAEFGPAHMLLLVRLIHRDPTLLLTQGGVHNEVQSSITLLEINGLVSLVHQTTPDVAQAEHAEALLANPEKIEVWNPAPINTFADVSSQVLFSTISQKLIQHQIANYTDLKALREILIC													
Hus	FKKPTDLLETRSYKLLSMVKLIHRDPTLLLCNPRKQGPETQSTAEILITGLVQVPSHPEVAQAEHAEALLVHLQDSDIQLNHPDAPVETFWIEISSQLFYICKLTSQMLSTEILKALREILIC													
Consensus	.KelpraeEgrahKcLLLiVrLIHRDPTLLLngrKqahEtQSSITLEINGLVqLhQshHP#VAQAEHAEALLaHa!#kI#i#NHP#APi#TFW!#SSQLfScqKLIqHQiansT#iLKALREILIC													
	651	660	670	680	690	700	710	720	730	740	750	760	770	780
Dne1	RNTFLQRKDYAH-----VGSQIR-----ICKQRIKMEVFFHYLWSVDLQVLTLSLSCFLLCEEREICSSOELLVGFIPHN													
Hus	RNKFLKKNQQRDRSSCHSLLYGVGCEHSATGNTQMSYDHDDEFRLACTPGASLRKGRGNSHDSSTAGCGTTPICRQARQKLEVALYMLANPDEVALVNSCFRHLCEEARICGVDVSVNMLPN													
Consensus	RNkFLqrnKaar.....VgC#ia.....ICrQaRiKIEValZMLAnpDl#AVLta#SCFRHLCEEARiCrCgsDElsvgni#PN													
	781	790	800	810	820	830	840	850	860	870	880	890	900	910
Dne1	YHIYQELAQLSATDSRICCFDNTGNVLSRLTLQKRINTLLRKEIENCVHGYPAMEETFRNHEVSKVLQTPYKCKGEDGQA--EVFHRGHRKRRASHQSSSEHDLF---EQTNEANHTMFLLAGGV													
Hus	YNTFHEFRSYNNSMSTGRRA-----LQKRYNALLRRIEHPTAGNIEAMEETHAKAEQATKLLNYPKAKHEDGQARESLHKTIVKRRHSYSGGSDILSDTDSLQEMINATGFLCAGGV													
Consensus	YniZqELiRqLSmasdgRaa.....LQKR!MaLLRiEiNctagqaeAME#ThanaeqasKliqnYPKaKgedGQA..EaIHRgigKRRASHqSgegdI#...#qi#EaANHTMFLcALGGV													
	911	920	930	940	950	960	970	980	990	1000	1010	1020	1030	1040
Dne1	CLHKRSSRQHLLQDSQNHASLGLRQNSLYSSSTSSGHGSLHPSTVSLSTLPPAPPDQVSYCPVYTFVGGLLRLLVCSNEKTGLNITQKVKELVGEHSTQLYPIFLDQVRAIVEKFFDQGGQVNVNVT													
Hus	CLQDRSSSGL-----ATYSPPHGAVSERKGSHTVMSSEGNTDS-----PVSRFNRDLISLHVCNHEKVGQLTRTNVKDLVGLLELSPALYPLFNKLKNTISKFFDQGGQVLLS--													
Consensus	CLqRSSSRq.....aqqnapfGala#rkgsniStnSgeGnidp.....PVsrFndrLLrLVcnnEK!GL#TrkNVK#LVGEtSpalYPIlfqIrai!eKFFDqGGQVln..													
	1041	1050	1060	1070	1080	1090	1100	1110	1120	1130	1140	1150	1160	1170
Dne1	DINTQFIEHTIYIHKSLDLPKANKDPNNDQSPSEHLGVTSEIGHMLGIVRYVRLDHTVYAIRIKTKLQQLVEVHAKRRDILAFRQEMKFRNKVEYLTDVHGTSHQIAPPSSARAILINTSLIFRD													
Hus	DSNTQFVEQTIATKMLLD-----NHTEGSSEHLGASIEATHMLNRYRYVRLDMVHAIQITKTLQQLVEVHARRDILSFCQEMKFRNKVEYLTDVHGTSHQIAPPSSARAILINTSLIFRD													
Consensus	DINTQF!EqTiaTKnILD.....NdqegpSEHLGqasTEghMLniVRYVRLdmVhAIrIKTKLQQLVEVHARRDILaFrQEMKFRNK#VEYLTDVHGTShqAdd...DaaCT.....RD													
	1171	1180	1190	1200	1210	1220	1230	1240	1250	1260	1270	1280	1290	1300
Dne1	LQQRHEAVYRLLRGLPLOPEESDRGLDHAKSALFLKYFTLFRNLLHDCIDSSEREKEMHNTPLPPRPRMARGKLTALRNATILRMSNLLGANDISGLMHSIDLGYNPOLQTRAFHEVLTQILQOGT													
Hus	LQQRHEAVYSLLAGLPLOPEEGVGLHEAKSALFLKYFTLFRNLLHDC---SEVEDENRQTG---GRKRGHSRRLASLRHCTVLRMSNLLNANVDSGLMHSIDLGYNKDLQTRAFHEVLTQILQOGT													
Consensus	LQQRHEAVaLLaGLPLOPEEGDrg#LH#AKSaLFLKYFTLFRNLLHDC...SEaEdEna#Tg...gRkRgaarrLaaLRnat!LRMSNLLnAN!DSGLMHSIDLGYNKDLQTRAFHEVLTqILQOGT													
	1301	1310	1320	1330	1340	1350	1360	1370	1380	1390	1400	1410	1420	1430
Dne1	EFDTLAETVLADRFEQLVQLYTHISDQKELPIAHMLANVYVTSQMDLARVLYTLFDRKILLSPLLNMFYREYVSDCHQTLFRGNSLASKINAFCKFYGRSYLQMLLEPLIRPLLDEEE--ETCFEY													
Hus	EFDTLAETVLADRFERLVELYTHIGDQKELPIAHMLANVYVPCSQMDLARVLYTLFDRKILLYQLLNMFYREYVSDCHQTLFRGNSLASKINAFCKFYGRSYLQMLLEPLIRPLLDEEE--ETCFEY													
Consensus	EFDTLAETVLADRFErLV#LYTHigDqKELPIAHMLANVYVpCsqMDLARVLYTLFDRkILLsqLLNMF#rEYVsdChQTLFRGNSLASKINaFCFKiYGRsYLqML#PLrPliDee#...etcFEY													



A



B

	1	10	20	30	40	50	60	70	80	90	100	110	120	130
Dne1	MSLADMGTASRSAGGEGGRHYDLATGGAGSGGHPVGGGLPGGRHTSLSTPSGVDGTPSTPRHRGGKLVTRVQHLDDSTHFQVQAKALGRVLFQVCRQLNLEADYFGLYQEVSTHTKYMLDLEKP													
Hus	MGEIEGTYRALPTSGTRLGGQTAIGVST---LEPEQLSPRNQEKHMRTVRLDSTVLEFDIEPKCDGQVLLTQVAKHLNLIECDYFGLFKVQSYM--DLLEPNKP													
Consensus\$aegeagsrahPtGGrIGGrnahg1ST...I#geqSLprrrqekH#rIRIq#LDs!e#F#!#aKadGrVLEQVcrqLNLIEADYFGLEx#Vqst..iL#LeKp													
Dne1	131	140	150	160	170	180	190	200	210	220	230	240	250	260
Hus	MKRQVGLSLIDPVLRFCKEYFPDPAQLLEEYTRYFLCLQIKRDLATGSLQCDNTRALNASYLVQASCGDFVPEDYDHYTLSSYRFPVNDQATMQRKTHEINKHYGSSPRAEDLNLLETARRCELVY													
Consensus	inRQVrIpl.#aVLRlA!K#F#PDPaQL#EYTRYFLaLQIKRDLaeerLqCnaNTRAL\$aShiIqaeG0%...#tIDrehLkanr%LPNQ#as\$#.KI#nHqrHcGSPRAEdI#LEIARcE#Yg													
Dne1	261	270	280	290	300	310	320	330	340	350	360	370	380	390
Hus	MKHMPAKQVQVPLNLAVAHMGITVFNITRINTFSMAKTRKISFKRRKRLVKLHPEGYYKYOTVEFFEGRNECKNFWKVCVENHGFRCRTAYQNTPRKTRVLSRGSSFRYSGRTKQIIEFVRENY													
Consensus	irHhAKdREGtkiNLAVAHMG!VFNITRINTFnaK!RKISFKRRKRL!KLHPEghGpYqDTIEF!LegR#ECKNFWK!CVENhgFFRcsa.QnkPrakarfLSRGSSFRYSGrTKQI!#zVr#ng													
Dne1	391	400	410	420	430	440	450	460	470	480	490	500	510	520
Hus	VKRQNFQRSSFRQGLNASSRSQSHYVNSSISANPLLPIDTAAADYRNQCSDSHTPLTKKAAOTLDRRRNDPIGHRSQVTAQAQVEIYQTKNYAADSPTSDEEACSAAGAEKOHHSVAVHDKLNSH													
Consensus	nKRIPYERHRSKTRTSLHA.....LTVDLPKQSYSTOGLRTS.....ASLSSANVSYFPPSSLSPPGLNPLKDSSSSLVDPQ---APVYKSTRAE nKRqn#R#KrrngpLn#.....\$TpdLpKqadfIDrrRdn.....aqlsa#VeiyqpknsaadpPglq#ea#Saaga#rQ...#apaidkIaa#													
Dne1	521	530	540	550	560	570	580	590	600	610	620	630	640	650
Hus	RSLSPQPSQNTSPNSHHQGRGPPARVHPGDHNTDGYGINGNHSLDARGETTPTPTRYDILGSDKSSLSRSEAGTYDVIQAEIQHAKRQELATGVATRSHQNGNGNGHTLSTQHDIEAEYK													
Consensus	RS---SGPSSSDGPTQSAHLIP--GPPVLRPGPG.....FSNDSP--QPSSSLKSHLSLCPQLQARLSTAEQASPLSPVL.....SGAGTARMDN---SGAGTARMDN---QEEQKH rS...qGpQsSdgPSHqSahq.GPdpaRpgPG.....nS#Drr.#isppplrdsLslcp#lqaaLraEaGasdViqaei.....sGaataRh#N.....#aEqKh													
Dne1	651	660	670	680	690	700	710	720	730	740	750	760	770	780
Hus	RKMPTEPSYFLAKELLTERTYKDLVLTFRQVLSLGDVEQ---LQPLFELLDLSLQHNLFRLDIEHRMYQNEGRGGH---FAHRTIGDYMHKHAALPIYQEVYATLDTLHCNHDHYEGDERFR													
Consensus	rhmPe#eaFYIAKEILATERTYIKDL#VInttFRqVLIle#aeq...\$alFenIDpla#h#rgrFLr#IeqR#aq#EGrgga....#aqRIGD!\$#n#aaLke#deYfQr#d#Lhc\$#dategderIr													
Dne1	781	790	800	810	820	830	840	850	860	870	880	890	900	910
Hus	QVYKEFEQKQCYLPTIGELLKPLNLLHYQLILERLCDYEGEEDYADAMVHLLVRSKIGIRSQLPDSANVELCELQRD--INFQALVQPHRLTRQGCILLKHSKRLQQRHFFLSDLLLYGSKS													
Consensus	ayYKEFEqKQCYLPLTfLLKpYqRLVHYRLLSRLCAHYSPGHROYADCHEALKATEVYITELQSSLRLLENLQKTELQRLVGVENLIAPGREFIREGCLHKLTKKGLQQRHFFLSDMLLYTSKS													
Dne1	911	920	930	940	950	960	970	980	990	1000	1010	1020	1030	1040
Hus	PLDQS--FRILGHVYVRSLLTENAEH----NTFSIFGGCAITVSAGTAEKTLMLALSKAARDIKNRPNNQLQLTTLKNCSSSEGLDLFGLSNGNNSLSSVYNGGGLTITQQKQLQQQQQNRT													
Consensus	pLdaS.FRrIghlPIRg\$LEa#n.....ncfS!zaaQcaItVa#grTra#K#eLH#a#Lna#aaaknrgdnnqLqLggLknrcspr.....ng##sSL#e#e#6rG.....#rgL#q#qQnR.													
Dne1	1041	1050	1060	1070	1080	1090	1100	1110	1120	1130	1140	1150	1160	1170
Hus	QPSRSNTALVCHVHRGATVGLGDHLIAEHQLSGYLLRKFKNSSGHAQLHYVFTSFLCYFYKSYQDEFALASLPLLGYTVGPPGHQDAVQKEFVFKLSEKNNHYFFRRESANTYRNALVLRSTTQTQ--													
Consensus	...aNTa\$HYCHrNasVgradHLIa#EnQLSGYLLRKFKNSSGHAQLHYVFTfNCLFFYKThQDYPLASLPLLGYsVSLPREADSIHKDYVFKLQKSHYFFFRRESKYTFERHNDYIKRASSSPGR													
Dne1	1171	1180	1190	1200	1204									
Hus	--DFKVVHSHAVLGN													
Consensus	..dfk#dcSHAS16n.....													

Figure 30 - Sequence analysis of CG1283 (Cdep)

(A) Protein domain structure of CG1283 (Cdep) from *Drosophila* (top) and mouse (bottom). (B) Amino acid comparison shows a 37.2 % of identity between *Drosophila* and *Mus musculus* proteins.

Top: *Drosophila melanogaster* 1167 aa and Lower: *Mus musculus* 1065 aa.

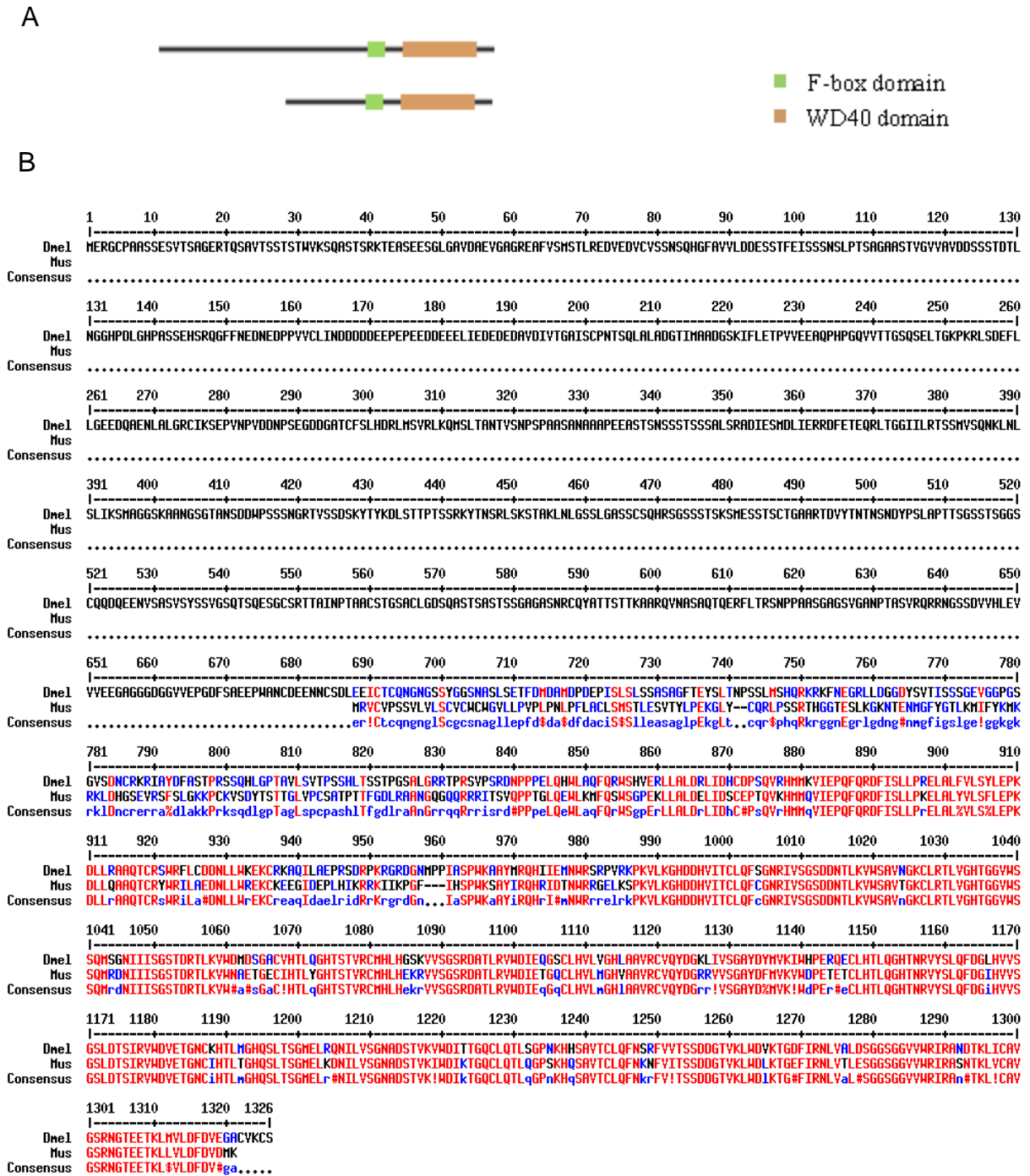


Figure 31 - Sequence analysis of CG15010 (Archipelago)

(A) Protein domain structure of CG15010 (Archipelago) from *Drosophila* (top) and mouse (bottom). (B) Amino acid comparison shows a 30.4 % of identity between *Drosophila* and *Mus musculus* proteins.

Top: *Drosophila melanogaster* 1326 aa and Lower: *Mus musculus* 629 aa.

3.9 - Archipelago is a negative regulator of dS6K levels

3.9.1 - Identification of Archipelago as a negative interactor of dS6K

Among the RNAi lines of 45 candidate genes which produced a strong interactions with *dS6K* (Table 3), we focused our attention on *archipelago* (*ago*). As mentioned in the introduction (section: 1.4.4.3) the protein Ago has been previously described to promote protein degradation of various growth regulators. Since dS6K is a positive regulator of cell growth (Montagne et al., 1999) and nothing is known about its degradation, it was tempting to speculate that Ago may also control the degradation process of dS6K. In the screen, both UAS-RNAi lines to *ago* (*ago*^{RNAi} R2 & *ago*^{RNAi} R3) were found to be strong enhancers of the dS6K-dependent growth phenotype either at 25°C or 29°C (Fig. 32). Although a subtle bent-down of the wing could be observed when *ago*^{RNAi} was induced alone with the *ap*-Gal4 driver (Fig. 32B,D,F,H), the strong bending observed when *dS6K* and *ago*^{RNAi} were co-induced together support the notion that Ago may be a negative regulator of dS6K.

To ensure that the wing phenotype was specific to Ago and did not result from any non-specific effect, potential off-targets of *ago*^{RNAi} were ordered from VDRC (CG16880, CG31132, CG4144, CG8108, CG15239, CG32464, CG3308, CG32685, CG6181, CG14107, CG12052 and CG9781). UAS-RNAi to these potential off-targets was co-induced with *dS6K* in the dorsal compartment of the developing wing using the *ap*-Gal4 driver both at 25°C and 29°C. Importantly, none of these RNAi enhanced the bent-down of the wing, which further argue for the specificity of Ago to regulate dS6K-dependent growth. To confirm that the *ago*^{RNAi} disrupts *ago* expression levels, RT (Reverse Transcriptase) Quantitative-PCR was performed. When induced by either of the ubiquitous *Da*-Gal4 or *Act*-Gal4 drivers, both of the *ago*^{RNAi} lines provoked a severe decrease of *ago* expression (Fig 33). Altogether, these findings strongly suggest that the *dS6K/ago*^{RNAi} genetic interaction reveals a new level for dS6K regulation.



Figure 32 - Genetic interaction at the wing between *dS6K* and *ago*^{RNAi}

The bending down of the adult wing due to *dS6K* overexpression in the dorsal compartment of the developing wing disc (A) is enhanced by co-induction of an RNAi to *archipelago* (*ago*) at 25°C (compare B to C and D to E) and 29°C (compare F to G and H to I). Two UAS-RNAi lines to *ago* were tested; both of these lines cause a bend-down phenotype when co-induced with *dS6K* in the dorsal compartment of the developing wing using *ap-Gal4* driver (C, G, E and I). Notably, the *ago*^{RNAi} itself seldom induces a slight bending down phenotype (B, F D and H).

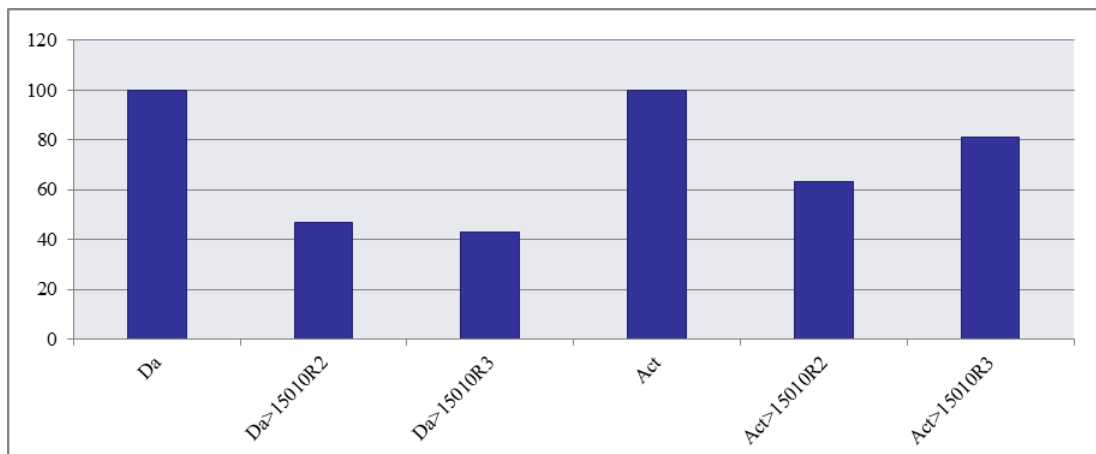


Figure 33 - Efficiency of *ago*^{RNAi} through quantitative PCR

Quantification of the RNAi suppression on *ago* expression levels using two ubiquitous Gal4 drivers (*Da-Gal4* and *Act-Gal4*). Note that the *Da-Gal4* driver is more efficient than the *Act-Gal4* driver to suppress *ago* expression levels as compared to controls (driver alone).

3.9.2- A putative Ago interaction motif in dS6K

Archipelago (*ago*) encodes a 1,326 amino-acid protein, that contains an F-box and seven WD repeats in its carboxyl terminal portion (section 1.4.4 in Introduction and Fig. 12 & Fig. 31). Extensive Y2H assay utilization of the BioGrid source indicates that Ago interacts with several protein targets including Cyclin E, dMyc, dS6K, RpS3, Hippo (Hpo), Supercoiling factor (Scf), Tracheless (Trh), Dysfusion (Dys), Plex A and the proteins encoded by CG13822, CG4998, CG2165 (Formstecher et al., 2005; Alfarano et al., 2005; Giot et al., 2003). The WD repeat domain of Ago has been reported to be necessary for binding to Cyclin E and dMyc. Comparison of their polypeptidic sequence suggests that the S/T-P-x-x-S/T motif might be the consensus recognized by Ago in the substrate (S: Serine; T: Threonine; P: Proline) (Moberg et al., 2004). Studies in *Saccharomyces cerevisiae* suggests that once phosphorylated, this motif constitutes an high-affinity phospho-epitope for binding to the WD repeat domain (Nash et al 2001) and the subsequent ubiquitination of the substrate for proteasome-dependent degradation (Hao et al., 2007; Orlicky et al., 2003; Moberg et al., 2001; Mortimer and Moberg, 2007; Mortimer and Moberg, 2009; Moberg et al., 2004). Sequence analysis revealed that this Ago binding consensus can be found in each of the interactor proteins mentioned above (Fig. 34). Primary structure of dS6K contains such an interacting motif in the auto-inhibitory domain of dS6K, which includes S₄₁₈, P₄₁₉ and T₄₂₂ (Fig. 34 & Fig. 35). This auto-inhibitory domain is conserved in the mammalian S6K and has been shown to be critical for its activation in mammalian cells (Dennis et al., 1998). In *Drosophila*, the activity of dS6K is regulated by the phosphorylation of multiple serine and threonine residues (Stewart et al., 1996), that sequentially involves the auto-inhibitory domain (S₄₁₈, T₄₂₂), the linker domain (T₃₉₈) and the catalytic domain (T₂₃₈) (Fig 35). We therefore, tested three different variants of *dS6K* in which acidic amino acids were substituted for the conserved S/T phosphorylation sites in the auto-inhibitory and in the linker domains (Fig. 35). Two amino acids in the dS6K auto-inhibitory domain S₄₁₈ and T₄₂₂ were substituted to aspartic acid (D) and glutamic acid (E) respectively (UAS-*dS6K*^{STDE}); the T₃₉₈ residue in the linker domain was replaced with a glutamic acid (UAS-*dS6K*^{TE}); and all the those substitutions were present in the third variant (UAS-*dS6K*^{STDETE}) (Fig. 35). When co-expressed with *ago*^{RNAi}, both UAS-*dS6K*^{TE} and UAS-*dS6K*^{STDE} produced a strong

genetic interaction (Fig. 35B, D, H, J) as compared to the *dS6K* variants induced alone (Fig. 35A, C, G, I). Strikingly, co-expression of *ago*^{RNAi} with the UAS-*dS6K*^{STDETE} variant did not enhance the wing phenotype, but rather suppressed the bending-down of the wing due to UAS-*dS6K*^{STDETE} induced alone (Fig. 35F, L). In summary, although these finding suggest that Ago regulates dS6K in a phosphorylation dependent manner, the molecular mechanism of this regulation remains to be elucidated.

IWKKFELLP T P P L S PSR	Hs c-Myc
ALRAPESLL T P P A S SHK	Dm CycE
ASPLPSGLL T P P Q S GKK	Hs Cyc E
SSSSGGFSG S P S S Y HSQ	CG4998-PA
SSSSGGFSG S P S S Y HSQ	CG4998-PB
YSGVEVRV T P S R T EIIIM	RpS3-PA
VTSVVDMK S P N I S SSCSF	Hippo (hpo) CG11228-PA
DESKKFDL T P E E S RRRL	supercoiling factor (scf)
GDQQTGPLP T P P G S ESSY	trh-PA
YHNAM T P P S S V S PRD S NQ	trh-PA
GDQQTGPLP T P P G S ESSY	trh-PB
YHNAM T P P S S V S PRD S NQ	trh-PB
THHNFQQHET S P T V S QQQH	Dysfusion (dys) : dys-PB
VHVVLQVRD S P D S T QQPV	Dysfusion (dys) : dys-PB
PADFIEQWNP S P P W S ESAQ	Dysfusion (dys) : dys-PB
PPGTPSSGYY S P H S S HPPAT	Dysfusion (dys) : dys-PB
L S P C I T TTPTPTSA T P H Q S G	Dysfusion (dys) : dys-PB
THHNFQQHET S P T V S QQQH	Dysfusion (dys) : dys-PC
VHVVLQVRD S P D S T QQPV	Dysfusion (dys) : dys-PC
PADFIEQWNP S P P W S ESAQ	Dysfusion (dys) : dys-PC
PPGTPSSGYY S P H S S HPPAT	Dysfusion (dys) : dys-PC
L S P C I T TTPTPTPTSA T P H Q S G	Dysfusion (dys) : dys-PC
THHNFQQHET S P T V S QQQH	Dysfusion (dys) : dys-PD
VHVVLQVRD S P D S T QQPV	Dysfusion (dys) : dys-PD
PADFIEQWNP S P P W S ESAQ	Dysfusion (dys) : dys-PD
PPGTPSSGYY S P H S S HPPAT	Dysfusion (dys) : dys-PD
L S P C I T TTPTPTPTSA T P H Q S G	Dysfusion (dys) : dys-PD
DMVDDGPNLE T P S D S DEEI	Dm Myc1
PRYNFNLPY T P A S S SPVK	Dm Myc2
DIATGRNTVD S P P T T GSDS	Dm Myc3
FNLPTYTPASS S P V K S VANS	Dm Myc4
VKSVANSRYP S P S S T PYQN	Dm Myc5
STPYQNCSSA S P S Y S PLSV	Dm Myc6
KVVGTSNGNT S P I S S GQDV	Dm Myc7
DSMEFYQTSR S P N L T ATFA	Plex A
ETLNISKYTSS S P T F S RAGSP	Plex A
TQLNVSSGMM S P D I S YIDED	CG2165
HRANRMPAR S P R R T PRQ	Dm dS6K

Figure 34 - The Ago substrates share a putative interactive motif

Amino acid comparison of Ago substrate proteins reveals that a single high-affinity phospho-epitope is well conserved. Note that some of the target proteins display multiple phospho-epitope sites. The central S/T residue marked by an arrowhead, followed by a proline (P) residue and a conserved S/T residue at position +4 are represented. Two candidates selected during screen which physically interact with Ago, show this conserved S/T site (Plex A, CG2165). A well conserved S/T site is also present in *Drosophila* S6 kinase (dS6K).

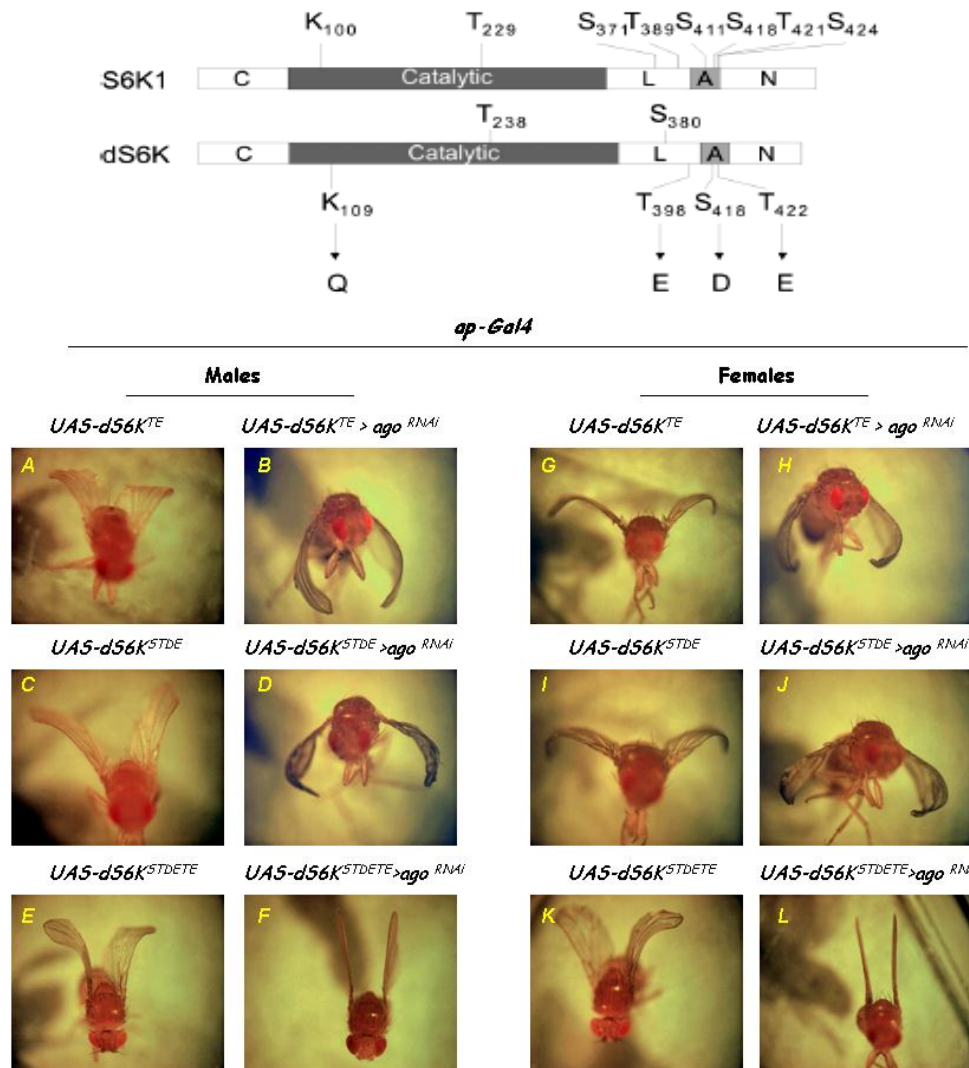


Figure 35 - Genetic interaction between *ago^{RNAi}* and different variants of *dS6K*

Upper Panel: Comparison of dS6K and mS6K1 showing the conserved T and S residues critical for kinase activation. Specific amino acid substitutions are indicated by arrows. The C-terminal (C), linker (L), autoinhibitory (A) and N-terminal (N) domains of the S6K are also indicated (From Barcelo and Stewart, 2002).

Lower panel: Using the *ap-Gal4* driver, the *dS6K* variants *dS6K^{TE}* (A,B,G,H), *UAS-dS6K^{STDE}* (C,D,I,J), *UAS-dS6K^{STDETE}* (E,F,K,L) were overexpressed either alone (A,C,E,G,I,K) or in combination with *ago^{RNAi}* (B,D,F,H,J,L). Males (left panel) and females (right panels) for all the phenotypes are shown separately.

3.9.3- Genetic interaction between *dS6K* and *ago* mutants

To further investigate the genetic interactions between *dS6K* and *ago*, we generated double mutants; either of them exhibit a severe phenotype, since the former is semi-lethal (Montagne et al., 1999) and the latter is lethal at early larval stage (data not shown). Since both genes are closely located on the left arm of chromosome 3, the mutants were recombined with an FRT cassette that allows for clonal analysis. We analyzed the FRT-associated mutations in the eye of heterozygous mutant flies using the *eyeless* promoter to drive flipase during eye development. As the FRT chromosome arm being wild-type for *dS6K* and *ago* also contained a homozygous cell-lethal *Minute* mutation (Montagne et al., 2010); the recombined sister cells, homozygote wild type for *dS6K* and/or *ago*, were eliminated during development. This led to adult eyes that were largely made up of homozygous mutant cells. This way, we analyzed *dS6K* null mutant (Montagne et al., 1999), *ago*¹ and *ago*³ mutants (Moberg et al., 2001) as well as the recombined double mutants. As expected, homozygous *dS6K* mutant eyes were smaller than controls (compare Fig 36B to 36A). In contrast homozygous mutant eyes for either the *ago*¹ or *ago*³ mutations, did not show a significant modification in eye size (Fig. 36E, I). The absence of visible effect is a consequence of opposite effects of the *ago* mutation, the loss-of-function of which has been earlier shown by others to provoke an increase of cellular growth and apoptosis simultaneously (Nicholson et al., 2009). Importantly, the size of double *dS6K-ago* mutant eye was nearly identical to the size of *dS6K* mutant eye (Fig. 36B, F, J). This epistasis of *dS6K* mutation over *ago* mutants was further confirmed by the statistical measurement of the eye surface normalized to the corresponding size of the thorax (Fig. 37). Although, most of the eyes are made up of homozygous mutant cells, few heterozygous ommatidia are not eliminated allowing such measurements (Nicholson et al., 2009). To specifically analyze the role of *dS6K* and *ago* mutations on cellular growth only, the experiment was performed in an H99 background, which suppresses apoptosis (White et al., 1994). The H99 deficiency, which removes the *hid*, *reaper* and *grim* pro-apoptotic genes, is also located on the left arm of the chromosome 3. Recombination of the H99 deficiency with *ago* mutations has been previously shown to be appropriate for the visualization of the overgrowth that results from loss-of-*ago* function (Nicholson et al., 2009). Consistently, homozygous *ago*¹ or *ago*³ mutant eyes were bigger when

combined with the H99 deficiency (Fig. 36G, K). Nonetheless, the triple FRT-*ago-dS6K*-H99 homozygous mutant eyes were smaller and their size was nearly similar to the size of double FRT-*dS6K*-H99 mutant eyes (compare Fig. 36H, 36L to 36D). Statistical measurement of the eye sizes normalized to the thorax size confirmed that, similar to the epistasis observed in the H99 wild-type background, the dS6K mutation was epistatic to the ago mutations in the H99 deletion background (Fig. 37). Altogether these findings indicate that the overgrowth resulting of loss-of *ago* function needs a functional dS6K activity to proceed.

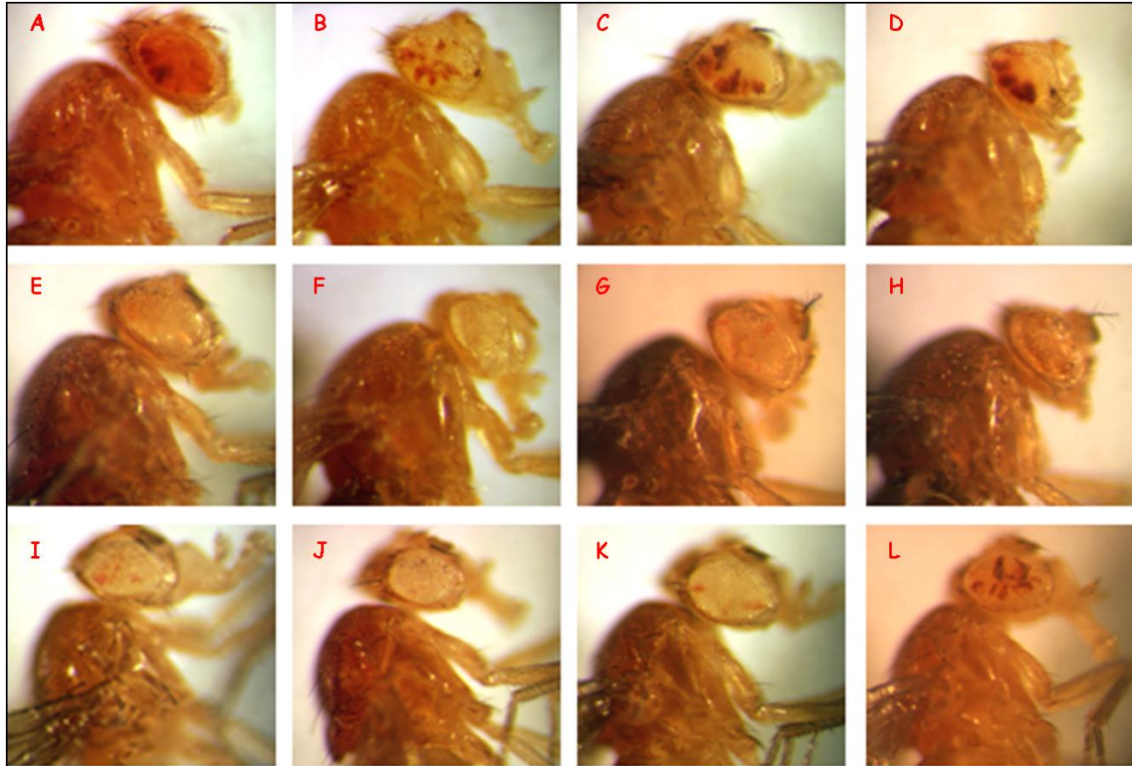


Figure 36 - Genetic interaction between *dS6K* and *ago* in homozygous mutant eyes

Light microscopic images of the corresponding genotypes of adult females (side image photos). Note that the eyes of the flies are mostly composed of homozygous mutant tissues. Upper panel (A-D): GFP-FRT, FRT-*dS6K*, FRT-H99 and FRT-*dS6KH99*, respectively. Middle panel (E-H): FRT-*ago*¹, FRT-*ago*¹*dS6K*, *ago*¹H99 and FRT-*ago*¹*dS6KH99*, respectively. Lower panel (I-L): FRT-*ago*³, FRT-*ago*³*dS6K*, *ago*³H99 and FRT-*ago*³*dS6KH99*, respectively.

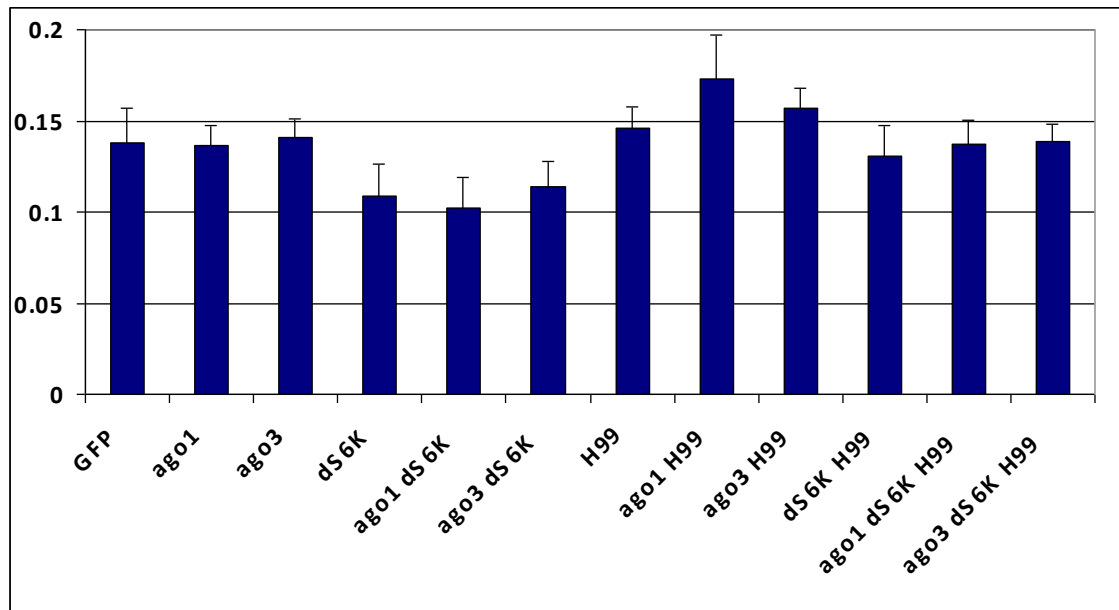


Figure 37 - A representation of the eye/thorax ration between *dS6K* and *ago* mutants

Graphical representation of the mean value of eye size normalized to the corresponding thorax; at least 15 individual females were used for each genotype. Both *ago* alleles do not modify eye size, either alone or in combination with *dS6K* mutation. In contrast, in combination with the H99 deficiency, *ago*¹ and to some extent *ago*³ mutations provoke an increase of eye size. The effect is clearly suppressed by the *dS6K* mutation showing; thereby that *dS6K* is epistatic to *ago*.

3.9.4 - Ago regulates dS6K levels

Our findings strongly support the notion that Ago negatively regulates dS6K. Since previous studies clearly established that Ago regulates ubiquitin ligation and the subsequent proteasome degradation (Hao et al., 2007; Orlicky et al., 2003; Moberg et al., 2001; Mortimer and Moberg, 2007; Mortimer and Moberg, 2009; Moberg et al., 2004), we hypothesized that Ago might regulate the degradation of dS6K. To investigate this issue, dS6K levels were first analyzed with a dS6K specific antibody (Montagne et al., 1999) in *ap-Gal4>ago^{RNAi}* wing imaginal discs where *ago* is repressed in the dorsal compartment. Nonetheless no difference could be detected in the levels of either the genuine (compare Fig 38A and 38C) or the over-expressed dS6K (compare Fig 38B and 38D).

Since, the genuine dS6K protein is barely detectable in *Drosophila* tissues, we took advantage of a transgene that constitutively expressed high levels of dS6K under the control of an *α -tubulin* promoter (Montagne et al., 1999). In contrast with the low expression of the genuine dS6K (Fig 38), the over-expressed kinase could be detected in most of the tissues. The dS6K expression levels was particularly high in the ring gland, where the detection was specific, as the signal dramatically dropped in flip-out clones expressing *dS6K^{RNAi}* (Fig. 39A-C). However, the levels of neither the genuine (data not shown), nor the over-expressed dS6K was modified in flip-out clones expressing *ago^{RNAi}* in imaginal discs (Fig. 39D-F). In contrast, a moderate increase of dS6K levels could be observed in *ago^{RNAi}* flip-out clones generated in the salivary gland (Fig. 39G-I). These findings suggest that in a given tissue, Ago can regulate dS6K level.

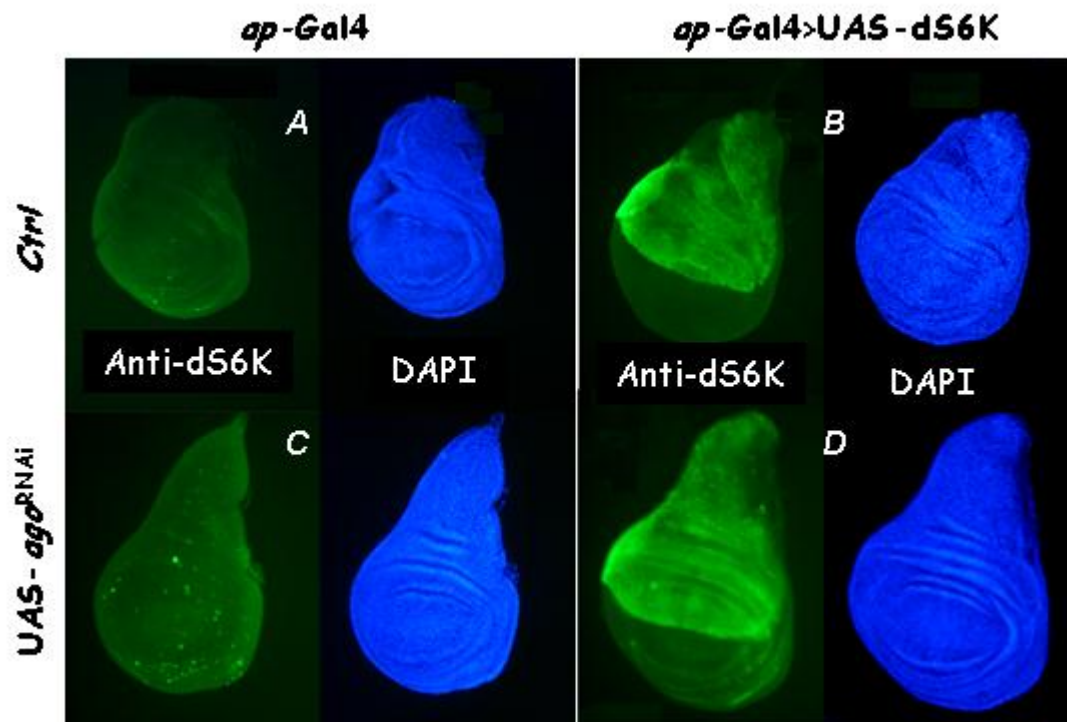


Figure 38 - Immunostaining to dS6K in wing imaginal disc of the 3rd instar larvae

Driving UAS-dS6K with the *ap-Gal4* driver strongly increases dS6K levels in the dorsal compartment of the wing imaginal disc (right panel: left B). An RNAi to *ago* does not modify neither endogenous nor over-expressed *dS6K* levels (left panel: left C & left D). A nuclear staining with DAPI is also shown (right A, B, C and D).

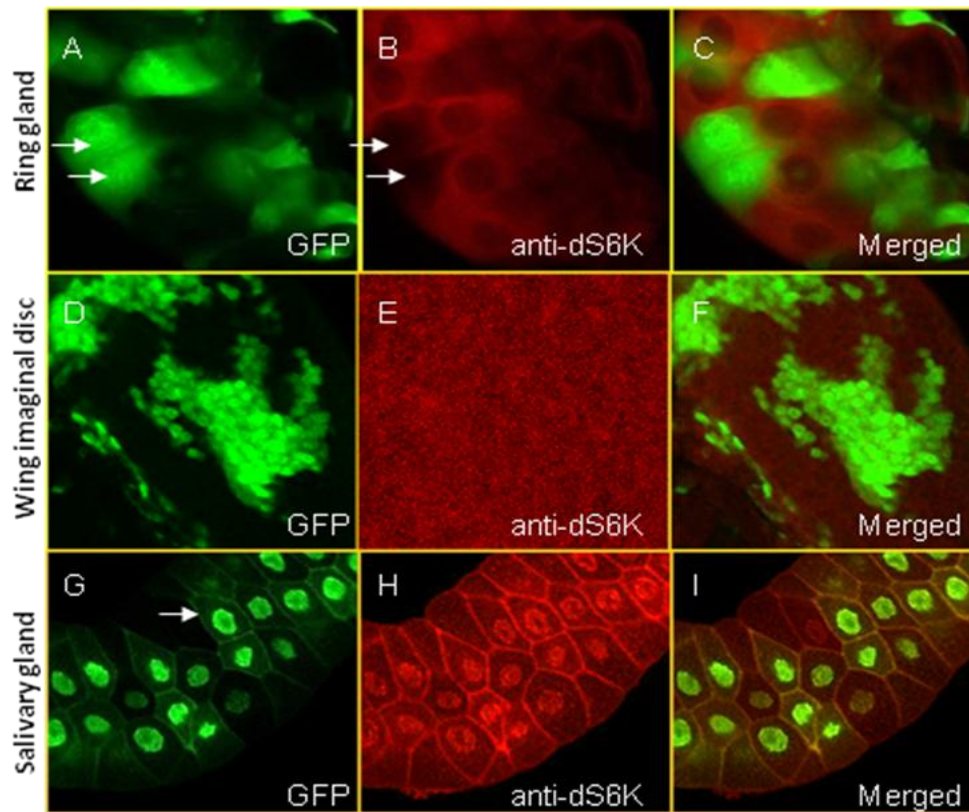


Figure 39 - dS6K expression level and flip-out clones

Upper panel (A-C): Immunostaining to dS6K (B) in the ring gland of the 3rd instar larvae containing GFP-marked clones (A) expressing *dS6K*^{RNAi}. The dS6K expression level is significantly reduced in clones (GFP positive cells) compared to neighboring control cells (GFP negative cells).

Middle Panel (D-F): Immunostaining to dS6K (E) in the wing imaginal disc of the 3rd instar larvae containing GFP-marked clones (D) expressing *ago*^{RNAi}. The dS6K expression level cannot be distinguished between clones (GFP positive) and the neighboring control cells (GFP negative cells).

Lower panel (G-I): Immunostaining to dS6K (H) in the salivary gland of the 3rd instar larvae containing GFP-marked clones (G) expressing *ago*^{RNAi}. The dS6K expression is increased in clones (GFP positive) compared to neighboring control cells (GFP negative cells).

C, F, I are merged images of A-B, D-E and G-H, respectively.

To get further insights into the role of Ago, the constitutive *dS6K* transgene was combined to the *ago* mutants. Consistent with the *ago*^{RNAi} flip-out clones, dS6K levels in imaginal discs of third instar larvae were unaffected in either FRT-*ago*¹ and FRT-*ago*³ mutant clones (Fig. 40A-C and data not shown). Surprisingly, FRT clones generated in endoreplicative tissues provoked a decrease of dS6K levels. In salivary glands (Fig. 40D-F), dS6K protein was barely detectable in FRT-*ago*¹ mutant clones; whereas it was reduced in fat body FRT-*ago*¹ clonal cells (Fig. 40G-I). This unexpected results may be an indirect consequence of the *ago* mutation, which may have strong deleterious effects as the nucleus of homozygous *ago*¹ mutant cell looks disorganized (Fig. 40I). Since nucleus disruption may be due to the pro-apoptotic effect of the *ago*¹ mutation, dS6K levels were then analyzed in double FRT-*ago*¹H99 mutant clones. In this genetic context, endoreplicative homozygous mutant cells were smaller but the nucleus was not disorganized, although its size was severely reduced as compared to the nuclei of control neighboring cells (Fig. 40J-L). This growth defect observed only in endoreplicative cells must be a consequence of impaired Cyclin E degradation, which typically occurs in *ago* mutant cells (Moberg et al., 2001; Shcherbata et al., 2004), since it was earlier described that the endoreplication process requires a cyclic expression of Cyclin E (Follette et al., 1998; Weiss et al., 1998; Edgar and Orr-Weaver, 2001). Nonetheless no modification of dS6K levels could be detected in the FRT-*ago*¹H99 mutant clones (Fig. 40K). Altogether, these findings suggest that in a strong *ago* mutant background many cellular functions may be affected; a genetic context that eventually does not allow the detection of potential cell-autonomous modification of dS6K protein levels.

Since, Western-blotting to the genuine dS6K was very efficient in S2 cells treated with dsRNA (Fig. 28), similar experiments were performed in third instar larvae expressing either of the *ago*^{RNAi} lines directed by the ubiquitous *da-Gal4* or *act-Gal4* drivers. This genetic context does not affect viability (data not shown), most probably because expression of the *ago* mRNA is suppressed but not abolished (Fig. 33). As shown in Fig. 41, driving *ago*^{RNAi} with either of the ubiquitous drivers led to an increase in dS6K levels. This increase in dS6K levels was however not observed in each experiment (data not shown), most probably because of the variability of the

RNAi response (Fig 33 and data not shown). This finding further suggests that Ago does not control dS6K stability in a dose-response manner, but rather in a threshold-dependent manner. We therefore switched to the *ago* mutant alleles, which have been reported to be embryonic lethal (Moberg et al., 2001). Interestingly, few transheterozygous *ago¹/ago³* mutant larvae could survive until second instar larval stage (data not shown). These larvae were then used to prepare protein extracts and analyzed by Western-blotting with either an antibody to dS6K or a phospho-specific antibody to the phosphorylated T₃₉₈ residue of dS6K. As compared to control larvae, dS6K levels were dramatically increased in the transheterozygote *ago¹/ago³* mutant larvae (Fig. 41B, C). This effect is likely restricted to the genuine inactivated dS6K, since the levels of phosphorylated dS6K at residue T₃₉₈ was not increased as compared to an internal control using a Tubulin-specific antibody (Fig. 41D). Quantification of the specific signals and normalization to the α -Tubulin corresponding values (Fig. 41B) confirms that dS6K levels are increased (Fig. 41C), while T398 phosphorylation is slightly decreased (Fig. 41D). In conclusion, our findings strongly support the notion that Ago regulates dS6K levels. Considering that the E3-ligase complex controls substrate ubiquitination and the subsequent targeting to the proteasome, it is likely that Ago regulates dS6K degradation.

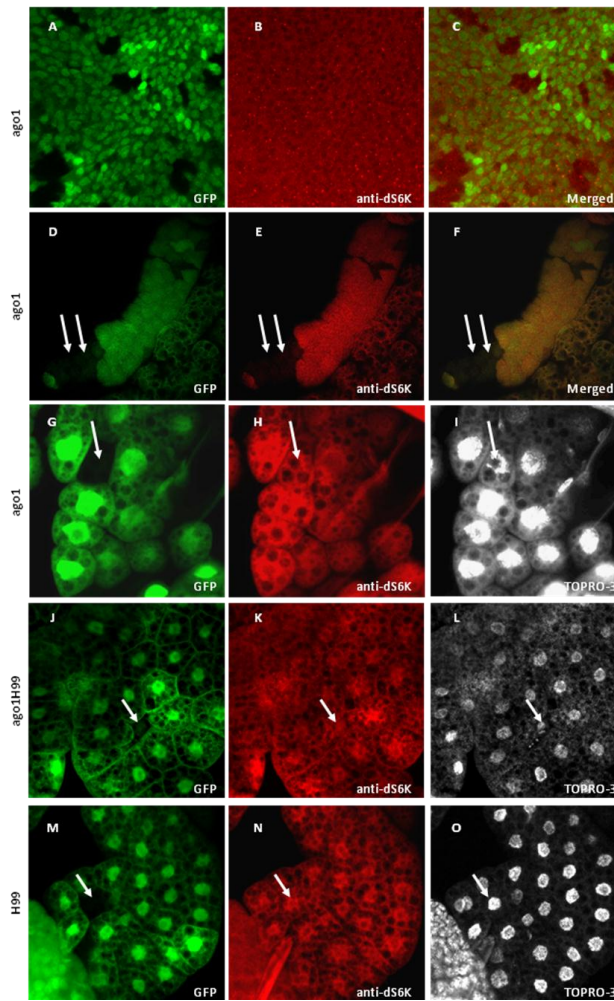


Figure 40 - dS6K expression level in *ago* mutant clones

(A-C): dS6K levels (B) in a wing imaginal disc are not significantly modified in *ago*¹ mutant clones labelled by the lack of GFP (A); (C) is a merged image. (D-F): loss of dS6K staining (arrows in E) in an *ago*¹ mutant clone (arrows in D) within a salivary gland; (F) is a merged image. (G-I): mild reduction of dS6K staining (arrow in H) and nucleus disruption (arrow in I) in an *ago*¹ mutant clone (G) within the larval fat body. (J-L): dS6K level is not significantly modified (arrow in K) in an *ago*¹-H99 double mutant clone (arrow in J) within a larval fat body; note that the nucleus is smaller but not disrupted (arrow in L). (M-O): dS6K level (arrow in N) and nucleus (arrow in O) are not significantly modified in an *H99* mutant clone (arrow in M) within a larval fat body.

(A,D,G,J,M) GFP detection. (B,E,H,K,N) immunostaining to dS6K. C and F are merged of A,B and D,E respectively. (I,L,O) DAPI staining.

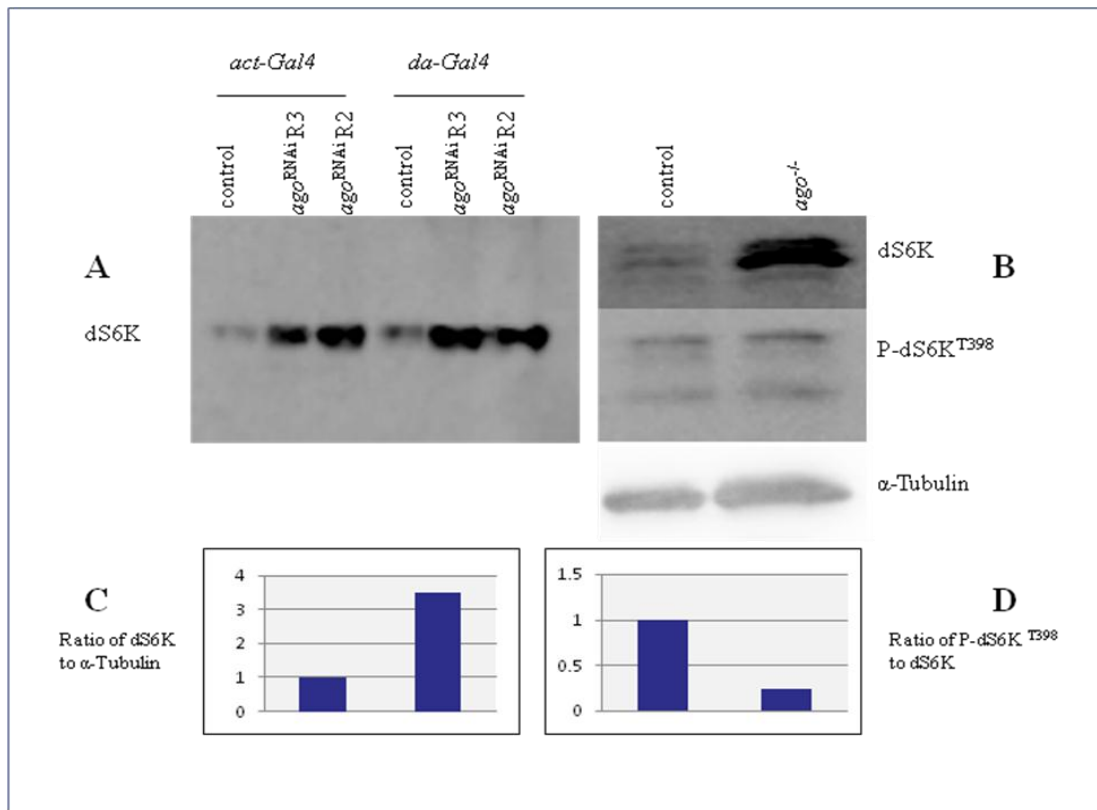


Figure 41 - Western blot analysis to dS6K in *ago*^{RNAi} and *ago* mutant larval extracts

(A) Western blot analysis with specific antibody to dS6K using protein extracts from 3rd instar larvae. Left panel: Both of the UAS-RNAi lines to *ago* when ubiquitously induced using either daughterless-Gal4 (*da*-Gal4) or actin-Gal4 (*act*-Gal4) driver causes an increase in the dS6K expression levels compared to controls. Right Panel: Western-blotting with protein extracts from 2nd instar larvae, using antibody specific to dS6K (top), phospho-T398 residue of dS6K (middle) and α -Tubulin (bottom). As compared to wild type (control), in trans-heterozygous *ago*^{1/ago}³ mutant combination (*ago*^{-/-}) dS6K levels are severely induced (quantification in C), whereas T398 phosphorylation is weakly decreased (quantification in D). Both dS6K and P-dS6K were quantified and normalized to α -Tubulin using ImageJ (C and D).

Chapter 4

Discussion and Perspectives

4.1 - Comparison of genome-wide RNAi screen in *Drosophila*

During my PhD research work, I used *Drosophila* as a model system for genome-wide screens. Taking advantage of the inducible UAS-RNAi lines from NIG, three screens have been performed to identify novel regulators of 1) steroidogenesis, 2) lipid metabolism and, 3) dS6K-dependent growth. I participated in the preparative step that was common of the two first screens scored in their F2 progeny, but, in fact, I did not perform the further screening steps of the first one. The third screen was scored in the F1 progeny. Considering the work published by others and the list of candidates identified, I decided to focus on the genes identified in this latter screen to complete my PhD work. In the following section, I will discuss in details the results of the screens for lipid metabolism and dS6K-dependent growth. However, as I was involved in the three distinct genome-wide RNAi screens, which, therefore, gave me an opportunity to compare the number of candidate genes retained through our strategies with the results of genome-wide screens recently published by others.

To identify novel regulators of Notch signalling and asymmetric cell division, Mummery-Widmer and colleagues screened a total of 20,262 transgenic RNAi lines corresponding to 11,619 protein-coding genes (Mummery-Widmer et al., 2009). The RNAi lines were induced using the *pannier* (*pnr*)-Gal4 driver that is active in the central part of the notum (dorsal thorax). The adults were further scored for notum defects or more appropriate to Notch signalling for bristle phenotypes. This way, 19.6 % of the RNAi lines produced a visible phenotype. A comparison with a list of genes required for Notch signalling or asymmetric cell division indicates that a huge proportion of the candidates were retained through the screen, ultimately validating the screening strategy. Using secondary assays, they finally identified 6 and 23 novel genes involved in asymmetric cell division and Notch signalling, respectively. In a screen for genes involved for intestinal bacterial infection, Cronin et al., challenged 13,053 RNAi lines representing 10,689 genes using a ubiquitous driver, and found 8.3 % of them as susceptible candidates. Using both a hemocyte- and a gut-specific driver, several of the selected RNAi lines were further analysed. The utmost novelty of their investigation was the identification of the JAK-STAT pathway to control the host defense in the gut by regulating epithelial homeostasis through stem cell proliferation (Cronin et al., 2009). To identify genes involved in obesity, Pospislik and colleagues used a ubiquitous driver to screen 11,594 RNAi lines corresponding to 10,489 distinct protein-coding genes. They found 516 RNAi lines (4.5 %) to modify triglyceride content, and which were further analysed with the tissue-specific drivers. This study revealed hedgehog signalling as an essential determinant for triglyceride accumulation in drosophila fat body cells and for the differentiation of white adipocytes in mouse as well (Pospislik et al., 2010). In a screen for genes involved in muscle morphogenesis and function, Schnorrer and colleagues, challenged a total of 17,759 RNAi lines representing 10,461 distinct genes. Using the *Mef2*-Gal4 muscle-specific driver 2,785 genes (26.6 %) were identified to produce lethality (20.2 %) or functional muscle defect without affecting viability (6.4 %). To identify genes involved in heart function, Neely and colleagues screened a total of 8,417 RNAi lines representing 7,061 drosophila genes conserved in mammals (Schnorrer et al., 2010). Furthermore, after several repeated screening steps by Neely et al., 498 genes were identified (7 %) showing enrichment in multiple pathways including TOR and insulin signalling, and

the CCR4-NOT complex implicated in transcriptional regulatory mechanisms. Specific knock-down in drosophila and mouse revealed that the role of the CCR4-NOT complex to control cardiac contractility is conserved throughout evolution (Neely et al., 2010).

In our screen for steroidogenesis using the *phm*-Gal4 driver, about 11,000 lines, representing roughly 7,000 genes were scored, allowing the identification of 620 candidates (8.86 %). The same collection of RNAi lines was also screened for the regulators of dS6K-dependent growth using *ap*-Gal4 driver, leading to the selection of 357 enhancer RNAi lines (3.2 %). A more narrow and stringent selection ends up with a list of 45 genes whose RNAi induced a strong enhancement (0.64 %). In the screen for lipid metabolism at the fat body, approximately 7,300 RNAi lines representing 4000 genes were scored in flip out clones, leading to the identification of 24 candidate genes (0,6 %), the corresponding RNAi of which provoked an increase of LD size.

Comparison of our findings and data published by others revealed that the percentage of candidate genes selected varies a lot regarding the screening strategy. This number can be very high when the Gal4 driver target an essential tissue and the phenotype monitored is not precisely defined. For instance, 20.2 % of the tested genes induced lethality when the RNAi are targeted to muscles (Schnorrer et al., 2010). The high number of candidates found in our screen for steroidogenesis, therefore, suggests that a significant number of the selected genes affect general cellular processes, rather than the steroidogenesis pathway *per se*. Congruently, the classification of the genes regarding their presumptive functions (Fig 19) revealed that some of these candidate genes retain housekeeping activities, for instance, general transcription factors for RNA polIII-dependent transcription or ribosome biogenesis. Thus, this screen needs further rounds of selection to restrict the candidate list to the genes that play specific roles, critical for steroidogenesis. These secondary assays will first rely on an *in silico* elimination of housekeeping genes and then on the direct observation of the prothoracic gland to discard the genes, the RNAi of which are deleterious for gland cell survival.

Strikingly, only 24 candidates (0.6 %) were identified through our screen for lipid metabolism at the fat body following the size of LDs, whereas Pospislik and colleagues identified 516 RNAi lines (4.5 %) as potential candidates when screening for triglyceride content (Pospislik et al., 2010). Although they screened about three times more RNAi lines than us, and hence, very low no. of genes that we found suggest that the modification of LDs size is controlled by a limited set of genes and thus constitutes a very specific parameter for screening.

The screen for dS6K regulators first led to the selection of 357 enhancer RNAi lines (3.2 %). Considering that we were searching for negative regulators of dS6K-dependent growth, this percentage seems rather high. Nonetheless, it could be speculated that RNAi expression of several negative regulators of growth might be selected through our screening strategy. However, an RNAi to the negative regulator may not be able to induce an overgrowth of the dorsal wing blade when induced alone with the *ap*-Gal4 driver, while co-induction of the UAS-dS6K might create a sensitized background appropriate to the visualized subtle extra-growth effects. In agreement with potential dS6K unrelated effects, a previous screen for positive regulator of dS6K-dependent growth following the same phenotypic enhancement identified a rather high number of candidates. This candidate list was easily decreased when considering only the strong enhancements, which finally revealed a small subset of gene products that most-likely intervene in the dS6K signalling pathway (Montagne et al 2010). Following the same strategy, our candidate list was restricted to only 45 strong enhancers (0.64 %) which were further used to generate an interaction map.

4.2 - RNAi screening for new regulators of lipid metabolism

Many of the analogous organ systems that control nutrient uptake, storage, and metabolism in humans are present in the fruit fly (Baker and Thummel, 2007). In *Drosophila*, the fat body accumulates nutrients mostly as LDs that contain triglycerides and proteins (Britton et al., 2002; Beller et al., 2008). Starvation has been known to induce an increase of size of lipid droplets. This phenotype is also observed upon modulation of various growth or metabolic regulators, in particular with the

intermediates of nutrient responsive TOR signaling pathway (Hietakangas and Cohen, 2009; Britton et al., 2002; Beller et al., 2008; Colombani et al., 2003; Zhang et al., 2000; DiAngelo and Birnbaum, 2009).

To identify novel regulators of growth and metabolism centred on the TOR/S6K cassette, we have retained the size of LDs as a specific hallmark to screen the RNAi collection of NIG that targets about half of the *Drosophila* genome. We, however, screened only 7,300 RNAi lines representing roughly one fourth of the genome. This way, 24 candidate genes were identified, the RNAi of which induced in fat body cells provokes an increase of the size of the LDs. The corresponding candidate genes fall in different functional categories: four encoded signalling molecules (*Pak3*, *twins*, CG2165 and *Rack1*), eight encoded enzymes of lipid metabolism (*sxe2*, *thiolase*, *start1*, CG3961, CG5122, CG4630, *cyp4g* and α/β hydrolase), three encoded ribosomal proteins (*mRpS31*, *mRpS35* and *mRpL28*), and four encoded proteins which are linked to development or activity of the CNS (*Fasciclin2*, *period*, *dunce* and *RhoGAP93B*). Strikingly, none of these RNAi lines produced a phenotype as strong as the one induced in our pilot experiment with an RNAi to *Rheb*, which encodes an upstream effector in the TOR signalling pathway. These findings suggest that one of the *Fasciclin* genes might control the regulation of lipid metabolism. This also gives an idea that the mild effect in the size of lipid droplets due to *Fasciclin2* could be due to any of the potential off-targets. This emphasizes a further detailed study for an invaluable insight of the overlapping of lipid metabolism and nervous system development processes. Although, only one fourth of the genome was screened, our finding indicates that *Rheb* and the downstream TOR play a major role in the regulation of LD size and further confirm that this pathway is central in responding to nutrients availability. Furthermore, the signalling molecules identified through our screen may be alternative modulator of this pathway.

During the course of our screen for LDs size modification, two distinct studies have been published that report screenings for lipid metabolism in *Drosophila*. As mentioned above, Pospislik and colleagues screened for triglyceride storage using 11,594 RNAi lines (Pospislik et al., 2010). Gene ontology highlighted the involvement of regulators of feeding control, nutrient transport, chromatin remodelling, cell cycle

and development, but also the components of protein translation and degradation machineries. In another study, Guo and colleagues screened the entire *Drosophila* genome with RNAi treatment in cultured S2 cells, following the aspect of LDs as a specific hallmark for lipid metabolism. The 180 genes identified this way, encode regulators and enzymes of lipid metabolism, members of translation machinery, subunits of RNAPolymerase II, splicosome or proteasome, and effector of vesicle trafficking. They also demonstrated 5-different phenotypic classes regarding the size, the number and the aspect of LDs. These phenotypic features, could not be directly transposed to fat body cells, since it was necessary to add high amounts of oleic acid in the media to trigger LD formation in the cultured S2 cells (Guo et al., 2008). These epithelial-like diploid cells are originated from embryo and do not appear to be specialized in lipid storage and homeostasis. Each of those screens including ours, are different and do not provide overlapping results. In particular, none of the candidate genes found in our LD size screen was found in the S2 cell screen and only a potential calcium transporter (CG2165) was found in the Pospislik screen, the gene disruption of which leads to a decrease in triglyceride content (Pospislik et al., 2010). Consistent with the search for regulators and effectors of lipid metabolism, each of the screens identified enzymes that catalyzed synthesis, modification or degradation of lipids. Strikingly, members of the translational machinery were also found in each of those screens, suggesting that translation efficiency contributes to the lipid metabolism. It is worth noting that LDs are typically constituted in lipids, mostly triglycerides, surrounded by a phospholipid monolayer and associated proteins (Farese and Walther, 2009; Goodman, 2008; Beller et al., 2006; Cermelli et al., 2006). Therefore, it can be speculated that the increase of LD size is a direct consequence of protein synthesis failure, since packaging of large LDs requires fewer proteins than small LDs for an identical amount of lipids. This interpretation is consistent with the identification of three ribosomal protein gene in our screen and with the increase of LD size observed in mutant cells for the *slif* amino acid transporter (Colombani et al., 2003). This further suggests that the increased of LD size induced by starvation, basically reflects an economic strategy for lipid packaging.

Unexpectedly, our screen for LD size identified several genes, for which the function was previously linked to the development or the activity of the CNS, indicating that these candidate genes also control basic metabolism. This is of particular interest, since lipid metabolism plays a critical role in the differentiation and activity of neurons. Considering that modification of lipid metabolism is proposed to play a critical role in several neurological diseases. Thus, our screen may lead to the identification of novel regulators that potentially affect lipid metabolism in neurons, an issue that we wish to follow in a future collaborative project.

In summary, these three distinct studies highlight the role of enzymes of lipid metabolism and protein translation machinery in triglyceride storage and physiology of LDs, although each of the screens identified a distinct set of candidate genes. In contrast to the others, only 24 potential candidates were retained through our screening strategy, suggesting that the increase of LD size is a very specific parameter that does not reflect all the physiological aspects of lipid metabolism. However, I did not continue this LD project when the S2 screen was published (Guo et al., 2008), and concentrated on the screen for negative regulators of dS6K-dependent growth.

4.3 - RNAi screening for negative regulators of dS6K-dependent-growth

Loss-of-function for dS6K provokes severe growth defect (Montagne et al., 1999). In contrast gain-of-function induced very subtle over-growth which could be visualized only when dS6K is induced in the developing dorsal wing compartment, leading to a bending-down of the adult wing. By monitoring an enhancement of the bending-down, this sensitized phenotype has been successfully used in a gain-of-function screen to identify novel positive regulators of dS6K-dependent growth (Montagne et al., 2010). This screen failed to identify negative regulators, since suppression of the bending-down of the adult wing happen to be a very frequent event. Hence, to identify novel negative regulators of dS6K-dependent growth we took advantage of the RNAi collection to screen for enhancement of the bending-down phenotype. This way,

11,000 lines roughly corresponding to 7,000 genes have been screened, leading to the selection of 45 genes, which fall in various functional categories, including ubiquitin ligase activity, metabolic enzymes and signalling molecules. Potentially, metabolic enzymes may act downstream of dS6K signalling to down-regulate processes, which could be activated by dS6K. Consistently these candidates catalyse enzymatic reactions of protein and lipid metabolism, two processes that may be regulated by the TOR signalling pathway (see above). Furthermore, dS6K has been shown to directly affect lipid storage regarding fly age (Cho et al., 2010). Signalling molecules rather act upstream of dS6K to integrate growth factor and nutrient signalling. Finally the candidate genes encoding protein with ubiquitin ligase activity might be of great help to characterize the mechanism of dS6K degradation since nothing is known yet about the regulation of this specific cellular process.

Systematic studies with *Drosophila* gene products revealed that seven proteins could physical interact with dS6K in Y2H assay (Formstecher et al., 2005). Interestingly, three of them (CG15010/*ago*, CG8843/*sec5*, CG12019/*cdc37*) were identified as potential negative regulators of dS6K; since their RNAi produced an enhancement of the bent-down wing phenotype. Although our screen uncovers only half of the *Drosophila* genome, the seven dS6K interactors were challenged in our sensitized setting. The RNAi to four of them (CG10622/*sucb*, CG10295/*Pak*, CG14216, CG8128) did not enhance the bent-down phenotype suggesting that they are not negative regulators of dS6K. In fact, an RNAi to a positive regulator of dS6K should suppress the bending-down of the adult wing, an event that is too much frequent (about 50%) to be retained as a relevant phenotype (data not shown).

The *Drosophila* genome-scale Databases for Y2H protein interactions (Bork et al., 2004; Formstecher et al., 2005) has been used in an attempt to set up a connecting network between the candidate genes identified in the screen. All the enhancer candidates were analyzed using web-based sources; “The biogrid” and “BOND”, and thus, scored for the interaction with other partners. The network established this way (Fig. 27) revealed that all the candidate genes, for which Y2H interactive data were available, could be linked together; although additional proteins were required to fulfil some gap in the network. Nonetheless, more than half of these additional genes

products, have been tested through our screen and only two of them were found to mildly enhance the bent-down wing phenotype. As mentioned above, these additional gene products are likely acting independently or as activators of dS6K, but certainly not as repressors, since only the latter could be identified in our screening strategy.

Protein-protein interaction networks are classically established with the list of candidate genes identified through genome-wide screening to highlight specific regulatory modules. Consistent with a role in regulating metabolism, the TOR signalling has been found as a critical determinant in the screen for triglyceride accumulation (Pospislik et al., 2010). This study also revealed that the Hedgehog signalling controls triglyceride accumulation, establishing a physiological link between morphogen signalling and metabolism. This link is further emphasized in our network, since several components of the Hedgehog signalling pathway (*patched*, *fused*, *cubitus interruptus*) appeared to be intermediates necessary for associating together our negative regulators of dS6K-dependent growth (Fig. 27). Alternatively identification of members of the Hedgehog signalling may only reflect the central role of this pathway in the morphogenesis of the wing (Ogden et al., 2004). The discovery that *ago* is a negative regulator of dS6K-dependent growth also emphasizes the role of proteasome-mediated degradation in this protein-protein interaction network. This finding might be of upmost interest, since Ago encodes an F-box Ubiquitin-ligase component, one of the very few proteins that physically interact with dS6K, thus providing a potential molecular insight into the regulation of dS6K degradation.

4.4 - Regulation of dS6K activity

In an attempt to identify some novel regulators of dS6K, the candidate genes, RNAi of which produced an extreme enhancement, were analyzed in S2 cells by Western-blotting after dsRNAi treatment. This way, three genes (*Cdep*, *Nf1*, CG10139) were found to regulate dS6K phosphorylation and one (*ago*) to regulate dS6K levels. The CG10139 encodes a small protein of 224 amino acids without a typical conserved domain. Sequence blast could not identify a mammalian homologue. The gene has not been studied yet and there is no available mutant (Giot et al., 2003; flybase.org). That

this gene is found only in insects suggesting that it might be a target for agronomic treatment. Nonetheless, extensive and deep analyses must be acquired to understand how CG10139 regulates the process of growth through dS6K phosphorylation.

The *Drosophila* CG8318 gene encodes a protein named as Neurofibromin 1 (NF1), the amino acid sequence of which is 60% identical to the unique human NF1 protein (Fig. 29). This is a large protein, which contains a GAP (GTPase activating protein) domain for Ras. In humans, mutation of the *Nf1* tumor suppressor gene causes a familial heritable syndrome. Loss-of-heterozygosity favours the development of nervous system tumors including neurofibromatosis (Ferner et al., 2007). Therefore, elevated Ras activity was thought to contribute to the development of these tumors. However, Ras inhibitors-based therapy has a limited success. Following a proteomic approach, Dasgupta and colleagues (Dasgupta et al., 2005) observed an increase of ribosomal proteins expression in extracts of *Nf1* mutant astrocytes associated with hyperphosphorylation of RPS6. They also observed that treatment with the TOR inhibitor rapamycin, impedes RPS6 phosphorylation and hyperproliferation of NF1 mutant astrocytes. Further studies have now clearly established that NF1 act as a repressor of the mTOR signalling both in cultured cells and in mouse tumors (Johannessen et al., 2005; Johannessen et al., 2008). Since both Ras and mTOR are aberrantly activated in *Nf1*-deficient tumors suggesting that the hyper-activated Ras in these tissues leads to the activation of the PI3K pathway which in turn relieves the TSC2-mediated down-regulation of mTORC1.

The finding that the *Drosophila* NF1 acts as a negative regulator of dS6K-dependent growth validates the relevance of our screen. Several other studies in *Drosophila* have shown that *Nf1* plays an important role in learning and memory (Margulies et al., 2005). In addition, one study has already shown that loss of *Drosophila* NF1 resulted in a reduction in size of larvae, pupae and adult (The et al., 1997). This size defect could be restored by manipulating PKA signalling but not Ras. This growth defective phenotype is intriguing, since NF1 is reported to be a tumor suppressor that inhibits cellular growth. Moreover, we found that RNAi disruption of the *Drosophila* NF1 enhances an overgrowth induced by dS6K-over-expression and increases dS6K phosphorylation. A possible explanation might be that NF1 is required to sustain

systemic growth but acts as a repressor of cell-autonomous growth. In agreement with such a model, several studies have shown that mutation of PI3K leads to a cell-autonomous growth defect (Weinkove et al., 1999), whereas down-regulation of this pathway in the prothoracic gland increases systemic growth (Colombani et al., 2005). Analysis of homozygous mutant clones in an otherwise heterozygote mutant background must be an appropriate approach to address this issue. An alternative hypothesis is that the *Nf1* null mutation could trigger a compensatory response that restrains cellular growth, whereas the down-regulation mediated by the RNAi is not sufficient to fully abolish NF1 expression and subsequently does not trigger this compensatory response. Hence, it could be speculated that this compensatory effect is lost in tumor cells.

The *Drosophila* CG1283 gene (*Cdep*) is conserved throughout evolution. It encodes a protein with several functional domains, including a FERM (Farp ezrin moesin radixin), a Rho GEF (Guanine nucleotide exchange factor) and 2 PH (pleckstrin homology) domains and hence, it is expected to be involved in adhesion, proliferation and/or differentiation (Koyano et al., 1997). An elevated expression level of *Cdep* was observed in hypertrophic stage of chondrocytes (Koyano et al., 2001). A recent study has revealed that it is required for TGF β mediated switch from cohesive to single cell motility in breast cancer progression. Nevertheless, these data do not reveal how *Cdep* contributes to cellular growth, since TGF β promotes tumor cell motility, but also can promote growth arrest (Giampieri et al., 2009). The *Drosophila* *Cdep* physically interacts with *Ci* (*Cubitus interruptus*), a component of the Hedgehog signalling, *Dof* that links together FGF and Ras signalling and *Hrs*, a predicted Tyrosine kinase substrate (Fig. 27; Giot et al., 2003; flybase.org). Our findings indicate that in *Drosophila* imaginal discs, *Cdep* acts as a negative regulator of dS6K-dependent growth. *Cdep* is likely an interesting candidate for further investigation. However, to get insight into the role of *Cdep* regarding cell growth will certainly require an in-depth analysis of its various functional domains.

Concurrent to the completion of our screen for repressors of dS6K-dependent growth, a genome-wide RNAi screen has been performed in S2 cells for identification of novel regulators of the TORC1/S6K module (Lindquist et al., 2011). Using a phospho-

specific antibody to the ribosomal protein s6, the S6K genuine target, an immunofluorescence assay was designed to follow the activity of the TORC1/S6K module. This way, 13,618 genes, representing roughly 97 % of the *Drosophila* genome, were monitored, leading the selection of 240 low-phospho-S6 and 139 high-phospho-S6 genes. The gene products selected in the latter group corresponds to potential repressors, but unexpectedly, none of them match to our list of candidates. These differential findings may rely on the readout. The bending-down of the wing is a highly sensitized phenotype; roughly a 1% increase in the length of the dorsal versus ventral blades produces an adult wing whose proximal/distal axis represents a quarter of circle (Montagne et al., 1999). Hence, our screening strategy can visualize very subtle modification of cellular growth. Moreover, the *ap*-Gal4 driver used for the screen is also active in some embryonic neurones and thus, might provoke lethality when driving RNAi to an essential gene (Montagne et al., 2010). In contrast, only strong modifications of the fluorescent signal due to phospho-specific antibody can be easily detectable in the screen with S2 cells. In addition, it has been observed that phosphorylation of S6 is severely impaired in *S6K1/2* double mutant but not totally abolished, suggesting that an alternative pathway contributes to this phosphorylation (Pende et al., 2004). In summary, Lindquist and colleagues performed a screen for strong regulators of S6 phosphorylation mostly dependent on the TORC1/S6K module (Lindquist et al., 2011), whereas our screen identified specific negative modulators that likely fine-tune the activity or levels of dS6K. Considering that both screens provide a list of novel signalling components for S6K, it will be of fundamental interest to determine whether they act in distinct or common molecular processes.

4.5 - Does Archipelago control dS6K degradation?

Ago, the F box component of SCF-ubiquitin ligase and the *Drosophila* ortholog of the mammalian F-box protein Fbw7 (SCFF^{bw7}) has been implicated in the control of dMyc, cyclin E, Notch and Trh (Moberg et al., 2001; Moberg et al., 2004; Tetzlaff et al., 2004; Mortimer and Moberg, 2007). It has previously been shown that ago mutant cells proliferate more than wild type cells and contain an increased levels of Cyc E

(Moberg et al., 2001). The overgrowth of *ago* mutant tissue implies that *ago* mutant cells grow at an accelerated rate in comparison to wild-type cells (Moberg et al., 2004). Because *Drosophila* Cyc E has also been shown to promote S phase entry but not growth (Neufeld and Edgar, 1998), the increased growth of *ago* cells suggested that there are other *ago* substrates that promote cell growth (Moberg et al., 2004). In addition, it has been shown that both dMyc and Cyc E interact with Ago through a well conserved S/T sites. These findings suggested that the increase of Cyc E and dMyc levels cooperate to promote growth in *ago* mutant cells (Moberg et al., 2004; Mortimer and Moberg, 2007).

ago encodes a 1326 amino-acids protein containing an F-box and seven WD repeats through which it interacts with its substrate, thereby regulating the turnover of its targeted protein (Skowrya et al., 1997; Mortimer and Moberg, 2007). An S/T site followed by proline (P) is present in all of the interactive proteins of Ago including the auto-inhibitory domain of dS6K, suggesting that it is putative Ago target (Fig. 34 & 35). Considering that Ago physically interacts with dS6K in Y2H assay (Formstecher et al., 2005), and that *ago*^{RNAi} was found in our screen to enhance a dS6K-dependent wing phenotype, we further investigated the potential role of Ago in the dS6K degradation. In favor of this hypothesis, we observed that overgrowth of *ago* mutant tissues requires a functional dS6K and that dS6K levels were dramatically increased in *ago* mutant larvae. Likewise, an increase of dS6K levels was observed in S2 cells treated with dsRNA to *ago*, in particular in serum-deprived S2 cells. Unexpectedly, the increase of dS6K levels was accompanied by a decrease of dS6K phosphorylation in both S2 cells and protein extracts of mutant larvae. It will be necessary then to determine whether the molecular processes controlled by dS6K are increased. To address this issue, a mammalian S6 transgene will be combined with *ago* mutants since the mammalian ribosomal protein S6 is a competent target for dS6k and a phospho-specific antibody is available to monitor S6 phosphorylation.

Surprisingly, we were unable to detect an increase of dS6K levels in clonal *ago* mutant cells of imaginal discs. In endoreplicative tissues an increase of dS6K immuno-staining could be observed in flip-out clones expressing *ago*^{RNAi}, but not in homozygote mutant clones. It has been earlier reported that Ago regulates growth differentially in different

tissues. Our findings suggest that at least in some tissues Ago does control dS6K degradation in a cell-autonomous manner and that the increased dS6K levels observed in *ago* mutant larvae is a consequence of systemic effect. This hypothesis is however unlikely, since Ago controls cell growth in a cell-autonomous and can directly bind to dS6K in yeast 2 hybrid assay. Alternatively, the pleiotropic function of Ago, which regulates CycE, dMyc, Notch and Trh (Moberg et al., 2001; Moberg et al., 2004; Mortimer and Moberg, 2007) may have indirect consequence on dS6K. It has been described that the regulators of cell cycle machinery, i.e., dMyc, Notch, dE2F work in a context-dependent-manner (Herranz and Milàn, 2008). Therefore, perturbation in Ago which is known to regulate these proteins could lead to some striking findings. Congruently, we observed a decrease of dS6K levels in clonal *ago* mutant fat body cells, which was reverted when the *ago* mutation was combined to the H99 deficiency. This genetic context suppressed apoptosis (Nicholson et al., 2009), although cell growth was still restricted, probably because of elevated Cyc E levels (Moberg et al., 2001; Shcherbata et al., 2004) the expression of which must be cyclic to sustain endoreplication and growth of the polytenic tissues. It is therefore, conceivable that in a context of cell competition the increase of dS6K levels could not be visualized because of cell interactions consequent to the pleiotropic effects of Ago.

Nonetheless to deeply investigate the physical interaction between Ago and dS6K, the immunoprecipitation assay will be performed in S2 cells over-expressing the different variants of each partner. This study will be completed by an *in vivo* analysis of the expression levels of each dS6K variant in the context of *ago* loss-of-function clones using either RNAi or mutants.

In summary our study supports the notion Ago controls dS6K degradation, although several issues have still to be addressed. This phenomenon should be investigated in mammalian cells, since both the TOR/S6K signalling pathway and the SCF-dependent proteasome degradation process are directly implicated in various human pathologies. Further investigations based on the other candidates selected through our screens may also contribute to the understanding of these regulations.

References

Adams, M. D., Celniker, S. E., Holt, R. A., Evans, C. A., Gocayne, J. D., Amanatides, P. G., Scherer, S. E., Li, P. W., Hoskins, R. A., Galle, R. F., *et al.* (2000). The genome sequence of *Drosophila melanogaster*. *Science* 287, 2185-2195.

Adams, M. D., and Sekelsky, J. J. (2002). From sequence to phenotype: reverse genetics in *Drosophila melanogaster*. *Nat Rev Genet* 3, 189-198.

Adams, R. R., Maiato, H., Earnshaw, W. C., and Carmena, M. (2001). Essential roles of *Drosophila* inner centromere protein (INCENP) and aurora B in histone H3 phosphorylation, metaphase chromosome alignment, kinetochore disjunction, and chromosome segregation. *J Cell Biol* 153, 865-880.

Adie, E. A., Adams, R. R., Evans, K. L., Porteous, D. J., and Pickard, B. S. (2006). SUSPECTS: enabling fast and effective prioritization of positional candidates. *Bioinformatics* 22, 773-774.

Aerts, S., Vilain, S., Hu, S., Tranchevent, L. C., Barriot, R., Yan, J., Moreau, Y., Hassan, B. A., and Quan, X. J. (2009). Integrating computational biology and forward genetics in *Drosophila*. *PLoS Genet* 5, e1000351.

Alessi, D. R., Andjelkovic, M., Caudwell, B., Cron, P., Morrice, N., Cohen, P., and Hemmings, B. A. (1996). Mechanism of activation of protein kinase B by insulin and IGF-1. *Embo J* 15, 6541-6551.

Alessi, D. R., Deak, M., Casamayor, A., Caudwell, F. B., Morrice, N., Norman, D. G., Gaffney, P., Reese, C. B., MacDougall, C. N., Harbison, D., *et al.* (1997). 3-Phosphoinositide-dependent protein kinase-1 (PDK1): structural and functional homology with the *Drosophila* DSTPK61 kinase. *Curr Biol* 7, 776-789.

Alfarano *et al.*, (2005). The Biomolecular Interaction Network Database and related tools 2005 update. *Nucleic Acids Res.* 33. D418-D424.

Anonymous, (2003). (The FlyBase Consortium). The FlyBase database of the *Drosophila* genome projects and community literature. *Nucleic Acid Res* 31,172-175.

Aravin, A. A., Naumova, N. M., Tulin, A. V., Vagin, V. V., Rozovsky, Y. M., and Gvozdev, V. A. (2001). Double-stranded RNA-mediated silencing of genomic tandem repeats and transposable elements in the *D. melanogaster* germline. *Curr Biol* 11, 1017-1027.

Arquier, N., and Leopold, P. (2007). Fly foie gras: modeling Fatty liver in *Drosophila*. *Cell Metab* 5, 83-85.

Asano, M. (2009). Endoreplication: the advantage to initiating DNA replication without the ORC? *Fly (Austin)* 3, 173-175.

Bai, C., Sen, P., Hofmann, K., Ma, L., Goebel, M., Harper, J. W., and Elledge, S. J. (1996). SKP1 connects cell cycle regulators to the ubiquitin proteolysis machinery through a novel motif, the F-box. *Cell* 86, 263-274.

Bai, J., Sepp, K. J., and Perrimon, N. (2009). Culture of *Drosophila* primary cells dissociated from gastrula embryos and their use in RNAi screening. *Nat Protoc* 4, 1502-1512.

Baker, K. D., and Thummel, C. S. (2007). Diabetic larvae and obese flies-emerging studies of metabolism in *Drosophila*. *Cell Metab* 6, 257-266.

Balakrishnan, A., Bleeker, F. E., Lamba, S., Rodolfo, M., Daniotti, M., Scarpa, A., van Tilborg, A. A., Leenstra, S., Zanon, C., and Bardelli, A. (2007). Novel somatic and germline mutations in cancer candidate genes in glioblastoma, melanoma, and pancreatic carcinoma. *Cancer Res* 67, 3545-3550.

Balendran, A., Currie, R., Armstrong, C. G., Avruch, J., and Alessi, D. R. (1999). Evidence that 3-phosphoinositide-dependent protein kinase-1 mediates phosphorylation of p70 S6 kinase in vivo at Thr-412 as well as Thr-252. *J Biol Chem* 274, 37400-37406.

-
- Bandi, H. R., Ferrari, S., Krieg, J., Meyer, H. E., and Thomas, G. (1993). Identification of 40 S ribosomal protein S6 phosphorylation sites in Swiss mouse 3T3 fibroblasts stimulated with serum. *J Biol Chem* 268, 4530-4533.
- Barcelo, H., and Stewart, M. J. (2002). Altering *Drosophila* S6 kinase activity is consistent with a role for S6 kinase in growth. *Genesis* 34, 83-85.
- Barolo, S., and Posakony, J. W. (2002). Three habits of highly effective signaling pathways: principles of transcriptional control by developmental cell signaling. *Genes Dev* 16, 1167-1181.
- Bateman, J. M., and McNeill, H. (2004). Temporal control of differentiation by the insulin receptor/tor pathway in *Drosophila*. *Cell* 119, 87-96.
- Bayascas, J. R., and Alessi, D. R. (2005). Regulation of Akt/PKB Ser473 phosphorylation. *Mol Cell* 18, 143-145.
- Beller, M., Riedel, D., Jansch, L., Dieterich, G., Wehland, J., Jackle, H., and Kuhnlein, R. P. (2006). Characterization of the *Drosophila* lipid droplet subproteome. *Mol Cell Proteomics* 5, 1082-1094.
- Beller, M., Sztalryd, C., Southall, N., Bell, M., Jackle, H., Auld, D. S., and Oliver, B. (2008). COPI complex is a regulator of lipid homeostasis. *PLoS Biol* 6, e292.
- Beller, M., Bulankina, A.V., Hsiao, H.H., Urlaub, H., Jäckle, H and Kühnlein, R.P. (2010). PERILIPIN-Dependent Control of Lipid Droplet Structure and Fat Storage in *Drosophila*. *Cell Metabolism* 12: 521–532.
- Bernstein, E., Caudy, A. A., Hammond, S. M., and Hannon, G. J. (2001). Role for a bidentate ribonuclease in the initiation step of RNA interference. *Nature* 409, 363-366.
- Biondi, R. M., Kieloch, A., Currie, R. A., Deak, M., and Alessi, D. R. (2001). The PIF-binding pocket in PDK1 is essential for activation of S6K and SGK, but not PKB. *Embo J* 20, 4380-4390.

Bjorklund, M., Taipale, M., Varjosalo, M., Saharinen, J., Lahdenpera, J., and Taipale, J. (2006). Identification of pathways regulating cell size and cell-cycle progression by RNAi. *Nature* 439, 1009-1013.

Bodart, J. F. (2010). Extracellular-regulated kinase-mitogen-activated protein kinase cascade: unsolved issues. *J Cell Biochem* 109, 850-857.

Bork, P., Jensen, L. J., von Mering, C., Ramani, A. K., Lee, I., and Marcotte, E. M. (2004). Protein interaction networks from yeast to human. *Curr Opin Struct Biol* 14, 292-299.

Brand, A. H., and Perrimon, N. (1993). Targeted gene expression as a means of altering cell fates and generating dominant phenotypes. *Development* 118, 401-415.

Brasaemle, D. L., Barber, T., Wolins, N. E., Serrero, G., Blanchette-Mackie, E. J., and Londos, C. (1997). Adipose differentiation-related protein is an ubiquitously expressed lipid storage droplet-associated protein. *J Lipid Res* 38, 2249-2263.

Brasaemle, D. L., Levin, D. M., Adler-Wailes, D. C., and Londos, C. (2000). The lipolytic stimulation of 3T3-L1 adipocytes promotes the translocation of hormone-sensitive lipase to the surfaces of lipid storage droplets. *Biochim Biophys Acta* 1483, 251-262.

Britton, J. S., and Edgar, B. A. (1998). Environmental control of the cell cycle in *Drosophila*: nutrition activates mitotic and endoreplicative cells by distinct mechanisms. *Development* 125, 2149-2158.

Britton, J. S., Lockwood, W. K., Li, L., Cohen, S. M., and Edgar, B. A. (2002). *Drosophila*'s insulin/PI3-kinase pathway coordinates cellular metabolism with nutritional conditions. *Dev Cell* 2, 239-249.

Bryk, B., Hahn, K., Cohen, S. M., and Teleman, A. A. (2010). MAP4K3 regulates body size and metabolism in *Drosophila*. *Dev Biol*.

Buchanan, M. E. and Davis, R.L. (2010). A distinct set of *Drosophila* brain neurons required for NF1-dependent learning and memory. *J. Neurosci.* 30, 10135-10143.

Bulankina, A. V. (2003) TIP47 is recruited to lipid droplets and important for the organelle biogenesis and function, Georg-August-Universität zu Göttingen.

Burgering, B. M., and Coffey, P. J. (1995). Protein kinase B (c-Akt) in phosphatidylinositol-3-OH kinase signal transduction. *Nature* 376, 599-602.

Burnett, P. E., Blackshaw, S., Lai, M. M., Qureshi, I. A., Burnett, A. F., Sabatini, D. M., and Snyder, S. H. (1998). Neurabin is a synaptic protein linking p70 S6 kinase and the neuronal cytoskeleton. *Proc Natl Acad Sci U S A* 95, 8351-8356.

Caldwell, P.E., Walkiewicz, M., Stern, M. (2005). Ras activity in the Drosophila prothoracic gland regulates body size and developmental rate via ecdysone release. *Curr. Biol.* 15(20): 1785-1795.

Calhoun, E. S., Jones, J. B., Ashfaq, R., Adsay, V., Baker, S. J., Valentine, V., Hempen, P. M., Hilgers, W., Yeo, C. J., Hruban, R. H., and Kern, S. E. (2003). BRAF and FBXW7 (CDC4, FBW7, AGO, SEL10) mutations in distinct subsets of pancreatic cancer: potential therapeutic targets. *Am J Pathol* 163, 1255-1260.

Calleja, V., Alcor, D., Laguerre, M., Park, J., Vojnovic, B., Hemmings, B. A., Downward, J., Parker, P. J., and Larijani, B. (2007). Intramolecular and intermolecular interactions of protein kinase B define its activation in vivo. *PLoS Biol* 5, e95.

Cantley, L. C. (2002). The phosphoinositide 3-kinase pathway. *Science* 296, 1655-1657.

Caplen, N. J., Fleenor, J., Fire, A., and Morgan, R. A. (2000). dsRNA-mediated gene silencing in cultured Drosophila cells: a tissue culture model for the analysis of RNA interference. *Gene* 252, 95-105.

Cardozo, T., and Pagano, M. (2004). The SCF ubiquitin ligase: insights into a molecular machine. *Nat Rev Mol Cell Biol* 5, 739-751.

Cermelli, S., Guo, Y., Gross, S. P., and Welte, M. A. (2006). The lipid-droplet proteome reveals that droplets are a protein-storage depot. *Curr Biol* 16, 1783-1795.

Cho, I., Horn, L., Felix, T.M., Foster, L., Gregory, G., Starz-Gaiano, M., Chambers, M.M., Luca, M.D and Leips, J. (2010). Age- and diet-specific effects of variation at S6 Kinase on life history, metabolic, and immune response traits in *Drosophila melanogaster*. *DNA Cell Biol.* 29(9), 473-485.

Choi, K. M., McMahon, L. P., and Lawrence, J. C., Jr. (2003). Two motifs in the translational repressor PHAS-I required for efficient phosphorylation by mammalian target of rapamycin and for recognition by raptor. *J Biol Chem* 278, 19667-19673.

Chung, J., Kuo, C. J., Crabtree, G. R., and Blenis, J. (1992). Rapamycin-FKBP specifically blocks growth-dependent activation of and signaling by the 70 kd S6 protein kinases. *Cell* 69, 1227-1236.

Clemens, J. C., Worby, C. A., Simonson-Leff, N., Muda, M., Maehama, T., Hemmings, B. A., and Dixon, J. E. (2000). Use of double-stranded RNA interference in *Drosophila* cell lines to dissect signal transduction pathways. *Proc Natl Acad Sci U S A* 97, 6499-6503.

Colombani, J., Bianchini, L., Layalle, S., Pondeville, E., Dauphin-Villemant, C., Antoniewski, C., Carré, C., Noselli, S and Léopold, P. (2005). Antagonistic Actions of Ecdysone and Insulins Determine Final Size in *Drosophila*. *Science* 310, 667-670.

Colombani, J., Raisin, S., Pantalacci, S., Radimerski, T., Montagne, J., and Leopold, P. (2003). A nutrient sensor mechanism controls *Drosophila* growth. *Cell* 114, 739-749.

Crespo, J. L., Diaz-Troya, S., and Florencio, F. J. (2005). Inhibition of target of rapamycin signaling by rapamycin in the unicellular green alga *Chlamydomonas reinhardtii*. *Plant Physiol* 139, 1736-1749.

Crespo, J. L., and Hall, M. N. (2002). Elucidating TOR signaling and rapamycin action: lessons from *Saccharomyces cerevisiae*. *Microbiol Mol Biol Rev* 66, 579-591, table of contents.

Cronin, S.J.F., Nehme, N.T., Limmer, S., Liegeois, S., Pospisilik, J.A., Schramek, D. Leibbrandt, A., Simoes, R.M., Gruber, S., Puc, U., Ebersberger, I., Zoranovic, T., Neely, G.G., Haeseler, A.V., Ferrandon, D and Penninger, J.M. (2009). Genome-Wide

RNAi Screen Identifies Genes Involved in Intestinal Pathogenic Bacterial Infection. *Science* 325: 340-343.

Dann, S. G., and Thomas, G. (2006). The amino acid sensitive TOR pathway from yeast to mammals. *FEBS Lett* 580, 2821-2829.

Dasgupta, B., Yi, Y., Chen, D.Y., Weber, J.D., and Gutmann, D.H. (2005). Proteomic analysis reveals hyperactivation of the mammalian target of rapamycin pathway in neurofibromatosis 1-associated human and mouse brain tumors. *Cancer Res.* 65, 2755–2760.

Dennis, P. B., Fumagalli, S., and Thomas, G. (1999). Target of rapamycin (TOR): balancing the opposing forces of protein synthesis and degradation. *Curr Opin Genet Dev* 9, 49-54.

Dennis, P. B., Jaeschke, A., Saitoh, M., Fowler, B., Kozma, S. C., and Thomas, G. (2001). Mammalian TOR: a homeostatic ATP sensor. *Science* 294, 1102-1105.

Dennis, P. B., Pullen, N., Kozma, S. C., and Thomas, G. (1996). The principal rapamycin-sensitive p70(s6k) phosphorylation sites, T-229 and T-389, are differentially regulated by rapamycin-insensitive kinase kinases. *Mol Cell Biol* 16, 6242-6251.

Dennis, P. B., Pullen, N., Pearson, R. B., Kozma, S. C., and Thomas, G. (1998). Phosphorylation sites in the autoinhibitory domain participate in p70(s6k) activation loop phosphorylation. *J Biol Chem* 273, 14845-14852.

DiAngelo, J. R., and Birnbaum, M. J. (2009). Regulation of fat cell mass by insulin in *Drosophila melanogaster*. *Mol Cell Biol* 29, 6341-6352.

Diaz-Benjumea, F. J., and Cohen, S. M. (1993). Interaction between dorsal and ventral cells in the imaginal disc directs wing development in *Drosophila*. *Cell* 75, 741-752.

Donaldson, T. D., and Duronio, R. J. (2004). Cancer cell biology: Myc wins the competition. *Curr Biol* 14, R425-427.

-
- Dong, J., and Pan, D. (2004). Tsc2 is not a critical target of Akt during normal *Drosophila* development. *Genes Dev* 18, 2479-2484.
- Doumanis, J., Wada, K., Kino, Y., Moore, A. W., and Nukina, N. (2009). RNAi screening in *Drosophila* cells identifies new modifiers of mutant huntingtin aggregation. *PLoS One* 4, e7275.
- Du, K., and Tschlis, P. N. (2005). Regulation of the Akt kinase by interacting proteins. *Oncogene* 24, 7401-7409.
- Dubois-Dalcq, M., Feigenbaum, V., and Aubourg, P. (1999). The neurobiology of X-linked adrenoleukodystrophy, a demyelinating peroxisomal disorder. *Trends Neurosci* 22, 4-12.
- Ducharme, N. A., and Bickel, P. E. (2008). Lipid droplets in lipogenesis and lipolysis. *Endocrinology* 149, 942-949.
- Durfee, T., Becherer, K., Chen, P. L., Yeh, S. H., Yang, Y., Kilburn, A. E., Lee, W. H., and Elledge, S. J. (1993). The retinoblastoma protein associates with the protein phosphatase type 1 catalytic subunit. *Genes Dev* 7, 555-569.
- Dutil, E. M., and Newton, A. C. (2000). Dual role of pseudosubstrate in the coordinated regulation of protein kinase C by phosphorylation and diacylglycerol. *J Biol Chem* 275, 10697-10701.
- Edgar, B. A. (2006). How flies get their size: genetics meets physiology. *Nat Rev Genet* 7, 907-916.
- Edgar, B. A., and Orr-Weaver, T. L. (2001). Endoreplication cell cycles: more for less. *Cell* 105, 297-306.
- Ekholm, S. V., and Reed, S. I. (2000). Regulation of G(1) cyclin-dependent kinases in the mammalian cell cycle. *Curr Opin Cell Biol* 12, 676-684.
- Elbashir, S. M., Lendeckel, W., and Tuschl, T. (2001). RNA interference is mediated by 21- and 22-nucleotide RNAs. *Genes Dev* 15, 188-200.

Erikson, E., and Maller, J. L. (1985). A protein kinase from *Xenopus* eggs specific for ribosomal protein S6. *Proc Natl Acad Sci U S A* 82, 742-746.

Farese, R. V., Jr., and Walther, T. C. (2009). Lipid droplets finally get a little R-E-S-P-E-C-T. *Cell* 139, 855-860.

Ferner, R. E., S. M. Huson, et al. (2007). "Guidelines for the diagnosis and management of individuals with neurofibromatosis 1. *J Med Genet* 44 (2), 81-8.

Fire, A. (1999). RNA-triggered gene silencing. *Trends Genet* 15, 358-363.

Fire, A., Xu, S., Montgomery, M. K., Kostas, S. A., Driver, S. E., and Mello, C. C. (1998). Potent and specific genetic interference by double-stranded RNA in *Caenorhabditis elegans*. *Nature* 391, 806-811.

Fire, A. Z. (2007). Gene silencing by double-stranded RNA. *Cell Death Differ* 14, 1998-2012.

Follette, P. J., Duronio, R. J., and O'Farrell, P. H. (1998). Fluctuations in cyclin E levels are required for multiple rounds of endocycle S phase in *Drosophila*. *Curr Biol* 8, 235-238.

Formstecher, E., Aresta, S., Collura, V., Hamburger, A., Meil, A., Trehin, A., Reverdy, C., Betin, V., Maire, S., Brun, C., et al. (2005). Protein interaction mapping: a *Drosophila* case study. *Genome Res* 15, 376-384.

Fraser, A. G., Kamath, R. S., Zipperlen, P., Martinez-Campos, M., Sohrmann, M., and Ahringer, J. (2000). Functional genomic analysis of *C. elegans* chromosome I by systematic RNA interference. *Nature* 408, 325-330.

Friberg, J. (2006). The control of growth and metabolism in *Caenorhabditis elegans*. Umeå Centre for Molecular Pathogenesis. Umeå University, Umeå, Sweden. Larseries Digital Print, Sunbyberg.

Fumagalli, S. a. G. T. (2000). S6 phosphorylation and signal transduction (New York: Cold Spring Harbor, New York).

Gangloff, Y. G., Mueller, M., Dann, S. G., Svoboda, P., Sticker, M., Spetz, J. F., Um, S. H., Brown, E. J., Cereghini, S., Thomas, G., and Kozma, S. C. (2004). Disruption of the mouse mTOR gene leads to early postimplantation lethality and prohibits embryonic stem cell development. *Mol Cell Biol* *24*, 9508-9516.

Gao, X., Zhang, Y., Arrazola, P., Hino, O., Kobayashi, T., Yeung, R. S., Ru, B., and Pan, D. (2002). Tsc tumour suppressor proteins antagonize amino-acid-TOR signaling. *Nat Cell Biol* *4*, 699-704.

Garami, A., Zwartkruis, F. J., Nobukuni, T., Joaquin, M., Rocco, M., Stocker, H., Kozma, S. C., Hafen, E., Bos, J. L., and Thomas, G. (2003). Insulin activation of Rheb, a mediator of mTOR/S6K/4E-BP signaling, is inhibited by TSC1 and 2. *Mol Cell* *11*, 1457-1466.

Garcia-Bellido, A., and Merriam, J. R. (1971). Parameters of the wing imaginal disc development of *Drosophila melanogaster*. *Dev Biol* *24*, 61-87.

Giampieri S, Manning C, Hooper S, Jones L, Hill CS, Sahai E. (2009). Localized and reversible TGF beta signalling switches breast cancer cells from cohesive to single cell motility. *Nat Cell Biol* *11* (11),1287-1296.

Giet, R., and Glover, D. M. (2001). *Drosophila* aurora B kinase is required for histone H3 phosphorylation and condensin recruitment during chromosome condensation and to organize the central spindle during cytokinesis. *J Cell Biol* *152*, 669-682.

Gilbert L.I., Rybczynski, R and J. T. Warren. (2002). Control and biochemical nature of the ecdysteroidogenic pathway. *Ann. Rev. Entomolo.* *47*, 883-916.

Giordano, E., Peluso, I., Senger, S., and Furia, M. (1999). minifly, a *Drosophila* gene required for ribosome biogenesis. *J Cell Biol* *144*, 1123-1133.

Giot, L., Bader, J. S., Brouwer, C., Chaudhuri, A., Kuang, B., Li, Y., Hao, Y. L., Ooi, C. E., Godwin, B., Vitols, E., *et al.* (2003). A protein interaction map of *Drosophila melanogaster*. *Science* *302*, 1727-1736.

-
- Gonczy, P., Echeverri, C., Oegema, K., Coulson, A., Jones, S. J., Copley, R. R., Duperon, J., Oegema, J., Brehm, M., Cassin, E., *et al.* (2000). Functional genomic analysis of cell division in *C. elegans* using RNAi of genes on chromosome III. *Nature* 408, 331-336.
- Gonzalez, A., Chaouiya, C., and Thieffry, D. (2008). Logical modelling of the role of the Hh pathway in the patterning of the *Drosophila* wing disc. *Bioinformatics* 24, i234-240.
- Goodman, J. M. (2008). The gregarious lipid droplet. *J Biol Chem* 283, 28005-28009.
- Gout, I., Minami, T., Hara, K., Tsujishita, Y., Filonenko, V., Waterfield, M. D., and Yonezawa, K. (1998). Molecular cloning and characterization of a novel p70 S6 kinase, p70 S6 kinase beta containing a proline-rich region. *J Biol Chem* 273, 30061-30064.
- Grandori, C., Cowley, S. M., James, L. P., and Eisenman, R. N. (2000). The Myc/Max/Mad network and the transcriptional control of cell behavior. *Annu Rev Cell Dev Biol* 16, 653-699.
- Graves, J. D., and Krebs, E. G. (1999). Protein phosphorylation and signal transduction. *Pharmacol Ther* 82, 111-121.
- Greenberg, A. S., Egan, J. J., Wek, S. A., Garty, N. B., Blanchette-Mackie, E. J., and Londos, C. (1991). Perilipin, a major hormonally regulated adipocyte-specific phosphoprotein associated with the periphery of lipid storage droplets. *J Biol Chem* 266, 11341-11346.
- Greenspan, M. D., and Yudkovitz, J. B. (1985). Mevinolinic acid biosynthesis by *Aspergillus terreus* and its relationship to fatty acid biosynthesis. *J Bacteriol* 162, 704-707.
- Gressner, A. M., and Wool, I. G. (1974). The phosphorylation of liver ribosomal proteins in vivo. Evidence that only a single small subunit protein (S6) is phosphorylated. *J Biol Chem* 249, 6917-6925.

Grewal, S. S. (2009). Insulin/TOR signaling in growth and homeostasis: a view from the fly world. *Int J Biochem Cell Biol* *41*, 1006-1010.

Gronke, S., Mildner, A., Fellert, S., Tennagels, N., Petry, S., Muller, G., Jackle, H., and Kuhnlein, R. P. (2005). Brummer lipase is an evolutionary conserved fat storage regulator in *Drosophila*. *Cell Metab* *1*, 323-330.

Guertin, D. A., Guntur, K. V., Bell, G. W., Thoreen, C. C., and Sabatini, D. M. (2006). Functional genomics identifies TOR-regulated genes that control growth and division. *Curr Biol* *16*, 958-970.

Guo, Y., Walther, T. C., Rao, M., Stuurman, N., Goshima, G., Terayama, K., Wong, J. S., Vale, R. D., Walter, P., and Farese, R. V. (2008). Functional genomic screen reveals genes involved in lipid-droplet formation and utilization. *Nature* *453*, 657-661.

Gutierrez, E., Wiggins, D., Fielding, B., and Gould, A. P. (2007). Specialized hepatocyte-like cells regulate *Drosophila* lipid metabolism. *Nature* *445*, 275-280.

Haemmerle, G., Lass, A., Zimmermann, R., Gorkiewicz, G., Meyer, C., Rozman, J., Heldmaier, G., Maier, R., Theussl, C., Eder, S., *et al.* (2006). Defective lipolysis and altered energy metabolism in mice lacking adipose triglyceride lipase. *Science* *312*, 734-737.

Hahn, K., Miranda, M., Francis, V. A., Vendrell, J., Zorzano, A., and Teleman, A. A. (2010). PP2A regulatory subunit PP2A-B' counteracts S6K phosphorylation. *Cell Metab* *11*, 438-444.

Hammond, S. M., Bernstein, E., Beach, D., and Hannon, G. J. (2000). An RNA-directed nuclease mediates post-transcriptional gene silencing in *Drosophila* cells. *Nature* *404*, 293-296.

Hannon, G. J. (2002). RNA interference. *Nature* *418*, 244-251.

Hannon, G. J., and Conklin, D. S. (2004). RNA interference by short hairpin RNAs expressed in vertebrate cells. *Methods Mol Biol* *257*, 255-266.

-
- Hanrahan, J., and Blenis, J. (2006). Rheb activation of mTOR and S6K1 signaling. *Methods Enzymol* 407, 542-555.
- Hao, B., Oehlmann, S., Sowa, M. E., Harper, J. W., and Pavletich, N. P. (2007). Structure of a Fbw7-Skp1-cyclin E complex: multisite-phosphorylated substrate recognition by SCF ubiquitin ligases. *Mol Cell* 26, 131-143.
- Hara, K., Maruki, Y., Long, X., Yoshino, K., Oshiro, N., Hidayat, S., Tokunaga, C., Avruch, J., and Yonezawa, K. (2002). Raptor, a binding partner of target of rapamycin (TOR), mediates TOR action. *Cell* 110, 177-189.
- Hariharan, I. K., and Bilder, D. (2006). Regulation of imaginal disc growth by tumor-suppressor genes in *Drosophila*. *Annu Rev Genet* 40, 335-361.
- Hariharan, I. K., and Haber, D. A. (2003). Yeast, flies, worms, and fish in the study of human disease. *N Engl J Med* 348, 2457-2463.
- Hay, N., and Sonenberg, N. (2004). Upstream and downstream of mTOR. *Genes Dev* 18, 1926-1945.
- Hayashi, A. A., and Proud, C. G. (2007). The rapid activation of protein synthesis by growth hormone requires signaling through mTOR. *Am J Physiol Endocrinol Metab* 292, E1647-1655.
- Heid, H. W., Moll, R., Schwetlick, I., Rackwitz, H. R., and Keenan, T. W. (1998). Adipophilin is a specific marker of lipid accumulation in diverse cell types and diseases. *Cell Tissue Res* 294, 309-321.
- Heitman, J., Movva, N. R., and Hall, M. N. (1991). Targets for cell cycle arrest by the immunosuppressant rapamycin in yeast. *Science* 253, 905-909.
- Herranz, H., and Milàan, M. (2008). Signalling molecules, growth regulators and cell cycle control in *Drosophila*. *Cell Cycle* 7 (21), 3335-321.
- Hietakangas, V., and Cohen, S. M. (2009). Regulation of tissue growth through nutrient sensing. *Annu Rev Genet* 43, 389-410.

-
- Hild, M., Beckmann, B., Haas, S. A., Koch, B., Solovyev, V., Busold, C., Fellenberg, K., Boutros, M., Vingron, M., Sauer, F., *et al.* (2003). An integrated gene annotation and transcriptional profiling approach towards the full gene content of the *Drosophila* genome. *Genome Biol* 5, R3.
- Ho, M. S., Ou, C., Chan, Y. R., Chien, C. T., and Pi, H. (2008). The utility F-box for protein destruction. *Cell Mol Life Sci* 65, 1977-2000.
- Ho, M. S., Tsai, P. I., and Chien, C. T. (2006). F-box proteins: the key to protein degradation. *J Biomed Sci* 13, 181-191.
- Hodges, A. K., Li, S., Maynard, J., Parry, L., Braverman, R., Cheadle, J. P., DeClue, J. E., and Sampson, J. R. (2001). Pathological mutations in TSC1 and TSC2 disrupt the interaction between hamartin and tuberlin. *Hum Mol Genet* 10, 2899-2905.
- Holz, M. K., Ballif, B. A., Gygi, S. P., and Blenis, J. (2005). mTOR and S6K1 mediate assembly of the translation preinitiation complex through dynamic protein interchange and ordered phosphorylation events. *Cell* 123, 569-580.
- Hubbard, E. J., Wu, G., Kitajewski, J., and Greenwald, I. (1997). sel-10, a negative regulator of lin-12 activity in *Caenorhabditis elegans*, encodes a member of the CDC4 family of proteins. *Genes Dev* 11, 3182-3193.
- Ikeya, T., Galic, M., Belawat, P., Nairz, K. and Hafen, E. (2002). Nutrientdependent expression of insulin-like peptides from neuroendocrine cells in the CNS contributes to growth regulation in *Drosophila*. *Curr. Biol.* 12, 1293-1300.
- Inoki, K., Li, Y., Zhu, T., Wu, J., and Guan, K. L. (2002). TSC2 is phosphorylated and inhibited by Akt and suppresses mTOR signaling. *Nat Cell Biol* 4, 648-657.
- Isaac, D. D., and Andrew, D. J. (1996). Tubulogenesis in *Drosophila*: a requirement for the trachealess gene product. *Genes Dev* 10, 103-117.
- Ito, T., Chiba, T., and Yoshida, M. (2001). Exploring the protein interactome using comprehensive two-hybrid projects. *Trends Biotechnol* 19, S23-27.

-
- Ivanov, D., Philippova, M., Allenspach, R., Erne, P., and Resink, T. (2004). T-cadherin upregulation correlates with cell-cycle progression and promotes proliferation of vascular cells. *Cardiovasc Res* 64, 132-143.
- Jacinto, E., and Hall, M. N. (2003). Tor signaling in bugs, brain and brawn. *Nat Rev Mol Cell Biol* 4, 117-126.
- Jacinto, E., Loewith, R., Schmidt, A., Lin, S., Ruegg, M. A., Hall, A., and Hall, M. N. (2004). Mammalian TOR complex 2 controls the actin cytoskeleton and is rapamycin insensitive. *Nat Cell Biol* 6, 1122-1128.
- Jacinto, E., and Lorberg, A. (2008). TOR regulation of AGC kinases in yeast and mammals. *Biochem J* 410, 19-37.
- Jackson, R. J., Hellen, C. U., and Pestova, T. V. (2010). The mechanism of eukaryotic translation initiation and principles of its regulation. *Nat Rev Mol Cell Biol* 11, 113-127.
- Jaeschke, A., Hartkamp, J., Saitoh, M., Roworth, W., Nobukuni, T., Hodges, A., Sampson, J., Thomas, G., and Lamb, R. (2002). Tuberous sclerosis complex tumor suppressor-mediated S6 kinase inhibition by phosphatidylinositide-3-OH kinase is mTOR independent. *J Cell Biol* 159, 217-224.
- Jin, Z., and El-Deiry, W. S. (2005). Overview of cell death signaling pathways. *Cancer Biol Ther* 4, 139-163.
- Johannessen et al., (2008). TORC1 Is Essential for NF1-Associated Malignancies. *Curr. Biol.* 18: 56-62.
- Johannessen, C.M., Reczek, E.E., James, M.F., Brems, H., Legius, E., and Cichowski, K. (2005). The NF1 tumor suppressor critically regulates TSC2 and mTOR. *Proc. Natl. Acad. Sci. USA* 102, 8573–8578.
- Johnson, S. P., and Warner, J. R. (1987). Phosphorylation of the *Saccharomyces cerevisiae* equivalent of ribosomal protein S6 has no detectable effect on growth. *Mol Cell Biol* 7, 1338-1345.

Johnston, L. A., and Gallant, P. (2002). Control of growth and organ size in *Drosophila*. *Bioessays* 24, 54-64.

Jones, S. M., and Kazlauskas, A. (2001). Growth factor-dependent signaling and cell cycle progression. *FEBS Lett* 490, 110-116.

Juhasz, G., Csikos, G., Sinka, R., Erdelyi, M., and Sass, M. (2003). The *Drosophila* homolog of Aut1 is essential for autophagy and development. *FEBS Lett* 543, 154-158.

Kamada, Y., Funakoshi, T., Shintani, T., Nagano, K., Ohsumi, M., and Ohsumi, Y. (2000). Tor-mediated induction of autophagy via an Apg1 protein kinase complex. *J Cell Biol* 150, 1507-1513.

Kamath, R. S., Fraser, A. G., Dong, Y., Poulin, G., Durbin, R., Gotta, M., Kanapin, A., Le Bot, N., Moreno, S., Sohrmann, M., *et al.* (2003). Systematic functional analysis of the *Caenorhabditis elegans* genome using RNAi. *Nature* 421, 231-237.

Kanemori, Y., and Sagata, N. (2006). [Regulation of the cell cycle and checkpoint by SCF(beta-TrCP)]. *Tanpakushitsu Kakusan Koso* 51, 1386-1390.

Katso, R., Okkenhaug, K., Ahmadi, K., White, S., Timms, J., and Waterfield, M. D. (2001). Cellular function of phosphoinositide 3-kinases: implications for development, homeostasis, and cancer. *Annu Rev Cell Dev Biol* 17, 615-675.

Kawasome, H., Papst, P., Webb, S., Keller, G. M., Johnson, G. L., Gelfand, E. W., and Terada, N. (1998). Targeted disruption of p70(s6k) defines its role in protein synthesis and rapamycin sensitivity. *Proc Natl Acad Sci U S A* 95, 5033-5038.

Kennerdell, J. R., and Carthew, R. W. (1998). Use of dsRNA-mediated genetic interference to demonstrate that frizzled and frizzled 2 act in the wingless pathway. *Cell* 95, 1017-1026.

Kennerdell, J. R., and Carthew, R. W. (2000). Heritable gene silencing in *Drosophila* using double-stranded RNA. *Nat Biotechnol* 18, 896-898.

Keyomarsi, K., and Herliczek, T. W. (1997). The role of cyclin E in cell proliferation, development and cancer. *Prog Cell Cycle Res* 3, 171-191.

Kim, D. H., Sarbassov, D. D., Ali, S. M., King, J. E., Latek, R. R., Erdjument-Bromage, H., Tempst, P., and Sabatini, D. M. (2002). mTOR interacts with raptor to form a nutrient-sensitive complex that signals to the cell growth machinery. *Cell* 110, 163-175.

Kim, D. H., Sarbassov, D. D., Ali, S. M., Latek, R. R., Guntur, K. V., Erdjument-Bromage, H., Tempst, P., and Sabatini, D. M. (2003). GbetaL, a positive regulator of the rapamycin-sensitive pathway required for the nutrient-sensitive interaction between raptor and mTOR. *Mol Cell* 11, 895-904.

Kim, K. R., Kim, Y. K., and Cha, H. J. (2008). Recombinant baculovirus-based multiple protein expression platform for *Drosophila* S2 cell culture. *J Biotechnol* 133, 116-122.

Kim, Y. J., Lee, M. C., Kim, S. J., and Chun, J. Y. (2000). Identification and characterization of multiple isoforms of a mouse ribosome receptor. *Gene* 261, 337-344.

Kim, Y. O., Park, S. J., Balaban, R. S., Nirenberg, M., and Kim, Y. (2004). A functional genomic screen for cardiogenic genes using RNA interference in developing *Drosophila* embryos. *Proc Natl Acad Sci U S A* 101, 159-164.

Kirisako, T., Baba, M., Ishihara, N., Miyazawa, K., Ohsumi, M., Yoshimori, T., Noda, T., and Ohsumi, Y. (1999). Formation process of autophagosome is traced with Apg8/Aut7p in yeast. *J Cell Biol* 147, 435-446.

Klambt, C., Glazer, L., and Shilo, B. Z. (1992). *breathless*, a *Drosophila* FGF receptor homolog, is essential for migration of tracheal and specific midline glial cells. *Genes Dev* 6, 1668-1678.

Klionsky, D. J., Cregg, J. M., Dunn, W. A., Jr., Emr, S. D., Sakai, Y., Sandoval, I. V., Sibirny, A., Subramani, S., Thumm, M., Veenhuis, M., and Ohsumi, Y. (2003). A unified nomenclature for yeast autophagy-related genes. *Dev Cell* 5, 539-545.

Knoblich, J. A., Sauer, K., Jones, L., Richardson, H., Saint, R., and Lehner, C. F. (1994). Cyclin E controls S phase progression and its down-regulation during *Drosophila* embryogenesis is required for the arrest of cell proliferation. *Cell* 77, 107-120.

Koyano Y, Kawamoto T, Kikuchi A, Shen M, Kuruta Y, Tsutsumi S, Fujimoto K, Noshiro M, Fujii K, Kato Y. (2001). Chondrocyte-derived ezrin-like domain containing protein (CDEP), a rho guanine nucleotide exchange factor, is inducible in chondrocytes by parathyroid hormone and cyclic AMP and has transforming activity in NIH3T3 cells. *Osteoarthritis Cartilage* 9, S64-S68.

Koyano, Y. et al. (1997). Molecular cloning and characterization of CDEP, a novel human protein containing the ezrin-like domain of the band 4.1 superfamily and the Dbl homology domain of Rho guanine nucleotide exchange factors. *Biochem Biophys Res Commun* 241, 369-75.

Kozma, S. C., Lane, H. A., Ferrari, S., Luther, H., Siegmann, M., and Thomas, G. (1989). A stimulated S6 kinase from rat liver: identity with the mitogen activated S6 kinase of 3T3 cells. *Embo J* 8, 4125-4132.

Kozma, S. C., and Thomas, G. (2002). Regulation of cell size in growth, development and human disease: PI3K, PKB and S6K. *Bioessays* 24, 65-71.

Kuhnlein, R. P. (2010). *Drosophila* as a lipotoxicity model organism--more than a promise? *Biochim Biophys Acta* 1801, 215-221.

Kumar, A., and Paietta, J. V. (1995). The sulfur controller-2 negative regulatory gene of *Neurospora crassa* encodes a protein with beta-transducin repeats. *Proc Natl Acad Sci U S A* 92, 3343-3347.

Kuttenkeuler, D., and Boutros, M. (2004). Genome-wide RNAi as a route to gene function in *Drosophila*. *Brief Funct Genomic Proteomic* 3, 168-176.

Lambertsson, A. (1998). The minute genes in *Drosophila* and their molecular functions. *Adv Genet* 38, 69-134.

-
- Lane, L. K. (1993). Functional expression of rat alpha 1 Na,K-ATPase containing substitutions for cysteines 454, 458, 459, 513 and 551. *Biochem Mol Biol Int* 31, 817-822.
- Laplante, M., and Sabatini, D. M. (2009). An emerging role of mTOR in lipid biosynthesis. *Curr Biol* 19, R1046-1052.
- Lawrence, P. A., and Morata, G. (1977). The early development of mesothoracic compartments in *Drosophila*. An analysis of cell lineage and fate mapping and an assessment of methods. *Dev Biol* 56, 40-51.
- Layalle, S., Arquier, N., Léopold, P. (2008). The TOR pathway couples nutrition and developmental timing in *Drosophila*. *Dev. Cell* 15(4): 568-77.
- Lee, S., Comer, F. I., Sasaki, A., McLeod, I. X., Duong, Y., Okumura, K., Yates, J. R., 3rd, Parent, C. A., and Firtel, R. A. (2005). TOR complex 2 integrates cell movement during chemotaxis and signal relay in *Dictyostelium*. *Mol Biol Cell* 16, 4572-4583.
- Leevers, S. J., and McNeill, H. (2005). Controlling the size of organs and organisms. *Curr Opin Cell Biol* 17, 604-609.
- Levine, B., and Klionsky, D. J. (2004). Development by self-digestion: molecular mechanisms and biological functions of autophagy. *Dev Cell* 6, 463-477.
- Li, L., Edgar, B. A and Grewal, S. S. (2010). Nutritional control of gene expression in *Drosophila* larvae via TOR, Myc and a novel cis-regulatory element. *BMC Cell Biology*. 11:7.
- Li, Y., Corradetti, M. N., Inoki, K., and Guan, K. L. (2004). TSC2: filling the GAP in the mTOR signaling pathway. *Trends Biochem Sci* 29, 32-38.
- Lindquist, R.A., Ottina, K.A., Wheeler, D.B. et al. (2011). Genome-scale RNAi on living-cell microarrays identifies novel regulators of *Drosophila melanogaster* TORC1-S6K pathway signaling. *Genome Res.* 21,000-000.

Lodish, H., Berk, A., Kaiser, C.A., Krieger, M., Scott, M.P, Bretscher, A., Ploegh, H and Matsudaira, P. (2008). *Molecular Cell Biology*. (Sixth Edition). W.H. Freeman and Company. New York.

Loewith, R., Jacinto, E., Wullschleger, S., Lorberg, A., Crespo, J. L., Bonenfant, D., Oppliger, W., Jenoe, P., and Hall, M. N. (2002). Two TOR complexes, only one of which is rapamycin sensitive, have distinct roles in cell growth control. *Mol Cell* *10*, 457-468.

Long, X., Lin, Y., Ortiz-Vega, S., Yonezawa, K., and Avruch, J. (2005a). Rheb binds and regulates the mTOR kinase. *Curr Biol* *15*, 702-713.

Long, X., Ortiz-Vega, S., Lin, Y., and Avruch, J. (2005b). Rheb binding to mammalian target of rapamycin (mTOR) is regulated by amino acid sufficiency. *J Biol Chem* *280*, 23433-23436.

Long, X., Spycher, C., Han, Z. S., Rose, A. M., Muller, F., and Avruch, J. (2002). TOR deficiency in *C. elegans* causes developmental arrest and intestinal atrophy by inhibition of mRNA translation. *Curr Biol* *12*, 1448-1461.

Lum, L., Yao, S., Mozer, B., Rovescalli, A., Von Kessler, D., Nirenberg, M., and Beachy, P. A. (2003). Identification of Hedgehog pathway components by RNAi in *Drosophila* cultured cells. *Science* *299*, 2039-2045.

Luong, N., Davies, C. R., Wessells, R. J., Graham, S. M., King, M. T., Veech, R., Bodmer, R., and Oldham, S. M. (2006). Activated FOXO-mediated insulin resistance is blocked by reduction of TOR activity. *Cell Metab* *4*, 133-142.

Malyukova, A., Dohda, T., von der Lehr, N., Akhoondi, S., Corcoran, M., Heyman, M., Spruck, C., Grander, D., Lendahl, U., and Sangfelt, O. (2007). The tumor suppressor gene hCDC4 is frequently mutated in human T-cell acute lymphoblastic leukemia with functional consequences for Notch signaling. *Cancer Res* *67*, 5611-5616.

Manning, J., Beutler, K., Knepper, M. A., and Vehaskari, V. M. (2002). Upregulation of renal BSC1 and TSC in prenatally programmed hypertension. *Am J Physiol Renal Physiol* 283, F202-206.

Margulies, C., Tully, T., & Dubnau, J. (2005). Deconstructing memory in *Drosophila*. *Curr Biol* 15, R700-13.

Marshall, S. (2006). Role of insulin, adipocyte hormones, and nutrient-sensing pathways in regulating fuel metabolism and energy homeostasis: a nutritional perspective of diabetes, obesity, and cancer. *Sci STKE* 2006, re7.

Martin, D. E., and Hall, M. N. (2005). The expanding TOR signaling network. *Curr Opin Cell Biol* 17, 158-166.

Martin, F. A., and Morata, G. (2006). Compartments and the control of growth in the *Drosophila* wing imaginal disc. *Development* 133, 4421-4426.

Martin, P. M., and Sutherland, A. E. (2001). Exogenous amino acids regulate trophoblast differentiation in the mouse blastocyst through an mTOR-dependent pathway. *Dev Biol* 240, 182-193.

Martin, S., and Parton, R. G. (2006). Lipid droplets: a unified view of a dynamic organelle. *Nat Rev Mol Cell Biol* 7, 373-378.

Matus, D. Q., Magie, C. R., Pang, K., Martindale, M. Q., and Thomsen, G. H. (2008). The Hedgehog gene family of the cnidarian, *Nematostella vectensis*, and implications for understanding metazoan Hedgehog pathway evolution. *Dev Biol* 313, 501-518.

McNeill, H., Craig, G. M., and Bateman, J. M. (2008). Regulation of neurogenesis and epidermal growth factor receptor signaling by the insulin receptor/target of rapamycin pathway in *Drosophila*. *Genetics* 179, 843-853.

Melendez, A., Tallozy, Z., Seaman, M., Eskelinen, E. L., Hall, D. H., and Levine, B. (2003). Autophagy genes are essential for dauer development and life-span extension in *C. elegans*. *Science* 301, 1387-1391.

Meyuhas, O. (2008). Physiological roles of ribosomal protein S6: one of its kind. *Int Rev Cell Mol Biol* 268, 1-37.

Miklos, G. L., and Rubin, G. M. (1996). The role of the genome project in determining gene function: insights from model organisms. *Cell* 86, 521-529.

Minella, A. C., Grim, J. E., Welcker, M., and Clurman, B. E. (2007). p53 and SCFFbw7 cooperatively restrain cyclin E-associated genome instability. *Oncogene* 26, 6948-6953.

Mirth, C. K., and Riddiford, L. M. (2007). Size assessment and growth control: how adult size is determined in insects. *Bioessays* 29, 344-355.

Miura, S., Gan, J. W., Brzostowski, J., Parisi, M. J., Schultz, C. J., Londos, C., Oliver, B., and Kimmel, A. R. (2002). Functional conservation for lipid storage droplet association among Perilipin, ADRP, and TIP47 (PAT)-related proteins in mammals, *Drosophila*, and *Dictyostelium*. *J Biol Chem* 277, 32253-32257.

Mizushima, N., Ohsumi, Y., and Yoshimori, T. (2002). Autophagosome formation in mammalian cells. *Cell Struct Funct* 27, 421-429.

Moberg, K. H., Bell, D. W., Wahrer, D. C., Haber, D. A., and Hariharan, I. K. (2001). Archipelago regulates Cyclin E levels in *Drosophila* and is mutated in human cancer cell lines. *Nature* 413, 311-316.

Moberg, K. H., Mukherjee, A., Veraksa, A., Artavanis-Tsakonas, S., and Hariharan, I. K. (2004). The *Drosophila* F box protein archipelago regulates dMyc protein levels in vivo. *Curr Biol* 14, 965-974.

Mohr, S., Bakal, C., and Perrimon, N. (2010). Genomic screening with RNAi: results and challenges. *Annu Rev Biochem* 79, 37-64.

Montagne, J., Lecerf, C., Parvy, J. P., Bennion, J. M., Radimerski, T., Ruhf, M. L., Zilbermann, F., Vouilloz, N., Stocker, H., Hafen, E., *et al.* (2010). The nuclear receptor DHR3 modulates dS6 kinase-dependent growth in *Drosophila*. *PLoS Genet* 6, e1000937.

-
- Montagne J. and Thomas, G. (2004). S6K integrates nutrient and mitogen signals to control cell growth. In: Hall M, Raff M, Thomas G (eds) Cell growth: control of cell size. Cold Spring Harbor Monograph Series 42. Cold Spring Harbor Press, 265-298.
- Montagne, J., Stewart, M. J., Stocker, H., Hafen, E., Kozma, S. C., and Thomas, G. (1999). Drosophila S6 kinase: a regulator of cell size. *Science* 285, 2126-2129.
- Moon, N. S., Di Stefano, L., and Dyson, N. (2006). A gradient of epidermal growth factor receptor signaling determines the sensitivity of rbf1 mutant cells to E2F-dependent apoptosis. *Mol Cell Biol* 26, 7601-7615.
- Mortimer, N. T., and Moberg, K. H. (2007). The Drosophila F-box protein Archipelago controls levels of the Trachealess transcription factor in the embryonic tracheal system. *Dev Biol* 312, 560-571.
- Mortimer, N. T., and Moberg, K. H. (2009). Regulation of Drosophila embryonic tracheogenesis by dVHL and hypoxia. *Dev Biol* 329, 294-305.
- Moscat, J., Rennert, P., and Diaz-Meco, M. T. (2006). PKCzeta at the crossroad of NF-kappaB and Jak1/Stat6 signaling pathways. *Cell Death Differ* 13, 702-711.
- Mummery-Widmer, J.L., Yamazaki, M., Stoeger, T., Novatchkova, M., Bhalerao, S., Chen, D., Dietzl, G., Dickson, B.J and Knoblich, J.A. (2009). Genome-wide analysis of Notch signalling in Drosophila by transgenic RNAi. *Nature* 458, 987-992.
- Murakami, I. (2004). The aperture problem in egocentric motion. *Trends Neurosci* 27, 174-177.
- Murphy, D. J. (2001). The biogenesis and functions of lipid bodies in animals, plants and microorganisms. *Prog Lipid Res* 40, 325-438.
- Myat, M. M. (2005). Making tubes in the Drosophila embryo. *Dev Dyn* 232, 617-632.
- Nagy, A., Perrimon, N., Sandmeyer, S., and Plasterk, R. (2003). Tailoring the genome: the power of genetic approaches. *Nat Genet* 33 *Suppl*, 276-284.

Nash, P., Tang, X., Orlicky, S., Chen, Q., Gertler, F.B., Mendenhall, M.D., Sicheri, F., Pawson, T., and Tyers, M. (2001). Multisite phosphorylation of a CDK inhibitor sets a threshold for the onset of DNA replication. *Nature* *414*, 514–521.

Neely et al., (2010). A global in vivo *Drosophila* RNAi screen identifies NOT3 as a conserved regulator of heart function. *Cell* *141*, 142-153.

Neufeld, T. P., and Edgar, B. A. (1998). Connections between growth and the cell cycle. *Curr Opin Cell Biol* *10*, 784-790.

Nicholson, S. C., Gilbert, M. M., Nicolay, B. N., Frolov, M. V., and Moberg, K. H. (2009). The archipelago tumor suppressor gene limits *rb/e2f*-regulated apoptosis in developing *Drosophila* tissues. *Curr Biol* *19*, 1503-1510.

Noda, T., and Ohsumi, Y. (1998). Tor, a phosphatidylinositol kinase homologue, controls autophagy in yeast. *J Biol Chem* *273*, 3963-3966.

Nojima, H., Tokunaga, C., Eguchi, S., Oshiro, N., Hidayat, S., Yoshino, K., Hara, K., Tanaka, N., Avruch, J., and Yonezawa, K. (2003). The mammalian target of rapamycin (mTOR) partner, raptor, binds the mTOR substrates p70 S6 kinase and 4E-BP1 through their TOR signaling (TOS) motif. *J Biol Chem* *278*, 15461-15464.

Nygaard, O., and Nilsson, L. (1990). Translational dynamics. Interactions between the translational factors, tRNA and ribosomes during eukaryotic protein synthesis. *Eur J Biochem* *191*, 1-17.

Nykanen, A., Haley, B., and Zamore, P. D. (2001). ATP requirements and small interfering RNA structure in the RNA interference pathway. *Cell* *107*, 309-321.

Ogden, S. K., Ascano, M., Jr., Stegman, M. A., and Robbins, D. J. (2004). Regulation of Hedgehog signaling: a complex story. *Biochem Pharmacol* *67*, 805-814.

Oldham, S., Montagne, J., Radimerski, T., Thomas, G., and Hafen, E. (2000). Genetic and biochemical characterization of dTOR, the *Drosophila* homolog of the target of rapamycin. *Genes Dev* *14*, 2689-2694.

Orlicky, S., Tang, X., Willems, A., Tyers, M., and Sicheri, F. (2003). Structural basis for phosphodependent substrate selection and orientation by the SCFCdc4 ubiquitin ligase. *Cell* 112, 243-256.

Ou, C. Y., Pi, H., and Chien, C. T. (2003). Control of protein degradation by E3 ubiquitin ligases in *Drosophila* eye development. *Trends Genet* 19, 382-389.

Patursky-Polischuk, I., Stolovich-Rain, M., Hausner-Hanochi, M., Kasir, J., Cybulski, N., Avruch, J., Ruegg, M. A., Hall, M. N., and Meyuhas, O. (2009). The TSC-mTOR pathway mediates translational activation of TOP mRNAs by insulin largely in a raptor- or rictor-independent manner. *Mol Cell Biol* 29, 640-649.

Parvy, J.P., Blais, C., Bernard, F., Warren, J.T., Petryk, A., Gilbert, L.I., O'Connor, M.B and Dauphin-Villemanta, C. (2005). A role for hFTZ-F1 in regulating ecdysteroid titers during post-embryonic development in *Drosophila melanogaster*. *Develop Biol* 282, 84-94.

Pearson, R. B., Dennis, P. B., Han, J. W., Williamson, N. A., Kozma, S. C., Wettenhall, R. E., and Thomas, G. (1995). The principal target of rapamycin-induced p70s6k inactivation is a novel phosphorylation site within a conserved hydrophobic domain. *Embo J* 14, 5279-5287.

Pende, M., Um, S. H., Mieulet, V., Sticker, M., Goss, V. L., Mestan, J., Mueller, M., Fumagalli, S., Kozma, S. C., and Thomas, G. (2004). S6K1(-)/S6K2(-) mice exhibit perinatal lethality and rapamycin-sensitive 5'-terminal oligopyrimidine mRNA translation and reveal a mitogen-activated protein kinase-dependent S6 kinase pathway. *Mol Cell Biol* 24, 3112-3124.

Petroski, M. D., and Deshaies, R. J. (2005). In vitro reconstitution of SCF substrate ubiquitination with purified proteins. *Methods Enzymol* 398, 143-158.

Pickart, C. M. (2001). Mechanisms underlying ubiquitination. *Annu Rev Biochem* 70, 503-533.

Pickart, C. M. (2004). Back to the future with ubiquitin. *Cell* 116, 181-190.

Pospisilik, J. A., Schramek, D., Schnidar, H., Cronin, S. J., Nehme, N. T., Zhang, X., Knauf, C., Cani, P. D., Aumayr, K., Todoric, J., *et al.* (2010). *Drosophila* genome-wide obesity screen reveals hedgehog as a determinant of brown versus white adipose cell fate. *Cell* *140*, 148-160.

Potter, C. J., Pedraza, L. G., and Xu, T. (2002). Akt regulates growth by directly phosphorylating Tsc2. *Nat Cell Biol* *4*, 658-665.

Pratt, C. H., Vadigepalli, R., Chakravarthula, P., Gonye, G. E., Philp, N. J., and Grunwald, G. B. (2008). Transcriptional regulatory network analysis during epithelial-mesenchymal transformation of retinal pigment epithelium. *Mol Vis* *14*, 1414-1428.

Pullen, N., and Thomas, G. (1997). The modular phosphorylation and activation of p70s6k. *FEBS Lett* *410*, 78-82.

Radimerski, T. (2002) A genetic and biochemical analysis of *Drosophila melanogaster* dS6K upstream and downstream signaling elements. University Basel, Basel.

Radimerski, T., Mini, T., Schneider, U., Wettenhall, R. E., Thomas, G., and Jenö, P. (2000). Identification of insulin-induced sites of ribosomal protein S6 phosphorylation in *Drosophila melanogaster*. *Biochemistry* *39*, 5766-5774.

Radimerski, T., Montagne, J., Hemmings-Mieszczak, M., and Thomas, G. (2002a). Lethality of *Drosophila* lacking TSC tumor suppressor function rescued by reducing dS6K signaling. *Genes Dev* *16*, 2627-2632.

Radimerski, T., Montagne, J., Rintelen, F., Stocker, H., van der Kaay, J., Downes, C. P., Hafen, E., and Thomas, G. (2002b). dS6K-regulated cell growth is dPKB/dPI(3)K-independent, but requires dPDK1. *Nat Cell Biol* *4*, 251-255.

Radimerski, T. (2002) A genetic and biochemical analysis of *Drosophila melanogaster* dS6K upstream and downstream signaling elements

University Basel, Basel.

Ramadan, N., Flockhart, I., Booker, M., Perrimon, N., Mathey-Prevot, B. (2007). Design and implementation of high-throughput RNAi screens in cultured *Drosophila* cells. *Nat. Prot.* 2(9): 2245-2264.

Reinke, A., Anderson, S., McCaffery, J. M., Yates, J., 3rd, Aronova, S., Chu, S., Fairclough, S., Iverson, C., Wedaman, K. P., and Powers, T. (2004). TOR complex 1 includes a novel component, Tco89p (YPL180w), and cooperates with Ssd1p to maintain cellular integrity in *Saccharomyces cerevisiae*. *J Biol Chem* 279, 14752-14762.

Rintelen, F., Stocker, H., Thomas, G., and Hafen, E. (2001). PDK1 regulates growth through Akt and S6K in *Drosophila*. *Proc Natl Acad Sci U S A* 98, 15020-15025.

Rohde, J. R., Bastidas, R., Puria, R., and Cardenas, M. E. (2008). Nutritional control via Tor signaling in *Saccharomyces cerevisiae*. *Curr Opin Microbiol* 11, 153-160.

Romeo, Y., and Lemaitre, B. (2008). *Drosophila* immunity: methods for monitoring the activity of Toll and Imd signaling pathways. *Methods Mol Biol* 415, 379-394.

Rossi, R., Pester, J. M., McDowell, M., Soza, S., Montecucco, A., and Lee-Fruman, K. K. (2007). Identification of S6K2 as a centrosome-located kinase. *FEBS Lett* 581, 4058-4064.

Rusten, T. E., Lindmo, K., Juhasz, G., Sass, M., Seglen, P. O., Brech, A., and Stenmark, H. (2004). Programmed autophagy in the *Drosophila* fat body is induced by ecdysone through regulation of the PI3K pathway. *Dev Cell* 7, 179-192.

Saitoh, M., ten Dijke, P., Miyazono, K., and Ichijo, H. (1998). Cloning and characterization of p70(S6K beta) defines a novel family of p70 S6 kinases. *Biochem Biophys Res Commun* 253, 470-476.

Sarbassov, D. D., Ali, S. M., Kim, D. H., Guertin, D. A., Latek, R. R., Erdjument-Bromage, H., Tempst, P., and Sabatini, D. M. (2004). Rictor, a novel binding partner of mTOR, defines a rapamycin-insensitive and raptor-independent pathway that regulates the cytoskeleton. *Curr Biol* 14, 1296-1302.

Sarbassov, D. D., Ali, S. M., and Sabatini, D. M. (2005a). Growing roles for the mTOR pathway. *Curr Opin Cell Biol* 17, 596-603.

Sarbassov, D. D., Guertin, D. A., Ali, S. M., and Sabatini, D. M. (2005b). Phosphorylation and regulation of Akt/PKB by the rictor-mTOR complex. *Science* 307, 1098-1101.

Saucedo, L. J., Gao, X., Chiarelli, D. A., Li, L., Pan, D., and Edgar, B. A. (2003). Rheb promotes cell growth as a component of the insulin/TOR signaling network. *Nat Cell Biol* 5, 566-571.

Schalm, S. S., and Blenis, J. (2002). Identification of a conserved motif required for mTOR signaling. *Curr Biol* 12, 632-639.

Schalm, S. S., Fingar, D. C., Sabatini, D. M., and Blenis, J. (2003). TOS motif-mediated raptor binding regulates 4E-BP1 multisite phosphorylation and function. *Curr Biol* 13, 797-806.

Schmelzle, T., and Hall, M. N. (2000). TOR, a central controller of cell growth. *Cell* 103, 253-262.

Schnorrer, F., Schönbauer, C., Langer, C.C.H., Dietzl, G., Novatchkova, M., Schernhuber, K., Fellner, M., Azaryan, A., Radolf, M., Stark, A., Keleman, K and Dickson, B.J. (2010). Systematic genetic analysis of muscle morphogenesis and function in *Drosophila*. *Nature* 464, 287-291.

Scott, R. C., Schuldiner, O., and Neufeld, T. P. (2004). Role and regulation of starvation-induced autophagy in the *Drosophila* fat body. *Dev Cell* 7, 167-178.

Sehgal, S. N., Baker, H., and Vezina, C. (1975). Rapamycin (AY-22,989), a new antifungal antibiotic. II. Fermentation, isolation and characterization. *J Antibiot (Tokyo)* 28, 727-732.

Sethi, J. K., and Vidal-Puig, A. (2010). Wnt signaling and the control of cellular metabolism. *Biochem J* 427, 1-17.

-
- Shcherbata, H. R., Althausen, C., Findley, S. D., and Ruohola-Baker, H. (2004). The mitotic-to-endocycle switch in *Drosophila* follicle cells is executed by Notch-dependent regulation of G1/S, G2/M and M/G1 cell-cycle transitions. *Development* *131*, 3169-3181.
- Shima, H., Pende, M., Chen, Y., Fumagalli, S., Thomas, G., and Kozma, S. C. (1998). Disruption of the p70(s6k)/p85(s6k) gene reveals a small mouse phenotype and a new functional S6 kinase. *Embo J* *17*, 6649-6659.
- Skowyra, D., Craig, K. L., Tyers, M., Elledge, S. J., and Harper, J. W. (1997). F-box proteins are receptors that recruit phosphorylated substrates to the SCF ubiquitin-ligase complex. *Cell* *91*, 209-219.
- Smith, E. M., Finn, S. G., Tee, A. R., Browne, G. J., and Proud, C. G. (2005). The tuberous sclerosis protein TSC2 is not required for the regulation of the mammalian target of rapamycin by amino acids and certain cellular stresses. *J Biol Chem* *280*, 18717-18727.
- Soulard, A., and Hall, M. N. (2007). SnapShot: mTOR signaling. *Cell* *129*, 434.
- Spencer, E., Jiang, J., and Chen, Z. J. (1999). Signal-induced ubiquitination of I κ B α by the F-box protein Slimb/ β -TrCP. *Genes Dev* *13*, 284-294.
- Spruck, C. H., Strohmaier, H., Sangfelt, O., Muller, H. M., Hubalek, M., Muller-Holzner, E., Marth, C., Widschwendter, M., and Reed, S. I. (2002). hCDC4 gene mutations in endometrial cancer. *Cancer Res* *62*, 4535-4539.
- St Johnston, D. (2002). The art and design of genetic screens: *Drosophila melanogaster*. *Nat Rev Genet* *3*, 176-188.
- Stanfel, M. N., Shamieh, L. S., Kaeberlein, M., and Kennedy, B. K. (2009). The TOR pathway comes of age. *Biochim Biophys Acta* *1790*, 1067-1074.
- Stark, C., Breitkreutz, B. J., Reguly, T., Boucher, L., Breitkreutz, A., and Tyers, M. (2006). BioGRID: a general repository for interaction datasets. *Nucleic Acids Res* *34*, D535-539.

Stewart, M. J., Berry, C. O., Zilberman, F., Thomas, G., and Kozma, S. C. (1996). The *Drosophila* p70s6k homolog exhibits conserved regulatory elements and rapamycin sensitivity. *Proc Natl Acad Sci U S A* 93, 10791-10796.

Stewart, M. J., and Thomas, G. (1994). Mitogenesis and protein synthesis: a role for ribosomal protein S6 phosphorylation? *Bioessays* 16, 809-815.

Stocker, H., Radimerski, T., Schindelholz, B., Wittwer, F., Belawat, P., Daram, P., Breuer, S., Thomas, G., and Hafen, E. (2003). Rheb is an essential regulator of S6K in controlling cell growth in *Drosophila*. *Nat Cell Biol* 5, 559-565.

Strohmaier, H., Spruck, C. H., Kaiser, P., Won, K. A., Sangfelt, O., and Reed, S. I. (2001). Human F-box protein hCdc4 targets cyclin E for proteolysis and is mutated in a breast cancer cell line. *Nature* 413, 316-322.

Stromhaug, P. E., and Klionsky, D. J. (2001). Approaching the molecular mechanism of autophagy. *Traffic* 2, 524-531.

Struhl, G., and Basler, K. (1993). Organizing activity of wingless protein in *Drosophila*. *Cell* 72, 527-540.

Sutherland, D., Samakovlis, C., and Krasnow, M. A. (1996). *branchless* encodes a *Drosophila* FGF homolog that controls tracheal cell migration and the pattern of branching. *Cell* 87, 1091-1101.

Szuplewski, S., Sandmann, T., Hietakangas, V., and Cohen, S. M. (2009). *Drosophila* Minus is required for cell proliferation and influences Cyclin E turnover. *Genes Dev* 23, 1998-2003.

Tabara, H., Grishok, A., and Mello, C. C. (1998). RNAi in *C. elegans*: soaking in the genome sequence. *Science* 282, 430-431.

Tanaka, T., Masuzaki, H., Yasue, S., Ebihara, K., Shiuchi, T., Ishii, T., Arai, N., Hirata, M., Yamamoto, H., Hayashi, T., *et al.* (2007). Central melanocortin signaling restores skeletal muscle AMP-activated protein kinase phosphorylation in mice fed a high-fat diet. *Cell Metab* 5, 395-402.

-
- Tansey, J. T., Sztalryd, C., Hlavin, E. M., Kimmel, A. R., and Londos, C. (2004). The central role of perilipin a in lipid metabolism and adipocyte lipolysis. *IUBMB Life* 56, 379-385.
- Tapon, N., Ito, N., Dickson, B. J., Treisman, J. E., and Hariharan, I. K. (2001). The *Drosophila* tuberous sclerosis complex gene homologs restrict cell growth and cell proliferation. *Cell* 105, 345-355.
- Tee, A. R., and Blenis, J. (2005). mTOR, translational control and human disease. *Semin Cell Dev Biol* 16, 29-37.
- Teleman, A. A., Chen, Y. W., and Cohen, S. M. (2005a). 4E-BP functions as a metabolic brake used under stress conditions but not during normal growth. *Genes Dev* 19, 1844-1848.
- Teleman, A. A., Chen, Y. W., and Cohen, S. M. (2005b). *Drosophila* Melted modulates FOXO and TOR activity. *Dev Cell* 9, 271-281.
- Teleman, A. A., Hietakangas, V., Sayadian, A. C., and Cohen, S. M. (2008). Nutritional control of protein biosynthetic capacity by insulin via Myc in *Drosophila*. *Cell Metab* 7, 21-32.
- Teleman, A. A., Maitra, S., and Cohen, S. M. (2006). *Drosophila* lacking microRNA miR-278 are defective in energy homeostasis. *Genes Dev* 20, 417-422.
- Tetzlaff, M. T., Yu, W., Li, M., Zhang, P., Finegold, M., Mahon, K., Harper, J. W., Schwartz, R. J., and Elledge, S. J. (2004). Defective cardiovascular development and elevated cyclin E and Notch proteins in mice lacking the Fbw7 F-box protein. *Proc Natl Acad Sci U S A* 101, 3338-3345.
- The, I., Hannigan, G.E, Cowley, G.S, Reginald, S., Zhong, Y., Gusella, J.F., Hariharan, I.K and Bernards, A. (1997) Rescue of *Drosophila* NF1 mutant phenotype by protein kinase A. *Science* 276:791–794.
- Timmons, L., and Fire, A. (1998). Specific interference by ingested dsRNA. *Nature* 395, 854.

Vanhaesebroeck, B., Leever, S. J., Ahmadi, K., Timms, J., Katso, R., Driscoll, P. C., Woscholski, R., Parker, P. J., and Waterfield, M. D. (2001). Synthesis and function of 3-phosphorylated inositol lipids. *Annu Rev Biochem* 70, 535-602.

Vargas, M.A., Lou, N., Yamaguchi and Kapahi, P. (2010). A role of S6 kinase in Serotonin in postmating dietary switch and balance of nutrients in *D. Melanogaster*. *Curr. Biol.* 20, 1006-1011.

Vidal, M., and Cagan, R. L. (2006). *Drosophila* models for cancer research. *Curr Opin Genet Dev* 16, 10-16.

Volarevic, S., Stewart, M. J., Ledermann, B., Zilberman, F., Terracciano, L., Montini, E., Grompe, M., Kozma, S. C., and Thomas, G. (2000). Proliferation, but not growth, blocked by conditional deletion of 40S ribosomal protein S6. *Science* 288, 2045-2047.

Volarevic, S., and Thomas, G. (2001). Role of S6 phosphorylation and S6 kinase in cell growth. *Prog Nucleic Acid Res Mol Biol* 65, 101-127.

Wang, C. W., and Klionsky, D. J. (2003). The molecular mechanism of autophagy. *Mol Med* 9, 65-76.

Wang, L., Tu, Z., and Sun, F. (2009). A network-based integrative approach to prioritize reliable hits from multiple genome-wide RNAi screens in *Drosophila*. *BMC Genomics* 10, 220.

Wang, R. C., and Levine, B. (2010). Autophagy in cellular growth control. *FEBS Lett* 584, 1417-1426.

Watson, K. L., Chou, M. M., Blenis, J., Gelbart, W. M., and Erikson, R. L. (1996). A *Drosophila* gene structurally and functionally homologous to the mammalian 70-kDa s6 kinase gene. *Proc Natl Acad Sci U S A* 93, 13694-13698.

Weinkove, D., Neufeld, T. P., Twardzik T., Waterfield, M. D and Leever, S. J. (1999). Regulation of imaginal disc cell size, cell number and organ size by *Drosophila* class I(A) phosphoinositide 3-kinase and its adaptor. *Curr Biol* 9,1019-29.

Weiss, A., Herzig, A., Jacobs, H., and Lehner, C. F. (1998). Continuous Cyclin E expression inhibits progression through endoreduplication cycles in *Drosophila*. *Curr Biol* 8, 239-242.

White, K., Grether, M. E., Abrams, J. M., Young, L., Farrell, K., and Steller, H. (1994). Genetic control of programmed cell death in *Drosophila*. *Science* 264, 677-683.

White, M. F. (2003). Insulin signaling in health and disease. *Science* 302, 1710-1711.

Winter, S. E. (2005) Repression of Dpp targets in the *Drosophila* wing by Brinker, University of Pittsburgh, Pennsylvania , USA.

Wool, I. G. (1996). Extraribosomal functions of ribosomal proteins. *Trends Biochem Sci* 21, 164-165.

Wullschleger, S., Loewith, R., and Hall, M. N. (2006). TOR signaling in growth and metabolism. *Cell* 124, 471-484.

Wullschleger, S., Loewith, R., Oppliger, W., and Hall, M. N. (2005). Molecular organization of target of rapamycin complex 2. *J Biol Chem* 280, 30697-30704.

Wu, Q., Zhang, Y., Xu, J and Shen, P. (2001) . Regulation of hunger driven behaviors by neural ribosomal S6 kinase in *Drosophila*. *PNAS* 102, 13289-13294.

Zaffran, S., Chartier, A., Gallant, P., Astier, M., Arquier, N., Doherty, D., Gratecos, D., and Semeriva, M. (1998). A *Drosophila* RNA helicase gene, *pitchoune*, is required for cell growth and proliferation and is a potential target of d-Myc. *Development* 125, 3571-3584.

Zamore, P. D. (2001). RNA interference: listening to the sound of silence. *Nat Struct Biol* 8, 746-750.

Zamore, P. D., Tuschl, T., Sharp, P. A., and Bartel, D. P. (2000). RNAi: double-stranded RNA directs the ATP-dependent cleavage of mRNA at 21 to 23 nucleotide intervals. *Cell* 101, 25-33.

Zhang, H., Stallock, J. P., Ng, J. C., Reinhard, C., and Neufeld, T. P. (2000). Regulation of cellular growth by the *Drosophila* target of rapamycin dTOR. *Genes Dev* 14, 2712-2724.

Zhang, Y., Billington, C. J., Jr., Pan, D., and Neufeld, T. P. (2006). *Drosophila* target of rapamycin kinase functions as a multimer. *Genetics* 172, 355-362.

Zhang, Y., Gao, X., Saucedo, L. J., Ru, B., Edgar, B. A., and Pan, D. (2003). Rheb is a direct target of the tuberous sclerosis tumour suppressor proteins. *Nat Cell Biol* 5, 578-581.

Zinke, I., Schutz, C. S., Katzenberger, J. D., Bauer, M., and Pankratz, M. J. (2002). Nutrient control of gene expression in *Drosophila*: microarray analysis of starvation and sugar-dependent response. *Embo J* 21, 6162-6173.